

Essays in Empirical Analysis of Energy Markets

Inauguraldissertation
zur
Erlangung des Doktorgrades
der
Wirtschafts- und Sozialwissenschaftlichen Fakultät
der
Universität zu Köln

2024

vorgelegt
von

M. Sc. Markos Farag

aus

Ägypten

Referent: Prof. Dr. Marc Oliver Bettzüge
Korreferent: Prof. Dr. Jörg Breitung

ACKNOWLEDGEMENTS

I would like to express my sincere thanks to Prof. Dr. Marc Oliver Bettzüge for his supervision of my thesis. His insights and feedback have been crucial in shaping my research interests and have significantly helped me improve my papers in a very constructive way. I am also grateful to Prof. Dr. Jörg Breitung for co-refereeing my thesis. Furthermore, my gratitude goes to Prof. Dr. Oliver Ruhnau for chairing the examination committee.

I am deeply grateful to my excellent colleagues at the Institute of Energy Economics at the University of Cologne (EWI) and the Chair of Energy Economics. Along with the shared enjoyable moments, our collaborative projects and discussions have broadened both my professional and personal perspectives. My special thanks go to my outstanding co-authors Samir Jeddi, Jan Hendrik Kopp, Oliver Ruhnau, Stephen Snudden, and Gregory Upton for the great teamwork and all the wonderful memories we created together.

Additionally, I would like to thank Gabriel Arce Alfaro, Christiane Baumeister, Jörg Breitung, Eren Çam, Reinhard Ellwanger, James D. Hamilton, Jan Hendrik Kopp, Mario Liebensteiner, Philip Schnaars, and David Schlund for their helpful comments and suggestions. I would also like to acknowledge my research stay at the Center for Energy Studies, facilitated and hosted by Gregory Upton, during which I worked primarily on Chapter 3.

The second chapter benefited from comments from participants at the US-AEE/IAEE North American Conference 2023 in Chicago, the Economics Seminar at Louisiana State University, the Bonn-Frankfurt-Mannheim PhD Conference 2024 in Bonn, and the Monitoring and Forecasting Macroeconomic and Financial Risk So.Fi.E. Summer School in Brussels. The third chapter benefited from comments from participants at the 14th RCEA Bayesian Econometrics Workshop in London and the 13th International Ruhr Energy Conference in Essen. The fourth chapter benefited from feedback from participants at the 44th IAEE Conference in Riyadh, the 12th International Ruhr Energy Conference in Essen, and the Hagen Workshop on Global Economic Studies 2022 in Berlin.

Finally, my deepest appreciation goes to Dora, my family, and my friends for their constant encouragement, understanding, and patience during this challenging journey.

Contents

List of Figures	ix
List of Tables	xii
1. Introduction	1
1.1. Outline	3
1.1.1. Can Futures Prices Predict the Real Price of Primary Com- modities?	3
1.1.2. Revisiting the Dynamics and Elasticities of the U.S. Natural Gas Market	3
1.1.3. Global Natural Gas Market Integration: The Role of LNG Trade and Infrastructure Constraints	4
1.1.4. Decomposing Return and Volatility Connectedness in North- west European Gas Markets: Evidence from the R2 con- nectedness approach.	4
1.2. Methodology	5
2. Can Futures Prices Predict the Real Price of Primary Com- modities?	9
2.1. Introduction	9
2.2. Literature Review	12
2.2.1. Period-Average Forecasts	12
2.2.2. Point-Sampled Forecasts	14
2.3. Methods	15
2.3.1. Expectations from Futures	15
2.3.2. Futures-Based Forecasts	17
2.3.3. Forecast Evaluation	18
2.4. Data	20
2.4.1. Data Sources	20
2.4.2. Alignment of Futures Contracts with Forecast Horizons . .	22

2.5.	Results	24
2.5.1.	Non-Parametric Forecasts	24
2.5.2.	Effects of Averaging Futures	29
2.5.3.	Parametric Forecasts	30
2.5.4.	Nominal Forecasts	31
2.5.5.	Direct Forecasts	33
2.5.6.	Robustness over time	34
2.6.	Conclusion	34
3.	Revisiting the Dynamics and Elasticities of the U.S. Natural Gas Market	37
3.1.	Introduction	37
3.2.	Literature review	40
3.3.	Methodology	44
3.3.1.	Structural VAR specification and estimation	44
3.3.2.	A structural VAR model of the U.S. natural gas market	45
3.3.3.	Prior information for contemporaneous parameters	48
3.4.	Data	50
3.5.	Results	52
3.5.1.	Posterior distributions for structural parameters	52
3.5.2.	Impulse response functions	54
3.5.3.	Forecast error variance decomposition	56
3.5.4.	Historical decomposition	57
3.6.	Sensitivity Analysis	60
3.6.1.	Sensitivity to the effects of excluding pandemic-related observations	60
3.6.2.	Sensitivity to the effects of the shale gas revolution	61
3.6.3.	Sensitivity to alternative prior assumptions and model identification	62
3.7.	Conclusion	63
4.	Global Natural Gas Market Integration: The Role of LNG Trade and Infrastructure Constraints	67
4.1.	Introduction	67
4.2.	Conceptual background	71
4.3.	Structural changes in the international natural gas market	72
4.4.	Methodology	74

4.5. Main results	76
4.5.1. Structural break	76
4.5.2. Examining the linear cointegration	77
4.5.3. Examining the nonlinear cointegration	78
4.5.4. Results of the (a)symmetric error correction model	79
4.6. Further results	81
4.7. Conclusion	82
5. Decomposing Return and Volatility Connectedness in North-west European Gas Markets: Evidence from the R^2 connectedness approach	85
5.1. Introduction	85
5.2. Literature review	88
5.3. Dynamics of gas prices and volatility in NWE	91
5.4. Methodology	96
5.5. The connectedness of NWE gas markets	98
5.5.1. Return connectedness results	99
5.5.2. Volatility connectedness results	102
5.5.3. Connectedness analysis using futures prices	104
5.6. Factors associated with the connectedness of NWE gas markets	106
5.7. Conclusion	110
A. Supplementary Material for Chapter 2	113
A.1. Additional data details	113
A.2. Additional results	114
B. Supplementary Material for Chapter 3	125
B.1. Detailed Bayesian identification and estimation of the SVAR model	125
B.2. Additional results: posterior distributions and historical decompositions	128
B.3. Detailed results of the sensitivity analyses	132
C. Supplementary Material for Chapter 4	141
D. Supplementary Material for Chapter 5	143
D.1. Additional data details	143
D.2. Additional results	144
Bibliography	155

List of Figures

2.1. Settlement and Delivery for Wheat and Crude oil on December 31	23
2.2. Evolution of MSFEs Criteria For Futures-Based Forecasts, One-Month Ahead.	35
3.1. Prior and posterior distributions of the contemporaneous coefficients in the matrix A	53
3.2. Structural impulse responses	54
3.3. Historical decomposition of U.S. real natural gas price movements from January 2022 to October 2023	58
4.1. Natural gas prices in log level	73
4.2. Δ YoY (%) in Russian gas exports, Gate terminal and U.S. export terminals utilization rates	73
4.3. Δ YoY (%)in LNG imports for major regions	74
5.1. TTF price series and price ratios of THE, NBP, and ZTP to TTF	93
5.2. TTF volatility series and volatility ratios of THE, NBP, and ZTP to TTF	94
5.3. Gas infrastructure utilization in NWE	95
5.4. Dynamic total connectedness of return series	100
5.5. Dynamic directional connectedness of return series	101
5.6. Dynamic total connectedness of volatility series	103
5.7. Dynamic directional connectedness of volatility series	104
5.8. Comparison of return connectedness indices: spot prices vs. futures prices	105
5.9. Return connectedness level and utilization rate of BBL and IZT gas pipelines (%)	107
A.1. Traded Volume vs MSFE Ratio for the One-Month Ahead.	118
A.2. Evolution of MSFEs Criteria For Futures-Based Forecasts, One-Year Ahead.	123

A.3. Evolution of MSFEs Criteria For Futures-Based Forecasts, Two-Year Ahead.	124
B.1. Historical decomposition of U.S. real natural gas price movements from January 2005 to December 2005	130
B.2. Historical decomposition of U.S. real natural gas price movements from January 2015 to December 2017	131
B.3. Impulse response functions for the model estimated from January 1992 to December 2019	132
B.4. Impulse response functions for the model estimated using the entire sample from January 1992 to October 2023, including observations during the COVID-19 pandemic.	133
B.5. Impulse response functions for the model estimated from January 2009 to October 2023, excluding the COVID-19 pandemic period from March 2020 to February 2021.	134
B.6. Impulse response functions from the model estimated using the full dataset from January 1992 to December 2023, excluding the period from March 2020 to February 2021, with weaker priors for supply and demand elasticities.	135
B.7. Posterior predictive densities of standardized structural shocks . .	137
B.8. Posterior distributions of the mutual independence test statistics $U(E)$, as per Matteson and Tsay (2017).	138
B.9. Impulse response functions with Non-Gaussianity as an additional source of identification.	139
B.10. Monthly U.S. domestic natural gas production and total supply (in billion cubic feet) from 1992 to 2023.	140
C.1. Worldwide and regional developments of natural gas a) production and b) demand from 2012 to 2022 (Billion cubic meters).	141
D.1. Connectedness with different rolling window sizes (150, 200, 250) for return and volatility series	147
D.2. Connectedness using Spearman correlation coefficient for return and volatility series	148
D.3. Dynamic total connectedness of realized weekly volatility series .	149
D.4. Dynamic directional connectedness of realized weekly volatility series	150
D.5. Comparison of directional connectedness indices: spot prices vs. futures prices	151

D.6. Dynamic total connectedness of volatility series using futures prices	152
D.7. Dynamic directional connectedness of volatility series using futures prices	153
D.8. volatility connectedness level and utilization rate of BBL and IZT gas pipelines	154

List of Tables

2.1. Summary of Studies Forecasting Period Average Commodity Prices using Futures	13
2.2. Summary of Studies Forecasting Point-Sampled Commodity Prices using Futures	14
2.3. Bloomberg Tickers for Commodity Futures, Sample Periods, and Contract Details	21
2.4. Futures-based Forecasts of Monthly Real Prices, Non-Parametric	25
2.5. Futures-based Forecasts of Monthly Real Prices, Non-Parametric, Monthly Average Futures	29
2.6. Futures-based Forecasts of Monthly Real Prices, Parametric	31
2.7. Futures-based Forecasts of Monthly Average Nominal Prices, Non-Parametric	32
2.8. Direct Futures-based Forecasts of Monthly Average Real Prices, Non-Parametric, End-of-Month Futures	33
3.1. Summary of studies analyzing the dynamics of the U.S. natural gas market using SVAR models	42
3.2. Summary of prior distributions affecting contemporaneous coefficients \mathbf{A}	48
3.3. Percent contribution of shocks to the overall variability of each variable	56
4.1. Linear cointegration analysis	77
4.2. Non-linear cointegration analysis	79
4.3. Results of symmetric and asymmetric ECM	80
4.4. Causality Tests for HH-TTF Spread	82
5.1. Regression analysis of factors associated with NWE gas markets connectedness	109
A.1. Bloomberg Tickers / Sources for Commodity Spot Prices and Sample Periods	114

A.2. Real-Time End-of-Month versus Monthly Average No-Change Forecast	115
A.3. Adjustment Variations in First-Month Futures Forecasting, Non-Parametric	117
A.4. Futures-based Forecasts of Monthly Average Real Prices, Non-Parametric, Constructed using Five Day End-of-Month Futures Average	119
A.5. MSFE Precision of Futures-based Forecasts of Monthly Real Prices, Parametric	120
A.6. Directional Accuracy of Futures-based Forecasts of Monthly Real Prices, Parametric	121
A.7. Futures-based Forecasts of Monthly Average Real Prices, Non-Parametric, Sample Starting 2000	122
B.1. Summary statistics for the contemporaneous coefficients in A . .	128
B.2. Percent contribution of shocks to the overall variability of each variable (with credibility sets)	129
C.1. Summary statistics of gas price series across different periods . .	142
C.2. Time series properties of the data	142
D.1. Descriptive statistics for NWE gas benchmarks	143
D.2. Averaged connectedness of return series	144
D.3. Averaged connectedness of volatility series	146

1. Introduction

Energy markets play a central role in the global economy, with commodities such as oil and natural gas serving as essential inputs across industrial sectors and influencing macroeconomic indicators like inflation, trade balances, and economic growth (Acaravci et al., 2012; Cunado & De Gracia, 2005; He et al., 2010). Fluctuations in energy prices directly affect production costs and consumer spending, making them a critical factor for policymakers, businesses, and consumers. Beyond their standalone importance, energy markets are increasingly interconnected with other commodity markets, such as agricultural and metal markets. Specifically, energy markets are linked to agriculture, particularly corn, due to the rise of biofuel production, which creates connections between agricultural commodities and energy (Tyner, 2010). Energy and metal markets are also closely linked, as energy is essential for metal extraction and processing, making metal prices sensitive to energy cost fluctuations. Additionally, rising energy prices often drive investors toward metals like gold, which serve as safe-haven assets during periods of market volatility (Ji et al., 2020; Rehman & Vo, 2021).

Starting in the late 1970s, energy markets in developed countries began a gradual shift from heavy regulation and state control toward deregulation and, in some cases, privatization. Previously, sectors such as natural gas and electricity were tightly regulated, while coal and crude oil prices were often controlled by a small group of powerful producers (Farag & Zaki, 2021b). Deregulation created new incentives for market-driven energy procurement and pricing, reducing reliance on regulatory oversight and cost recovery through ratepayers (Kaminski, 2012). Natural gas markets, in particular, experienced significant deregulation efforts, with notable reforms in both Europe and the United States. In Europe, the First Gas Directive of 1998 marked the beginning of a series of regulatory reforms aimed at enhancing competition, increasing cross-border trade, and improving transparency within the natural gas market. This was followed by the Second and Third Energy Packages, which further dismantled monopolistic structures and integrated the European market (Bianco et al., 2015; Demir & Demir, 2020). Similarly, the United States pursued a phased deregulation process, beginning with the Natural Gas Policy Act of 1978 and culminating in the Natural Gas Wellhead Decontrol Act of 1989, which fully deregulated wellhead prices and allowed market forces to dictate prices (Hou & Nguyen, 2018; Makhholm, 2010). These parallel efforts in Europe and the U.S. transformed regional natural gas markets, fostering competitive pricing, enhancing cross-border trade, and contributing to a more dynamic and integrated energy market.

1. Introduction

As energy markets became increasingly market-oriented, futures contracts emerged as critical tools for managing price volatility and enhancing market transparency. The introduction of energy futures—beginning with heating oil futures on the New York Mercantile Exchange (NYMEX) in 1978—brought greater efficiency and liquidity to energy markets, enabling faster price discovery and providing mechanisms for hedging against price risks (Kim et al., 2024). Since then, energy futures markets have expanded to include contracts on crude oil, natural gas, and gasoline, among others, allowing a broader range of market participants, from producers to institutional investors, to manage exposure to price fluctuations (Hanly, 2017).

This thesis is organized into four main chapters, each addressing a distinct aspect of energy markets, with a particular focus on the predictive power of futures prices and the dynamics of natural gas markets. Chapter 2 investigates the predictive power of futures prices for 17 primary commodities, including five key energy commodities. Chapter 3 focuses on the U.S. natural gas market, exploring how supply and demand shocks affect price fluctuations and market dynamics. Chapter 4 examines the integration of natural gas markets across Europe, North America, and Japan. Finally, Chapter 5 concentrates on the interconnectedness of price returns and volatility within the Northwest European natural gas markets, analyzing how price movements and volatility are transmitted across this regional market. Each chapter is based on a paper to which all authors contributed equally.

1. **Can Futures Prices Predict the Real Price of Primary Commodities?**. Joint work with Stephen Snudden and Gregory Upton. USAEE Working Paper No. 24-629.
2. **Revisiting the Dynamics and Elasticities of the U.S. Natural Gas Market**.
3. **Global Natural Gas Market Integration: The Role of LNG Trade and Infrastructure Constraints**. Joint work with Samir Jeddi and Jan Hendrik Kopp. Published in *The World Economy*, 2025.
4. **Decomposing Return and Volatility Connectedness in Northwest European Gas Markets: Evidence from the R2 connectedness approach**. Joint work with Oliver Ruhnau. EWI Working Paper No. 2024/6.

The remainder of the introduction is divided into two sections: Section 1.1 provides an outline of the content of the four essays. Section 1.2 discusses the methodological approaches of the essays, as well as limitations and potential areas of further research.

1.1. Outline

1.1.1. Can Futures Prices Predict the Real Price of Primary Commodities?

Primary commodities play an indispensable role in the production of a wide array of goods and services, shaping global trade, influencing aggregate price levels, and affecting broader economic outcomes. These commodities are also central to global decarbonization efforts. One approach to forecasting primary commodity prices is to use futures contract prices. This method offers practical advantages, as data from futures markets are widely available and based on real-time decisions of market participants. However, prior studies have produced mixed results regarding their predictive performance. This chapter investigates whether using end-of-month futures prices, rather than monthly averages, enhances forecast accuracy. The analysis uses both non-parametric and parametric forecasting approaches, comparing them against a random walk benchmark across multiple forecast horizons. Results indicate that non-parametric forecasts, which rely on the latest available market data rather than averaging prices over the month, consistently reduce forecast errors for most commodities, especially at shorter horizons. The findings suggest that futures-based forecasts are a valuable tool for predicting commodity prices, particularly when recent trading data is prioritized over time-averaged prices, providing practical insights for researchers, policymakers, and market participants interested in more accurate commodity price forecasts.

1.1.2. Revisiting the Dynamics and Elasticities of the U.S. Natural Gas Market

The third chapter focuses on the dynamics of the U.S. natural gas market, exploring the distinct roles of supply, demand, and trade shocks in influencing price fluctuations. As a critical component of the U.S. energy landscape, natural gas affects a wide range of sectors, from manufacturing to residential heating, and has recently gained importance in global markets due to rising liquefied natural gas (LNG) exports. Traditional structural analyses of the U.S. natural gas market, often adapted from oil market models, have generally emphasized the role of domestic demand while largely overlooking the impact of external trade flows, such as imports and exports. These omissions may lead to an incomplete representation of the market's dynamics, particularly in capturing the role of export demand within observed demand-side shocks. To address this gap, this chapter develops a Structural Vector Autoregression (SVAR) model that explicitly incorporates external trade flows, allowing for a clearer distinction between domestic and export-driven demand shocks and providing new insights into the relative importance of different structural shocks.

The model, estimated using monthly data through 2023, captures short-term market dynamics more precisely than models estimated with quarterly data.

1. Introduction

Extending the dataset through 2023 also captures recent market shifts, particularly those related to the increase in natural gas exports to Europe following the Russian invasion of Ukraine. Key findings reveal that short-run supply and demand elasticities in the U.S. natural gas market are low, indicating limited responsiveness to price changes. The analysis shows that domestic consumption and inventory demand shocks are the primary drivers of short-term price fluctuations, while the effects of supply, economic activity, and export demand shocks become more pronounced over longer horizons. Additionally, a decomposition of gas price movements during the period 2022–2023 highlights how domestic factors—particularly consumption and inventory demand—drove significant price variations, with export demand shocks also playing a role due to increased LNG exports to Europe and operational disruptions at LNG facilities. These findings underscore the need to adapt global oil market frameworks for use in regional natural gas markets, as well as the importance of accounting for the unique dynamics of external trade in the U.S. market.

1.1.3. Global Natural Gas Market Integration: The Role of LNG Trade and Infrastructure Constraints

The integration of global gas markets has been driven by the rise of LNG trade and a shift from oil-indexed to hub-based pricing, which has increased market liquidity and created new opportunities for spatial arbitrage. This chapter examines the integration of global natural gas markets, focusing on the North American, European, and East Asian regions from 2016 to 2022. Using daily futures prices for Henry Hub (North America), Title Transfer Facility (Europe), and East Asia Index (East Asia), this chapter explores whether these markets exhibit cointegration over this period. To capture the potential impact of recent geopolitical and market disruptions—especially Russia’s reduction of gas supplies to Europe and the resulting surge in LNG demand—the analysis divides the data into two subsamples: pre-October 2021 and post-October 2021. In the first subsample, we find evidence of linear and nonlinear cointegration among all three markets. However, in the second subsample, as LNG infrastructure reached capacity limits, we observe a breakdown in integration between the American and European markets and a nonlinear cointegration between European and Asian prices.

1.1.4. Decomposing Return and Volatility Connectedness in Northwest European Gas Markets: Evidence from the R2 connectedness approach.

The integration of European gas markets has accelerated over recent decades, driven by regulatory reforms and the expansion of liquefied natural gas (LNG) infrastructure, which has increased interdependence among regional gas hubs. Previous studies by Chen et al. (2022) and Szafranek et al. (2023) have shown that these shocks have also led to reduced market connectedness in terms of price returns

between gas hubs. Building on this prior analysis, this chapter extends the study of connectedness by addressing the following research questions: *Do European gas markets influence each other's price returns and volatility contemporaneously, or are there delays in this transmission? How does the timing of connectedness vary between tight and stable market conditions? How quickly does connectedness recover following major disruptions?*

The findings reveal that contemporaneous spillovers tend to dominate over lagged effects, even during periods of significant external disruption. This suggests that regional gas markets exhibit rapid adjustments to new information, with price connections reestablishing quickly after shocks subside. Market connectedness dipped notably during peak disruptions but rebounded to pre-crisis levels once conditions stabilized. These patterns indicate that, despite external stressors, the underlying structure of Northwest European gas markets remains capable of reverting to high levels of integration once immediate pressures are alleviated.

1.2. Methodology

The methodology in this thesis employs a range of econometric techniques to analyze various aspects of energy markets, focusing on forecasting, structural modeling, market integration, and interconnectedness.

In **Chapter 2**, the methodology focuses on constructing and evaluating commodity price forecasts using futures market data to predict the monthly average real spot price. To create period-average spot price forecasts from futures data, the study explores three main approaches: (1) averaging futures prices over the last few trading days of each month to capture recent market expectations; (2) using the monthly average of daily futures prices, which accounts for any mid-month contract rollovers; and (3) focusing on the futures price at the close of the last trading day of each month for its up-to-date information. Each approach is empirically tested across multiple commodities to assess its predictive power. The chapter also addresses practical challenges associated with using futures prices for forecasting, including irregular delivery schedules and the unique settlement procedures tied to front-month contracts for each commodity. To overcome these issues, a continuous monthly futures curve is generated, aligning each observation with its respective forecast month. This approach better reflects real-time commodity trading practices, thereby enhancing the relevance and applicability of the findings. The study constructs monthly, recursive, real-time, and out-of-sample forecasts following Baumeister and Kilian (2012). To generate real-time forecasts of real prices, the vintages of the seasonally adjusted U.S. Consumer Price Index (CPI) are obtained from the real-time database maintained by the Philadelphia Federal Reserve. The data begins in January 1973, and the historical average of the CPI is used to estimate expected inflation for constructing real prices. The analysis employs both non-parametric and parametric techniques and compares their predictive performance. Forecasting performance is evaluated against a

1. Introduction

baseline random walk model using the Mean Squared Forecast Error (MSFE) ratio and directional accuracy metrics.

In **Chapter 3**, the methodology involves developing a Structural Vector Autoregression (SVAR) model to analyze the U.S. natural gas market. This model builds on and extends the SVAR framework originally developed by Baumeister and Hamilton (2019) for the global oil market. This extension ensures that the total available supply is accurately allocated among domestic consumption, exports, and inventory changes. Additionally, unlike Baumeister and Hamilton (2019)’s model, this chapter does not include measurement error in inventory data, given the high accuracy of U.S. underground natural gas storage reports. The SVAR model includes five equations that describe the behavior of natural gas supply, economic activity, domestic consumption demand, and inventory and export demand. Accordingly, the model allows for specific structural shocks, such as supply shocks due to geopolitical events, economic activity shocks linked to broader economic cycles, and speculative demand shocks affecting inventory levels.

The SVAR model is estimated using the Bayesian approach introduced by Baumeister and Hamilton (2015), which allows for the incorporation of prior information about the structural parameters. Priors are set based on empirical estimates from the literature, reflecting the generally low elasticity of natural gas supply and demand in the short run. For example, the short-run supply elasticity is assumed to be low, consistent with infrastructure and production constraints, while demand elasticities are informed by studies showing limited responsiveness to price changes. To account for potential uncertainty in these estimates, the model applies truncated Student- t distributions for most priors, allowing for flexibility in the presence of extreme values.

In **Chapter 4**, the methodology assesses the integration of regional natural gas markets—specifically North America, Europe, and Asia—using cointegration techniques. First, we evaluate the stationarity of each price series with the Augmented Dickey-Fuller (ADF), Phillips-Perron (PP), and Kwiatkowski-Phillips-Schmidt-Shin (KPSS) tests to confirm that they exhibit unit roots, a prerequisite for cointegration analysis. Next, we employ both the traditional two-step cointegration model by Engle and Granger (1987) and an extension by Enders and Siklos (2001), which accounts for potential asymmetry in the adjustment process through the Momentum Threshold Autoregressive (M-TAR) model. In the Engle-Granger framework, we estimate the long-run equilibrium relationship between pairs of gas prices (e.g., TTF and EAX) and then test for symmetric adjustment. In the M-TAR model, we incorporate asymmetric adjustments by allowing for differing speeds of reversion depending on whether deviations are above or below a threshold. The threshold is estimated endogenously following Chan (1993).

In **Chapter 5**, the methodology utilizes the R^2 decomposed connectedness approach to assess spillover effects and interdependencies among European gas markets. This method is based on the framework developed by Balli et al. (2023).

It captures both immediate and lagged interactions among variables, allowing for a comprehensive breakdown of spillovers into contemporaneous and lagged components. The analysis also estimates four connectedness metrics: the Total Connectedness Index (TCI), which measures the overall degree of interconnect- edness across all markets; the “TO” connectedness, which quantifies how much a specific market contributes to the variability in other markets; the “FROM” connectedness, which measures the extent to which each market’s variability is explained by shocks from other markets; and the “NET” connectedness, defined as the difference between TO and FROM values, indicating whether a market is a net transmitter or receiver of shocks. These measures provide insights into the dynamic relationships and influence patterns within the European gas market, especially under varying market conditions.

Beyond this discussion, the respective chapters provide comprehensive descrip- tions of the methodological approaches.

2. Can Futures Prices Predict the Real Price of Primary Commodities?

2.1. Introduction

Primary commodities play an indispensable role in the production of a wide array of goods and services, shaping global trade, influencing aggregate price levels, and affecting broader economic outcomes (Duarte et al., 2021; Gelos & Ustyugova, 2017). These commodities are also central to global decarbonization efforts. For example, the anticipated rise in demand for metals—crucial for electrification and battery production—underscores their significance in transitioning to a low-carbon energy system (Bazilian et al., 2023). Similarly, bio-based feedstocks offer a promising pathway to decarbonize liquid fuel markets, potentially competing with fossil-based alternatives (Zabed et al., 2017). Economic decisions today are heavily influenced by expectations of future commodity prices, particularly real average price levels, which reflect broader macroeconomic conditions and long-term flows of costs and revenues. Given their importance in economic planning and forecasting, there is an increasing demand for reliable methods to predict these averages.

One approach to forecasting primary commodity prices is to use futures contract prices¹ as forecasts of future spot prices. This method offers practical advantages, as data from futures markets are widely available and based on real-time decisions of market participants. These strengths have led to its adoption by leading international organizations and central banks, including the International Monetary Fund (IMF) and the European Central Bank (ECB) for forecasting purposes (ECB, 2024; IMF, 2024). However, despite the convenience of using futures forecasts, empirical evidence on their effectiveness in predicting commodity price levels remains mixed (see, for example, Alquist & Kilian, 2010; Chernenko et al., 2004; Chinn & Coibion, 2014; Ellwanger & Snudden, 2023b; Kumar, 1992). Thus, the motivating question for this research is: *Are futures markets useful real-time predictors of the real average spot price of primary commodities?*

To reconcile the mixed evidence, this study reviews the methods used in prior studies, as detailed in Section 2.2. We identify three key areas where improvements can be made to the methods used for forecasting average commodity prices over a given period.

¹A futures contract is a standardized agreement between two parties to buy or sell a specific quantity of a commodity at a specified future date for a predetermined price (Hull & Basu, 2016).

2. Can Futures Prices Predict the Real Price of Primary Commodities?

First, prior analyses of period-average forecasts often constructed them by averaging futures prices over a certain period (typically daily values over a month). This method is expected to reduce forecast accuracy, especially at shorter horizons, due to the loss of information from temporal aggregation (Amemiya & Wu, 1972; Ogbonna et al., 2024; Tiao, 1972; Zellner & Montmarquette, 1971). This loss in accuracy is also intuitive because averaging older futures market expectations tends to dilute the value of futures prices by incorporating outdated information. An example of this issue is evident in the behavior of West Texas Intermediate (WTI) crude oil front-month futures prices in April 2020, at the onset of the COVID-19 pandemic. Prices fell sharply from \$28.34 on April 3rd to -\$37.63 on April 20th, before recovering to \$15.06 by the last trading day of the month. Using the monthly average price for April in a forecast would incorporate outdated market expectations.

It remains an open empirical question whether using the most recent trading information, instead of averages, improves forecast accuracy across commodity markets (Conlon et al., 2022). This study evaluates the impact of three approaches to using futures prices: averaging over the month, averaging the last week of the month, and using end-of-month prices to assess how each method affects the accuracy and precision of futures-based forecasts.

Secondly, the review shows that prior studies examining futures-based period-average forecasts of primary commodities have evaluated forecast gains against the period-average no-change forecast, which assumes that the period-average level of commodity prices in each future period will equal the current period-average level. However, such gains are theoretically expected *by construction*, as models for forecasting period-average levels are expected to outperform the period-average no-change benchmark if daily commodity prices follow a random walk (Marcellino, 1999; Weiss, 1984). In contrast, this study follows recent advances by aiming to forecast the period average while comparing against the end-of-period no-change forecast (Ellwanger & Snudden, 2023a). This approach is equivalent to the random walk forecast commonly used in studies of point-sampled futures-based forecasts (e.g., Chinn & Coibion, 2014; Kumar, 1992; Kwas & Rubaszek, 2021). This allows us to quantify differences in forecast accuracy between the two naive benchmarks for all commodities and, for the first time, to test futures-based forecasts of period averages against the traditional random walk.

Lastly, prior studies examining real-time forecasts of period-average commodity prices in levels have been limited to crude oil and retail gasoline. This study broadens that scope by evaluating the usefulness of real-time predictions of the monthly average real primary commodity prices for 17 commodities across the energy, metals, and agriculture markets, including a novel analysis of ethanol using recently available futures data. This diverse selection introduces distinct trading characteristics and challenges, such as variable delivery schedules and varied front-

month contract settlement procedures across these commodities.² To address these complexities, we propose techniques that ensure our forecasts account for the varying structures and trading practices of each market. Furthermore, our real-time forecasts of period averages build on prior studies of nominal point-sampled forecasts (Chinn & Coibion, 2014; Reeve & Vigfusson, 2011; Reichsfeld & Roache, 2011), providing an updated assessment of the performance of futures-based forecasts over the last decade.

The results can be summarized as follows. First, we find that futures-based forecasts often outperform the traditional random walk no-change forecast for most primary commodities. The most effective approaches leverage the latest expectations from futures markets rather than averaging prices from multiple trading days. For example, short-horizon mean-squared forecast errors are reduced for most commodities when using end-of-month closing values, compared to the common practice of averaging futures prices. Similarly, simple non-parametric forecasts consistently outperform more complex parametric approaches. Using the proposed techniques, several commodities show predictability at short horizons and most show predictability at horizons of six months and beyond.

Second, the analysis reveals that futures markets exhibit different forecast accuracies across commodities. Energy commodities' futures-based forecasts consistently outperform no-change forecasts across most horizons. Performance for base metal commodities is more varied, particularly at shorter horizons, with only copper, lead, and zinc showing some consistency in accuracy. Beyond the short-term, the largest gains are observed for copper and nickel. Moreover, little evidence of predictability was found for real gold prices, though the nominal price of gold shows predictability starting around the one-year-ahead horizon, especially in terms of directional accuracy. Finally, agricultural commodities, particularly corn and soybeans, demonstrate predictive improvements across most horizons.

Lastly, the findings reveal two key trends in the performance of futures-based forecasts over time. First, forecast accuracy improved around 2010 and has generally remained stable for most commodities since then. This improvement coincides with the financialization of commodity markets, which enhanced market liquidity and price discovery. Second, during the past two years of our evaluation period have we observed reduced performance for wheat and natural gas, particularly at longer horizons.

The main conclusion is that futures-based forecasts can effectively predict period-average commodity spot prices across various commodities and forecast horizons by using the latest available futures market data. This simple, non-parametric approach is also practical, as it is cost-effective and quick to implement in real time. The findings provide valuable guidance for researchers, policymakers,

²For further details on delivery schedules, settlement dates, and contract alignment, see the Data Sources section (Section 2.4.1) for a discussion of specific futures contract characteristics and their alignment with forecast horizons.

2. Can Futures Prices Predict the Real Price of Primary Commodities?

and companies on how to best utilize futures market information to construct accurate forecasts.

The remainder of the paper is structured as follows. Section 2.2 reviews the relevant literature on using futures prices to predict commodity spot prices. Section 2.3 explores the real-time forecast methodology and the choice of no-change benchmark. Section 2.4 discusses the data used and describes the idiosyncrasies in trading rules for each commodity. Section 2.5 presents our results, and Section 2.6 concludes.

2.2. Literature Review

Relevant literature is categorized into two broad groups: forecasts of period-average spot prices and point-sampled spot prices. Assumptions related to temporal aggregation are discussed, as they are particularly relevant to this analysis. Additionally, the primary commodities studied, forecast horizons, and whether the analyses consider real or nominal spot prices are summarized. Finally, the discussion highlights whether the forecasts were conducted out-of-sample and utilized real-time methods. Real-time out-of-sample forecasts require that both the data and model estimation rely only on information available at the time of the forecast.

2.2.1. Period-Average Forecasts

Table 2.1 summarizes studies that forecast period-average commodity prices, often from a macroeconomic perspective, as these prices are closely linked to inflation and terms of trade. For example, central banks construct period-average real commodity price forecasts for their economic projections (e.g., Bank of Japan, 2024; European Central Bank, 2024).

Most studies in Table 2.1 examine monthly average forecasts, with all analyzing forecasts in levels, and all except four focusing on real forecasts. Earlier studies typically concentrated on one-year horizons, but two-year horizons have become more common since Baumeister and Kilian (2015). Recent works, such as Chu et al. (2022) and Ellwanger and Snudden (2023b), have extended these horizons to five years. Out-of-sample and real-time forecasts are common across all these studies. The literature primarily focuses on crude oil, with exceptions such as Baumeister et al. (2017), which examines gasoline prices, and Bowman and Husain (2006), which analyzes metal and agricultural commodities from 1993 to 2003. The current study aims to expand this field by evaluating the usefulness of futures-based forecasts for 17 primary commodities.

Table 2.1 further indicates that most studies use average futures prices to construct futures-based forecasts. However, this method may reduce forecast accuracy due to information loss from temporal aggregation (Amemiya & Wu,

1972; Tiao, 1972).³ In this context, studies in Table 2.1 that rely on averaging futures prices generally conclude that futures-based forecasts are not useful (e.g., Alquist & Kilian, 2010; Baumeister & Kilian, 2012). In contrast, research that avoids averaging over the month, such as Pagano and Pisani (2009), Funk (2018), and Ellwanger and Snudden (2023b), finds that futures exhibit some degree of predictive power. This study empirically evaluates the impact of three approaches to using futures prices: averaging over the month, averaging the last week of the month, and using end-of-month prices.

Table 2.1.: Summary of Studies Forecasting Period Average Commodity Prices using Futures

Author(s)	Commodities	Frequency	Horizons	Futures Sampling	No-Change Benchmark	Real or Nominal	Level or Returns	Out-of-Sample	Real-time
Bowman and Husain (2006)	Agricultural, Metals	Quarterly	1 – 8	Quarterly average	Average	Nominal	Level	Yes	No
Pagano and Pisani (2009)	Crude Oil	Monthly	2 – 12	3rd week average	Average	Nominal	Level	Yes	Yes
Baumeister and Kilian (2012)	Crude Oil	Monthly	1 – 12	Monthly average	Average	Real	Level	Yes	Yes
Alquist et al. (2013)	Crude Oil	Monthly	1 – 12	Monthly average	Average	Real	Level	Yes	Yes
Baumeister and Kilian (2014)	Crude Oil	Quarterly	1 – 4	Quarterly average	Average	Real	Level	Yes	Yes
Manescu and Van Robays (2016)	Crude Oil	Quarterly	1 – 11	Monthly average	Average	Real	Level	Yes	Yes
Baumeister et al. (2015)	Crude Oil	Monthly, Quarterly	1 – 24	Monthly average	Average	Real	Level	Yes	Yes
Baumeister and Kilian (2015)	Crude Oil	Monthly	1 – 24	Monthly average	Average	Real	Level	Yes	Yes
	Crude Oil	Quarterly	1 – 8	Quarterly average	Average	Real	Level	Yes	Yes
Drachal (2016)	Crude Oil	Monthly	1	Monthly average	Average	Nominal	Level	Yes	Yes
Wang et al. (2017)	Crude Oil	Monthly	1 – 24	Monthly average	Average	Real	Level	Yes	Yes
Baumeister et al. (2017)	Gasoline	Monthly	1 – 24	Monthly average	Average	Real	Level	Yes	Yes
	Gasoline	Quarterly	1 – 8	Quarterly average	Average	Real	Level	Yes	Yes
Funk (2018)	Crude Oil	Monthly	1 – 24	Last 5 days average	Average	Real	Level	Yes	Yes
Chu et al. (2022)	Crude Oil	Monthly	1 – 60	Monthly average	Average	Nominal	Level	Yes	Yes
Ellwanger and Snudden (2023b)	Crude Oil	Monthly	1 – 60	EoM, Average	Average	Real	Level	Yes	Yes

Notes: “Commodities” specifies the commodities examined in the respective study. “Frequency” refers to the frequency at which the forecasts were evaluated. “Horizon” corresponds to the unit of time specified by the “Frequency”. “Futures Sampling” describes how the futures prices were sampled for the predictions, with “EoM” referring to End-of-Month. The “Level or returns” column specifies whether the forecast target is the level of the spot price or the return on the spot price. The “Out-of-Sample” and “Real-time” columns indicate whether the study employs such forecast methods.

In addition to the forecast itself, the benchmark used for comparison is also important. Notably, all prior studies in Table 2.1 compare futures forecasts against the period-average no-change benchmark. However, improvements relative to this benchmark are theoretically expected, even if the underlying commodity price follows a random walk (Conlon et al., 2022; Ellwanger & Snudden, 2023a; Weiss, 1984; Working, 1960). For the first time, this study maintains its focus on forecasting the period average, while testing this forecast against the traditional random walk hypothesis, which is commonly used in finance and in the point-sampled literature discussed in the next subsection.

³For a comprehensive discussion on temporal aggregation methods and their applications in time series analysis, see Silvestrini and Veredas (2008).

2. Can Futures Prices Predict the Real Price of Primary Commodities?

2.2.2. Point-Sampled Forecasts

This subsection reviews the studies that have examined futures-based forecasts of point-sampled commodity spot prices (see Table 2.2). Point-sampled prices are commonly used in financial applications because profits accrue between asset purchase and settlement. Additionally, point-sampling is standard practice for calculating returns to avoid spurious predictability (see, e.g., Bork et al., 2022; Conlon et al., 2022; Working, 1960).

Table 2.2.: Summary of Studies Forecasting Point-Sampled Commodity Prices using Futures

Author(s)	Commodities	Frequency	Horizons	Futures Sampling	No-Change Benchmark	Real or Nominal	Level or Returns	Out-of-Sample	Real-time
Fama and French (1987)	Agricultural, Livestock, Metals, Wood	Monthly	2-10	EoM	EoM	Nominal	Returns	No	No
Kumar (1992)	Crude Oil	Monthly	1-9	EoM, Ave.	EoM	Nominal	Level	Yes	Yes
Abosedra and Baghestani (2004)	Energy	Monthly	1-12	EoM	EoM	Nominal	Returns	No	No
Chernenko et al. (2004)	Energy	Monthly	3-12	15th day of Month	EoM	Nominal	Returns	No	No
Chinn et al. (2005)	Energy	Monthly	3-12	EoM	EoM	Nominal	Level	Yes	No
Alquist and Kilian (2010)	Crude Oil	Monthly	1-12	Last 5 days average	EoM	Nominal	Level	Yes	Yes
Reeve and Vigfusson (2011)	Agricultural, Livestock, Energy, Metals	Monthly	3-12	EoM	EoM	Nominal	Returns	Yes	Yes
Reichsfeld and Roache (2011)	Agricultural, Energy, Metals	Weekly	12-104	EoW	EoW	Nominal	Returns	Yes	No
Alquist et al. (2013)	Crude Oil	Monthly	1-12	Last 5 days average	EoM	Nominal	Level	Yes	Yes
Chinn and Coibion (2014)	Agricultural, Energy, Metals	Monthly	3-12	EoM	EoM	Nominal	Returns	Yes	Yes
Jin (2017)	Crude Oil	Weekly	1-24	EoW	EoW	Real	Level	Yes	No
Miao et al. (2017)	Crude Oil	Weekly	1-8	EoW	EoW	Nominal	Level	Yes	Yes
Conlon et al. (2022)	Crude Oil	Monthly	1	EoM	EoM	Real	Return	Yes	No
Kwas and Rubaszek (2021)	Agricultural, Energy, Metals	Monthly	1-12	EoM	EoM	Nominal	Level	Yes	Yes

Notes: See the notes below Table 2.1. “EoW” refers to End-of-Week.

Table 2.2 shows that studies of point-sampled forecasts cover a range of commodities, including non-oil energy commodities, agricultural products, and metals. Most of these studies focus on returns, with all except two examining nominal forecasts. The majority of studies use real-time methods, with out-of-sample forecasts becoming standard in the literature following Chinn et al. (2005).

These studies consistently compare forecasts against the point-sampled no-change benchmark, thereby appropriately testing the null hypothesis of no predictability. Moreover, most of these studies utilize point-sampled futures to construct forecasts. The exceptions are Alquist and Kilian (2010) and Alquist et al. (2013), which use an average of the last five business days of the month. However, Kumar (1992) examines both end-of-period and alternative forms of averaging for crude oil and finds that any averaging reduces the accuracy of out-of-sample point forecasts.

The literature on point forecasts suggests that futures prices frequently outperform no-change forecasts. Predictive ability varies across commodities and forecasting horizons. For example, Chinn et al. (2005), Reeve and Vigfusson (2011), and Chinn and Coibion (2014) show that futures markets are predictive for energy and agricultural commodities across all horizons. However, these studies

observe limited predictive power for precious and base metals. Similar findings are reported by Reichsfeld and Roache (2011) and Abosedra and Baghestani (2004), who also note that the performance of futures prices depends on market conditions and varies over time. Furthermore, Reeve and Vigfusson (2011) note that although futures prices may contain a risk premium, adjusting for this premium in real-time forecasting does not materially improve the performance of futures price predictions.

2.3. Methods

Consistent with the existing literature and standard reporting, the monthly average spot price is calculated as the simple average of daily closing prices observed over the calendar month: $\bar{S}_t = \frac{1}{n_t} \sum_{i=1}^{n_t} S_{t,i}$, where \bar{S}_t is the average spot price in month t , $S_{t,i}$ denotes the daily closing spot price on day i of month t , and n_t is the total number of trading days in month t . The nominal monthly average is deflated by the consumer price index (CPI) to derive the monthly average real price: $\bar{R}_t = \bar{S}_t/p_t$, where p_t is the CPI in month t . We utilize all information available in real time at the end of month t to construct h -month-ahead forecasts of the future level of the monthly average real spot price, $E_{t,n_t}(\bar{R}_{t+h})$, where E_{t,n_t} denotes the expectation based on information up to last day n_t of month t .

2.3.1. Expectations from Futures

How can a forecaster use futures market information to construct forecasts of future monthly average spot prices? Consider a scenario where markets are complete, there is no risk premium, and all market participants have homogeneous and rational expectations, meaning they all have the same unbiased view of the future spot price. Additionally, assume that settlement and delivery occur on the same day. Under these conditions, the price of a futures contract, $F_{t,i}^{h,d}$, reflects the consensus of individual market participants' expectations of the future spot price:

$$F_{t,i}^{h,d} = E_{t,i}(S_{t+h,d}), \quad (2.1)$$

Here, $F_{t,i}^{h,d}$ is the futures price observed at the close of trading on day i of month t , for delivery on day d in month $t+h$, $E_{t,i}$ denotes the expectation operator based on information available up to trading day i in month t , and $S_{t+h,d}$ is the spot price on day d in month $t+h$. Thus, the futures price reflects the market participants' expected price for delivery on day d in month $t+h$.

Consider now three approaches used to sample futures prices for predicting period-average spot prices.

The first approach, used by Alquist and Kilian (2010) and Funk (2018), focuses on averaging futures prices over the final 3-5 trading days of the month. Alquist and Kilian (2010) applies this method to predict end-of-month spot prices, while

2. Can Futures Prices Predict the Real Price of Primary Commodities?

Funk (2018) uses it to forecast monthly average real spot prices. The averaging is performed as follows:

$$\tilde{F}_t^{h,d} = \frac{1}{k} \sum_{i=n_t-k+1}^{n_t} F_{t,i}^{h,d} = \frac{1}{k} \sum_{i=n_t-k+1}^{n_t} E_{t,i}(S_{t+h,d}) \quad (2.2)$$

where $\tilde{F}_t^{h,d}$ is the average futures price over the final k trading days of month t . The summation from $i = n_t - k + 1$ to n_t selects the last k days of the month. By averaging over these days, the aim is to capture recent market expectations, but including even a few older observations may dilute the most current information.

The second approach, common in forecasting applications of monthly average prices (see, e.g., Alquist et al., 2013; Baumeister & Kilian, 2012), uses the monthly average of the futures price:

$$\bar{F}_t = \frac{1}{n_t} \sum_{i=1}^{n_t} F_{t,i}^{h_i,d_i} \quad (2.3)$$

where \bar{F}_t is the average futures price over all trading days in month t , $F_{t,i}^{h_i,d_i}$ is the futures price observed on trading day i of month t , for delivery on day d_i in month $t + h_i$, and h_i and d_i may vary during the month due to contract rollovers. Suppose that during month t , the futures contract rolls over from delivery in month $t + h$ to delivery in month $t + h + 1$ on trading day k . Then, for trading days $i = 1$ to k : $F_{t,i}^{h,d} = E_{t,i}(S_{t+h,d})$, whereas for trading days $i = k + 1$ to n_t : $F_{t,i}^{h+1,d'} = E_{t,i}(S_{t+h+1,d'})$. Accordingly, the monthly average futures price becomes:

$$\bar{F}_t = \frac{1}{n_t} \left(\sum_{i=1}^k E_{t,i}(S_{t+h,d}) + \sum_{i=k+1}^{n_t} E_{t,i}(S_{t+h+1,d'}) \right) \quad (2.4)$$

This means that the average includes expectations for delivery in both month $t + h$ and month $t + h + 1$. As a result, \bar{F}_t mixes expectations for different delivery periods, which may not align with the forecast target of the monthly average spot price in month $t + h$.

The third approach uses only the most recent futures market expectations, specifically the closing price on the last trading day of the month, $F_{t,n_t}^{h,d} = E_{t,n_t}(S_{t+h,d})$. This method is appealing because the end-of-month futures price reflects the most up-to-date market expectations for future spot prices. However, whether this approach yields more accurate forecasts is an empirical question. This study conducts an empirical evaluation of all three approaches across seventeen primary commodities.

Additionally, recall that the objective of this analysis is to forecast the monthly average price of the commodity, $E_{t,n_t}(\bar{S}_{t+h})$. In contrast, the futures contract may refer to an alternative average period or a specific day d , $E_{t,t}(S_{t+h,d})$. If this is the case, there may be forecast gains from reconciling the market's forecast

with the monthly average forecast. That is, the futures market may not directly provide an expectation of the monthly average forecast. For this reason, this study carefully reviews the differences in the delivery and settlement dates for the different commodities. Alternative approaches to reconciling potential discrepancies between market expectations and the forecaster's objective are also quantified.

2.3.2. Futures-Based Forecasts

A common method for constructing a futures-based forecast of a real spot price is to deflate the futures curve as follows:

$$\hat{R}_{t+h,d|t} = F_{t,n_t}^{h,d} / E_{t,n_t}(p_{t+h|t}), \quad \forall h \quad (2.5)$$

where $\hat{R}_{t+h,d|t}$ is the forecast of the real spot price on day d in month $t+h$, based on information up to the last trading day n_t of month t , $F_{t,n_t}^{h,d}$ is the futures price observed on the last trading day n_t of month t , for delivery on day d in month $t+h$, and $E_{t,n_t}(p_{t+h|t})$ represents the expected U.S. consumer price deflator h periods ahead. It is common practice to express this relationship using the log-percentage spread between the futures price and the spot price, as follows (e.g. Alquist & Kilian, 2010):

$$\hat{R}_{t+h,d|t} = R_{t,n_t} \left(1 + \ln F_{t,n_t}^{h,d} - \ln S_{t,n_t} - E_{t,n_t}(\pi_t^h) \right), \quad \forall h \quad (2.6)$$

where $E_{t,n_t}(\pi_t^h)$ is the expected U.S. inflation rate over the next h periods. This is still an h -month-ahead forecast for the delivery period d .

The non-parametric method proposed by Ellwanger and Snudden (2023b) assumes proportionality and uses the futures-market forecast of the spot price during the delivery period, $\hat{R}_{t+h,d|t}$, as the forecast for the monthly average, $\hat{R}_{t+h|t}$. This is particularly appealing for commodities where the delivery period is any day within the month, for example for natural gas, crude oil, and precious metals (see section 2.4.1). Alternatively, the delivery date may refer to a specific day within a month, for example for base metals. In the case of using a daily point forecast as a period average forecast, Ellwanger et al. (2023) theoretically demonstrate that a point forecast within a month converges to the monthly average as data persistence increases and at longer forecast horizons.

In contrast to these non-parametric approaches, parametric methods allow us to relax the assumptions of proportionality and unbiasedness. Specifically, to account for the possibility that the spread may be a biased predictor of future average prices, we relax the assumption of a zero intercept in Equation 2.6 and estimate α accordingly. Similarly, we relax the proportionality restriction to estimate β . Finally, we explore the simultaneous relaxation of both the unbiasedness and

2. Can Futures Prices Predict the Real Price of Primary Commodities?

proportionality restrictions.

$$\hat{\bar{R}}_{t+h|t} = R_{t,n_t} \left(1 + \hat{\alpha} + \hat{\beta} \left(\ln F_{t,n_t}^{h,d} - \ln S_{t,n_t} - E_{t,n_t} \left(\pi_t^h \right) \right) \right), \quad \forall h. \quad (2.7)$$

The parameters $\hat{\alpha}$ and $\hat{\beta}$ are obtained in real time through recursive least-squares regression estimates. Empirical evidence on the differences in forecast performance across these approaches is then explored.

2.3.3. Forecast Evaluation

If commodity prices follow a random walk, the change in spot prices cannot be predicted. Suppose the daily price of a certain commodity follows such a pattern, where $R_{t,i}$, the real price on trading day i of month t , is given by the following equation:

$$R_{t,i} = R_{t,i-1} + \epsilon_{t,i}, \quad \text{for } i = 1, 2, \dots, n_t. \quad (2.8)$$

where n_t is the total number of trading days in month t , $\epsilon_{t,i}$ is a mean-zero independent and identically distributed (*iid*) error term with variance σ_ϵ^2 . The last observed price in month t is R_{t,n_t} , the real price on the last trading day of the month. The *iid* assumption leads to constant forecast error variance, with no patterns or trends to exploit. Over longer horizons, however, the forecast error variance increases linearly with time, as the uncertainty compounds. This means that, while the random walk remains a challenging benchmark in the short run, the inherent unpredictability of prices results in growing forecast uncertainty over time, making it less reliable for longer-term forecasts. Consequently, any potential gains from alternative forecasting models may be more evident in long-run horizons where the random walk's forecast performance deteriorates due to increased uncertainty.

In this analysis, we aim to predict a commodity's monthly average real price h periods ahead. We can express the monthly average of nominal prices deflated by CPI equivalently as the monthly average of daily real prices:

$$\bar{R}_t \equiv \frac{\frac{1}{n_t} \sum_{i=1}^{n_t} S_{t,i}}{p_t} \equiv \frac{1}{n_t} \sum_{i=1}^{n_t} \frac{S_{t,i}}{p_t} \equiv \frac{1}{n_t} \sum_{i=1}^{n_t} R_{t,i}.$$

That is, the monthly average real price is the temporal aggregate of daily real prices. The conditional expectation, $E_t(\bar{R}_{t+h})$, of the average price h periods ahead, given time t information, is:

$$E_{t,n_t}(\bar{R}_{t+h}) = R_{t,n_t} \quad \forall h.$$

If daily prices follow a random walk, only the last daily observation reflects the traditional random walk forecasts for all future values, whether averaged or not. Moreover, Ellwanger and Snudden (2023a) show that when daily prices follow

a random walk, the monthly average no-change forecast, \bar{R}_t , produces strictly larger forecast errors than $R_{t,n}$ in theory.

Moreover, forecast improvements relative to the monthly average no-change forecast are expected for all autoregressive integrated moving average representations of the daily data (Marcellino, 1999; Weiss, 1984), including the special case where the daily real price follows a random walk. Thus, comparisons with the monthly average no-change forecast do not reflect the traditional random walk used in finance and could result in spurious predictability.

We empirically compare the forecasting accuracy of the end-of-month no-change benchmark with the period average no-change for monthly average real prices across seventeen primary commodities. The results, detailed in Table A.2, suggest that the end-of-month no-change serves as a more stringent benchmark, particularly at shorter horizons. It improves upon the period average no-change by up to 48% in the MSFE ratio and by 52% in directional accuracy. Both the magnitude and convergence of forecasts at longer horizons, in terms of directional accuracy and mean-squared precision, reflect patterns expected if the daily data closely follow a random walk.

Thus, all forecasts in this study are tested against the end-of-month no-change benchmark. This provides the first instance of futures-based forecasts of period average commodity prices are evaluated against the traditional random walk hypothesis. We use two forecast evaluation criteria: the Mean Squared Forecast Error (MSFE) ratio and mean directional accuracy, also known as success ratios. The MSFE ratio for the h -step-ahead forecast, $MSFE_h^{ratio}$, is calculated as the quotient of the MSFE of the model-based forecast divided by the MSFE of the no-change benchmark. The formula is as follows:

$$MSFE_h^{ratio} = \frac{\sum_{q=1}^Q (\bar{R}_{q+h} - \hat{R}_{q+h|q})^2}{\sum_{q=1}^Q (\bar{R}_{q+h} - R_{q,n_q})^2}, \quad (2.9)$$

Here, $\hat{R}_{q+h|q}$ represents the model forecast for the h -step-ahead average price \bar{R}_{q+h} , and $R_{q,n}$ is the end-of-month no-change forecast for the evaluation sample $q = 1, 2, \dots, Q$. The null hypothesis, which states that the model-based forecast has equal MSFE to the no-change forecast, is tested following Diebold and Mariano (1995) and constructed using Newey and West (1987) standard errors, with results compared against standard normal critical values. Values of the MSFE ratio below one indicate improvements over the end-of-period no-change forecast.

Directional accuracy is evaluated using mean directional accuracy. This metric measures the fraction of times the end-of-month no-change forecast correctly predicts the direction of change in the monthly average real price of a commodity. When the underlying level follows a random walk (which, by nature, is unpredictable), the expected SR for any forecast model is 0.5. In simple terms, this means that no forecast model can outperform a random guess, or a coin flip. Such

2. Can Futures Prices Predict the Real Price of Primary Commodities?

models are considered to exhibit 'no directional accuracy. The calculation is as follows:

$$SR_h = \frac{1}{Q} \sum_{q=1}^Q \mathbb{1} \left\{ \text{sgn}(\bar{R}_{q+h} - R_{q,n_q}) = \text{sgn}(\hat{R}_{q+h|q} - R_{q,n_q}) \right\} \quad (2.10)$$

where sgn is a sign function and $\mathbb{1}$ is an indicator function. The test statistic is calculated following Pesaran and Timmermann (2009). The null hypothesis states that the futures-based forecast has a 50 percent success rate in predicting the direction of change in the real price of the respective commodity. Therefore, a success ratio above 0.5 indicates an improvement over a random change in direction.

2.4. Data

This study examines 17 commodity spot prices across four major categories: energy (West Texas Intermediate (WTI) crude oil, Henry Hub natural gas, heating oil, RBOB gasoline, and ethanol), precious metals (gold, silver, and platinum), base metals (copper, aluminum, nickel, tin, lead, and zinc), and agricultural commodities (wheat, corn, and soybeans).

To construct real-time forecasts of these commodities' real prices, we use vintages of the seasonally adjusted U.S. Consumer Price Index (CPI) from the real-time database maintained by the Philadelphia Federal Reserve. The data begin in January 1973, and the historical average of the CPI is used to generate the expected rate of inflation, which is then applied to calculate the real prices.

2.4.1. Data Sources

The daily closing prices for commodity futures and spot data, which reflect real-time prices, are sourced from Bloomberg, except for the spot prices of crude oil and heating oil, which are obtained from the U.S. Energy Information Administration (EIA). Table 2.3 provides details on the futures data, including Bloomberg tickers, commodity grades, and the initial data availability dates for futures contracts over three specified horizons: 1-month, 12-month, and 24-month. The table also outlines the settlement dates, delivery periods, and active trading months for these contracts, in accordance with the specifications for each commodity's futures contracts.

Table A.1 in the Appendix provides details on the spot price series, including the respective region, Bloomberg ticker, and start date for each series. These spot price series are carefully selected to ensure alignment with the futures contracts in two key aspects. First, the spot data match the futures data in terms of trading exchange and delivery location. For example, Cushing, Oklahoma, serves as the

Table 2.3.: Bloomberg Tickers for Commodity Futures, Sample Periods, and Contract Details

Commodity	Exchange	Grade/Name	Ticker	Sample Start			Maximum		Listed Contracts	Settlement Date	Delivery Period
				1-month	12-month	24-month	Max	Start date			
Energy											
Crude oil	NYMEX	WTI	CL	1990.01	1990.01	1990.11	129	2019.11	Monthly	3BD before 25th of Jan.	First to last BD of Feb.
Natural Gas	NYMEX	Henry Hub	NG	1990.04	1990.06	1995.09	151	2008.02	Monthly	3rd Last BD of Jan.	First to last day of Feb.
Heating Oil	NYMEX	NY Harbor ULSD	HO	1990.01	1990.01	2007.04	44	2012.04	Monthly	Last BD of Dec.	From the 9th to the 30th of Jan.
Gasoline	NYMEX	RBOB	XB	2005.10	2005.10	2007.02	44	2015.11	Monthly	Last BD of Dec.	From the 9th to the 30th of Jan.
Ethanol	CBOT	ASTM D4806, CA	DL	2005.05	2005.08	2007.01	36	2008.02	Monthly	3rd BD of Jan.	From 1st BD of Jan. to 2nd BD post-settlement.
Precious Metals											
Gold	COMEX	Min of 995 fineness	GC	1990.01	1990.01	1990.01	72	1990.12	2,4,6,8,10,12	3rd Last BD of Feb.	First to last BD of Feb
Silver	COMEX	Min of 999 fineness	SI	1990.01	1990.01	1990.01	44	1993.07	3,5,7,9,12	3rd Last BD of Mar.	First to last BD of Mar
Platinum	NYMEX	Min of 99.95% pure	PL	1990.01	-	-	12	1990.01	1,4,7,10	3rd Last BD of Jan.	First to last BD of Jan
Base Metals											
Aluminum	LME	High grade primary	LA	1997.07	1997.07	1997.07	123	2008.09	Monthly	Tue before 3rd Wed of Jan	Two BD after settlement
Copper	LME	Grade A	LP	1997.06	1997.07	1997.07	123	2008.09	Monthly	Tue before 3rd Wed of Jan	Two BD after settlement
Lead	LME	Min of 99.97% purity	LL	1997.07	1997.10	2008.09	63	2008.09	Monthly	Tue before 3rd Wed of Jan	Two BD after settlement
Zinc	LME	Min of 99.97% purity	LX	1997.07	1997.07	1997.07	63	2008.09	Monthly	Tue before 3rd Wed of Jan	Two BD after settlement
Nickel	LME	Min of 99.80% purity	LN	1997.07	1997.07	1997.07	63	2008.09	Monthly	Tue before 3rd Wed of Jan	Two BD after settlement
Tin	LME	Min of 99.85% purity	LT	1997.07	1997.10	-	16	1998.01	Monthly	Tue before 3rd Wed of Jan	Two BD after settlement
Agricultural											
Corn	CBOT	No. 2 Yellow	C	1990.01	1990.01	1993.03	39	2006.09	3,5,7,9,12	BD Before 15th of Mar.	From Mar. 1st BD to 2nd BD post-settlement
Soybeans	CBOT	No. 2 Yellow	S	1990.01	1990.01	1993.01	40	2009.11	1,3,5,7,8,9,11	BD Before 15th of Jan	From Jan. 1st BD to 2nd BD post-settlement
Wheat	CBOT	No. 2 Soft Red Winter	W	1990.01	1990.01	1992.09	30	2000.09	3,5,7,9,12	BD Before 15th of Mar.	From Mar. 1st BD to 2nd BD post-settlement

Note: *Exchange* is the marketplace where each commodity's contract is listed. *Grade/Name* specifies the quality or type of the commodity being traded. *Ticker* is the Bloomberg ticker used for downloading the data. *Sample Start* indicates the starting month and year from which the data was used in the analysis. *Maximum horizon* represents the longest period, in months, over which the contract is available for trading. *Listed Contracts* refer to the specific months for which futures contracts are available for trading and delivery. The numbers represent the months the contracts are listed, with 1 = January, 2 = February, ..., and 12 = December. *Settlement Date* is the date by which the contract must be settled or expire. *Delivery Period* is the time frame within which the physical delivery of the commodity is expected to occur. For further details, refer to the individual contract specifications from the corresponding exchange. The last two columns assume that the forecaster uses the front contract on the last business day (BD) of December, with examples provided for heating oil and gasoline for the last business day of December 2024.

2. Can Futures Prices Predict the Real Price of Primary Commodities?

designated delivery location for crude oil, while Chicago is the delivery region for agricultural commodities, consistent with futures contracts that specify no price differentials at these locations. Second, this consistency extends to the grade of the commodity traded, which is particularly relevant for agricultural commodities. For instance, both the spot and futures prices for wheat are for No. 2 Soft Red Winter. However, for soybeans, where futures are for No. 2 yellow soybeans with a 6-cent premium for No. 1, the spot price is adjusted by subtracting 6 cents, as the spot price is only available for No. 1 yellow soybeans.

2.4.2. Alignment of Futures Contracts with Forecast Horizons

Table 2.3 shows that futures contracts are listed for delivery every month for energy and base metals (see the column “Listed Contracts”). In contrast, for precious metals and agricultural commodities, contracts are only listed for specific delivery months. For example, wheat futures contracts are available for delivery in March, May, July, September, and December. To ensure a forecast can be constructed for every month of the forecast evaluation sample, we follow Chinn and Coibion (2014) and interpolate missing monthly values in the futures curve using the observed contracts. Specifically, the delivery dates of each contract are aligned with the closest corresponding monthly horizon. A linear interpolation is then applied to the missing data along the futures curve. We find that alternative interpolation methods have almost no effect on forecast performance beyond the one-month-ahead forecasts.

Aligning the contracts with the forecast horizons is more crucial than interpolating missing contracts along the futures curve. The “Settlement Date” and “Delivery Period” columns in Table 2.3 show that, for base and precious metals, trading of a futures contract observed on the last day of the month concludes in the third week of the contract month, with delivery occurring just two business days after settlement.⁴ Thus, the delivery period of the front-month contract reflects the market’s expectations for one month ahead. A similar situation occurs with precious metals, where the settlement and delivery dates overlap within the same month. However, aligning the contracts with the forecast horizon requires more careful consideration for other commodities.

Consider the crude oil futures market. According to the contract specifications, the front contract observed at the end of each month is settled in the following month, three business days before the 25th, and corresponds to delivery two months ahead. Figure 2.1ii illustrates this visually: the front contract on December 31 is settled on January 22 (indicated by the blue arrow) and corresponds to delivery in February (indicated by the gray arrow). Following Ellwanger and Snudden (2023b), we align the front contract with the two-month-ahead horizon and impute

⁴For example, if one is trading the front-month futures contract for aluminum on December 31st, the settlement date is scheduled for the Tuesday preceding the third Wednesday of January, with the delivery period encompassing the two business days following settlement.

the one-step-ahead forecast using the curvature of the futures curve for up to 12 contracts.

The contract specification for natural gas is similar to that of crude oil, in that trading of the front-month contract terminates on the third-to-last business day of the month before the contract month, with delivery occurring during the following month. In this case, we also consider constructing one-month-ahead forecasts by averaging the spot price and the front-month contract (two-month forecast). As reported in Appendix Table A.3, this method performs similarly to using the average curvature, and both methods substantially outperform alternative assumptions for the one-month-ahead forecast.

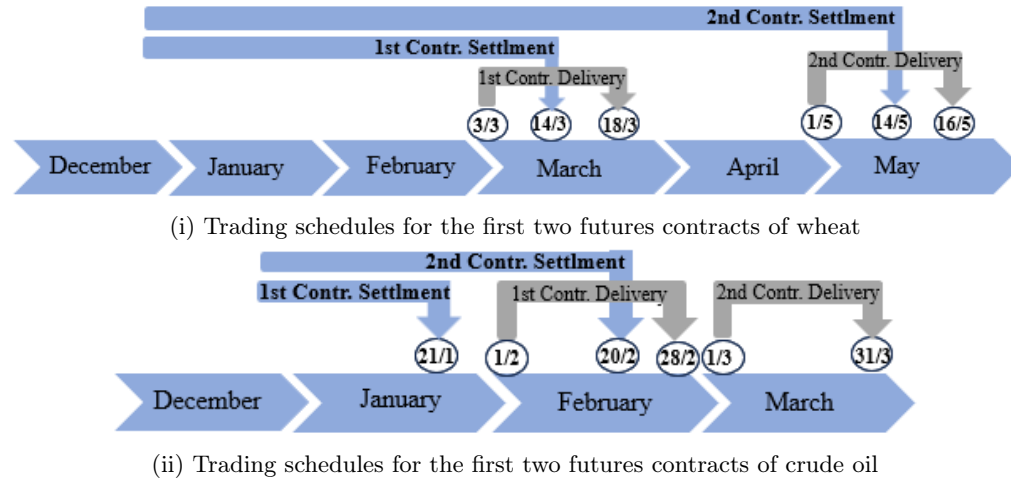


Figure 2.1.: Settlement and Delivery for Wheat and Crude oil on December 31

Note: Settlement and delivery procedures for the two contracts of wheat and crude oil for a trade conducted on December 31, 2024. “Contr.” refers to “Contract”. Settlement dates indicate the official end of the trading contract, while the delivery period specifies when the physical commodity is scheduled to be delivered. Circled numbers represent specific settlement and delivery dates (formatted as dd/mm).

The front-month contract for other energy commodities, such as heating oil, settles at the end of the month, with delivery occurring at the beginning of the next month. This means that such contracts may experience reduced liquidity as they approach expiration and move toward physical delivery. Moreover, the beginning-of-month delivery suggests that an accurate prediction of the monthly average can be constructed using a weighted average of the forecasts from the first and second contracts (see, for example, Ellwanger et al., 2023). To investigate this, we construct a one-month-ahead forecast using the average of the first and second contracts and compare this to the alternative approach of averaging the current spot price with the second contract. We find that such assumptions reduce the one-month-ahead mean-squared error by as much as 46 percent. For these commodities, the average of the spot and the second-month contract is used as the forecast for the month ahead.

2. Can Futures Prices Predict the Real Price of Primary Commodities?

For agricultural commodities, delivery also takes place at the beginning of the month. For example, the front contracts for wheat observed on December 31 are scheduled for delivery between the 1st and 18th of March (see Figure 2.1i). Therefore, we consider that averaging the current month's and the preceding month's futures prices provides a better representation of the current monthly average spot price. We find that this calculation yields consistent, albeit small, improvements in forecast performance one month ahead, and we use this method as the baseline for forecasting agricultural commodities.

Note that these time alignment assumptions only affect the results of the one-month-ahead forecast. For a detailed comparison of all proposed one-month-ahead assumptions for the affected commodities, including outcomes using the front contract without time alignment considerations, see Appendix Table A.3.

2.5. Results

This section is organized as follows: It begins with non-parametric forecasts that use end-of-month futures prices (subsection 2.5.1), followed by an evaluation of the effect of averaging futures prices (subsection 2.5.2). Next, parametric forecasts are introduced, exploring different parameter estimation scenarios (subsection 2.5.3). In subsection 2.5.4, forecasts of nominal average prices are investigated, abstracting from inflation adjustments. Direct forecasts are then explored, using futures contract values directly for forecasting rather than calculating a spread over the spot price (subsection 2.5.5). Finally, robustness checks are conducted in subsection 2.5.6 to assess forecast stability over time and across different sample start dates.

Our baseline forecast evaluation sample begins in 2010, when futures prices for longer horizons became consistently available and regularly observed across all commodities starting in the mid-2000s, as indicated in Table 2.3.

2.5.1. Non-Parametric Forecasts

Results for the non-parametric futures-based forecasts of the monthly average real spot price, following Equation 2.6, are reported in Table 2.4. These baseline results utilize end-of-month futures prices and are compared against the end-of-month no-change forecast. Results are shown for different forecast horizons (1 month, 3 months, 6 months, etc.). The top panel presents the mean squared forecast error (MSFE) ratio. An MSFE ratio of less than 1 indicates that the futures-based forecast outperformed the traditional random walk. P-values, shown in parentheses, test the null hypothesis of equal MSFEs. The bottom panel reports the success ratio, which shows the proportion of times the futures-based forecasts correctly predicted the directional change in the real commodity price level. A success ratio above 0.5 suggests improvement over random chance, with the

p-value for testing the null hypothesis of no directional accuracy provided in brackets.

Table 2.4.: Futures-based Forecasts of Monthly Real Prices, Non-Parametric

	1	3	6	9	12	15	18	21	24
Commodity	MSFE Ratio								
Crude Oil	0.99 (0.313)	0.94 (0.021)	0.88 (0.037)	0.86 (0.066)	0.82 (0.054)	0.77 (0.022)	0.71 (0.012)	0.66 (0.007)	0.61 (0.003)
Natural Gas	1.02 (0.663)	1.01 (0.532)	0.97 (0.387)	1.07 (0.665)	1.07 (0.672)	0.97 (0.395)	0.97 (0.396)	0.97 (0.394)	0.97 (0.419)
Heating Oil	1.04 (0.767)	0.98 (0.340)	0.96 (0.251)	0.91 (0.038)	0.87 (0.005)	0.85 (0.001)	0.82 (0.000)	0.78 (0.000)	0.74 (0.000)
Gasoline	0.81 (0.004)	0.75 (0.002)	0.69 (0.004)	0.81 (0.041)	0.88 (0.078)	0.81 (0.023)	0.74 (0.009)	0.73 (0.008)	0.69 (0.002)
Ethanol	0.72 (0.125)	0.74 (0.120)	0.84 (0.233)	0.83 (0.174)	0.77 (0.118)	0.71 (0.048)	0.68 (0.042)	0.63 (0.041)	0.59 (0.027)
Gold	1.01 (0.607)	1.00 (0.426)	1.00 (0.510)	0.99 (0.404)	0.98 (0.344)	0.97 (0.286)	0.96 (0.225)	0.95 (0.159)	0.93 (0.118)
Silver	1.04 (0.885)	1.00 (0.495)	0.99 (0.288)	0.98 (0.157)	0.97 (0.124)	0.96 (0.076)	0.93 (0.029)	0.89 (0.018)	0.87 (0.016)
Platinum	1.02 (0.860)	0.98 (0.067)	0.93 (0.008)	0.91 (0.010)	0.89 (0.009)	0.88 (0.001)	0.86 (0.000)	0.85 (0.000)	0.85 (0.000)
Aluminum	1.00 (0.527)	1.01 (0.647)	0.98 (0.250)	0.95 (0.118)	0.96 (0.077)	0.96 (0.105)	0.97 (0.157)	0.97 (0.191)	0.96 (0.172)
Copper	0.98 (0.042)	0.98 (0.170)	0.97 (0.118)	0.94 (0.086)	0.93 (0.072)	0.92 (0.061)	0.90 (0.040)	0.88 (0.037)	0.88 (0.057)
Lead	0.97 (0.036)	0.97 (0.008)	0.93 (0.008)	0.87 (0.010)	0.86 (0.010)	0.85 (0.022)	0.84 (0.030)	0.83 (0.013)	0.81 (0.010)
Zinc	0.97 (0.097)	0.95 (0.083)	0.93 (0.081)	0.89 (0.028)	0.90 (0.049)	0.91 (0.089)	0.92 (0.121)	0.92 (0.162)	0.93 (0.233)
Nickel	1.00 (0.633)	1.00 (0.529)	0.97 (0.143)	0.95 (0.106)	0.94 (0.097)	0.89 (0.046)	0.85 (0.022)	0.82 (0.011)	0.80 (0.007)
Tin	1.00 (0.508)	1.03 (0.697)	1.02 (0.623)	1.01 (0.526)	0.98 (0.424)	0.95 (0.226)	0.95 (0.189)	0.98 (0.338)	0.99 (0.442)
Corn	1.03 (0.580)	0.75 (0.054)	0.67 (0.031)	0.70 (0.046)	0.71 (0.051)	0.67 (0.036)	0.63 (0.033)	0.61 (0.028)	0.57 (0.012)
Soybeans	0.86 (0.125)	0.77 (0.039)	0.73 (0.032)	0.78 (0.052)	0.84 (0.148)	0.77 (0.121)	0.72 (0.080)	0.72 (0.070)	0.67 (0.032)
Wheat	1.10 (0.911)	1.06 (0.761)	1.02 (0.565)	0.98 (0.456)	0.96 (0.414)	0.96 (0.386)	0.94 (0.292)	0.93 (0.222)	0.89 (0.166)
	Success Ratio								
Crude Oil	0.55 (0.091)	0.52 (0.208)	0.58 (0.093)	0.62 (0.031)	0.68 (0.002)	0.69 (0.000)	0.66 (0.002)	0.64 (0.005)	0.75 (0.000)
Natural Gas	0.52 (0.321)	0.54 (0.169)	0.61 (0.000)	0.63 (0.004)	0.64 (0.006)	0.66 (0.003)	0.63 (0.017)	0.64 (0.006)	0.62 (0.021)
Heating Oil	0.52 (0.300)	0.56 (0.072)	0.61 (0.019)	0.69 (0.000)	0.77 (0.000)	0.82 (0.000)	0.81 (0.000)	0.83 (0.000)	0.81 (0.000)
Gasoline	0.62 (0.001)	0.62 (0.004)	0.71 (0.000)	0.65 (0.001)	0.62 (0.001)	0.62 (0.001)	0.65 (0.002)	0.69 (0.000)	0.70 (0.000)
Ethanol	0.55 (0.086)	0.59 (0.015)	0.66 (0.000)	0.64 (0.001)	0.64 (0.024)	0.69 (0.000)	0.64 (0.001)	0.68 (0.000)	0.73 (0.000)
Gold	0.47 (0.444)	0.55 (0.114)	0.48 (0.170)	0.54 (0.140)	0.52 (0.616)	0.57 (0.000)	0.55 (0.000)	0.56 (0.000)	0.50 (0.000)
Silver	0.47 (0.753)	0.50 (0.779)	0.59 (0.353)	0.66 (0.069)	0.67 (0.037)	0.66 (0.004)	0.67 (0.000)	0.67 (0.000)	0.63 (0.009)
Platinum	0.49 (0.370)	0.56 (0.238)	0.66 (0.016)	0.64 (0.114)	0.72 (0.011)	0.76 (0.002)	0.79 (0.000)	0.82 (0.000)	0.84 (0.000)
Aluminum	0.47 (0.702)	0.45 (0.862)	0.46 (0.682)	0.47 (0.598)	0.50 (0.466)	0.49 (0.504)	0.53 (0.235)	0.56 (0.061)	0.56 (0.064)
Copper	0.53 (0.024)	0.53 (0.000)	0.60 (1.000)	0.61 (1.000)	0.63 (1.000)	0.63 (1.000)	0.60 (1.000)	0.59 (1.000)	0.59 (1.000)
Lead	0.56 (0.060)	0.61 (0.005)	0.60 (0.057)	0.62 (0.020)	0.58 (0.011)	0.65 (0.009)	0.66 (0.144)	0.65 (0.080)	0.67 (0.061)
Zinc	0.53 (0.519)	0.50 (0.548)	0.52 (0.346)	0.51 (0.344)	0.57 (0.086)	0.61 (0.021)	0.60 (0.020)	0.59 (0.012)	0.58 (0.120)
Nickel	0.50 (1.000)	0.49 (0.790)	0.50 (0.569)	0.50 (1.000)	0.50 (1.000)	0.50 (1.000)	0.49 (1.000)	0.56 (0.000)	0.55 (0.000)
Tin	0.53 (1.000)	0.50 (1.000)	0.48 (1.000)	0.52 (1.000)	0.52 (1.000)	0.54 (1.000)	0.58 (1.000)	0.57 (1.000)	0.54 (1.000)
Corn	0.56 (0.028)	0.63 (0.001)	0.64 (0.004)	0.57 (0.110)	0.51 (0.444)	0.52 (0.355)	0.55 (0.177)	0.56 (0.093)	0.59 (0.024)
Soybeans	0.56 (0.051)	0.53 (0.260)	0.60 (0.021)	0.63 (0.012)	0.58 (0.074)	0.58 (0.150)	0.55 (0.144)	0.58 (0.087)	0.62 (0.004)
Wheat	0.55 (0.088)	0.56 (0.075)	0.58 (0.034)	0.49 (0.840)	0.48 (0.881)	0.49 (0.733)	0.53 (0.441)	0.54 (0.485)	0.55 (0.371)

Notes: This table presents the performance of futures-based forecasts for monthly average spot prices using end-of-month futures prices. The forecasting horizons (in months) are listed in the column headers (e.g., 1, 3, 6, etc.). The “MSFE Ratio” compares the forecast accuracy of futures-based models to a random walk (no-change) forecast, where values below 1 indicate that the futures-based forecast is more accurate. Values in parentheses are p-values from the Diebold and Mariano (1995) test for equal MSFE, which assesses whether the difference in forecast accuracy is statistically significant. The “Success Ratio” represents the percentage of correct directional forecasts, with values above 0.5 indicating that the futures-based forecast correctly predicts the direction of price movement more than half the time. Values in parentheses are p-values for the null hypothesis of no directional accuracy relative to the random walk, based on Pesaran and Timmermann (2009).

For energy commodities, the analysis reveals significant predictive capacity for futures-based forecasts, particularly in terms of directional accuracy. Across all forecast horizons examined, directional accuracy exceeds 0.5, highlighting the effectiveness of futures-based forecasts in predicting market trends. The null hypothesis of no directional gains is rejected at the 5 percent significance level by the nine-month forecasting horizon. For the one-month-ahead forecast, directional accuracy is statistically significant at the 1 percent level for gasoline and at the 10 percent level for ethanol and crude oil. Notably, at the two-year horizon, directional accuracy for heating oil reaches 81 percent, while crude oil,

2. *Can Futures Prices Predict the Real Price of Primary Commodities?*

ethanol, and gasoline show substantial forecasting accuracy, at approximately 70 percent. Additionally, improvements in forecasting are observed in terms of MSFE precision for gasoline and crude oil at shorter-term horizons. All energy commodities, except for natural gas, exhibit significant forecast accuracy at longer horizons, with MSFE reductions approaching 40 percent at the 24-month horizon for crude oil and ethanol.

When compared to previous studies, such as Baumeister and Kilian (2012), our analysis using end-of-month futures prices demonstrates stronger predictive performance across most forecast horizons. For example, the MSFE ratios in Baumeister and Kilian (2012) range from 0.997 at the one-month horizon to 0.912 at twelve months, and these values are not statistically significant. In our extended sample, which runs through 2022, we observe consistently lower MSFE ratios, starting at 0.99 at the one-month horizon, improving to 0.82 at twelve months, and further to 0.61 at twenty-four months, all of which are statistically significant beyond the one-month horizon. Additionally, our success ratios surpass those in Baumeister and Kilian (2012), where their highest reported value is 0.569 at the twelve-month horizon, while our corresponding success ratio is 0.68, reaching 0.75 at twenty-four months. When comparing our results to those obtained using forecast combination methods, we observe stronger performance at longer horizons. While Baumeister and Kilian (2015) find that combining forecasts provides statistically significant gains at shorter horizons, our analysis shows more pronounced improvements, particularly over longer periods. Specifically, at the twenty-four-month horizon, Baumeister and Kilian (2015) report an MSFE ratio of 1.029 and a success ratio of 0.561, both of which are outperformed by our corresponding values. Furthermore, when comparing our results to those of Ellwanger and Snudden (2023b), who also use end-of-month futures prices to generate futures-based forecasts but compare forecast gains to a monthly-average no-change benchmark, we observe differences that underscore the importance of the benchmark used for comparison. Ellwanger and Snudden (2023b) report an MSFE ratio of 0.59 at the one-month horizon and a success ratio of 0.72, reflecting significant forecast gains over the average-month benchmark. However, we find that these forecast gains diminish when the comparison is made against the end-of-month no-change benchmark. This highlights how the choice of benchmark can significantly influence forecast performance evaluations. Finally, our findings align with those of Kwas and Rubaszek (2021) in the point forecast literature on crude oil. For other energy commodities, such as gasoline and heating oil—primarily examined within the point forecast literature, as discussed in Subsection 2.2.2—our results are consistent with those of Chinn et al. (2005) and Chinn and Coibion (2014), where futures-based forecasts consistently outperform the no-change alternative.

Precious metals demonstrate limited predictability at short horizons, with no forecast gains observed at the one-month horizon. However, futures-based forecasts for silver and platinum show significant improvements in directional accuracy at longer horizons, starting at six months for silver and three months for platinum. The medium- to long-term forecast accuracy, particularly in terms of

MSFE precision, is statistically significant at the five percent level, beginning at three months for platinum and fifteen months for silver. Gold presents the greatest challenge for prediction, as futures-based forecasts were only marginally—and generally insignificantly—better than the no-change forecast in terms of the MSFE ratio.

For base metals, the results indicate varied forecast performance. In terms of both directional accuracy and mean-squared precision, copper and lead exhibit significant improvements starting at the one-month horizon. At longer horizons, most metals demonstrate gains in directional accuracy. Furthermore, all analyzed metals, except tin, show significant reductions in MSFE by the one-year forecast horizon. Although these improvements are not as pronounced as those observed for energy commodities, a notable mean-squared reduction of up to twenty percent is seen at the two-year horizon. This result is the first in the literature to demonstrate the utility of futures in forecasting the average price of metals. Our results for zinc are consistent with Reeve and Vigfusson (2011), who found that futures prices have predictive power. However, our findings differ from Reeve and Vigfusson (2011) and Chinn and Coibion (2014) for other base metals. While these studies report limited predictive ability for futures prices, our extended sample suggests that futures prices do, in fact, demonstrate predictive power for these metals, especially at medium- and long-term horizons.

For agricultural commodities, enhanced forecast performance is notable in terms of directional accuracy across almost all horizons, with improvements in mean-squared precision becoming evident from the three-month horizon onward. However, wheat shows forecast gains primarily in directional accuracy at shorter horizons and exhibits an eleven percent improvement in mean-squared precision at the two-year mark, though this is not statistically significant. The reductions in the MSFE ratio are particularly substantial at the two-year horizon for soybeans and corn, with ratios of 0.67 and 0.57, respectively. These outcomes suggest that futures-based forecasts are reliable predictors for most agricultural commodities, with the exception of wheat.

Overall, the results indicate that the non-parametric approach to constructing futures forecasts consistently provides predictive power for monthly average spot prices across a diverse array of commodities and time horizons. In particular, futures-based forecasts of monthly average prices generally outperform the traditional random walk forecast for most primary commodities, especially over medium- and long-term horizons.

To better understand these results, two common views on the relationship between futures and spot prices can be considered.

Risk premium and market liquidity The first view posits that the futures price typically reflects the sum of the expected spot price and a risk premium (Fama & French, 1987; Pindyck, 2001). Hamilton and Wu (2014) document that the oil futures risk premium has, on average, diminished since 2005, attributing this decline to the growing influence of index-fund investing. This shift transferred

2. Can Futures Prices Predict the Real Price of Primary Commodities?

the role of risk-bearing from commercial hedgers to financial investors, thereby reducing the compensation required for holding long positions. Ellwanger and Snudden (2023b) observe significant improvements in crude oil forecasting performance starting in 2007, coinciding with increases in the volume of futures contracts traded, particularly for longer maturities. These improvements in forecasting performance may be linked to increased market liquidity. Our results suggest that such improvements in forecasting accuracy extend to other commodities as well. For example, Figure A.1 shows the trading volume for first-month futures contracts for the 17 commodities considered in this analysis, alongside the MSFE ratio for the one-month-ahead forecast⁵. The figure illustrates that forecast accuracy improvements, particularly evident from 2010 onwards, correlate with increased trading volumes. This suggests a potential link between market liquidity and predictive accuracy.

Theory of storage The theory of storage explains the relationship between spot and futures prices of commodities through the “cost-of-carry model,” which balances the costs and benefits of holding inventories. According to this theory, the difference between the futures price and the spot price, known as the basis, is determined by the cost of carrying the commodity until the delivery date. This cost includes the interest forgone on funds used to purchase the commodity, the marginal storage cost, and is offset by the marginal convenience yield—the benefit of holding the inventory. The convenience yield reflects the value of having inventories on hand, particularly when supply is scarce, as it allows holders to respond to unexpected demand or price increases. Importantly, the theory predicts a negative relationship between inventories and the convenience yield: as inventories decline, the convenience yield rises because the benefits of holding inventories are greater during periods of scarcity (Brennan, 1976; Fama & French, 1987; Telser, 1958; Working, 1949). High storage costs or low convenience yields can lead to futures prices exceeding spot prices (a situation known as contango), reflecting the market’s anticipation of higher future costs or lower storage benefits. Conversely, high convenience yields, which signal significant benefits from holding inventories, can result in futures prices being lower than spot prices (a condition known as backwardation), indicating the market’s expectation of tight supply or high future demand. This dynamic illustrates how futures prices encapsulate market participants’ collective assessments of future storage conditions, making them effective predictors of future spot prices by reflecting the costs and benefits associated with commodity storage (Pindyck, 2001). This perspective may also explain the heterogeneity observed in our analysis regarding the forecasting power of futures prices across different commodity categories. In line with this, Symeonidis et al. (2012) identify a strong correlation between storage-related factors and the adjusted basis for energy and agricultural commodities, attributing this relationship to factors like high storage and transportation costs. In contrast, metals, particularly precious metals, exhibit a lower correlation with storage-

⁵See Subsection 2.5.6 for more details on these time-varying MSFE ratios.

related factors, likely due to their low storage costs relative to their value and high inventory levels compared to demand.

2.5.2. Effects of Averaging Futures

We next investigate whether averaging futures prices over the month affects forecast performance, a technique utilized in several prior studies (see, e.g., Alquist et al., 2013; Baumeister & Kilian, 2012; Chu et al., 2022; Drachal, 2016). The results are shown in Table 2.5, with bolded values indicating whether the MSFE ratio and success ratio improve upon the baseline results in Table 2.4.

Table 2.5.: Futures-based Forecasts of Monthly Real Prices, Non-Parametric, Monthly Average Futures

Commodity	1	3	6	9	12	15	18	21	24
	MSFE Ratio								
Crude Oil	1.82 (1.000)	1.00 (0.514)	0.89 (0.040)	0.87 (0.102)	0.83 (0.074)	0.77 (0.028)	0.71 (0.013)	0.66 (0.007)	0.61 (0.003)
Natural Gas	1.56 (0.999)	1.03 (0.653)	1.06 (0.708)	1.13 (0.763)	1.11 (0.742)	1.01 (0.541)	1.01 (0.539)	0.99 (0.467)	0.99 (0.463)
Heating Oil	1.74 (0.999)	1.08 (0.860)	1.00 (0.477)	0.94 (0.133)	0.88 (0.015)	0.86 (0.005)	0.83 (0.001)	0.79 (0.001)	0.74 (0.000)
Gasoline	1.33 (0.967)	0.81 (0.012)	0.70 (0.004)	0.82 (0.053)	0.89 (0.101)	0.82 (0.033)	0.75 (0.012)	0.73 (0.008)	0.69 (0.002)
Ethanol	1.32 (0.772)	0.75 (0.123)	0.83 (0.227)	0.81 (0.154)	0.75 (0.109)	0.69 (0.049)	0.66 (0.042)	0.61 (0.037)	0.57 (0.025)
Gold	1.24 (0.992)	1.05 (0.884)	1.06 (0.893)	1.01 (0.552)	1.01 (0.553)	0.99 (0.432)	0.98 (0.378)	0.97 (0.270)	0.93 (0.134)
Silver	0.96 (0.445)	1.03 (0.649)	1.00 (0.507)	0.98 (0.371)	0.96 (0.258)	0.93 (0.116)	0.92 (0.066)	0.89 (0.041)	0.88 (0.049)
Platinum	1.42 (0.998)	1.04 (0.799)	0.95 (0.160)	0.92 (0.043)	0.90 (0.027)	0.87 (0.002)	0.88 (0.001)	0.88 (0.000)	0.88 (0.000)
Aluminum	1.72 (0.995)	1.08 (0.897)	1.01 (0.534)	0.95 (0.215)	0.96 (0.127)	0.93 (0.048)	0.94 (0.079)	0.95 (0.119)	0.93 (0.114)
Copper	1.56 (1.000)	1.08 (0.865)	1.01 (0.566)	0.97 (0.316)	0.95 (0.202)	0.91 (0.068)	0.89 (0.048)	0.88 (0.048)	0.87 (0.056)
Lead	1.42 (0.995)	0.98 (0.378)	0.96 (0.238)	0.88 (0.040)	0.85 (0.024)	0.82 (0.015)	0.81 (0.018)	0.82 (0.016)	0.79 (0.007)
Zinc	1.74 (0.999)	1.05 (0.795)	0.96 (0.294)	0.89 (0.069)	0.90 (0.105)	0.91 (0.129)	0.93 (0.182)	0.94 (0.251)	0.94 (0.255)
Nickel	1.51 (0.998)	1.09 (0.913)	1.00 (0.448)	0.97 (0.338)	0.96 (0.299)	0.88 (0.068)	0.84 (0.040)	0.81 (0.019)	0.79 (0.011)
Tin	1.82 (0.999)	1.20 (0.989)	1.06 (0.764)	1.02 (0.559)	1.00 (0.483)	0.94 (0.227)	0.93 (0.170)	0.96 (0.227)	0.97 (0.223)
Corn	1.16 (0.763)	0.86 (0.111)	0.73 (0.035)	0.73 (0.052)	0.75 (0.063)	0.68 (0.036)	0.64 (0.033)	0.62 (0.028)	0.58 (0.014)
Soybeans	1.48 (0.997)	0.84 (0.081)	0.76 (0.043)	0.79 (0.055)	0.83 (0.144)	0.77 (0.119)	0.73 (0.088)	0.73 (0.078)	0.68 (0.035)
Wheat	1.71 (0.980)	1.14 (0.842)	1.08 (0.710)	0.98 (0.457)	0.94 (0.361)	0.92 (0.297)	0.93 (0.258)	0.93 (0.229)	0.88 (0.174)
	Success Ratio								
Crude Oil	0.46 (0.821)	0.50 (0.408)	0.58 (0.029)	0.60 (0.021)	0.63 (0.002)	0.68 (0.000)	0.62 (0.009)	0.62 (0.008)	0.72 (0.000)
Natural Gas	0.52 (0.308)	0.50 (0.500)	0.58 (0.017)	0.61 (0.010)	0.64 (0.005)	0.64 (0.005)	0.63 (0.011)	0.63 (0.010)	0.62 (0.017)
Heating Oil	0.50 (0.518)	0.55 (0.184)	0.60 (0.015)	0.65 (0.004)	0.75 (0.000)	0.79 (0.000)	0.80 (0.000)	0.79 (0.000)	0.77 (0.000)
Gasoline	0.59 (0.008)	0.65 (0.000)	0.68 (0.000)	0.62 (0.011)	0.64 (0.000)	0.62 (0.002)	0.61 (0.012)	0.68 (0.000)	0.67 (0.000)
Ethanol	0.52 (0.328)	0.59 (0.021)	0.64 (0.000)	0.62 (0.007)	0.64 (0.020)	0.70 (0.000)	0.65 (0.000)	0.68 (0.000)	0.72 (0.000)
Gold	0.53 (0.233)	0.53 (0.242)	0.46 (0.765)	0.55 (0.149)	0.55 (0.205)	0.54 (0.294)	0.54 (0.129)	0.56 (0.053)	0.49 (0.134)
Silver	0.54 (0.158)	0.58 (0.032)	0.56 (0.093)	0.56 (0.142)	0.51 (0.680)	0.55 (0.342)	0.57 (0.184)	0.57 (0.148)	0.58 (0.111)
Platinum	0.49 (0.616)	0.56 (0.061)	0.58 (0.081)	0.60 (0.031)	0.63 (0.024)	0.66 (0.001)	0.61 (0.086)	0.63 (0.070)	0.59 (0.479)
Aluminum	0.53 (0.280)	0.52 (0.290)	0.50 (0.479)	0.56 (0.100)	0.55 (0.138)	0.51 (0.343)	0.53 (0.194)	0.57 (0.056)	0.56 (0.050)
Copper	0.62 (0.001)	0.53 (0.240)	0.58 (0.191)	0.57 (0.402)	0.56 (0.801)	0.60 (0.443)	0.59 (0.356)	0.58 (0.383)	0.60 (0.095)
Lead	0.59 (0.010)	0.53 (0.272)	0.58 (0.021)	0.62 (0.002)	0.57 (0.046)	0.62 (0.012)	0.65 (0.026)	0.68 (0.002)	0.66 (0.031)
Zinc	0.52 (0.480)	0.53 (0.268)	0.58 (0.029)	0.60 (0.007)	0.64 (0.000)	0.68 (0.000)	0.68 (0.000)	0.60 (0.004)	0.58 (0.108)
Nickel	0.53 (0.219)	0.46 (0.841)	0.48 (0.659)	0.55 (0.117)	0.55 (0.094)	0.57 (0.037)	0.60 (0.007)	0.59 (0.063)	0.62 (0.005)
Tin	0.47 (0.785)	0.45 (0.905)	0.52 (0.240)	0.52 (0.398)	0.61 (0.000)	0.61 (0.000)	0.61 (0.042)	0.60 (0.040)	0.59 (0.029)
Corn	0.58 (0.008)	0.62 (0.001)	0.66 (0.001)	0.61 (0.017)	0.54 (0.285)	0.54 (0.264)	0.58 (0.076)	0.59 (0.023)	0.58 (0.029)
Soybeans	0.53 (0.234)	0.55 (0.137)	0.63 (0.002)	0.64 (0.005)	0.61 (0.010)	0.57 (0.166)	0.58 (0.037)	0.61 (0.022)	0.63 (0.003)
Wheat	0.58 (0.023)	0.61 (0.007)	0.59 (0.019)	0.55 (0.248)	0.52 (0.527)	0.50 (0.562)	0.53 (0.426)	0.55 (0.334)	0.56 (0.274)

Notes: See the notes below Table 2.4. This table presents the performance of futures-based forecasts for monthly average spot prices using monthly average futures prices. Bold values indicate improvements over the baseline results in Table 2.4.

The results show lower forecast precision, particularly for short-term horizons when averaging futures prices, most notably at the one-month horizon. For example, the MSFE ratio is over 50 percent higher for energy commodities. Only for silver are there MSFE gains at the one-month horizon from averaging, although these gains are statistically insignificant. Consistent with theory, the effects of

2. Can Futures Prices Predict the Real Price of Primary Commodities?

averaging on forecast accuracy are less pronounced at longer horizons. At the one-year horizon and beyond, both methods yield similar predictive effectiveness, although end-of-month futures generally provide slight advantages. This suggests that while averaging futures prices may still offer long-term predictive value, end-of-month futures data is preferable for short-term forecast accuracy.

Differences in directional accuracy, measured by the Success Ratio (SR), do not mirror the magnitude of the decline seen in MSFE across all commodities at short horizons. In fact, averaging slightly improves the SR for a few commodities, notably lead, copper, and wheat. This highlights the differences between the two forecast evaluation criteria, as the success ratio is invariant to the magnitude of the forecast error. That said, end-of-month futures data, rather than averaging, continues to enhance forecast directional accuracy for most commodities and horizons.

To further examine the influence of averaging, we construct the futures curve using the average of the last five trading days of the month, similar to using the last trading week. The results are provided in Appendix Table A.4. The findings again suggest a general decline in forecast accuracy when averaging, compared to forecasts constructed using end-of-month futures prices. This decline is most pronounced for MSFEs at shorter horizons. However, the decrease in forecast accuracy is typically smaller than when averaging the entire month's prices, consistent with the informational loss from temporal aggregation. In cases where directional accuracy improves relative to using end-of-month prices, the differences in forecast accuracy are generally small and inconsistent across commodities or horizons. We again find small gains in directional accuracy for wheat at very short horizons and for gold at the one-month horizon, but these gains come with a decline in MSFE precision.

2.5.3. Parametric Forecasts

The results of the prior two subsections have used non-parametric methods to construct forecasts. Next, we utilize real-time parametric estimates using Equation 2.7 and compare them with the simpler non-parametric results. These forecasts estimate $\hat{\beta}$, thereby relaxing the proportionality assumption, while setting $\hat{\alpha}$ to zero. The results are presented in Table 2.6. Additionally, we explore two other scenarios: one where $\hat{\beta}$ is set to zero and $\hat{\alpha}$ is estimated, and another where both $\hat{\alpha}$ and $\hat{\beta}$ are estimated simultaneously. Neither of the latter two cases produces improvements in forecast precision relative to simply estimating $\hat{\beta}$. For brevity, detailed results for these two forecasts are provided in Appendix Tables A.5 and A.6.

The results indicate that parametric forecasts are both more complex to estimate and generally result in worse performance compared to the non-parametric approach. While there are isolated instances where parametric estimates marginally outperform, these differences are small and inconsistent across forecast horizons. A

notable exception is the directional accuracy for gold, which improves at the 15- to 21-month horizons, although this improvement does not extend to other horizons or to MSFE precision. Forecasts that relax the proportionality assumption for nickel show consistent improvements in MSFE at 18 months and beyond; however, these gains do not persist across other horizons or in terms of directional accuracy. We recommend that forecasters utilize the simpler non-parametric approach, as these results do not suggest that the parametric approach provides consistent gains in forecast accuracy.

Table 2.6.: Futures-based Forecasts of Monthly Real Prices, Parametric

	1	3	6	9	12	15	18	21	24
Commodity	MSFE Ratio								
Crude Oil	1.00 (0.147)	1.00 (0.009)	0.98 (0.014)	0.97 (0.029)	0.95 (0.027)	0.91 (0.010)	0.88 (0.007)	0.85 (0.004)	0.82 (0.002)
Natural Gas	1.00 (0.166)	0.97 (0.036)	0.95 (0.190)	1.00 (0.515)	1.06 (0.684)	1.03 (0.582)	1.07 (0.662)	1.10 (0.710)	1.12 (0.738)
Heating Oil	1.00 (0.184)	0.99 (0.096)	0.99 (0.037)	0.98 (0.009)	0.96 (0.003)	0.94 (0.001)	0.92 (0.000)	0.90 (0.000)	0.86 (0.000)
Gasoline	0.98 (0.004)	0.82 (0.001)	0.75 (0.014)	0.82 (0.047)	0.90 (0.104)	0.87 (0.137)	0.81 (0.140)	0.80 (0.134)	0.71 (0.040)
Ethanol	0.87 (0.036)	0.69 (0.021)	0.98 (0.481)	1.29 (0.754)	0.90 (0.369)	0.69 (0.087)	0.65 (0.055)	0.63 (0.045)	0.81 (0.115)
Gold	1.00 (0.644)	1.00 (0.333)	1.00 (0.124)	1.00 (0.049)	1.00 (0.010)	1.00 (0.001)	1.00 (0.001)	1.00 (0.002)	0.99 (0.007)
Silver	1.00 (0.375)	1.00 (0.178)	1.00 (0.048)	1.00 (0.017)	1.00 (0.022)	1.00 (0.017)	0.99 (0.007)	0.98 (0.006)	0.98 (0.007)
Platinum	1.00 (0.718)	1.00 (0.011)	1.00 (0.001)	1.00 (0.000)	1.00 (0.000)	0.99 (0.000)	0.99 (0.000)	0.99 (0.000)	0.98 (0.000)
Aluminum	1.00 (0.751)	1.00 (0.700)	1.00 (0.238)	1.00 (0.092)	1.00 (0.073)	1.00 (0.166)	1.00 (0.273)	1.00 (0.354)	1.00 (0.361)
Copper	1.00 (0.950)	1.00 (0.048)	1.00 (0.042)	0.99 (0.029)	0.98 (0.019)	0.97 (0.019)	0.96 (0.015)	0.95 (0.019)	0.93 (0.033)
Lead	1.00 (0.995)	1.00 (0.001)	0.99 (0.006)	0.97 (0.008)	0.96 (0.007)	0.94 (0.017)	0.92 (0.024)	0.89 (0.010)	0.86 (0.007)
Zinc	1.00 (0.971)	1.00 (0.043)	0.99 (0.043)	0.98 (0.016)	0.97 (0.029)	0.96 (0.052)	0.95 (0.069)	0.93 (0.099)	0.93 (0.161)
Nickel	1.00 (0.283)	1.00 (0.304)	0.99 (0.094)	0.97 (0.079)	0.93 (0.067)	0.84 (0.037)	0.76 (0.020)	0.71 (0.010)	0.69 (0.007)
Tin	1.00 (0.228)	1.00 (0.577)	1.00 (0.512)	1.00 (0.413)	0.99 (0.302)	0.98 (0.154)	0.97 (0.131)	0.98 (0.208)	0.99 (0.284)
Corn	1.00 (0.090)	0.98 (0.014)	0.95 (0.015)	0.95 (0.027)	0.94 (0.030)	0.90 (0.017)	0.85 (0.011)	0.81 (0.011)	0.77 (0.008)
Soybeans	1.00 (0.022)	0.98 (0.016)	0.95 (0.017)	0.93 (0.011)	0.91 (0.018)	0.87 (0.017)	0.84 (0.012)	0.82 (0.013)	0.78 (0.011)
Wheat	1.00 (0.086)	1.00 (0.210)	0.99 (0.234)	0.99 (0.203)	0.97 (0.138)	0.95 (0.086)	0.94 (0.030)	0.93 (0.018)	0.91 (0.037)
	Success Ratio								
Crude Oil	0.55 (0.091)	0.52 (0.208)	0.58 (0.093)	0.62 (0.031)	0.68 (0.002)	0.69 (0.000)	0.66 (0.002)	0.64 (0.005)	0.75 (0.000)
Natural Gas	0.52 (0.321)	0.54 (0.169)	0.61 (0.000)	0.63 (0.004)	0.64 (0.006)	0.66 (0.003)	0.63 (0.017)	0.64 (0.006)	0.62 (0.021)
Heating Oil	0.52 (0.300)	0.56 (0.072)	0.61 (0.019)	0.69 (0.000)	0.77 (0.000)	0.82 (0.000)	0.81 (0.000)	0.83 (0.000)	0.81 (0.000)
Gasoline	0.62 (0.001)	0.62 (0.004)	0.71 (0.000)	0.65 (0.001)	0.62 (0.001)	0.62 (0.001)	0.65 (0.002)	0.69 (0.000)	0.70 (0.000)
Ethanol	0.54 (0.207)	0.60 (0.024)	0.68 (0.000)	0.65 (0.008)	0.63 (0.129)	0.67 (0.000)	0.62 (0.024)	0.67 (0.002)	0.73 (0.000)
Gold	0.53 (0.556)	0.47 (0.630)	0.52 (0.422)	0.49 (0.570)	0.58 (0.155)	0.70 (0.000)	0.67 (0.000)	0.65 (0.000)	0.50 (0.000)
Silver	0.49 (0.535)	0.50 (0.779)	0.59 (0.353)	0.66 (0.069)	0.67 (0.037)	0.66 (0.004)	0.67 (0.000)	0.67 (0.000)	0.63 (0.009)
Platinum	0.49 (0.370)	0.56 (0.238)	0.66 (0.016)	0.64 (0.114)	0.72 (0.011)	0.76 (0.002)	0.79 (0.000)	0.82 (0.000)	0.84 (0.000)
Aluminum	0.53 (0.351)	0.55 (0.138)	0.46 (0.682)	0.47 (0.598)	0.50 (0.466)	0.49 (0.504)	0.53 (0.235)	0.56 (0.061)	0.56 (0.064)
Copper	0.47 (0.976)	0.53 (0.000)	0.60 (1.000)	0.61 (1.000)	0.63 (1.000)	0.63 (1.000)	0.60 (1.000)	0.59 (1.000)	0.59 (1.000)
Lead	0.44 (0.940)	0.61 (0.005)	0.60 (0.057)	0.62 (0.020)	0.58 (0.011)	0.65 (0.009)	0.66 (0.144)	0.65 (0.080)	0.67 (0.061)
Zinc	0.46 (0.547)	0.51 (0.506)	0.52 (0.346)	0.51 (0.344)	0.57 (0.086)	0.61 (0.021)	0.60 (0.020)	0.59 (0.012)	0.58 (0.120)
Nickel	0.50 (1.000)	0.49 (0.290)	0.50 (0.569)	0.50 (0.500)	0.50 (1.000)	0.50 (1.000)	0.49 (1.000)	0.56 (0.000)	0.55 (0.000)
Tin	0.53 (1.000)	0.50 (1.000)	0.48 (1.000)	0.52 (1.000)	0.52 (1.000)	0.54 (1.000)	0.58 (1.000)	0.57 (1.000)	0.54 (1.000)
Corn	0.55 (0.127)	0.64 (0.000)	0.65 (0.001)	0.58 (0.066)	0.52 (0.404)	0.50 (0.486)	0.55 (0.177)	0.56 (0.093)	0.58 (0.035)
Soybeans	0.55 (0.147)	0.53 (0.251)	0.60 (0.023)	0.63 (0.012)	0.57 (0.091)	0.58 (0.150)	0.56 (0.117)	0.58 (0.087)	0.61 (0.034)
Wheat	0.55 (0.069)	0.57 (0.057)	0.58 (0.033)	0.51 (0.622)	0.50 (0.774)	0.49 (0.659)	0.53 (0.441)	0.53 (0.536)	0.56 (0.269)

Notes: See the notes below Table 2.4. This table presents the performance of futures-based forecasts using the futures-spot spread model, where β is estimated in Equation 2.7 and the constant is set to zero. Bold values indicate improvements over the baseline results in Table 2.4.

2.5.4. Nominal Forecasts

This subsection considers forecasts of nominal monthly average spot prices, as shown in Table 2.7. This exercise isolates the importance of the observed measure of inflation, incorporating both the real-time nowcast and forecast. Monthly average h -step-ahead nominal futures-based spread forecasts are constructed as

2. Can Futures Prices Predict the Real Price of Primary Commodities?

follows:

$$\hat{S}_{t+h,d|t} = S_{t,n_t} \left(1 + \ln(F_{t,n_t}^{h,d}/S_{t,n_t}) \right), \quad (2.11)$$

This is similar to the baseline spread model for real forecasts, Equation 2.6, but uses the nominal spot price, S_{t,n_t} , and abstracts from inflation.

Table 2.7.: Futures-based Forecasts of Monthly Average Nominal Prices, Non-Parametric

	1	3	6	9	12	15	18	21	24
Commodity	MSFE Ratio								
Crude Oil	0.98 (0.232)	0.95 (0.038)	0.91 (0.051)	0.90 (0.092)	0.88 (0.068)	0.84 (0.019)	0.79 (0.006)	0.75 (0.002)	0.71 (0.001)
Natural Gas	1.03 (0.690)	1.04 (0.723)	0.98 (0.437)	1.10 (0.716)	1.09 (0.717)	0.99 (0.447)	0.97 (0.394)	0.97 (0.402)	0.98 (0.431)
Heating Oil	1.04 (0.739)	0.97 (0.302)	0.98 (0.336)	0.93 (0.076)	0.89 (0.014)	0.88 (0.007)	0.86 (0.004)	0.85 (0.003)	0.81 (0.002)
Gasoline	0.82 (0.003)	0.76 (0.003)	0.72 (0.005)	0.85 (0.041)	0.91 (0.084)	0.86 (0.013)	0.79 (0.003)	0.79 (0.002)	0.77 (0.000)
Ethanol	0.78 (0.194)	0.76 (0.121)	0.87 (0.265)	0.84 (0.149)	0.78 (0.100)	0.72 (0.033)	0.71 (0.026)	0.67 (0.022)	0.65 (0.015)
Gold	0.99 (0.240)	0.98 (0.137)	0.98 (0.193)	0.96 (0.060)	0.95 (0.037)	0.94 (0.035)	0.93 (0.031)	0.92 (0.030)	0.91 (0.037)
Silver	1.05 (0.889)	1.01 (0.635)	1.00 (0.577)	1.00 (0.367)	1.00 (0.356)	1.00 (0.370)	0.99 (0.269)	0.99 (0.190)	0.98 (0.124)
Platinum	1.02 (0.922)	1.00 (0.376)	0.99 (0.342)	1.00 (0.552)	1.03 (0.866)	1.09 (0.991)	1.15 (0.999)	1.21 (1.000)	1.26 (1.000)
Aluminum	1.02 (0.854)	1.02 (0.859)	1.01 (0.577)	0.99 (0.360)	0.99 (0.388)	0.99 (0.457)	1.00 (0.511)	1.01 (0.532)	1.01 (0.532)
Copper	0.99 (0.100)	1.00 (0.387)	0.99 (0.132)	0.97 (0.018)	0.97 (0.008)	0.97 (0.012)	0.96 (0.006)	0.96 (0.013)	0.96 (0.027)
Lead	0.98 (0.147)	0.99 (0.273)	0.97 (0.075)	0.92 (0.011)	0.92 (0.009)	0.94 (0.053)	0.96 (0.172)	0.98 (0.295)	0.97 (0.269)
Zinc	0.99 (0.281)	0.96 (0.084)	0.95 (0.051)	0.90 (0.002)	0.90 (0.003)	0.91 (0.005)	0.91 (0.006)	0.92 (0.016)	0.92 (0.052)
Nickel	1.01 (0.851)	1.01 (0.808)	1.00 (0.375)	0.99 (0.101)	0.98 (0.082)	0.96 (0.020)	0.94 (0.008)	0.93 (0.004)	0.92 (0.003)
Tin	1.02 (0.855)	1.05 (0.833)	1.05 (0.772)	1.03 (0.668)	1.01 (0.547)	0.97 (0.253)	0.97 (0.169)	1.00 (0.485)	1.01 (0.661)
Corn	1.01 (0.513)	0.77 (0.046)	0.70 (0.024)	0.74 (0.050)	0.77 (0.068)	0.74 (0.043)	0.71 (0.032)	0.69 (0.020)	0.64 (0.005)
Soybeans	0.84 (0.127)	0.76 (0.025)	0.74 (0.016)	0.80 (0.038)	0.87 (0.169)	0.83 (0.153)	0.78 (0.083)	0.76 (0.043)	0.71 (0.005)
Wheat	1.09 (0.862)	1.07 (0.783)	1.04 (0.601)	0.99 (0.469)	0.99 (0.461)	0.99 (0.482)	1.00 (0.483)	0.99 (0.446)	0.96 (0.338)
	Success Ratio								
Crude Oil	0.56 (0.066)	0.56 (0.203)	0.59 (0.104)	0.62 (0.037)	0.70 (0.002)	0.70 (0.001)	0.73 (0.000)	0.71 (0.000)	0.76 (0.000)
Natural Gas	0.53 (0.265)	0.55 (0.184)	0.59 (0.003)	0.60 (0.036)	0.66 (0.007)	0.62 (0.013)	0.62 (0.009)	0.60 (0.020)	0.60 (0.031)
Heating Oil	0.49 (0.770)	0.58 (0.050)	0.62 (0.002)	0.64 (0.006)	0.66 (0.001)	0.66 (0.001)	0.70 (0.000)	0.68 (0.000)	0.67 (0.003)
Gasoline	0.60 (0.005)	0.60 (0.013)	0.74 (0.000)	0.64 (0.001)	0.70 (0.000)	0.67 (0.000)	0.66 (0.002)	0.71 (0.000)	0.76 (0.000)
Ethanol	0.53 (0.236)	0.63 (0.001)	0.66 (0.000)	0.65 (0.000)	0.61 (0.028)	0.66 (0.001)	0.68 (0.000)	0.67 (0.000)	0.71 (0.000)
Gold	0.49 (0.525)	0.58 (0.028)	0.60 (0.209)	0.57 (0.118)	0.55 (0.092)	0.61 (0.001)	0.64 (0.000)	0.61 (0.000)	0.62 (1.000)
Silver	0.51 (0.395)	0.47 (0.763)	0.48 (0.371)	0.43 (0.570)	0.42 (0.866)	0.46 (1.000)	0.48 (1.000)	0.52 (0.000)	0.56 (0.000)
Platinum	0.49 (0.636)	0.52 (0.109)	0.48 (0.518)	0.44 (0.552)	0.36 (0.989)	0.35 (1.000)	0.32 (1.000)	0.33 (1.000)	0.28 (1.000)
Aluminum	0.48 (0.446)	0.49 (0.693)	0.50 (0.268)	0.53 (0.080)	0.53 (0.019)	0.51 (0.003)	0.50 (0.100)	0.45 (1.000)	0.41 (1.000)
Copper	0.58 (0.001)	0.55 (0.093)	0.55 (0.118)	0.56 (0.076)	0.57 (0.062)	0.56 (0.116)	0.57 (0.115)	0.60 (0.065)	0.56 (0.193)
Lead	0.57 (0.026)	0.55 (0.105)	0.60 (0.000)	0.63 (0.000)	0.60 (0.000)	0.54 (0.001)	0.54 (0.000)	0.55 (0.000)	0.56 (0.000)
Zinc	0.49 (0.443)	0.60 (0.025)	0.66 (0.001)	0.72 (0.000)	0.68 (0.001)	0.61 (0.050)	0.63 (0.054)	0.60 (0.094)	0.55 (0.269)
Nickel	0.49 (0.874)	0.51 (0.739)	0.55 (0.202)	0.55 (0.170)	0.58 (0.146)	0.64 (0.003)	0.70 (0.000)	0.65 (0.000)	0.63 (0.000)
Tin	0.48 (0.591)	0.44 (0.853)	0.46 (0.727)	0.49 (0.576)	0.52 (0.342)	0.50 (0.517)	0.50 (0.534)	0.54 (0.209)	0.59 (0.021)
Corn	0.58 (0.025)	0.62 (0.002)	0.62 (0.009)	0.57 (0.137)	0.52 (0.523)	0.57 (0.144)	0.63 (0.019)	0.63 (0.022)	0.62 (0.018)
Soybeans	0.60 (0.003)	0.58 (0.059)	0.68 (0.000)	0.68 (0.000)	0.66 (0.004)	0.59 (0.081)	0.66 (0.005)	0.66 (0.007)	0.71 (0.001)
Wheat	0.53 (0.248)	0.57 (0.088)	0.53 (0.539)	0.51 (0.968)	0.58 (0.446)	0.53 (0.828)	0.57 (0.683)	0.57 (0.491)	0.58 (0.290)

Notes: See the notes below Table 2.4. This table presents the performance of futures-based forecasts of nominal monthly prices using the end-of-month futures curve. Bold values indicate improvements over the baseline results in Table 2.4.

The MSFE performance of nominal forecasts is broadly consistent with the baseline findings, with only minor improvements in accuracy compared to forecasting real prices. Small gains in forecast directional accuracy relative to real forecasts are observed in some cases, particularly at horizons of three months and beyond. By the two-year horizon, the differences in directional accuracy become more noticeable, especially for gasoline, nickel, and soybeans. However, these forecast gains are not reflected in the MSFE ratio. A notable exception is that nominal gold prices now exhibit predictability, in stark contrast to real gold prices. Specifically, forecasts for the nominal monthly average price of gold show gains in both directional accuracy and mean-squared precision around the one-year horizon. This is likely due to the unique role that gold plays as a hedge

against inflation, providing an interesting example of the distinct characteristics that differentiate commodity markets.

2.5.5. Direct Forecasts

This subsection examines the effect of using the values of futures contracts directly for forecasting, as in Equation 2.5, rather than calculating a spread over the spot price, as in Equation 2.6. These forecasts eliminate the log approximations used in the baseline spread model, Equation 2.6. The results are shown in Table 2.8. The results do not reveal any improvements over the baseline results, presented in Table 2.4, showing only marginal differences in forecast performance between the direct and spread models. Only for ethanol do we find consistent, small improvements in forecast precision, particularly at horizons of less than one year. Additionally, we do not find any improvements over the baseline results in terms of directional accuracy.

Table 2.8.: Direct Futures-based Forecasts of Monthly Average Real Prices, Non-Parametric, End-of-Month Futures

Commodity	1	3	6	9	12	15	18	21	24
Crude Oil	0.99 (0.305)	0.94 (0.020)	0.88 (0.034)	0.86 (0.060)	0.82 (0.048)	0.77 (0.018)	0.72 (0.010)	0.68 (0.005)	0.63 (0.002)
Natural Gas	1.02 (0.653)	1.00 (0.527)	0.96 (0.360)	1.05 (0.626)	1.05 (0.631)	0.97 (0.411)	0.98 (0.436)	0.98 (0.443)	0.98 (0.460)
Heating Oil	1.04 (0.779)	0.98 (0.353)	0.96 (0.217)	0.91 (0.040)	0.86 (0.005)	0.85 (0.001)	0.81 (0.000)	0.78 (0.000)	0.73 (0.000)
Gasoline	0.81 (0.004)	0.74 (0.001)	0.69 (0.003)	0.81 (0.031)	0.87 (0.055)	0.80 (0.015)	0.74 (0.005)	0.73 (0.004)	0.69 (0.001)
Ethanol	0.71 (0.106)	0.67 (0.057)	0.73 (0.103)	0.75 (0.086)	0.71 (0.067)	0.67 (0.033)	0.65 (0.031)	0.61 (0.031)	0.57 (0.021)
Gold	1.01 (0.604)	1.00 (0.424)	1.00 (0.509)	0.99 (0.403)	0.98 (0.343)	0.97 (0.285)	0.96 (0.224)	0.95 (0.158)	0.93 (0.117)
Silver	1.04 (0.884)	1.00 (0.492)	0.99 (0.287)	0.98 (0.156)	0.97 (0.123)	0.96 (0.076)	0.93 (0.029)	0.90 (0.018)	0.87 (0.016)
Platinum	1.02 (0.859)	0.98 (0.066)	0.93 (0.008)	0.91 (0.010)	0.89 (0.008)	0.88 (0.001)	0.86 (0.000)	0.85 (0.000)	0.86 (0.000)
Aluminum	1.00 (0.526)	1.01 (0.648)	0.98 (0.252)	0.95 (0.119)	0.96 (0.078)	0.96 (0.109)	0.97 (0.163)	0.97 (0.199)	0.96 (0.181)
Copper	0.98 (0.042)	0.98 (0.169)	0.97 (0.118)	0.94 (0.087)	0.94 (0.073)	0.92 (0.061)	0.90 (0.040)	0.88 (0.037)	0.88 (0.056)
Lead	0.97 (0.035)	0.97 (0.008)	0.93 (0.008)	0.87 (0.010)	0.86 (0.009)	0.86 (0.022)	0.84 (0.029)	0.83 (0.013)	0.81 (0.010)
Zinc	0.97 (0.096)	0.95 (0.083)	0.93 (0.080)	0.90 (0.029)	0.90 (0.049)	0.92 (0.090)	0.92 (0.121)	0.92 (0.159)	0.93 (0.227)
Nickel	1.00 (0.632)	1.00 (0.526)	0.98 (0.143)	0.96 (0.106)	0.94 (0.097)	0.90 (0.046)	0.85 (0.022)	0.82 (0.011)	0.80 (0.007)
Tin	1.00 (0.503)	1.02 (0.689)	1.02 (0.607)	1.00 (0.507)	0.98 (0.408)	0.95 (0.226)	0.95 (0.192)	0.98 (0.337)	0.99 (0.439)
Corn	1.05 (0.622)	0.76 (0.054)	0.68 (0.028)	0.70 (0.040)	0.71 (0.046)	0.68 (0.032)	0.64 (0.026)	0.62 (0.022)	0.58 (0.009)
Soybeans	0.86 (0.130)	0.77 (0.037)	0.74 (0.029)	0.78 (0.044)	0.83 (0.122)	0.77 (0.100)	0.72 (0.064)	0.71 (0.053)	0.68 (0.026)
Wheat	1.11 (0.922)	1.07 (0.779)	1.03 (0.588)	0.99 (0.481)	0.97 (0.436)	0.96 (0.407)	0.96 (0.340)	0.95 (0.280)	0.90 (0.203)
Success Ratio									
Crude Oil	0.55 (0.091)	0.52 (0.208)	0.58 (0.093)	0.62 (0.031)	0.68 (0.002)	0.69 (0.000)	0.66 (0.002)	0.64 (0.005)	0.75 (0.000)
Natural Gas	0.52 (0.321)	0.54 (0.169)	0.61 (0.000)	0.63 (0.004)	0.64 (0.006)	0.66 (0.003)	0.63 (0.017)	0.64 (0.006)	0.62 (0.021)
Heating Oil	0.52 (0.300)	0.56 (0.072)	0.61 (0.019)	0.69 (0.000)	0.77 (0.000)	0.82 (0.000)	0.81 (0.000)	0.83 (0.000)	0.81 (0.000)
Gasoline	0.62 (0.001)	0.62 (0.004)	0.71 (0.000)	0.65 (0.001)	0.62 (0.001)	0.62 (0.001)	0.65 (0.002)	0.69 (0.000)	0.70 (0.000)
Ethanol	0.55 (0.086)	0.59 (0.015)	0.66 (0.000)	0.64 (0.001)	0.64 (0.024)	0.69 (0.000)	0.64 (0.001)	0.68 (0.000)	0.73 (0.000)
Gold	0.47 (0.444)	0.55 (0.114)	0.48 (0.170)	0.54 (0.140)	0.52 (0.616)	0.57 (0.000)	0.55 (0.000)	0.56 (0.000)	0.50 (0.000)
Silver	0.47 (0.753)	0.50 (0.779)	0.59 (0.353)	0.66 (0.069)	0.67 (0.037)	0.66 (0.004)	0.67 (0.000)	0.67 (0.000)	0.63 (0.009)
Platinum	0.49 (0.370)	0.56 (0.238)	0.66 (0.016)	0.64 (0.114)	0.72 (0.011)	0.76 (0.002)	0.79 (0.000)	0.82 (0.000)	0.84 (0.000)
Aluminum	0.47 (0.702)	0.45 (0.862)	0.46 (0.682)	0.47 (0.598)	0.50 (0.466)	0.49 (0.504)	0.53 (0.235)	0.56 (0.061)	0.56 (0.064)
Copper	0.53 (0.024)	0.53 (0.000)	0.60 (1.000)	0.61 (1.000)	0.63 (1.000)	0.63 (1.000)	0.60 (1.000)	0.59 (1.000)	0.59 (1.000)
Lead	0.56 (0.060)	0.61 (0.005)	0.60 (0.057)	0.62 (0.020)	0.58 (0.011)	0.65 (0.009)	0.66 (0.144)	0.65 (0.080)	0.67 (0.061)
Zinc	0.53 (0.519)	0.50 (0.548)	0.52 (0.346)	0.51 (0.344)	0.57 (0.086)	0.61 (0.021)	0.60 (0.020)	0.59 (0.012)	0.58 (0.120)
Nickel	0.50 (1.000)	0.49 (0.290)	0.50 (0.069)	0.50 (0.500)	0.50 (0.000)	0.50 (0.000)	0.49 (0.000)	0.56 (0.000)	0.55 (0.000)
Tin	0.53 (1.000)	0.50 (1.000)	0.48 (1.000)	0.52 (1.000)	0.52 (1.000)	0.54 (1.000)	0.58 (1.000)	0.57 (1.000)	0.54 (1.000)
Corn	0.56 (0.028)	0.63 (0.001)	0.64 (0.004)	0.57 (0.110)	0.51 (0.444)	0.52 (0.355)	0.55 (0.177)	0.56 (0.093)	0.59 (0.024)
Soybeans	0.56 (0.051)	0.53 (0.260)	0.60 (0.021)	0.63 (0.012)	0.58 (0.074)	0.58 (0.150)	0.55 (0.144)	0.58 (0.087)	0.62 (0.004)
Wheat	0.55 (0.088)	0.56 (0.075)	0.58 (0.034)	0.49 (0.840)	0.48 (0.881)	0.49 (0.733)	0.53 (0.441)	0.54 (0.485)	0.55 (0.371)

Notes: See the notes below Table 2.4. This table presents the forecast performance of regressions using the futures-spot spread without relying on log approximations. Bold values indicate improvements over the baseline results in Table 2.4.

2.5.6. Robustness over time

This subsection assesses the robustness of forecast performance over time and with respect to alternative sample start dates. Previous results suggest that futures-based forecast performance may exhibit time variation. Specifically, Hamilton and Wu (2014) suggest that the oil futures risk premium has become both smaller and more volatile since 2005. Similarly, Bohl et al. (2023) observe that financialization has improved the informational efficiency of futures markets across 34 commodities, covering energy, agriculture, and metals, allowing prices to better reflect new information.

We consider an earlier starting point for the forecast evaluation sample, January 2000 instead of 2010, and report two methods to assess the temporal stability of our baseline futures-based forecasts. First, we present the evolution of the one-month-ahead MSFE ratios over time (see Figure 2.2). The evolution of the evaluation criteria for one- and two-year horizons is provided in Figures A.2 and A.3 in the Appendix. Additionally, a table of end-of-period ratios and corresponding tests for the alternative forecast evaluation periods is provided in Table A.7.

The results reveal that starting around 2010, futures-based forecasts consistently began to outperform random walk predictions for the majority of commodities studied. These improvements in forecast accuracy correlate with increased trading volumes (see Appendix Figure A.1), suggesting a link between market depth and predictive performance. This finding also aligns with Funk (2018) and Ellwanger and Snudden (2023b), who find that futures-based models for oil forecasting experienced significant improvements in accuracy post-2010, demonstrating superior performance over medium- and long-term horizons.

However, the results reveal a decrease in forecasting accuracy for natural gas over the past two years. This decline is particularly pronounced at horizons of up to one year and explains the poor forecast performance observed in the baseline sample. Before this recent episode, natural gas had shown some of the best forecast performance across commodity markets.

2.6. Conclusion

This study examines the effectiveness of futures prices in predicting the real average spot prices of 17 primary commodities, addressing the practical challenges of using futures prices for forecasting. These challenges include irregular delivery schedules and the unique settlement procedures associated with front-month contracts for each commodity. To overcome these issues, we generate a continuous monthly futures curve, aligning each observation with its respective forecast month. This approach better reflects real-time commodity trading practices, thereby enhancing the relevance and applicability of our findings.

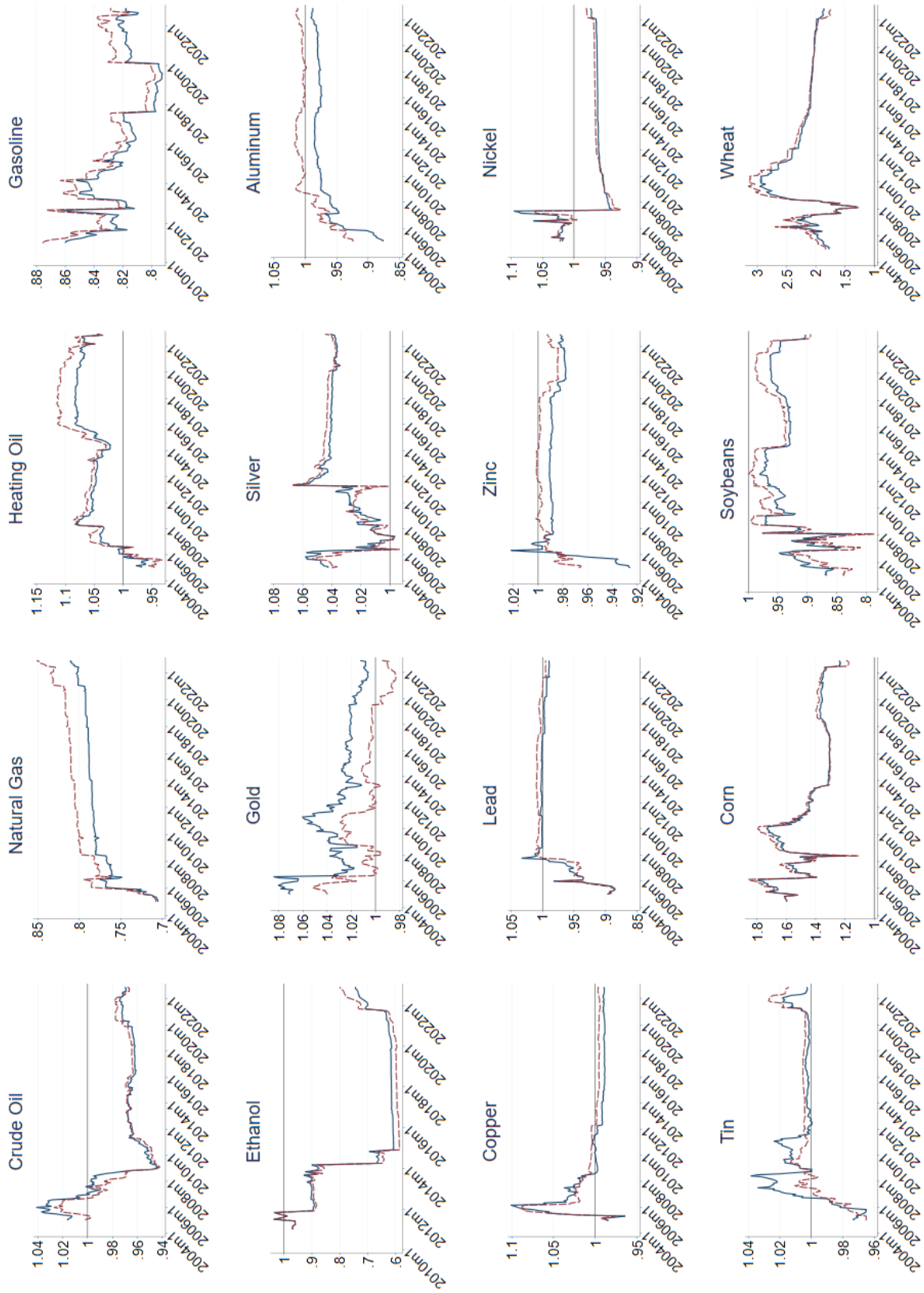


Figure 2.2.: Evolution of MSFEs Criteria For Futures-Based Forecasts, One-Month Ahead.

Note: The blue line represents the performance of futures-based forecasts of real prices using End-of-Month futures, while the red line shows the performance of futures-based forecasts of nominal prices using EoM. A horizontal reference line at 1 serves as a benchmark for evaluating MSFE values, which are reported relative to the no-change forecast.

2. Can Futures Prices Predict the Real Price of Primary Commodities?

Our results suggest that the average price of many primary commodities is predictable in real-time, particularly at horizons of six months and beyond. Notably, energy commodities, base metals, and certain agricultural products exhibit substantial improvements in forecast accuracy. This finding contributes to the broader understanding of futures markets' predictive capabilities and highlights the heterogeneity across different commodity sectors. The observed predictability provides valuable insights for market participants and policymakers, aiding in more informed decision-making related to resource allocation, investment, and policy formulation.

We conclude with three practical recommendations for constructing futures-based forecasts. First, we find empirical support for using the latest market expectations embedded in end-of-month futures prices, as these generally outperform forecasts based on averaged futures prices. This approach is also convenient for constructing real-time forecasts, given that futures prices are publicly available and continuously updated. Second, our analysis does not suggest significant gains from adopting parametric approaches; thus, we recommend utilizing simple non-parametric approaches. Third, forecasters should carefully consider the expectations embedded in futures contracts in relation to the specific forecast horizons they are targeting. By following these guidelines, we believe forecasters can more effectively utilize futures prices for real-time forecasts of period-average commodity prices.

Ultimately, the potential gains from ongoing refinements in futures-based forecasts highlight the importance of further research. This study underscores both the current capabilities and limitations of using futures markets for price forecasting. Further improvements in the precision, robustness, and applicability of these forecasts, particularly for under-explored commodities, are warranted. Future research could also quantify the impact of storage characteristics on the predictive power of futures prices by incorporating measurable indices that capture the physical and economic characteristics that vary across commodities.

3. Revisiting the Dynamics and Elasticities of the U.S. Natural Gas Market

3.1. Introduction

The U.S. natural gas market plays a pivotal role in the nation’s energy landscape, influencing sectors ranging from manufacturing to residential services (Gautam & Paudel, 2018). In addition to meeting domestic needs, the market provides significant economic opportunities through natural gas exports (P. Bernstein et al., 2016). According to the Energy Information Administration’s (EIA) *Annual Energy Outlook 2023*, natural gas production is projected to grow steadily through 2050. This growth is expected to be driven by increased domestic consumption, particularly in the industrial sector, as well as by the expansion of natural gas exports due to rising global demand for liquefied natural gas (LNG) (EIA, 2023b). These trends underscore the enduring economic importance of the U.S. natural gas market, both domestically and internationally. Therefore, understanding the joint dynamics of supply, domestic demand, export demand, and prices is essential for informed policy decisions.

The literature on U.S. natural gas market dynamics predominantly relies on structural vector autoregression (SVAR) models, originally developed for the global oil market to analyze the distinct roles of supply and demand shocks in driving oil price fluctuations. One strand of this literature follows the recursive structural VAR specification used in the trivariate oil market model by Kilian (2009) (e.g., Hailemariam and Smyth (2019)). This approach examines the joint dynamics of the percentage change in U.S. natural gas production, the log of real natural gas prices, and an index of cyclical variation in U.S. real economic activity, using monthly data.⁶ Variations in these variables are explained by three shocks: a natural gas supply shock, an aggregate demand shock, and a gas-market-specific demand shock. The other strand of this literature utilizes quarterly data and follows the four-variable specification used in oil market models proposed by Kilian and Murphy (2014) and Baumeister and Hamilton (2019) (e.g., Wiggins and Etienne (2017)). This approach extends the trivariate specification by incorporating natural gas inventories and adopting alternative

⁶Recursive identification orders variables so that shocks to earlier variables in the VAR do not contemporaneously affect later ones. In natural gas market models, this typically means that gas production is ordered first, economic activity second, and gas prices last, allowing prices to react instantly to production and activity changes but not vice versa.

3. Revisiting the Dynamics of the U.S. Natural Gas Market

identification strategies, such as sign restrictions⁷, that explicitly account for inventory demand shocks. Despite differences in identification approaches, the overarching conclusion from both strands is that natural gas price fluctuations are primarily demand-driven. A detailed review of this literature is provided in Section 5.2.

While these two strands of literature have enhanced our understanding of U.S. natural gas market dynamics, key features such as imports and exports, which are integral to the market's supply and demand structure, have not been fully considered. As a result, these omissions may lead to an incomplete representation of the market's dynamics, particularly in capturing the role of export demand in the observed demand-side shocks.

This study extends the literature by proposing an SVAR model that incorporates external gas flows into its structural framework. This extension ensures proper allocation of the total available supply among domestic consumption, export demand, and inventory changes, preventing any misrepresentation of the supply-demand balance that could occur if external flows were excluded.⁸ Within this framework, the model explicitly accounts for shocks to export demand for natural gas, thereby enhancing the understanding of demand-driven dynamics previously established in the literature. Furthermore, the analysis employs the Bayesian approach introduced by Baumeister and Hamilton (2015, 2019), which incorporates uncertainty in identifying assumptions and provides a framework for summarizing beliefs about key structural parameters, such as supply and demand elasticities. In doing so, this study revisits the dynamics and elasticities of natural gas supply and demand, providing new evidence on the relative importance of structural shocks in this market and contributing to the literature on the short-run response of energy commodities' supply and demand to price changes.

The model is estimated using a monthly dataset extending through 2023, which is particularly relevant for three reasons. First, using monthly data reduces the information loss typically associated with temporal aggregation in models that use quarterly data. Temporal aggregation can affect the structural interpretation and identification of VAR models, as it may obscure within-period relationships that are critical for accurately capturing structural shocks. In particular, exclusion restrictions and elasticity bounds, which are essential for identifying structural shocks, are more credible at a monthly frequency than at a quarterly one (Beetsma et al., 2009; Kilian & Lütkepohl, 2017). Second, extending the dataset through 2023 captures recent market shifts, particularly those related to the increase in

⁷The sign restriction approach is an identification method in which certain effects or responses are restricted in direction (positive or negative), rather than fixed at exactly zero. However, this method alone is insufficient because it can result in multiple equally plausible but conflicting models, necessitating additional economically motivated constraints to achieve reliable identification (see Kilian and Murphy (2012) and Baumeister and Hamilton (2019) for more details).

⁸See Section 3.3.2 for a detailed explanation of how this specification, which incorporates external gas flows, corrects potential misrepresentations in the supply-demand balance and improves the estimation of domestic consumption elasticity.

natural gas exports to Europe in the aftermath of the Russian invasion of Ukraine. This is relevant to ongoing policy discussions about the role of export demand shocks in natural gas price variation during this period (see, for example, EIA (2023a) and EVA (2023)). Finally, the analysis accounts for extreme observations during the COVID-19 pandemic, demonstrating that failing to control for these outliers can result in counterintuitive economic responses.

The results can be summarized as follows: First, the estimated short-run price elasticity of gas supply is 0.019, indicating that the supply curve remains price inelastic within the month. This minimal responsiveness aligns with the findings of Ponce and Neumann (2014) and Mason and Roberts (2018), highlighting the dominance of physical and technical constraints over economic incentives in the short term. On the demand side, the short-run price elasticity of domestic gas demand is -0.177, suggesting a modest decrease in demand in response to price increases. This estimate is consistent with the findings of Labandeira et al. (2017), who report an average short-run price elasticity of -0.180.

Second, the results show that a negative supply shock leads to an initial sharp decline in gas supply, which partially reverses within the first three months. The supply disruption raises natural gas prices, prompting an immediate drawdown of inventories to mitigate the shortfall, though they recover within four months. A shock to domestic consumption gradually increases supply and raises prices, leading to a small, temporary decline in economic activity. As a result of this shock, inventories drop immediately, reach their lowest point in the fourth month, and recover to their original level within a year. Both supply and domestic consumption shocks reduce exports, with the impact being more significant for supply shocks. Inventory demand shocks trigger an immediate but short-lived spike in prices, while export demand shocks cause both short- and medium-term price increases and a gradual rise in natural gas supply.

The analysis reveals that these effects are distorted if extreme values from the COVID-19 pandemic are not accounted for. For example, without adjusting for these outliers, the findings incorrectly suggest that a reduction in gas supply, which typically raises gas prices, increases U.S. economic activity. This underscores the importance of accounting for extreme events, such as the COVID-19 pandemic, in structural analyses to avoid misleading inferences about the true economic impacts of shocks.

Third, the analysis of the overall importance of each shock in determining gas price fluctuations reveals that domestic consumption demand shocks and inventory demand shocks are the primary drivers of short-term price variations, accounting for over 85% of the fluctuations at the one-month horizon. However, as the analysis extends to longer periods, up to 16 months, the influence of these shocks, though still dominant, diminishes slightly. Meanwhile, contributions from supply, economic activity, and export demand shocks become more pronounced, indicating a gradual shift in the dynamics affecting gas prices over time. Moreover, the analysis shows that consumption demand shocks and export demand shocks

3. Revisiting the Dynamics of the U.S. Natural Gas Market

are the primary drivers of natural gas inventories and exports, respectively, with their effects persisting but decreasing over the 16-month horizon. Compared to Arora and Lieskovsky (2014), who identified a minimal short-run impact of supply shocks and a dominant role for speculative demand shocks, this study finds a more substantial short-run effect from supply shocks and a weaker influence from speculative demand. Furthermore, unlike Wiggins and Etienne (2017), who reported that supply and aggregate income shocks had roughly equal influence, this study concludes that these factors initially play a lesser role, with their significance increasing over time. This study's findings are consistent with those of Rubaszek et al. (2021) in emphasizing the role of consumption demand and inventory demand shocks, but they differ in the relative strength of these effects. These differences across studies may stem from variations in data frequency and model specifications.

Lastly, the decomposition of natural gas price movements from January 2022 to October 2023 reveals that domestic factors, particularly consumption demand and inventory demand shocks, were the primary drivers of price fluctuations, especially during periods of extreme weather and low storage levels. Export demand shocks also played a significant role, especially following the Russian invasion of Ukraine in early 2022, which led to increased U.S. LNG exports to Europe. Additionally, the shutdown and subsequent reactivation of the Freeport LNG terminal in 2022 and 2023 had notable impacts on gas prices, underscoring the influence of export dynamics on the U.S. market. For example, maintenance and operational incidents at the terminal contributed to price reductions in mid-2022 and price increases after its reactivation in early 2023. A decomposition analysis of price fluctuations during the 2005 hurricanes shows that supply shocks led to significant price increases immediately following Hurricanes Katrina and Rita in August, but their effects diminished quickly, with demand factors regaining dominance in the subsequent months. This demonstrates that, while supply shocks can cause significant initial price increases, their effects are short-lived, with demand factors eventually regaining dominance.

The rest of the paper is organized as follows: Section 5.2 reviews the relevant literature. Section 5.4 describes the methodology, detailing the SVAR model adapted and extended for this analysis. Section 5.3 explains the data utilized and outlines the adjustments made to account for extreme observations stemming from the COVID-19 pandemic. Section 5.5 presents the estimation results. Section 3.6 discusses robustness checks to validate the reliability of the findings, and Section 5.7 concludes.

3.2. Literature review

The deregulation of the U.S. natural gas market was a gradual process shaped by policy changes, economic forces, and technological advancements. Initially, the natural gas wellhead price was regulated by the Federal Power Commission (FPC),

which was later reconstituted as the Federal Energy Regulatory Commission (FERC). This regulation resulted in significant supply shortages. In response, the Natural Gas Policy Act of 1978 facilitated incremental price adjustments toward market levels to address these shortages. Subsequent reforms included the introduction of Special Marketing Programs (SMPs) and FERC mandates requiring the separation of sales and transportation services, enabling direct transactions between customers and suppliers. This evolution towards a competitive market was further reinforced by the Natural Gas Wellhead Decontrol Act of 1989, which fully deregulated wellhead prices (Hou & Nguyen, 2018; Makhholm, 2010). From the mid-1990s onward, market forces exclusively determined U.S. natural gas prices (Ebinger et al., 2012; Joskow, 2013).

These significant market changes have prompted a corresponding shift in academic research. Initially, the literature primarily focused on the dynamics between natural gas and crude oil prices. Earlier studies, such as those by Serletis and Herbert (1999), Bachmeier and Griffin (2006), Villar and Joutz (2006), and Brown and Yttcel (2008), established a long-run relationship driven by the substitutability between refined petroleum products and natural gas across various consumption sectors. In contrast, more recent studies by Erdős and Ormos (2012), Geng et al. (2016b), and Zhang and Ji (2018) have observed a decoupling of oil and gas prices in the North American market. They attribute this trend to the switch to gas-on-gas competition pricing, the increased natural gas availability in the U.S., and a diminishing substitution effect with petroleum products. Consequently, contemporary research has shifted toward examining the relative importance of fundamental factors in the natural gas market through structural models. Table 3.1 summarizes studies employing the Structural VAR model, detailing their variables, specifications, identification strategies, data frequencies, and key findings.

The studies summarized in Table 3.1 cover a diverse range of variables, frequencies, and periods, with a common focus on fundamental factors influencing the dynamics of the U.S. natural gas market. Most of these studies exclude oil prices from their analysis, except for Hou and Nguyen (2018) and Nguyen and Okimoto (2019). Monthly data are used by Arora (2014), Hailemariam et al. (2019), and Rubaszek and Uddin (2020), who construct a three-variable model comprising the quantity of natural gas produced, industrial production as a measure of real economic activity, and the real price of natural gas. In contrast, quarterly data are used by Wiggins and Etienne (2017) and Rubaszek et al. (2021), who expand their variable sets to include natural gas inventories and use real GDP as a measure of economic activity.

3. Revisiting the Dynamics of the U.S. Natural Gas Market

Table 3.1.: Summary of studies analyzing the dynamics of the U.S. natural gas market using SVAR models

Authors (year)	Variables	Model specification	Identification strategy	Data freq.	Study period	Key findings
Arora and Lieskovsky (2014)	Production, consumption, price	SVAR	Recursive	M	1993M11–2012M12	Prices are mainly driven by specific demand shocks related to inventory.
Wiggins and Etienne (2017)	Production, GDP, price, inventory	TVP-VAR	Sign-restrictions	Q	1976Q1–2015Q2	The effects of supply and demand shocks vary significantly over time, with minimal impact from inventory demand shocks.
Hou and Nguyen (2018)	Production, IP, oil price, price	MS-VAR	Recursive	M	1980M2–2016M11	Prices are mainly driven by specific demand shocks related to inventory.
Nguyen and Okimoto (2019)	Oil price, production, IP, price	TSVAR	Recursive	M	1980M2–2016M11	Price response is asymmetric, varying according to the business cycle.
Hailemariam and Smyth (2019)	Production, IP, price	SHVAR	Recursive	M	1978M1–2018M7	Prices are largely explained by demand-specific shocks related to inventory.
Rubaszek and Uddin (2020)	Production, ADS, price, inventory	TSVAR	Recursive	M	1995M1–2018M8	Price response is asymmetric, varying according to the inventory level.
Rubaszek et al. (2021)	Production, GDP, price, gas inventory	BSVAR	Prior distributions and sign restrictions	Q	1993Q1–2020Q3	Prices are primarily driven by consumption demand shocks, followed by inventory demand shocks.

Note: In the “Variables” column, variables are listed according to the sequence adopted by each study for identifying causal relationships within their respective SVAR models. The terms “production”, “consumption”, “price”, and “inventory” refer to natural gas production, natural gas consumption, real natural gas price, and natural gas inventory, respectively. Additionally, “IP” and “ADS” refer to industrial production and the Aruoba-Diebold-Scotti business conditions index, respectively. In the “Model specification” column, abbreviations are defined as follows: VAR: Vector Autoregression, TVP-VAR: Time-Varying Parameter VAR, MS-VAR: Markov-Switching VAR, TSVAR: Threshold SVAR, SHVAR: Structural Heterogeneous VAR, BSVAR: Bayesian SVAR. The “Data freq.” column provides the data frequency in which the analysis is conducted, with “M” and “Q” referring to monthly and quarterly data frequencies, respectively.

Model specifications across these studies show significant variation. Arora and Lieskovsky (2014) employ a standard SVAR model, attributing price fluctuations primarily to gas-specific demand shocks related to speculative or precautionary purposes. Wiggins and Etienne (2017) apply a Time-Varying Parameter Vector Autoregression (TVP-VAR) model with smoothly and continuously evolving parameters, enabling them to assess the dynamic effects of various structural shocks on natural gas prices. Their results show that supply and demand shocks are the primary drivers of U.S. natural gas price fluctuations since deregulation, with speculative activities having only a minor impact during certain periods. However, Hailemariam and Smyth (2019) argue that the continuous changes in parameters may not reflect the actual changes in the underlying dynamics, especially in regimes characterized by constant coefficients. Therefore, they implement a Structural Heterogeneous Autoregressive VAR (SHVAR) model, allowing coefficients and volatilities to change at specific dates and to differ across

equations. They find that most variations in natural gas prices are attributable to gas-specific demand shocks related to storage, aligning with Arora and Lieskovsky (2014)'s conclusions. Further exploring nonlinearity, Rubaszek and Uddin (2020) employ a threshold SVAR model and find that the dominant role of these gas-specific demand shocks persists across both high and low inventory regimes. Lastly, Rubaszek et al. (2021) adopt a Bayesian SVAR framework, introduced by Baumeister and Hamilton (2019), which incorporates Bayesian inference to account for uncertainty in both parameter estimates and the structural features of the model. Their analysis shows that consumption demand shocks explain a dominant fraction of natural gas price variation.

Regarding the identification strategy, most studies, such as Arora and Lieskovsky (2014), Hou and Nguyen (2018), Nguyen and Okimoto (2019), and Hailemariam et al. (2019), predominantly adopt the recursive identification approach used by Kilian (2009) in the oil market. This approach is applied to analyze the joint dynamics of the percentage change in U.S. natural gas production, the logarithm of real natural gas prices, and an index representing cyclical fluctuations in U.S. real economic activity, based on monthly data. However, this identification strategy imposes exclusion restrictions that assume zero short-run supply elasticity, which may oversimplify real market dynamics, particularly given the non-zero elasticity of supply.⁹ To address these limitations, Wiggins and Etienne (2017) follow a sign-restriction-based identification approach, building on the works of Kilian and Murphy (2012), Baumeister and Peersman (2013), and Kilian and Murphy (2014). Unlike the recursive method, which produces unique parameter estimates, sign-identified models generate a range of possible solutions as long as the responses of endogenous variables adhere to a predetermined sign pattern. Wiggins and Etienne (2017) extend the three-variable model of natural gas by incorporating natural gas inventories as a fourth variable, allowing them to capture the effects of speculative behavior and storage dynamics on price fluctuations. Furthermore, Rubaszek et al. (2021) adopt the identification approach of Baumeister and Hamilton (2019), originally developed for the oil market, which involves a fully Bayesian setup that relaxes the dogmatic priors of the recursive identification and combines sign restrictions with weakly informative prior distributions on structural parameters to disentangle supply and demand shocks.

In summary, the variations in findings across studies analyzing factors affecting U.S. gas price fluctuations can largely be attributed to differences in model specification, identification assumptions, and variable selection. This divergence reflects the evolving understanding of interactions within the U.S. natural gas market. While earlier studies primarily relied on recursive identification and often overlooked the impact of inventories, recent research has adopted alternative approaches that enable them to account for inventories and has utilized quarterly

⁹The traditional Cholesky identification can be interpreted as a special case of Bayesian inference where exact prior knowledge is assumed about some elements of the structure, leading to identical inferences between the Cholesky and Bayesian posterior medians for those parameters (see Baumeister and Hamilton (2019) for more details).

data. However, the roles of natural gas imports and exports have not been fully considered, which can lead to misrepresentations in the supply-demand balance. Therefore, this study extends the literature by proposing an SVAR model that incorporates imports into the supply flow and explicitly allows for shocks to export demand, as well as those shocks examined in Rubaszek et al. (2021)’s analysis. This enables a clear distinction between domestic and export-driven demand shocks and contributes to the ongoing discussion about the role of export demand shocks in natural gas price variation. Additionally, this study uses monthly data to minimize the information loss typically associated with temporal aggregation. Finally, the analysis accounts for extreme values from the COVID-19 pandemic to avoid misleading inferences about the true economic impacts of shocks.

3.3. Methodology

This section outlines the approach for specifying and estimating an SVAR model of the U.S. natural gas market. Subsection 3.3.1 describes the specification of the SVAR model and the estimation procedures employed. Building on this foundation, Subsection 3.3.2 develops a specific model for the U.S. natural gas market. Finally, Subsection 3.3.3 details the prior assumptions applied to the model’s contemporaneous structural parameters.

3.3.1. Structural VAR specification and estimation

Consider the following SVAR specification for a n -dimensional time series vector y_t :

$$\mathbf{A}y_t = \mathbf{B}x_{t-1} + u_t \quad (3.1)$$

where y_t is an $n \times 1$ vector of endogenous variables, \mathbf{A} is an $(n \times n)$ matrix summarizing their contemporaneous structural relations, x_{t-1} is a $(k \times 1)$ vector (with $k = mn+1$) containing a constant and m lags of y ($x_{t-1} = (y'_{t-1}, y'_{t-2}, \dots, y'_{t-m}, 1)'$), and u_t is an $(n \times 1)$ vector of structural disturbances assumed to be independent and identically distributed (i.i.d.) $\mathcal{N}(0, \mathbf{D})$ and mutually uncorrelated (\mathbf{D} is diagonal).

This study follows the identification and estimation strategy introduced by Baumeister and Hamilton (2015) and further developed by Baumeister and Hamilton (2019) to construct a specific four-variable oil market model, which was later applied to the U.S. natural gas market by Rubaszek et al. (2021). This strategy yields a set-identified SVAR model through two primary steps. The first step involves specifying informative prior beliefs about the values of the structural parameters represented by a density $p(\mathbf{A}, \mathbf{D}, \mathbf{B})$. The second step generates draws from the posterior distribution of the structural coefficients to assess how the data influences the prior beliefs. Further details regarding the two steps are provided in the Appendix.

3.3.2. A structural VAR model of the U.S. natural gas market

To investigate the dynamics of the U.S. natural gas market, this study follows the model specification of Baumeister and Hamilton (2019). The original model comprises four structural equations that articulate the behavior of buyers and sellers in the global oil market, along with the determinants of global economic growth. However, due to the distinct characteristics of the U.S. gas market, particularly regarding natural gas imports and exports, modifications are necessary. This study adapts Baumeister and Hamilton (2019)'s framework by incorporating natural gas imports and exports into the specification. This extension is essential for precisely estimating the price elasticity of domestic natural gas demand, as it ensures the total available supply is accurately allocated among domestic consumption, exports, and inventory changes. Furthermore, unlike Baumeister and Hamilton (2019), which assumes the presence of additive measurement error in inventory levels, this study assumes no such measurement error. This is because the data for underground natural gas storage in the U.S. are highly accurate.¹⁰

To explain how the elasticity of domestic consumption can be approximated using the proposed SVAR model, let Q_t denote the total available natural gas supply in the U.S. market for period t . This supply includes dry natural gas production, net imports of pipeline natural gas from Canada, and imports of LNG.¹¹ Additionally, let EX_t represent the U.S. natural gas exports, which include pipeline natural gas exports to Mexico and LNG exports.¹² Let I_t denote the U.S. natural gas inventories in month t , representing the working gas in underground storage. Lastly, let C_t be the domestic consumption in month t . These variables are linked through the following accounting identity:

$$C_t = Q_t - EX_t - i_t^*. \quad (3.2)$$

¹⁰Data on underground natural gas storage in the U.S. are collected through the EIA-191 survey, which achieves nearly 100% final monthly and annual response rates from operators of underground facilities in the U.S. The data are based on metered quantities, and respondents are required to report whether the data are actual or estimated, with revisions incorporated as needed. This ensures high accuracy in the reported storage volumes. See EIA (2024) for more details.

¹¹Aggregating domestic production and imports into a single total supply measure is done for two reasons: first, the interest in this analysis lies in the total available supply shocks and in estimating U.S. total gas supply elasticity, which reflects both domestic and import responses and allows for a clearer focus on analyzing the effect of export demand shocks. Second, as Figure B.10 shows, imports have minimal impact on total supply variability, justifying their combined treatment in the SVAR model. Another specification could isolate gas production in the supply equation, while the final equation would account for net exports. This specification was tested, and the main conclusions regarding market dynamics and estimated elasticities remained unchanged. Detailed results are available upon request.

¹²This approach to constructing the total supply and export variables closely follows the industry-standard methods employed by the Energy Information Administration (EIA), as detailed in their 'Weekly Natural Gas Storage Report' and 'Natural Gas Annual' reports, which describe the dynamics of supply and demand in the U.S. natural gas market.

3. Revisiting the Dynamics of the U.S. Natural Gas Market

where $i_t^* = I_t - I_{t-1}$ represents the inventory change from period $t - 1$ to t . This equation posits that the natural gas supply, which is neither exported nor allocated to inventory changes, is consumed domestically. By dividing both sides by Q_{t-1} , the previous period's natural gas supply $t - 1$, the following equation is obtained:

$$\frac{C_t}{Q_{t-1}} = \frac{Q_t}{Q_{t-1}} - \frac{EX_t}{Q_{t-1}} - \frac{i_t^*}{Q_{t-1}}. \quad (3.3)$$

To further analyze changes from one period to the next, both sides of the equation are adjusted by adding $(EX_{t-1}/Q_{t-1}) - (Q_{t-1}/Q_{t-1})$ to reflect these changes and standardize the comparison by setting the baseline at the previous period's supply:

$$\frac{C_t - (Q_{t-1} - EX_{t-1})}{Q_{t-1}} = \frac{Q_t - Q_{t-1}}{Q_{t-1}} - \frac{(EX_t - EX_{t-1})}{Q_{t-1}} - \frac{i_t^*}{Q_{t-1}}. \quad (3.4)$$

Here, the left-hand side approximates the growth rate of domestic consumption, denoted by c_t . Similarly, $q_t = \frac{(Q_t - Q_{t-1})}{Q_{t-1}}$ represents the growth rate of natural gas supply. Therefore, the relationship can be approximately expressed as:

$$c_t \approx q_t - \frac{\Delta EX_t}{Q_{t-1}} - \frac{i_t^*}{Q_{t-1}}. \quad (3.5)$$

Considering the domestic demand for natural gas, this study hypothesizes a demand equation of the form:

$$c_t = \beta_{cy}\mathbf{y}_t + \beta_{cp}p_t + \mathbf{b}'x_{t-1} + u_t^{cd} \quad (3.6)$$

where \mathbf{y}_t denotes economic activity that may influence demand within the same month, p_t is the price of natural gas, \mathbf{b} is a vector of coefficients associated with lagged variables x_{t-1} , and u_t^{cd} represents unanticipated shocks to domestic demand. The coefficient β_{cy} is the elasticity of domestic consumption demand with respect to economic activity, indicating how consumption changes in response to income variations, and β_{cp} is the elasticity of domestic demand with respect to price, reflecting consumption sensitivity to price changes. Combining Equation 3.5 with 3.6, the relationship can be expressed as:

$$q_t - \frac{\Delta EX_t}{Q_{t-1}} - \frac{i_t^*}{Q_{t-1}} \approx \beta_{cy}\mathbf{y}_t + \beta_{cp}p_t + \mathbf{b}'x_{t-1} + u_t^{cd} \quad (3.7)$$

Rearranging for q_t and defining $ex_t = \frac{\Delta EX_t}{Q_{t-1}}$ and $i_t = \frac{i_t^*}{Q_{t-1}}$:

$$q_t = \beta_{qy}\mathbf{y}_t + \beta_{qp}p_t + i_t + ex_t + \mathbf{b}'x_{t-1} + u_t^{cd} \quad (3.8)$$

Accordingly, the structural model for the U.S. natural gas market is represented by the following simultaneous equations:

$$\text{Total supply: } q_t = \alpha_{qp}p_t + \mathbf{b}'_1x_{t-1} + u_t^s \quad (3.9)$$

$$\text{Economic activity: } \mathbf{y}_t = \alpha_{yp}p_t + \mathbf{b}'_2x_{t-1} + u_t^{ea} \quad (3.10)$$

$$\text{Domestic consumption demand: } q_t = \beta_{qy}\mathbf{y}_t + \beta_{qp}p_t + i_t + ex_t + \mathbf{b}'_3x_{t-1} + u_t^{cd} \quad (3.11)$$

$$\text{Inventory demand: } i_t = \psi_1q_t + \psi_2\mathbf{y}_t + \psi_3p_t + \mathbf{b}'_4x_{t-1} + u_t^{id} \quad (3.12)$$

$$\text{Exports demand: } ex_t = \lambda_1q_t + \lambda_2\mathbf{y}_t + \lambda_3p_t + \lambda_4i_t + \mathbf{b}'_5x_{t-1} + u_t^{exd} \quad (3.13)$$

where $u_t = [u_t^s, u_t^{ea}, u_t^{cd}, u_t^{id}, u_t^{exd}]' \sim \mathcal{N}(0, \mathbf{D})$ are uncorrelated structural shocks.

Equation 3.9 states that U.S. natural gas supply is influenced by natural gas prices through the contemporaneous structural coefficient α_{qp} . Assuming that both gas supply and real gas prices are expressed in log deviations, the coefficient α_{qp} can be interpreted as the short-run price elasticity of natural gas supply. The structural shock u_t^s is identified as a ‘U.S. natural gas supply shock,’ which can be triggered by geopolitical events, strikes, natural disasters (such as hurricanes), or production decisions.

Equation 3.10 characterizes real economic activity, which is instantaneously affected by natural gas prices via α_{yp} . The second structural shock, u_t^{ea} , corresponds to an ‘economic activity shock’ that reflects unexpected changes in the demand for natural gas driven by overall economic conditions, such as recessions or booms in the U.S. Equation 3.11 models domestic consumption demand. The coefficient β_{qp} represents the short-run price elasticity of natural gas demand, indicating how demand varies in response to price changes. Similarly, β_{qy} characterizes the response of demand to increased economic activity, reflecting how consumption adjusts to changes in the economic environment. The third structural shock, u_t^{cd} , is interpreted as a ‘U.S. natural gas domestic consumption demand shock’.

Lastly, Equations 3.12 and 3.13 capture the demand for gas inventories and exports, respectively. Inventory demand is allowed to respond contemporaneously to natural gas supply, real economic activity, and real gas prices through coefficients ψ_1 , ψ_2 , and ψ_3 , respectively. The term u_t^{id} represents a separate shock to natural gas inventory demand, often described in the literature as a ‘speculative demand shock.’ Similarly, Equation 3.13 allows exports to be affected contemporaneously by those variables as well as by inventories via coefficients λ_1 , λ_2 , λ_3 , and λ_4 . The term u_t^{exd} represents a shock to natural gas export demand, driven by unanticipated fluctuations in global demand for U.S. natural gas exports, international market dynamics, shifts in international gas prices, or changes in trade policies.

3.3.3. Prior information for contemporaneous parameters

This study specifies a set of prior beliefs regarding the elements of the contemporaneous matrix \mathbf{A} , based on economic theory and empirical evidence from previous studies. These priors represent initial assumptions about the parameters before observing the data. The detailed specifications of these priors, along with the sign restrictions for each contemporaneous coefficient, are summarized in Table 3.2.

Table 3.2.: Summary of prior distributions affecting contemporaneous coefficients \mathbf{A}

Parameter	Meaning	Student- t distribution			
		Location	Scale	dof	Restriction
α_{qp}	Natural gas supply elasticity	0.1	0.2	3	$\alpha_{qp} > 0$
α_{yp}	Effect of p on activity	-0.05	0.05	3	$\alpha_{yp} < 0$
β_{qy}	Income elasticity of natural gas demand	0.7	0.2	3	$\beta_{qy} > 0$
β_{qp}	Natural gas demand elasticity	-0.3	0.2	3	$\beta_{qp} < 0$
ψ_1	Effect of q on inventories	0	0.5	3	none
ψ_2	Effect of y on inventories	0	0.5	3	none
ψ_3	Effect of p on inventories	0	0.5	3	none
λ_1	Effect of q on exports	0	0.5	3	none
λ_2	Effect of y on exports	0	0.5	3	none
λ_3	Effect of p on exports	0	0.5	3	none
λ_4	Effect of inventories on exports	0	0.5	3	none

Note: “Location” refers to the mode of the t -distribution, “Scale” represents its standard deviation, and “dof” denotes the degrees of freedom. “Restriction” indicates whether a sign restriction has been enforced. In the second column, p refers to the real natural gas price, q denotes total natural gas supply, and y represents real U.S. GDP.

Priors for parameters of the gas supply equation. Barret (1992) provided an early estimate of natural gas supply elasticity at 0.014, based on an analysis of annual data from 1960 to 1990, highlighting the historically perceived inelastic nature of natural gas supply. Using monthly data from August 1987 to October 2012, Ponce and Neumann (2014) also noted a lack of short-run responsiveness from producers to price changes, a phenomenon attributed to the significant infrastructure investments required to scale production. However, they report a substantial long-run price elasticity of supply at 0.76, suggesting a delayed but significant supply response to price adjustments. Furthermore, Arora (2014) explored monthly data spanning from 1993 to May 2013 and estimated short-run and long-run elasticity at 0.07 and 0.42, respectively. Lastly, Mason and Roberts (2018) examined natural gas production in Wyoming from 1994 to 2012 and found that the price elasticity of intra-well production from previously drilled wells is

highly inelastic at 0.03, while the elasticity of initial or peak-production rates is negative at -0.12.¹³

Based on these findings, this study assumes a truncated Student- t prior for α_{qp} , denoted as $\alpha_{qp} \sim t_{0,\infty}(0.1, 0.2, 3)$, centered at 0.1, with a scale of 0.2 and 3 degrees of freedom. The mode of the distribution is set at 0.1, indicating a prior belief that the most probable value of the short-run supply elasticity is around 0.1, suggesting inelastic but positive responsiveness of supply to price changes. The scale parameter of 0.2 represents moderate uncertainty around this mode, acknowledging variability in empirical estimates and the possibility that the true elasticity may differ due to factors such as infrastructure constraints or market conditions. The degrees of freedom, set at 3, impart heavier tails to the distribution compared to a normal distribution. This accommodates the possibility of more extreme elasticity values observed in the literature. The heavy tails ensure that while the prior centers on 0.1, there remains a non-negligible probability for higher elasticity values, reflecting long-run adjustments and the dynamic nature of natural gas markets.

Priors for parameters of the real economic activity equation. The structural parameter α_{yp} measures the effect of natural gas price fluctuations on real economic activity. As noted by Kilian (2008), energy price shocks can impact the economy by reducing discretionary income, increasing price uncertainty, promoting heightened precautionary savings, and shifting consumption patterns, particularly for energy-intensive goods. These dynamics suggest that the elasticity of economic activity with respect to natural gas prices is expected to be negative. Consistent with Baumeister and Hamilton (2019), this study adopts a truncated Student- t prior for α_{yp} , denoted as $\alpha_{yp} \sim t_{-\infty,0}(-0.05, 0.05, 3)$, centered at -0.05 with a scale of 0.05 and 3 degrees of freedom.

Priors for parameters of the consumption demand equation. The consumption demand equation includes two structural parameters: the short-run price elasticity of natural gas demand (β_{qp}) and the effect of real economic activity on U.S. natural gas consumption demand (β_{qy}). The literature on natural gas demand elasticity offers a range of estimates. For example, Al-Sahlawi (1989) consolidated research from 1966 to 1984, noting short-term price elasticity of demand ranging from -0.05 to -0.95, predominantly around -0.30, and a wider long-run elasticity between -0.12 and -4.60. Joutz et al. (2009) analyzed data from 1980 to 2001, revealing short- and long-run elasticities of -0.09 and -0.18, respectively. Furthermore, R. Bernstein and Madlener (2011) found that the long-run U.S. price elasticity of residential natural gas demand is -0.16, and the short-run equivalent is -0.04. More recently, Joshi (2021) extended this timeline to 2015, observing a broader range of elasticities between -0.062 and -0.547, reflecting evolving market dynamics, particularly the effect of liberalization. Arora (2014) reported short-run elasticities between -0.10 and -0.16 and long-run values from -0.24 to -0.29. Therefore, this

¹³The authors explain this negative coefficient by the endogenous selection of wells: higher prices make less productive wells viable, thereby lowering average productivity.

study assumes a truncated Student- t prior $\beta_{qp} \sim t_{-\infty,0}(-0.30, 0.2, 3)$ centered at -0.30, with a scale of 0.20 and 3 degrees of freedom. Regarding the β_{qy} , the research conducted by Al-Sahlawi (1989) reviewed studies from the mid-1960s to 1984, indicating that the short-term income elasticity of natural gas demand ranges between 0.0 and 1.5, with minimal divergence observed between short- and long-term elasticities. This range was further contextualized by Burke and Yang (2016), who analyzed 44 countries over 1978–2011, predominantly OECD, finding an average income elasticity of 0.70 in a fixed-effects model. Accordingly, this study assumes a truncated Student- t prior for the parameter representing the relationship between income and natural gas demand (β_{qy}). This prior is defined as $\beta_{qy} \sim t_{0,\infty}(0.7, 0.2, 3)$, centered at 0.7 with a scale of 0.2 and 3 degrees of freedom.

Priors for parameters of the inventory and exports equations. Due to the absence of reliable empirical information to construct precise priors for the parameters in these equations, this study follows the approach proposed by Baumeister and Hamilton (2018). Specifically, it adopts non-informative priors, assuming these coefficients follow unrestricted Student- t distributions centered at zero, with a scale parameter of 0.5 and 3 degrees of freedom. This choice of a prior centered at zero reflects a neutral starting point, avoiding any inherent bias toward positive or negative effects. The chosen scale parameter and degrees of freedom allow for a modest degree of uncertainty, thereby giving the data a more significant role in shaping the posterior distributions.

3.4. Data

The dataset comprises monthly data spanning from January 1992 to October 2023. This period captures the influence of market forces on the dynamics of the natural gas market, as elaborated in Section 5.2. The selected variables include total natural gas supply (Q_t), real monthly Gross Domestic Product (GDP) (\mathbf{Y}_t), real natural gas prices (P_t), natural gas inventories (I_t), and natural gas exports (EX_t). Accordingly, the vector of endogenous variables used in the analysis is presented as follows:

$$y_t = [q_t, \mathbf{y}_t, p_t, i_t, ex_t] \quad (3.14)$$

where $q_t = 100 \times \ln(Q_t/Q_{t-1})$, $\mathbf{y}_t = 100 \times \ln(\mathbf{Y}_t/\mathbf{Y}_{t-1})$, $p_t = 100 \times \ln(P_t/P_{t-1})$, $i_t = 100 \times [I_t - I_{t-1}/Q_{t-1}]$, and $ex_t = 100 \times [EX_t - EX_{t-1}/Q_{t-1}]$. Data on real monthly U.S. GDP are obtained from IHS Markit, part of S&P Global, following Neukirchen et al. (2023).¹⁴ U.S. natural gas prices are sourced from the World

¹⁴This choice is necessitated by the fact that official U.S. GDP data are released only on a quarterly basis. According to IHS Markit, their index “is an indicator of real aggregate output that is conceptually consistent with real GDP in the National Income and Product Accounts (NIPA),” employing “calculation and aggregation methods comparable to those of the official GDP from the U.S. Bureau of Economic Analysis” to produce “a monthly index whose variation at the quarterly frequency mirrors that of official GDP, offering a meaningful and comprehensive measure of monthly changes in output” (IHS Markit, 2022).

Bank Commodity Price Database and converted into a real price index using the U.S. Consumer Price Index (CPI) from the U.S. Bureau of Labor Statistics. Data on natural gas market fundamentals, such as supply, working natural gas underground storage, imports, and exports, are sourced from the EIA Monthly Energy Review database. Following Hou and Nguyen (2018), Rubaszek and Uddin (2020) and Rubaszek et al. (2021), all variables are seasonally adjusted using the X-13ARIMA-SEATS method.

Data during the COVID-19 pandemic The disruptive impact of the 2020 pandemic significantly affected U.S. natural gas supply and demand, as well as a broad range of economic indicators. For detailed descriptions and analyses of these disruptions, see Nyga-Łukaszewska and Aruga (2020) and Baumeister (2023). This divergence suggests that structural and reduced-form parameters during the most acute phase of the pandemic, particularly in 2020 and early 2021, should be estimated separately due to the distinct nature of shocks and relationships. However, the limited number of observations available during this period makes estimating a full set of parameters impractical.

Several approaches have been proposed for handling extreme observations in such contexts. Ng (2021) argues that the principal components of economic data now capture both typical economic fluctuations and pandemic-related variations. To address this, Ng proposes adjusting each economic variable by incorporating COVID-19 indicators—such as positivity rates, hospitalizations, and deaths—to create a “de-covid” dataset, which allows for a more accurate estimation of underlying economic factors. Lenza and Primiceri (2022) propose explicitly modeling the increase in shock volatility. Specifically, they introduce a scaling factor in a VAR model, which adjusts the residual covariance matrix during the pandemic period, allowing for different levels of volatility in March, April, and May 2020, with a decay parameter for subsequent months. This approach aims to provide more accurate parameter estimates and predictions by accounting for the elevated uncertainty during the pandemic. Similarly, Carriero et al. (2022) introduce a BVAR model with outlier-augmented stochastic volatility, which combines transitory and persistent changes in volatility to handle extreme observations during COVID-19. This approach models large, infrequent volatility outliers as a separate state, allowing the model to account for sudden spikes in volatility without treating them as permanent. In contrast to these more complex methodologies, Schorfheide and Song (2024) opt for a simpler solution by recommending the exclusion of data points associated with the COVID-19 pandemic in the estimation of their Mixed-Frequency VAR model. This straightforward approach avoids the intricacies and potential complications of modifying the underlying model structure, focusing instead on maintaining the model’s performance by selectively omitting extreme observations. Baumeister and Hamilton (2024) also follow this straightforward approach by excluding extreme values.

Following Schorfheide and Song (2024) and Baumeister and Hamilton (2024), this paper excludes data from March 2020 through February 2021—the period

most affected by the pandemic—from the analysis. This decision is based on the premise that including this data could introduce significant volatility and anomalies into the model, potentially distorting the relationships under study.

3.5. Results

This section presents the findings from the estimated SVAR model for the U.S. natural gas market. Subsection 3.5.1 examines the posterior distributions of the structural parameters, highlighting the impact of the observed data on these estimates. Subsection 3.5.2 discusses the Impulse Response Functions (IRFs), which illustrate the dynamic effects of structural shocks on the model’s variables. Subsection 3.5.3 quantifies the contributions of different shocks to the forecast error variance of each variable in the model. Finally, Subsection 3.5.4 provides a historical decomposition, tracing the cumulative impact of various shocks on U.S. natural gas prices during key periods.

3.5.1. Posterior distributions for structural parameters

Figure 3.1 compares the prior and posterior distributions for the structural parameters in the **A** matrix, with red lines representing the priors and grey histograms representing the posteriors. This comparison evaluates the impact of the observed data on updating the initial beliefs discussed in Subsection 3.3.3 and assesses the extent to which these priors influence the outcomes of the subsequent analysis.

The results reveal that the posterior distribution for the short-run price elasticity of natural gas supply is tightly concentrated around a value close to zero, suggesting the data are quite informative and lead to a substantial revision of the prior belief. The posterior median of this parameter is 0.019, indicating that a 1% increase in price is associated with only a 0.019% increase in the total supply of natural gas in the U.S., reflecting minimal supply adjustments to price changes within the month. This minimal responsiveness is consistent with the findings of Ponce and Neumann (2014), Hou and Nguyen (2018), and Rubaszek et al. (2021), who report that natural gas supply in the U.S. is inelastic. Such inelasticity can be attributed to infrastructure costs, regulatory constraints, and the technical and logistical complexities of rapidly adjusting production levels in response to market fluctuations (Egging & Holz, 2016; Mason & Roberts, 2018). These factors underscore the dominance of physical and technical considerations over economic incentives in short-term supply responsiveness.

For the effect of natural gas prices on U.S. real economic activity, the posterior distribution of α_{yp} is centered near zero, with a median value of -0.004. This implies that increases in the real price of natural gas are associated with only a negligible reduction in real economic activity within a monthly period. This

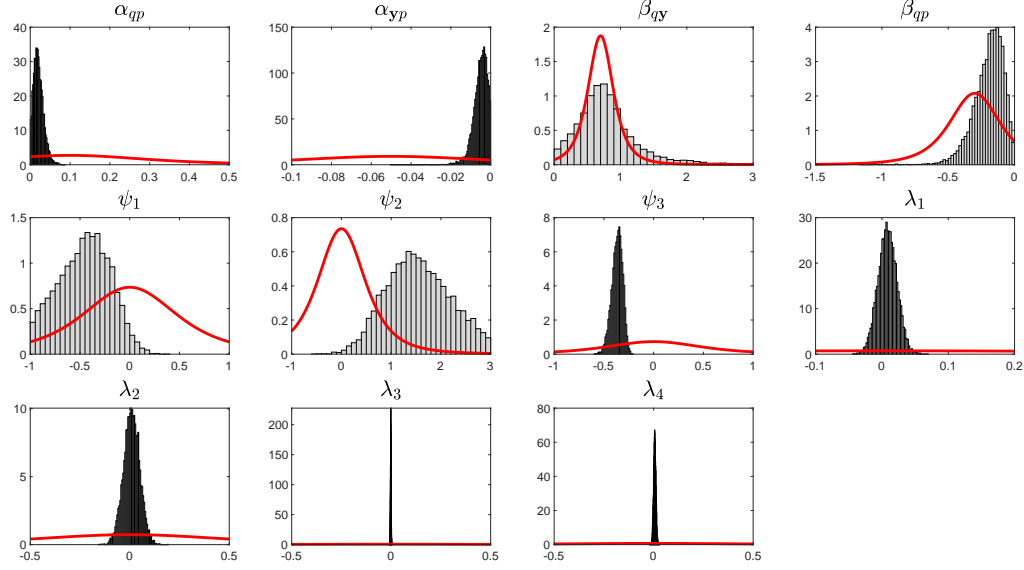


Figure 3.1.: Prior and posterior distributions of the contemporaneous coefficients in the matrix \mathbf{A} .

Note: The solid red curves represent the prior knowledge, and the gray histograms represent the posterior densities.

result aligns with the findings of Cavalcanti and Jalles (2013) and Alexeev and Chih (2021), who observe that gas and oil price shocks have minor effects on U.S. economic growth.

Regarding the domestic consumption equation, the first structural parameter, β_{qy} , represents the impact of economic activity on domestic natural gas demand. While the median value of this coefficient, 0.788, is similar to its prior, the posterior distribution shows a notable shift toward higher values, indicating that the data provide moderate support for the prior belief. This value is consistent with the findings of Burke and Yang (2016), who report that natural gas demand elasticity with respect to GDP ranges between 0.40 and 1.12. The second structural parameter, β_{qp} , measures the price elasticity of natural gas demand. The posterior median of this parameter is -0.177, which is lower than its prior value, indicating that the data provided significant insights into this relationship. This result implies that a 1% increase in natural gas prices leads to a 0.177% decrease in demand, highlighting short-run inelasticity. This estimate aligns with the findings of Labandeira et al. (2017), who report an average short-run price elasticity of -0.180, and is less inelastic than the -0.130 estimated by Arora (2014).

Summary statistics for the posterior estimates of these parameters, along with other relevant magnitudes, are reported in column 1 of Table B.1 in the Appendix.

3.5.2. Impulse response functions

Figure 3.2 presents the posterior medians (pointwise) along with 68% and 90% credible intervals for the impulse response functions (IRFs) up to 16 months, each standardized to reflect a 1% increase in natural gas prices on impact. Specifically, u_t^s represents an unanticipated disruption in the natural gas supply. The IRFs illustrate the dynamic responses of the five endogenous variables to structural innovations.

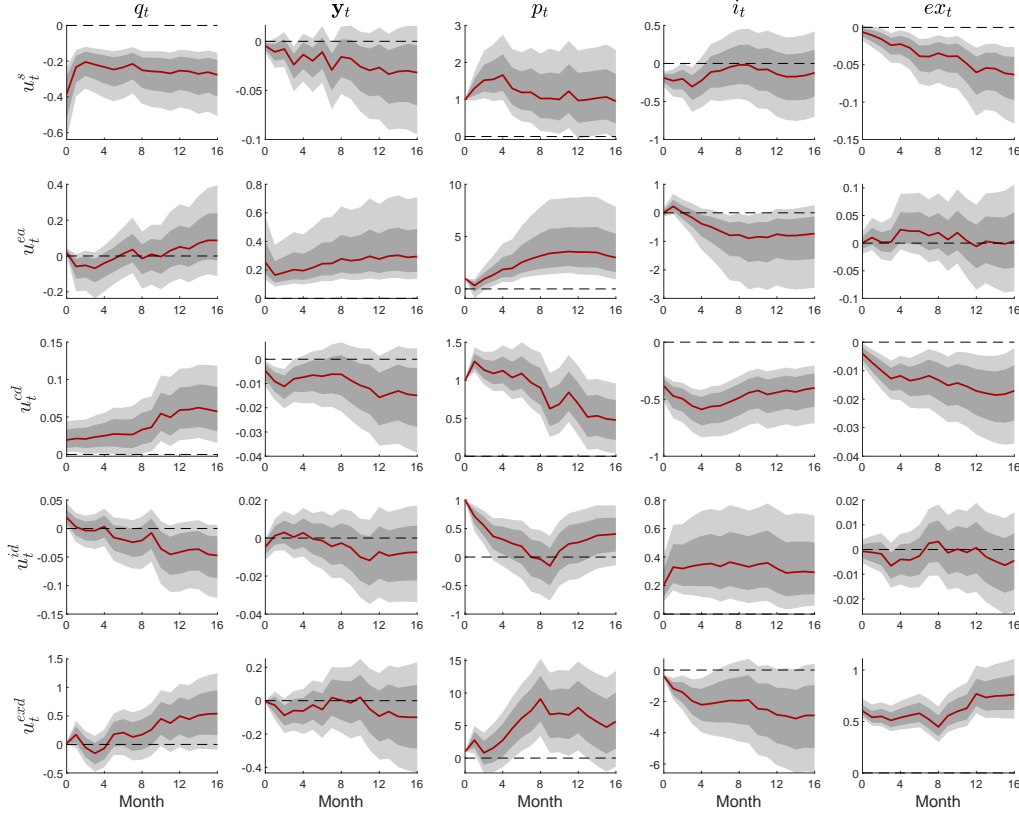


Figure 3.2.: Structural impulse responses

Note: The rows represent the responses to different shocks, denoted as u_t^s (supply shock), u_t^{ea} (economic activity shock), u_t^{cd} (consumption demand shock), u_t^{id} (inventory demand shock), and u_t^{exd} (export demand shock). The columns represent the variables: q_t (total U.S. natural gas supply), y_t (real U.S. GDP), p_t (real gas price), i_t (U.S. gas inventories), and ex_t (U.S. gas exports). The red solid lines represent the Bayesian posterior median, while the dark- and light-shaded grey areas denote the 68% and 90% posterior credible regions, respectively.

First, consider the effect of a negative flow supply shock, as shown in the first row. This shock causes a sharp initial decline in gas supply, which partially reverses within the first three months. This pattern aligns with the principle that supply constraints in one U.S. location, or in imports from a single source, often prompt compensatory increases in production or enhanced import flows from other locations. The results further indicate that a natural gas supply shock lowers real economic activity after a significant lag; however, this effect is insignificant

when considering the 90% credible sets. At the same time, this supply disruption leads to an immediate increase in the real price of natural gas, peaking after three months and then reverting to its initial value after one year. Natural gas inventories are immediately drawn down to mitigate the supply shortfall, though this effect dissipates within four months, as the credible sets return to include zero. Additionally, there is a reduction in natural gas exports, reflecting the decreased availability for foreign markets. These dynamics are consistent with findings from analyses of the U.S. natural gas and oil markets by Hailemariam and Smyth (2019) and Valenti et al. (2023), respectively, and with findings from analyses of the global crude oil market by Kilian and Murphy (2014) and Baumeister and Hamilton (2019).

The second row shows that an unexpected increase in economic activity does not influence natural gas supply. However, this economic shock leads to an increase in the real price of gas, peaking after almost one year. Changes in natural gas inventories are negligible in the short run; however, a drawdown occurs as time progresses. Natural gas exports remain unaffected. These responses to the economic activity shock are generally consistent with the results observed in Rubaszek and Uddin (2020) and Valenti et al. (2023).

The third row shows that a domestic consumption demand shock leads to a slight increase in supply on impact to meet rising demand. This increase continues gradually, peaking at twelve months before stabilizing, suggesting a lagged supply adjustment process in response to the shock. Real gas prices respond positively on impact but start to decrease after the second month, reaching a minimum after one year before stabilizing, likely reflecting market adjustments in response to the increased supply. Economic activity responds to the increase in gas prices with a small, temporary decrease. This finding aligns with Hailemariam and Smyth (2019), who also observed similar economic impacts from gas demand shocks. Inventory levels show a negative response on impact, reaching their lowest level in the fourth month before gradually recovering to their original level after one year. Meanwhile, natural gas exports exhibit a relatively small negative response to the positive demand shock, highlighting a shift in gas flows to meet domestic demand.

The fourth row examines responses to a positive shock to inventory demand, often characterized in the literature as a speculative demand shock. Such a shock could arise from increased precautionary demand for natural gas, driven by heightened uncertainty about future demand or supply conditions (see Kilian and Murphy (2014)). The results reveal that this shock is associated with an immediate jump in the real price of natural gas, which quickly diminishes and becomes statistically insignificant by the fourth month, indicating a short-lived market reaction. This shock also leads to a persistent increase in gas inventories. These findings are consistent with those of Kilian and Murphy (2014), who observe that oil prices initially overshoot in response to such shocks before gradually declining, with minimal effects on supply and global economic activity.

3. Revisiting the Dynamics of the U.S. Natural Gas Market

The last row presents the IRFs to an export demand shock. Natural gas supply shows no immediate reaction to this shock but begins to increase gradually thereafter. On impact, the real price of natural gas responds positively and continues to exhibit a substantial and statistically significant response in the following months, though this significance diminishes after one year. These trends suggest that market adjustments, primarily driven by changes in supply-demand dynamics from export activities, take several months to fully stabilize. In contrast, gas inventories initially decrease to meet the heightened export demands, but this decrease becomes statistically insignificant by the fourth month, as indicated by the 90% credible sets.

3.5.3. Forecast error variance decomposition

This section quantifies the impact of each shock on the variables in the estimated SVAR model by calculating the variance of the model's forecast error and determining the share of that variance attributable to each shock at different time horizons. The results, presented in Table 3.3, show the average contributions of each shock to the overall variation in natural gas supply, real economic activity, real price of natural gas, natural gas inventories, and natural gas exports, expressed in percentage terms.

Table 3.3.: Percent contribution of shocks to the overall variability of each variable

Horizon	Natural gas supply					Economic activity					Real natural gas price				
	u_t^s	u_t^{ea}	u_t^{cd}	u_t^{id}	u_t^{exd}	u_t^s	u_t^{ea}	u_t^{cd}	u_t^{id}	u_t^{exd}	u_t^s	u_t^{ea}	u_t^{cd}	u_t^{id}	u_t^{exd}
1	94.29	1.24	1.77	1.76	0.34	0.45	95.97	1.62	1.30	0.16	8.48	3.61	54.06	31.54	0.73
2	92.33	1.52	2.04	2.13	1.18	0.75	94.21	2.03	1.65	0.80	8.82	4.67	52.45	31.09	1.65
3	90.96	1.86	2.33	2.40	1.67	2.06	91.53	2.55	1.99	1.12	8.86	5.23	51.19	31.41	2.00
6	85.88	3.04	3.12	3.96	3.28	3.69	87.17	3.26	2.88	2.14	10.04	6.87	48.27	29.92	3.75
12	76.30	4.99	5.80	6.70	5.37	6.88	77.74	4.99	4.80	4.70	10.54	7.63	46.16	28.56	6.15
16	74.57	5.54	6.13	7.11	5.81	7.38	76.01	5.40	5.10	5.16	10.71	7.95	45.60	27.92	6.81

Horizon	Natural gas inventories					Natural gas exports				
	u_t^s	u_t^{ea}	u_t^{cd}	u_t^{id}	u_t^{exd}	u_t^s	u_t^{ea}	u_t^{cd}	u_t^{id}	u_t^{exd}
1	3.16	1.22	76.90	16.62	1.36	1.01	0.67	2.16	0.47	94.94
2	3.47	2.51	75.20	16.47	1.70	1.59	1.18	2.99	0.78	92.67
3	4.27	3.29	73.27	15.98	2.38	2.54	1.47	3.75	1.83	89.59
6	6.07	5.44	68.79	15.60	3.16	4.62	3.62	4.59	2.83	83.50
12	7.44	7.22	63.57	15.71	5.04	7.19	5.96	5.74	5.12	75.14
16	7.82	7.48	62.34	15.91	5.43	7.92	6.44	6.11	5.89	73.73

Note: This table provides posterior median estimates of the contribution of each shock to the forecast error variance of each variable. Credibility sets are available in Table B.2 in the Appendix. Horizons are expressed in months. The terms u_t^s , u_t^{ea} , u_t^{cd} , u_t^{id} , and u_t^{exd} refer to supply, economic activity, consumption demand, inventory demand, and exports demand shocks, respectively.

For the real gas price at the 1-month horizon, consumption demand shocks account for 53.85% of the variation, followed by inventory demand shocks, which contribute an additional 32.07%. By the 16-month horizon, these contributions adjust slightly to 45.35% for consumption demand and 28.17% for inventory demand, reflecting a sustained but diminishing influence on gas price movements.

Moreover, the impact of supply shocks, economic activity shocks, and export demand shocks on price variations is minimal initially but increases gradually, suggesting a prolonged adjustment process. Specifically, their combined impact accounts for less than 13% of the price variation initially but becomes more significant by the 16-month horizon, with economic activity shocks increasing from 3.57% to 7.96% and export demand shocks from 0.70% to 6.84%.

These results can be compared with those discussed in Section 5.2. According to Arora and Lieskovsky (2014), supply shocks initially have a minimal impact (3.2%) that increases significantly in the long run (16%), and the ‘other’ shock, which includes the demand and supply of natural gas for speculative or precautionary purposes, dominate the short term (76%). In contrast, this study finds a relatively higher effect from supply shocks in the short run and a much lower effect from speculative demand shocks. The findings from Rubaszek et al. (2021) align more closely with this study regarding the significant role of consumption demand shocks and inventory demand shocks. However, Rubaszek et al. (2021) reports a stronger effect in both the short run (79%) and the long run (65%) for consumption demand shocks, with lesser impacts from inventory demand shocks (12% in the short run and 19% in the long run). Compared to Wiggins and Etienne (2017), who report a balanced contribution from supply and aggregate income shocks (20%–30%), this study initially finds these factors to play a lesser role, with their significance increasing over time. The discrepancies between this study’s results and those reported by Rubaszek et al. (2021) and Wiggins and Etienne (2017) may be attributed to differences in data frequency or model specifications.

Regarding the other endogenous variables, Table 3.3 indicates that the variation in natural gas supply is predominantly driven by supply shocks (u_t^s), accounting for 94% on impact and 75% in the long run. This underscores the significant role of supply conditions in the short term, which marginally decreases as other factors come into play over time. In the case of natural gas inventories, consumption demand shocks (u_t^{cd}) are initially the most influential, explaining 76.34% of the variation, but this influence diminishes to 61.87% by the 16th month, indicating a sustained and significant impact over time. Finally, natural gas exports are primarily influenced by export demand shocks (u_t^{exd}), which account for 95.09% of the variation initially, decreasing to 73.18% by the 16th month, underscoring the critical role of external market demands in shaping U.S. natural gas export volumes.

3.5.4. Historical decomposition

The estimates obtained from structural IRFs and structural FEVDs describe the average movements in the U.S. gas market over the analyzed period, representing unconditional expectations. The main objective of this section is to decompose the movements in real gas prices and trace the cumulative effects of each shock from January 2022 to October 2023. This period was marked by escalating geopolitical tensions triggered by the Russian invasion of Ukraine in early 2022,

3. Revisiting the Dynamics of the U.S. Natural Gas Market

which significantly increased U.S. natural gas exports to Europe and sparked policy discussions concerning the impact of these exports on U.S. gas price fluctuations in 2022 (see EIA (2023a) and EVA (2023)). Figure 3.3 presents the historical decomposition of natural gas price movements from January 2022 to October 2023.

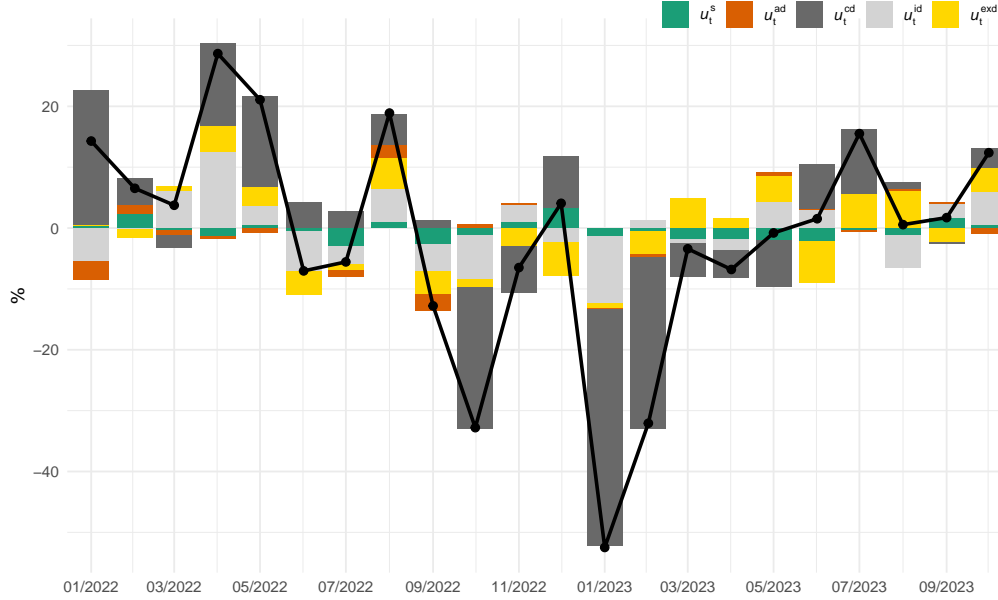


Figure 3.3.: Historical decomposition of U.S. real natural gas price movements from January 2022 to October 2023

Note: Each bar in the graph represents the median estimate of historical contribution of separate shocks—supply (u_t^s), aggregate demand (u_t^{ad}), consumption demand (u_t^{cd}), inventory demand (u_t^{id}), and export demand (u_t^{exd})—for each month during the specified period. The colors correspond to these specific shocks, as labeled directly on the figure. The solid black line represents the logarithmic changes in the real prices of U.S. natural gas.

The results reveal that natural gas dynamics during this period were predominantly influenced by consumption demand shocks (dark gray bars) and inventory demand shocks (light gray bars). For example, early 2022 experienced notably positive cumulative effects from consumption demand shocks due to weather-induced spikes in natural gas usage in the Northeast and Midwest. Speculative demand shocks also contributed positively, particularly in March and April 2022, likely due to low storage levels at the onset of the injection season. Similarly, throughout the first half of 2023, fluctuations in gas prices were primarily driven by domestic consumption shocks and inventory dynamics. The marked decline in gas prices, especially in January and February—typically peak months for heating—was largely due to milder-than-average temperatures, which reduced consumption in the residential and commercial sectors (Fleury, 2024).

The findings also show that accumulated export demand shocks (yellow bars) consistently influenced gas price dynamics throughout the period, with impacts

alternating between positive and negative across different months. For example, these shocks contributed to price spikes in April, May, and August 2022, which were associated with increased LNG exports to Europe during these months.¹⁵ Conversely, they also contributed to the price declines in June, July, and other months of 2022, which can be attributed to the explosion and subsequent shutdown of the Freeport LNG export terminal.¹⁶ This incident led to a significant reduction in U.S. LNG exports, contributing to a domestic surplus of natural gas. In contrast, the results indicate that accumulated export demand shocks have driven much of the gas price increases since March 2023. This rise could be attributed to the reactivation of the Freeport terminal in early 2023, alongside increased pipeline exports to Mexico during the summer, marking a return to positive contributions from exports to natural gas price fluctuations. However, the decline in export demand shocks in June 2023 can be explained by extensive maintenance activities at key LNG export facilities. For example, the Sabine Pass LNG terminal underwent major maintenance, reducing its feed gas deliveries from an average of 4.6 Bcf/d in May to nearly 3 Bcf/d in June. Additionally, the Freeport LNG plant in Texas faced operational issues in mid-June, further lowering overall feed gas deliveries (S&P Global Commodity Insights, 2023). This underscores how maintenance events at export infrastructure can affect price fluctuations.

Overall, the historical decomposition of U.S. natural gas prices from 2022 to 2023 highlights the consistent and substantial impact of accumulated demand-side shocks as the primary drivers of gas price dynamics. The analysis further shows that within these demand-side shocks, domestic consumption demand and inventory demand shocks were the dominant influences. Additionally, while less dominant, export demand shocks also played a crucial role in shaping price dynamics. Significant export shocks often correlated with movements in gas prices, with increases in export shocks generally aligning with upward price movements.

In addition to the 2022–2023 analysis, further investigations are conducted into the historical decomposition of natural gas price fluctuations during two other significant periods. The first examination focuses on 2005, specifically analyzing the impact of Hurricanes Katrina and Rita in August of that year on U.S. natural gas price dynamics. The results, presented in Figure B.1, show that the price increases in August, September, and October 2005 were primarily driven by natural gas supply shocks. This can be attributed to the loss of offshore gas production following the hurricanes, which caused a more than 20 percent drop in domestic U.S. gas production. In the remaining months of 2005, consumption demand and speculative demand shocks were the primary drivers of gas price

¹⁵For example, according to the EIA monthly statistics, U.S. LNG exports to the Netherlands in August 2022 (50,020 MMcf) surged to the highest level of the year, marking a 53% increase compared to July (32,637 MMcf) and 62% higher than September (30,924 MMcf), illustrating a significant spike in U.S. LNG exports to Europe during this month.

¹⁶Freeport LNG is a U.S. liquefaction and export facility for Liquefied Natural Gas (LNG) located in Freeport, Texas. It ranks as the seventh-largest LNG export facility globally and the second-largest in the United States. Additional details about this terminal and the incident that occurred in June 2022 can be found on its official website.

3. Revisiting the Dynamics of the U.S. Natural Gas Market

dynamics. These findings demonstrate that supply shocks, such as those caused by hurricanes, lead to significant price increases in the immediate aftermath, but their effects diminish quickly, with demand factors regaining dominance in the subsequent months.

The second analysis, covering January 2015 to December 2017, evaluates the relative importance of various shocks, with a particular focus on export demand shocks. This period is significant due to the rapid expansion in export capacity, which led to the U.S. becoming a major gas exporter by 2017. The findings, presented in Figure B.2, underscore the evolving impact of export dynamics on gas price fluctuations. Overall, the results indicate that during this period, price dynamics were primarily driven by shocks from consumption demand, speculative demand, and natural gas supply. In terms of export demand shocks, the results reveal that in 2015, accumulated export shocks had a minimal impact on gas price dynamics. However, from the second half of 2016 onwards, there is a notable increase in the influence of export shocks on gas prices. Additionally, the analysis identifies a negative export demand shock in August 2017, likely due to the impact of Hurricane Harvey. The hurricane caused widespread disruptions, including the closure of several regional ports by the U.S. Coast Guard on August 28, which halted LNG exports, particularly from Cheniere Energy's Sabine Pass facility, where no LNG tankers departed for several days. Moreover, pipeline flows from Texas to Mexico decreased due to the shutdown of compressor stations (NGI, 2017). These findings suggest that the influence of export demand shocks has grown over time, corresponding with the expansion of U.S. natural gas export infrastructure.

3.6. Sensitivity Analysis

This section presents a series of sensitivity analyses to evaluate the robustness of the SVAR model's findings for the U.S. natural gas market. Subsection 3.6.1 assesses the impact of excluding observations from the COVID-19 pandemic period on the model's results. Subsection 3.6.2 investigates how the findings are influenced by the shale gas revolution, focusing on data from 2009 onwards. Finally, Subsection 3.6.3 examines the effects of using weaker priors for short-run supply and demand elasticities, evaluating how these adjustments influence the posterior distributions and impulse response functions.

3.6.1. Sensitivity to the effects of excluding pandemic-related observations

This subsection evaluates the impact of excluding observations from March 2020 to February 2021, a period significantly affected by the COVID-19 pandemic. To investigate whether this exclusion alters the results, two exercises are conducted:

The first exercise involves a pre-pandemic analysis, where the model is estimated using data only up to December 2019. The posterior medians for the contemporaneous coefficients in \mathbf{A} are reported in the column labeled “S1” in Table B.1. Posterior IRFs are presented in Figure B.3 in the Appendix. The results reveal that the magnitudes of the structural parameters and the IRFs are very similar to those obtained in the baseline analysis, except for the IRFs related to export shocks, which show significance only in the short run. This difference in the response of prices to export shocks may suggest an increased sensitivity of U.S. gas prices to export shocks in recent years, particularly in 2022 and 2023.

The second exercise estimates the model using the entire sample period from January 1992 to October 2023, without excluding any observations. The posterior medians for the contemporaneous coefficients in \mathbf{A} are reported in the column labeled “S2” in B.1, and the posterior IRFs are plotted in Figure B.4 in the Appendix. The results show that while the structural parameters are largely similar to those in the baseline model, the IRFs reveal some counterintuitive outcomes, particularly in the response of economic activity to various shocks. For instance, the findings suggest that a reduction in gas supply, which typically increases gas prices, appears to boost U.S. economic activity (as shown in the (1,2) panel of Figure B.4). Given these results, caution is advised when interpreting the findings from this full-sample analysis. These anomalies imply that external disruptions, such as pandemics, can significantly alter traditional economic responses, highlighting the need for adjustments in economic modeling and policy considerations during such periods.

Overall, these results underscore the importance of adapting models to account for the unique effects of such disruptions in order to avoid counterintuitive economic responses. For subsequent sensitivity analyses, the model will continue to exclude observations from March 2020 to February 2021, following the approach used in the baseline analysis, to ensure consistency in evaluating the model’s robustness.

3.6.2. Sensitivity to the effects of the shale gas revolution

The baseline analysis of this study spans the period from 1992 to 2023, a time-frame selected to comprehensively examine the factors influencing U.S. gas prices following the deregulation of the U.S. natural gas market. To assess the sensitivity of the baseline results, this exercise uses data from January 2009 onward. This approach aligns with literature focusing on this period to examine the effects of the shale gas revolution, as seen in studies by Arora and Lieskovsky (2014), Geng et al. (2016a), Hailemariam and Smyth (2019), and Hu et al. (2020).

Corresponding summary statistics of the coefficients from the contemporaneous matrix are labeled as “S3” in Table B.1. Under this shorter sample, the posterior median of demand elasticity is relatively smaller at -0.130. This finding aligns with Arora (2014), who observe that demand elasticity becomes slightly more inelastic after the shale revolution, which could be explained by less adjustment

in consumption behavior when prices are low compared to when they are high. This result could also be attributed to the reduced impact of both the income and substitution effects. When prices are low, the expenditure on natural gas constitutes a smaller portion of consumers' budgets, leading to a lesser impact on their overall purchasing power, thus minimizing the income effect. Additionally, the incentive to switch to substitutes is reduced because alternatives like coal have become less competitive, leading to a greater reliance on natural gas and thereby weakening the substitution effect (Mason et al., 2015). The results also show that the posterior median of supply elasticity remains low at 0.024. This low supply elasticity is consistent with survey evidence for oil shale producers, as summarized by Golding (2019), who explains that U.S. shale producers are unlikely to respond quickly to price increases due to a sector-wide focus on achieving returns and positive cash flow, along with extensive hedging to secure revenue targets. Golding also notes that large public companies face investor pressure to maintain spending discipline, while smaller firms, though more likely to increase production, have limited impact due to capital constraints and less prolific acreage. The IRFs, presented in Figure B.5 in the Appendix, show the same qualitative pattern as the baseline. However, the response of real gas prices to supply and demand shocks becomes less persistent. This change could reflect a more adaptable U.S. gas market, primarily influenced by technological and infrastructural advances during the shale gas revolution. These advances have facilitated quicker adjustments to supply shocks and demand changes.

3.6.3. Sensitivity to alternative prior assumptions and model identification

This subsection evaluates the robustness of the baseline model to alternative assumptions regarding prior distributions and model identification strategies. Specifically, it investigates whether the key findings are sensitive to changes in these assumptions. Two exercises are conducted: first, by employing significantly weaker priors for the short-run supply and demand elasticities; and second, by incorporating non-Gaussianity as an additional source of identification.

The first exercise assesses the influence of prior assumptions on the posterior distributions of key structural parameters, specifically the short-run supply elasticity α_{qp} and the demand elasticity β_{qp} . In contrast to the baseline analysis, which employs scale parameters $\sigma^{\alpha_{qp}} = 0.2$ and $\sigma^{\beta_{qp}} = 0.2$ for the supply and demand price elasticity coefficients, respectively, this analysis tests the effect of significantly weaker priors by setting both $\sigma^{\alpha_{qp}}$ and $\sigma^{\beta_{qp}}$ to 1.0. This adjustment increases the variance of the priors for these two coefficients by a factor of 25 compared to the baseline specification, thereby reducing the influence of prior information on the estimation outcomes. The posterior medians of the supply and demand elasticities are presented in column "S4" of Table B.1, and the IRFs are shown in Figure B.10 in the Appendix. Overall, both the structural parameters and the IRFs remain relatively unchanged compared to the results obtained from

the baseline specification. This observation aligns with the findings of Baumeister and Hamilton (2019), who note that many key conclusions of their Bayesian model change very little when substantially less weight is placed on different components of the prior information.

The second exercise incorporates non-Gaussianity as an additional source of identification, following the identification strategy proposed by Braun (2023). This approach leverages the statistical properties of the error terms by assuming that the structural shocks are mutually independent and display some degree of non-Gaussianity. It integrates economically motivated prior distributions, as introduced by Baumeister and Hamilton (2019), with identification by non-Gaussianity. Accordingly, this approach ensures that economic interpretations remain relevant throughout the analysis. The structural shocks are modeled using Dirichlet Process Mixture Models, where each shock’s marginal distribution is estimated nonparametrically. This allows the analysis to reduce the reliance on strong economic priors, making the model more data-driven. Summary statistics for this exercise are presented in column “S5” of Table B.1, and the corresponding IRFs are shown in Figure B.9 in the Appendix. The results closely align with those from the baseline analysis, indicating that the key findings are robust even when non-Gaussianity in the error terms is utilized as an additional source of identification.

The outcomes of these exercises demonstrate that the baseline results are not highly sensitive to the specific identifying assumptions employed. Whether the priors on the short-run elasticities are weak or strong, or whether non-Gaussianity is incorporated as an additional identification strategy, the key structural parameters and the dynamic responses of the system remain largely consistent.

3.7. Conclusion

This paper proposes a Structural Vector Autoregression (SVAR) model that incorporates natural gas imports and exports to provide a more comprehensive understanding of U.S. natural gas market dynamics. The model extends previous studies by allowing for a clearer distinction between domestic and export-driven demand shocks. The findings contribute to the ongoing discourse by providing new insights into the relative importance of various structural shocks and revisiting the estimates of natural gas supply and demand elasticities.

The findings of this study reveal the significant inelasticity of natural gas supply in the short run, as reflected by a near-zero elasticity estimate—a pattern consistent with previous research (e.g., Labandeira et al., 2017; Ponce & Neumann, 2014). This limited responsiveness to price changes reveals the infrastructural, regulatory, and technical constraints that impede short-run adjustments in supply. Similarly, the small price elasticity of demand indicates limited consumer responsiveness

3. Revisiting the Dynamics of the U.S. Natural Gas Market

to price fluctuations within the month. These results suggest that short-term economic and policy interventions may have limited effectiveness in altering natural gas supply and demand. The impulse response analysis reveals that a negative supply shock leads to an immediate but short-lived spike in prices, with inventories being drawn down and exports temporarily reduced, while an unexpected rise in economic activity gradually increases prices without affecting supply. In response to a domestic consumption demand shock, prices initially rise but decline after two months, reaching a low point around one year as supply adjusts. Speculative inventory demand shocks cause a temporary increase in prices, followed by stabilization. Export demand shocks result in a price increase in the short and medium term.

The FEVD analysis indicates that short-term fluctuations in natural gas prices are predominantly driven by consumption and inventory demand shocks, which together account for over 85% of the price variation at the one-month horizon. Over time, the influence of export demand shocks, supply, and economic activity becomes more pronounced, reflecting a gradual adjustment process in the market. Historical decomposition results for the period from 2022 to 2023 suggest that natural gas price dynamics were largely shaped by demand-side factors, particularly domestic consumption and inventory demand shocks. Additionally, export demand shocks, though less dominant, consistently influenced natural gas prices throughout this period. These shocks alternated between positive effects, driven by increased exports, and negative effects, resulting from maintenance disruptions at key LNG facilities that caused temporary declines in exports. The analysis of past events, such as the hurricanes in 2005, highlights how supply shocks from natural disasters or other large-scale disruptions can lead to significant immediate price increases, though their impact tends to diminish quickly as demand factors regain influence in the following months. This underscores the dominant role of demand-side factors in shaping natural gas price dynamics.

An important consideration in this analysis is the exclusion of COVID-period observations from the sample, along with the pooling of pre- and post-COVID data. Sensitivity analyses show that this approach prevents counterintuitive economic responses that would occur if these observations were included. For example, retaining the COVID-period data results in findings that suggest that a reduction in gas supply—which typically increases gas prices—would instead stimulate U.S. economic activity. Similarly, it suggests that an export demand shock would lead to a sharp decline in economic activity. Dropping extreme observations has proven effective in avoiding these counterintuitive outcomes.

The main implication of this study is that adapting structural models developed for the global oil market to regional energy markets, such as the U.S. and European natural gas markets, requires specific adjustments to model specifications. These adjustments are necessary to ensure that the unique domestic and external dynamics of regional markets are accurately captured, leading to more informed economic and policy decisions.

One limitation of this paper's model is that it does not incorporate wellhead production rates and the utilization of pipeline and LNG export infrastructure. Future research could extend this model by including these rates. A potential avenue for future research could examine whether the nonlinear dynamics of the U.S. natural gas market are driven by these utilization rates. In this case, these rates could be used as a threshold variable, with the analysis divided into two regimes based on whether the rates are below or above a certain threshold.

4. Global Natural Gas Market Integration: The Role of LNG Trade and Infrastructure Constraints

4.1. Introduction

International trade in natural gas has traditionally been divided into three main regional markets: Asia, Europe, and North America (Economides & Wood, 2009; Geng et al., 2014; Melamid, 1994). Historically, this segmentation has been driven by limited Liquefied Natural Gas (LNG) transport capacity between. However, the literature suggests that these markets are gradually becoming more integrated (Li et al., 2014; Neumann, 2009). Market integration refers to the extent to which regional markets share information and align prices (Fackler & Goodwin, 2001; McNew & Fackler, 1997). Investigating this phenomenon has significant implications for supply security, as market participants in one region must increasingly consider conditions in other regions to ensure their own supply.

The integration process among the three regional gas markets has been driven by several key factors. First, some regions have experienced surplus natural gas production, while others have seen increasing consumption.¹⁷ This imbalance has necessitated expanding the international gas trade, with LNG emerging as a critical solution. Increasing export capacities and the growth of the LNG fleet have significantly improved the technical and economic feasibility of inter-regional trade (Barnes & Bosworth, 2015; Li et al., 2014). Second, many commercial agreements have shifted from traditional oil-indexed pricing in long-term contracts to greater reliance on hub-based pricing. For example, the share of Gas-on-Gas (G-o-G) competition¹⁸ in global gas consumption rose from 31% in 2005 to 49% in 2021, while oil indexation declined from 24% to 19% over the same period (IGU, 2021). The literature also suggests that the relationship between oil and natural gas prices has become more volatile, indicating a decoupling of the two commodities (Chiappini et al., 2019; Neumann, 2009). At the same time, the G-o-G competition has seen a rise in spot and short-term transactions, where shifts in regional supply and demand prompt LNG exporters to redirect spot volumes (IGU, 2021). These

¹⁷Figure C.1 in the Appendix compares the development of gas production and consumption between 2012 and 2022. It shows that production has significantly increased in export regions that do not have pipeline connections to the main gas import regions. This has been facilitated by the export of LNG.

¹⁸Gas-on-Gas (G-o-G) competition refers to a pricing mechanism in which natural gas prices are determined by supply and demand dynamics in competitive markets (GIIGNL, 2022; IGU, 2021).

4. Global natural gas market integration

developments have increased market liquidity, enhanced opportunities for spatial arbitrage, and boosted the presence of physical traders. Third, advancements in shale gas exploration technology have fueled a rapid increase in production in North America, commonly referred to as the shale gas revolution. As a result, the United States began exporting LNG in 2016 and has quickly become a major player in the global market, with export capacities expanding year over year (Farag, 2024; Melikoglu, 2014; Wiggins & Etienne, 2017).¹⁹ Finally, European and Asian countries have adopted supply diversification strategies that combine pipelines and LNG imports to mitigate supply risks (Farag & Zaki, 2021a; Hinchey, 2018; Ritz, 2019).

Several studies have focused on global gas market integration, primarily relying on price data to measure the degree of integration. The hypothesis is that the greater convergence between gas prices signifies stronger spatial arbitrage and higher levels of market integration.²⁰

Silverstovs et al. (2005) investigated the integration of the North American, European, and Asian gas markets using monthly prices from November 1993 to March 2004. Their cointegration analysis provided evidence of integration between the Asian and European markets, while the North American market remained decoupled. The authors explain that the European and Asian natural gas markets are integrated due to similar long-term contracts and oil-indexed pricing mechanisms, which align price movements in these regions. In contrast, the North American market operates under a different, more competitive pricing system that decouples it from the oil-linked European and Asian markets, resulting in a lack of integration across the Atlantic. A similar conclusion was reached by Li et al. (2014), who examined the integration of international natural gas markets across North America, Europe, and Asia from 1997 to 2011, using a convergence test and Kalman filter analysis.²¹ In contrast, Neumann (2009) found evidence of increasing integration between North American and European gas markets. Using the Kalman filter to analyze data from 1999 to 2008, Neumann observed rising price convergence, particularly after 2003. This trend was attributed to the role of LNG in linking previously segmented markets across the Atlantic during this period.

However, Nick and Tischler (2014) pointed out that linear cointegration models, which assume symmetric adjustments, may be misspecified for natural gas markets where adjustments to price deviations can be asymmetric. Factors such as transaction costs and different responses to widening or narrowing spreads contribute

¹⁹For example, the U.S. significantly expanded its LNG liquefaction capacity, from 16 bcm in 2016 to 131 bcm in 2022, accounting for 62% of the global increase during this period (Rystad Energy, 2023).

²⁰For a detailed review of the empirical methods used to examine the degree of spatial integration in natural gas markets, see Dukhanina and Massol (2018) and Farag and Ruhnau (2024).

²¹The convergence test used in Li et al. (2014) is the Phillips and Sul (2007) test, which examines whether natural gas prices across regions are moving toward a common long-term trend. The Kalman filter is applied to estimate time-varying relationships between price pairs, allowing the authors to track the gradual evolution of these relationships.

to this asymmetry, making nonlinear cointegration a more appropriate approach. To address this, they examined the degree of integration between North American and European gas prices using a nonlinear cointegration approach that accounts for transaction costs. Their results provided strong evidence of nonlinearity in the sub-samples analyzed (2000–2008 and 2009–2012). More recently, Chiappini et al. (2019) applied the momentum-threshold autoregression (M-TAR) model of Enders and Siklos (2001) with daily price data from 2004 to 2018, confirming the presence of nonlinearities and asymmetries in price adjustments in the global gas market. Their analysis also shows that the degree of interdependence between the North American and European markets has increased, whereas this has not occurred between the North American and Asian markets.

The reviewed literature shows that conclusions on regional gas market integration depend on the methods used and the key market mechanisms at play during the analyzed period. In terms of methods, accurately modeling this convergence requires accounting for transaction costs and asymmetric dynamics in the adjustment process. Regarding market mechanisms, LNG trade offers more opportunities for spatial arbitrage, contributing to increased price convergence among the North American, European, and Asian markets. However, it remains unclear how recent developments in the global gas market—especially the U.S.’s emergence as a major LNG exporter since 2016 and the supply disruptions caused by geopolitical tensions between Europe and Russia, amid a tight LNG market—have impacted the market integration.

This paper contributes to the literature by analyzing global gas market integration from 2016 to 2022²², using daily futures prices across the three main regional gas markets. The North American market is represented by the Henry Hub (HH) benchmark, the Northwest European market by the Title Transfer Facility (TTF) benchmark, and the East Asian market by the East Asian Index (EAX). This analysis is particularly relevant for two main reasons. First, this period coincides with the U.S.’s entry into the global LNG trade, a development that may have reshaped relationships within the global gas market. Therefore, this study provides new insights into cointegration under different market conditions. Second, various factors during this period have supported arbitrage in the global gas market, particularly between the U.S. and the other two regions, driven by the expansion of U.S. LNG export infrastructure and the rise in spot LNG trade (Rystad Energy, 2023). However, this period has also been marked by factors that hinder arbitrage, such as the U.S. LNG export infrastructure and European import infrastructure operating at maximum capacity. To capture the potential effects of these dynamics, we conduct the cointegration analysis over two subsamples, splitting the data on October 1, 2021. This timing aligns with significant market disruptions, including Russia’s reduction of gas flows to Europe and the tightening global LNG market due to supply outages and capacity constraints (Fulwood et al., 2022; McWilliams et al., 2023).

²²The sample period ends in 2022 due to data availability constraints.

4. Global natural gas market integration

Our results show that during the first subsample (January 2016 – September 2021) the Asian and European gas prices are cointegrated. This finding is consistent with previous studies, such as Chiappini et al. (2019), which also identified cointegration between European and Asian gas markets in earlier periods. The persistence of this integration during our sample period can be attributed to the growth of LNG trade, which has facilitated arbitrage opportunities between Europe and Asia. Both regions are subject to global supply-demand dynamics and spot market pricing mechanisms, reinforcing their integration. While Chiappini et al. (2019) found no cointegration between American and Asian prices but did find cointegration between American and European prices, our analysis reveals that American prices were cointegrated with both European and Asian prices during this period. These differences likely reflect changes in the global gas market, particularly the U.S.’s transition to a net exporter, which has reshaped its relationship with the European and Asian markets. However, our findings are consistent with those of Nick and Tischler (2014) and Chiappini et al. (2019), supporting the conclusion that regional gas prices are nonlinearly cointegrated. This implies that adjustments toward equilibrium happen at different speeds based on the direction of deviation from the equilibrium.

In the second subsample (October 2021 – November 2022), we find no evidence of linear cointegration for any price pairs based on the Engle-Granger approach. However, when we apply the Enders-Siklos threshold cointegration method, we find evidence of threshold cointegration only for the EAX-TTF price pair. This suggests the presence of a non-linear, asymmetric relationship between these two markets during the second subsample period, while the other pairs (HH-TTF and HH-EAX) do not exhibit such a relationship. The lack of cointegration between the American and European markets may be attributed to LNG infrastructure congestion during this period, which acts as a physical barrier to arbitrage.²³ To further investigate the decoupling of the American and European gas markets observed in the second subsample, we examine the relationship between the HH-TTF price spread and LNG infrastructure congestion. Using the Toda and Yamamoto (1995) approach, we analyze the predictive relationship between LNG infrastructure congestion and the HH-TTF price spread. In the second subsample, we find significant Granger causality from congestion to the HH-TTF spread, suggesting that infrastructure constraints are influencing price differentials. These findings underscore the critical role of infrastructure capacity in facilitating or impeding market integration between regional gas markets.

The remainder of the paper is organized as follows: Section 4.2 outlines the conceptual background. Following this, Section 4.3 discusses structural changes in the regional gas market, focusing on regional price patterns, LNG infrastructure utilization, and LNG trade dynamics in Northwest Europe (NWE) and East Asia.

²³For detailed data on LNG terminal utilization rates during this period, see Figure 4.2 in Section 4.3, which illustrates the increase in European LNG import terminal utilization and U.S. export terminal capacity constraints.

Section 5.4 details the methodology. Section 4.5 presents the empirical results of our analysis. Finally, Section 4.7 concludes.

4.2. Conceptual background

The concept of market integration can be traced back to Cournot, who stated that it is “an entire territory, of which the parts are so united by the relations of unrestricted commerce, that prices take the same level throughout with ease and rapidity” (Cournot, 1838). Empirical studies have examined market integration along vertical (prices at different stages of the supply chain), horizontal (prices across locations), and inter-temporal (spot and futures market prices) dimensions, often employing cointegration methods (Ihle & von Cramon-Taubadel, 2008; Roman & Žáková Kroupová, 2022). This study focuses on the horizontal dimension of market integration, which is theoretically motivated by the Enke-Samuelson-Takayama-Judge spatial equilibrium model (Enke, 1951; Samuelson, 1952; Takayama & Judge, 1971).

In the presence of transaction costs, the condition for arbitrage can be represented as follows:

$$p^A > p^B + \tau^{B,A} \quad (4.1)$$

where p^A and p^B denote prices in markets A and B , respectively, $\tau^{B,A}$ represents the transaction cost of exporting natural gas from market B to market A . Therefore, arbitrage activity may only be triggered if the implied gross profit of the trade covers transaction costs.

However, this spatial equilibrium model does not account for the infrastructure constraints on arbitrage between markets. If the import infrastructure in market A and the export infrastructure in market B are fully utilized, the price difference cannot be mitigated through arbitrage. The impact of infrastructure constraints on price relationships fundamentally differs from that of transaction costs. While transaction costs represent tangible expenses incurred during trade—such as transportation and handling fees—infrastructure constraints act as physical barriers that limit arbitrage, regardless of the price differential or the associated transaction costs (Kuper & Mulder, 2016). This distinction is crucial, as it highlights a boundary to market integration: even if the price difference ($p^A - p^B$) exceeds transaction costs ($\tau^{B,A}$), no arbitrage mechanism can equilibrate the markets if the infrastructure is fully utilized.

The above equation is appropriate for understanding price arbitrage between the U.S. and Europe or the U.S. and Asia, where direct LNG trade occurs. The U.S., being a net exporter, directly supplies LNG to both regions. However, between Asia and Europe, no significant direct LNG trade can be observed during the study period. Instead, arbitrage occurs through indirect trade via third-party LNG traders who reroute shipments based on market conditions. To represent this, let p^A and p^E be the prices in Asia and Europe, respectively, $\tau^{S,A}$ and $\tau^{S,E}$

be the transaction costs (including transportation) from swing supplier S to Asia and Europe, respectively, and $q^{S,A}$ and $q^{S,E}$ be the volumes exported from swing supplier S to Asia and Europe, respectively. Assuming that there are no binding infrastructure constraints at both the swing supplier and the importing regions, we have the following condition $p^A - \tau^{S,A} > p^E - \tau^{S,E}$. This means that swing supplier S will export LNG to Asia if the netback price in Asia ($p^A - \tau^{S,A}$) is greater than the netback price in Europe ($p^E - \tau^{S,E}$). If the netback is higher in Europe, the supplier will prefer to export there.

4.3. Structural changes in the international natural gas market

This section provides a descriptive overview of key trends in the global gas market, focusing on regional price fluctuations, LNG terminal utilization, and shifting trade dynamics. These elements are crucial for understanding the factors influencing market integration. By examining price patterns across North America, Europe, and East Asia, along with the impact of infrastructure constraints, this section lays the groundwork for the subsequent empirical analysis.

Figure 4.1 shows the logarithmic prices for Henry Hub (HH) in the North American market, Title Transfer Facility (TTF) in the European market, and the East Asian Index (EAX) in the East Asian region.²⁴ The figure demonstrates that there was a substantial decline in prices in March 2020, likely due to the outbreak of COVID-19 and its impact on natural gas demand. This was further exacerbated by historically mild temperatures.²⁵ Figure 4.1 also shows that the European and Asian gas prices began to rise in the second half of 2021. This can be attributed to the resurgence of demand from the industrial and heating sectors as economic activity rebounded and extreme weather events occurred. From this period onward, it is also evident that the HH series was not significantly affected by these increases.²⁶

Figure 4.2 highlights the major shifts in the natural gas market starting in October 2021 (indicated by the grey-shaded area). Figure 4.2(a) shows a sharp year-on-year (YoY) decline in Russian gas exports to Europe, reflecting a deliberate reduction in daily flows to the level of nominations from long-term

²⁴These prices are derived from the bid-offer ranges observed at the respective hubs for delivery in the subsequent month (front-month gas futures). In cases where price data were missing for certain days, the observations were forward-filled using the price from the most recent preceding day.

²⁵For example, the decreased demand for heating in the residential and commercial sectors due to milder temperatures led to a drop of more than 3% year-over-year during the first quarter of 2020. This resulted from a decrease of over 5% in heating degree days across the main consumption regions (IEA, 2020a).

²⁶Note that an outage at the Freeport LNG export terminal—the second-largest LNG export facility in the U.S.—in June 2022 temporarily relieved pressure on the U.S. gas market (IGU, 2022).

4.3. Structural changes in the international natural gas market

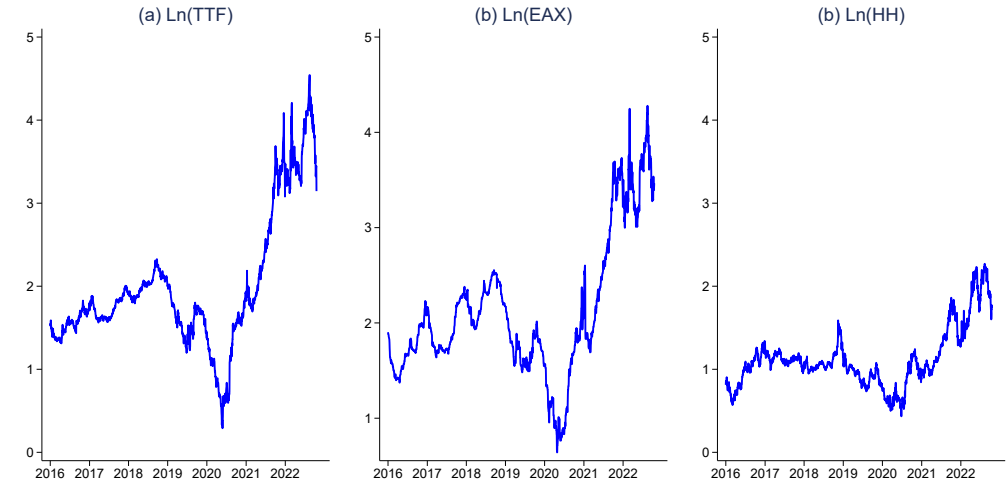


Figure 4.1.: Natural gas prices in log level

contracts, with no additional volumes supplied to the European spot market (Fulwood et al., 2022). This reduction forced Europe to increase its reliance on LNG imports, as seen in Figure 4.2(b), which depicts a notable increase in the utilization rate of the Gate terminal in the Netherlands, the largest LNG import terminal in Northwest Europe. The heightened demand for LNG also caused congestion at other European import terminals (GIE, 2024). Simultaneously, as shown in Figure 4.2(c), the utilization rate of U.S. gas export terminals increased, nearing full capacity and reflecting a high level of exports. However, capacity constraints at both European import and U.S. export terminals limited the ability to significantly increase LNG trade between the two regions.

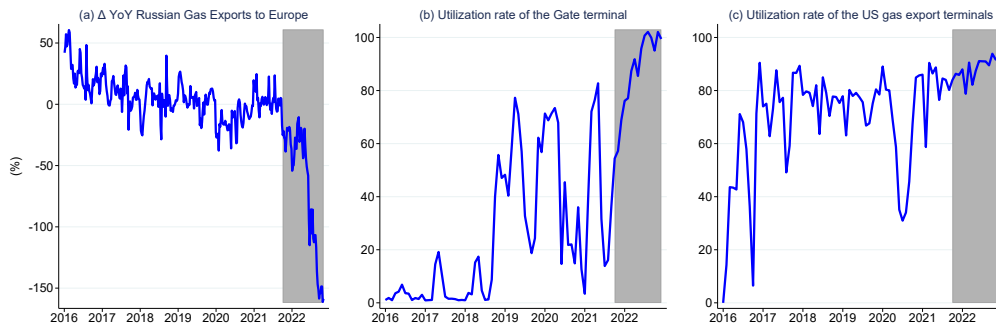


Figure 4.2.: Δ YoY (%) in Russian gas exports, Gate terminal and U.S. export terminals utilization rates

Notes: Own construction based on data obtained from EIA (2023a); ENTSOG (2023); GIE (2024)

4. Global natural gas market integration

Figure 4.3(a) shows that LNG imports to Europe increased in the last quarter of 2021, driven by reduced Russian gas supplies. This reduction led to energy security concerns and spurred efforts to diversify away from traditional pipeline sources (Aitken & Ersoy, 2023). In contrast, Figure 4.3(b) indicates that the growth rate of LNG imports in China began to slow, reflecting the country's slow economic growth during this period (Rystad Energy, 2023). Meanwhile, Figure 4.3(c) shows that LNG imports in Japan and Korea remained relatively stable, reflecting steady demand in these mature markets (Rystad Energy, 2023). These varying import patterns underscore differing regional demand dynamics and suggest that Europe, Japan, Korea, and China are experiencing unique drivers and pressures in their LNG markets, likely influenced by geopolitical, economic, and policy-related factors. As a result, these dynamics are expected to affect the relationship between Asian and European gas prices as of the last quarter of 2021, given the relatively lower LNG import levels in East Asia, largely due to China's import patterns, and the increasing LNG imports in Northwest European (NWE) markets.

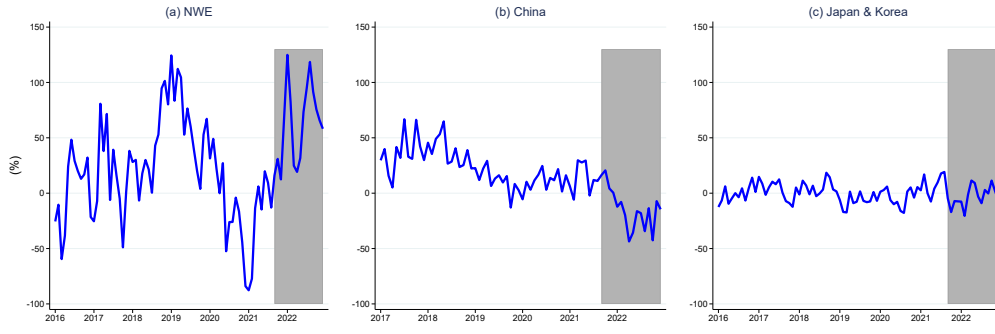


Figure 4.3.: Δ YoY (%) in LNG imports for major regions
Notes: Own construction based on data obtained from JODI (2024)

4.4. Methodology

Our analysis examines the integration of the three regional gas markets using the cointegration approach. Before conducting this analysis, we apply the Augmented Dickey-Fuller (ADF) test, the Phillips-Perron (PP) test, and the Kwiatkowski-Phillips-Schmidt-Shin (KPSS) test to the three gas price series to evaluate their stationarity properties. The ADF and PP tests test the null hypothesis of non-stationarity (i.e., the presence of a unit root), while the KPSS test tests the null hypothesis of stationarity. If the results indicate that the price series exhibit a unit root, we proceed with cointegration analysis to examine equilibrium relationships.

Previous studies have often utilized the traditional symmetric cointegration framework to analyze the integration of gas prices at both regional and intrare-

gional levels (e.g., Siliverstovs et al. (2005); Asche et al. (2002)). However, conventional cointegration tests may be misspecified when the adjustment process is asymmetric. The methodology proposed by Enders and Siklos (2001) extends the widely used Engle and Granger (1987) two-step cointegration procedure by incorporating asymmetric adjustments in the long-run relationships between gas prices. This extension, known as the Momentum Threshold Autoregressive (M-TAR) model, has been shown to perform better in the presence of asymmetry, providing more reliable results than methods that assume symmetric price adjustments. This approach has been extensively applied to analyze asymmetric adjustment in cointegration relationships between various energy prices (e.g., Chang et al., 2012; Chiappini et al., 2019; Hammoudeh et al., 2008).

In both the symmetric Engle and Granger (1987) framework and the asymmetric Enders and Siklos (2001) extension, the first step is to estimate the following model, which represents the equilibrium relationship between two regional gas price series, using ordinary least squares (OLS):

$$P_t^1 = \beta_0 + \beta_1 P_t^2 + \varepsilon_t \quad (4.2)$$

where P_t^1 and P_t^2 represent the logarithmic forms of two gas price series. We estimate three sets of gas price pairs: (TTF, EAX); (HH, TTF); and (HH, EAX). The residuals, $\hat{\varepsilon}_t$, obtained from Equation 4.2, are subsequently used in the second step of the Engle and Granger (1987) linear cointegration analysis (Equation 4.3) and in the second step of the M-TAR model for nonlinear cointegration as proposed by Enders and Siklos (2001) (Equation 4.4):

$$\Delta \hat{\varepsilon}_t = \rho_0 \hat{\varepsilon}_{t-1} + \sum_{j=1}^p \delta_j \Delta \hat{\varepsilon}_{t-j} + u_t \quad (4.3)$$

$$\Delta \hat{\varepsilon}_t = \rho_1 I_t \hat{\varepsilon}_{t-1} + \rho_2 (1 - I_t) \hat{\varepsilon}_{t-1} + \sum_{i=1}^K \vartheta_i \Delta \hat{\varepsilon}_{t-i} + u_t \quad (4.4)$$

The adjustment speed coefficients, ρ_0 , ρ_1 , and ρ_2 , correspond to the symmetric (ρ_0) and asymmetric (ρ_1 and ρ_2) cointegration models. Additionally, the inclusion of lagged values of $\Delta \hat{\varepsilon}_t$ helps to ensure that the residuals are serially uncorrelated. The Heaviside indicator function, I_t , is defined as 1 if $\Delta \hat{\varepsilon}_{t-1} \geq \tau$ and 0 if $\Delta \hat{\varepsilon}_{t-1} < \tau$, where τ is the threshold value, estimated using the consistent search method of Chan (1993).

We test for evidence of asymmetric adjustments using two hypotheses. First, we test the joint null hypothesis of no-cointegration ($H_0 : \rho_1 = \rho_2 = 0$), with the critical values obtained from Enders and Siklos (2001). If the null hypothesis of no-cointegration is rejected, we test for the null hypothesis of symmetry ($H_0 : \rho_1 = \rho_2$) using a standard F-test.

4.5. Main results

This section presents the empirical analysis of the integration of the three regional gas markets. The analysis is structured as follows: First, we test for a potential structural break on October 1, 2021, by applying the Chow test to the log price differentials between each pair of prices, motivated by significant developments in the global gas market. Next, we examine the linear cointegration relationships between each pair of gas prices using the Engle-Granger two-step approach. We then conduct a nonlinear cointegration analysis, employing the MTAR model to investigate potential asymmetries in price adjustments. Finally, we estimate both symmetric and asymmetric error correction models to assess the short-term dynamics and adjustments toward the equilibrium for each price pair.

4.5.1. Structural break

We hypothesize that the relationships among our variables of interest may be affected by a potential structural break on October 1, 2021. This break date is motivated by major developments in the natural gas markets, as discussed in section 4.3. For instance, in the latter half of 2021, geopolitical tensions—particularly Russia’s deliberate reduction of gas exports to Europe—significantly disrupted supply. This led to a major shock in the global gas market, leading to tighter market conditions.

To formally test for this break, we follow Büyük şahin et al. (2013) and Luong et al. (2019), conducting a Chow (1960) test on the log price differentials for each price pair. We perform the test using the following specification:

$$S_t = \theta + \lambda TR_t + \phi S_{t-1} + \phi S_{t-2} + \phi S_{t-3} + \epsilon_t, \quad (4.5)$$

Here, TR_t represents a linear trend, θ is a constant term, and ϕS_{t-1} , ϕS_{t-2} , and ϕS_{t-3} represent the lagged values of the dependent variable, where ϕ_1 , ϕ_2 , and ϕ_3 are the coefficients on the lagged terms.

The resulting F-statistics are 17.413 (significant at the 1% level), 4.328 (significant at the 1% level), and 2.867 (significant at the 5% level) for the spreads EAX-TTF, HH-TTF, and HH-EAX, respectively, with 5 and 1764 degrees of freedom. Given these significant statistics, we conclude that a structural break occurred around October 1, 2021. Consequently, the analysis is conducted over the period from January 1, 2016, to November 1, 2022, divided into two subsamples, with October 1, 2021, as the split date.

Summary statistics for the three price series over the two subsamples are provided in Table C.1 in the Appendix, which shows a shift towards higher prices and greater variability in the gas markets after September 2021. The results of the unit root tests for the log levels and their differences are also presented in Table C.2. The results show that all the time series in log levels are I(1)

variables, meaning they are non-stationary in levels but become stationary after first differencing. Therefore, cointegration analysis is an appropriate tool to investigate their joint properties.

4.5.2. Examining the linear cointegration

In the context of testing for linear cointegration, we apply the two-step approach proposed by Engle and Granger (1987). This approach involves first estimating the equilibrium relationship for each price pair according to the specification in Equation 4.2. In the second step, we obtain the residuals from this regression and apply the Engle-Granger residual-based cointegration test to determine if the residuals are stationary.

Table 4.1 presents the results of the two-step analysis, with the last column providing the test statistics for the stationarity of the residuals, which indicate whether the variables are cointegrated. For the EAX-TTF pair, the estimated β_1 is 0.973 in the first subsample, indicating that a 1% increase in the TTF price is associated with a 0.973% increase in the EAX price. However, β_1 drops to 0.663 in the second subsample. The estimated β_1 coefficients from the cointegration regressions of HH against EAX and TTF are relatively lower. In the first subsample, the estimated β_1 is 0.397 for HH-TTF and 0.376 for HH-EAX. In the second subsample, the estimated β_1 for HH-TTF remains stable at 0.385, while HH-EAX declines sharply from 0.376 to 0.214, indicating a weakening price linkage.

The Engle-Granger test statistics in the last column of Table 4.1 indicate that the three price pairs are cointegrated in the first subsample. However, in the second subsample, the test statistics are not statistically significant, providing no evidence of linear cointegration.

Table 4.1.: Linear cointegration analysis

Price pair	Subsample	β_0		β_1		R^2	EG(1987)
EAX-TTF	First	0.244 ^a	[0.015]	0.973 ^a	[0.009]	0.895	-5.087 ^a
	Second	1.122 ^a	[0.098]	0.663 ^a	[0.027]	0.687	-2.841
HH-TTF	First	0.323 ^a	[0.012]	0.397 ^a	[0.007]	0.682	-4.478 ^a
	Second	0.404 ^b	[0.160]	0.382 ^a	[0.044]	0.215	-1.908
HH-EAX	First	0.284 ^a	[0.014]	0.376 ^a	[0.007]	0.645	-4.718 ^a
	Second	1.036 ^a	[0.214]	0.212 ^a	[0.060]	0.043	-1.628

Note: The first subsample includes data from January 1, 2016, to September 30, 2021, while the second subsample includes data from October 1, 2021, to November 1, 2022. Standard errors of the estimated coefficients are given in the squared brackets. The column titled “ R^2 ” gives the goodness of fit for the regressions. The last column displays the Engle and Granger (1987) test statistic (EG(1987)) for cointegration, with a significant test statistic suggesting that the residuals are stationary, thus confirming cointegration between the variables. The number of lags was selected using the AIC. The critical values of this test are obtained from MacKinnon (2010). The symbols ^a and ^b denote significance at the 1% and 5% levels, respectively.

4.5.3. Examining the nonlinear cointegration

In the preceding subsection, the Engle-Granger test, which assumes a linear and symmetric adjustment process, indicates that there is no evidence of cointegration for any of the price pairs during the second period. This subsection examines estimates from the MTAR model proposed by Enders and Siklos (2001), which explicitly accounts for potential asymmetries in the adjustment process toward equilibrium. This analysis aims to determine whether there is evidence of asymmetries in the first subsample, which would suggest that the adjustment process occurs at different speeds depending on the direction of deviations from equilibrium (positive vs. negative), rather than symmetrically. Additionally, we seek to establish whether the MTAR model provides evidence of cointegration for any of the price pairs in the second subsample period.

Table 4.2 presents the results of the MTAR cointegration test. Column (1) shows the estimated threshold values, which indicate the point at which adjustments switch between regimes for positive and negative deviations from equilibrium. Although the estimated thresholds are close to zero, our analysis shows that models with an estimated threshold value perform better, according to the information criteria, than models assuming a fixed threshold of zero. Columns (2) and (3) show the estimated parameters of ρ_1 and ρ_2 , as specified in Equation 4.4. Here, ρ_1 represents the speed of adjustment in response to positive deviations from equilibrium, whereas ρ_2 represents the speed of adjustment for negative deviations. If the absolute value of ρ_1 is greater than that of ρ_2 , this indicates that the adjustment process is faster in response to positive deviations from equilibrium. Conversely, if $|\rho_2|$ is greater, the adjustment is faster in response to negative deviations from equilibrium. For example, in the relationship between EAX and TTF in the first subsample, the estimated threshold is -0.023, with adjustment coefficients of -0.026 for positive deviations and -0.120 for negative deviations. This result indicates that positive deviations from equilibrium (where $\Delta\varepsilon_{t-1} \geq -0.023$) are eliminated at a relatively slower rate of 2.6% per day. In contrast, negative deviations from equilibrium are adjusted at a much faster rate of 12% per day. Consequently, there is substantially slower convergence toward equilibrium for positive deviations (above the threshold) than for negative deviations (below the threshold). These findings suggest that arbitrageurs are more active in exploiting larger profitable opportunities depending on the direction the spread is moving from its equilibrium position. This also implies that during the first subsample period, the market adjusts more rapidly when EAX prices are decreasing relative to TTF prices. This conclusion is consistent with Chiappini et al. (2019), although the estimated speeds of adjustment in both regimes during our sample period are higher than their estimates. In the second subsample, the estimated threshold is 0.015, with adjustment coefficients of -0.208 for positive deviations and -0.070 for negative deviations. This outcome indicates that positive deviations from equilibrium are eliminated rapidly, at a rate of 20.8% per day. The results for

negative deviations do not show significant adjustment, as the coefficient for negative shocks is statistically insignificant.

Column (4) in the table presents the test of the joint null hypothesis of no cointegration with MTAR adjustment ($H_0 : \rho_1 = \rho_2 = 0$). The results indicate that this null hypothesis is rejected for each price pair in the first subsample, as the test statistic exceeds the critical values provided by (Enders & Siklos, 2001). Given this result, we proceed to test the null hypothesis of $H_0 : \rho_1 = \rho_2$. The results, shown in Column (5), indicate that this null hypothesis is rejected, supporting the presence of asymmetric adjustment. However, in the second subsample, Column (4) shows that the null hypothesis of no cointegration is rejected only for the EAX-TTF price pair. The lack of nonlinear cointegration for the HH-TTF and HH-EAX pairs suggests a decoupling of the U.S. gas market from the European and Asian markets during this period.

Table 4.2.: Non-linear cointegration analysis

Price pair	Subsample	(1)	(2)	(3)	(4)	(5)
		Threshold	ρ_1	ρ_2	$\Phi(H_0 : \rho_1 = \rho_2 = 0)$	$F(H_0 : \rho_1 = \rho_2)$
EAX-TTF	First	-0.023	-0.026 ^a (-2.390)	-0.120 ^b (-7.276)	27.555 ^b	25.492 ^b [0.000]
	Second	0.050	-0.208 ^b (-3.230)	-0.070 (-1.622)	5.909 ^c	3.665 ^c [0.057]
HH-TTF	First	0.012	-0.008 (-0.671)	-0.044 ^b (-5.035)	12.849 ^b	5.586 ^b [0.018]
	Second	-0.068	-0.020 (-1.308)	-0.090 ^a (-2.029)	2.915	2.218 [0.138]
HH-EAX	First	0.033	-0.083 ^b (-4.480)	-0.025 ^a (-3.427)	15.521 ^b	8.665 ^b [0.003]
	Second	0.010	-0.002 (-0.119)	-0.031 ^a (-2.011)	2.029	1.393 [0.239]

Note: The first subsample includes data from January 1, 2016, to September 30, 2021, while the second subsample includes data from October 1, 2021, to November 1, 2022. Column (1) provides the estimated threshold values. Columns (2) and (3) provide the estimated coefficients ρ_1 and ρ_2 in Equ. (4.3). t-statistics for the estimated coefficients are given in the brackets. The threshold is estimated using Chan (1993)'s approach with a ten percent trimming level. Column (4) shows the null hypothesis $\Phi(H_0 : \rho_1 = \rho_2 = 0)$ tests for the threshold cointegration with the critical values from Enders and Siklos (2001) as follows: C.V(1%) is 8.310; C.V(5%) is 6.050; C.V(10%) is 5.060. Column (5) gives the second null hypothesis $F(H_0 : \rho_1 = \rho_2 = 0)$. The symbols ^a, ^b, and ^c denote significance at the 1%, 5%, and 10% levels, respectively.

4.5.4. Results of the (a)symmetric error correction model

In this step, we estimate both symmetric and asymmetric error correction models (ECMs) to examine the adjustment processes of individual prices toward the equilibrium. We estimate the symmetric or asymmetric ECM for each price pair based on the cointegration results from the previous subsection.

4. Global natural gas market integration

Table 4.3 presents the estimation results for the two subsamples.²⁷ The magnitude of the Error Correction Term (ECT) indicates the speed at which deviations from equilibrium are corrected. For instance, if the ECT is -0.250, it suggests that approximately 25% of the deviation is corrected each day, implying that full correction to equilibrium would take about four days. The results indicate that, for the EAX-TTF pair in the first subsample, the ECT for EAX in the high regime is -0.003 and statistically insignificant, suggesting no adjustment for positive deviations. In the low regime, the ECT for EAX is -0.090 and statistically significant, indicating a correction toward equilibrium for negative deviations. For TTF, the ECT is -0.020 and statistically significant in the high regime and -0.020 and statistically significant in the low regime, indicating adjustments in both cases. In the second subsample, the ECT for EAX is -0.116 and statistically significant in the high regime and -0.105 and statistically significant in the low regime, indicating strong adjustments for both positive and negative deviations. For TTF, the ECT is 0.105 and statistically insignificant in the high regime and -0.035 and statistically insignificant in the low regime, suggesting a lack of significant adjustments. Comparing the two subsamples, the first shows active adjustments for both EAX and TTF, with significant responses to arbitrage opportunities. In contrast, the second subsample reveals a pronounced response in the EAX market, particularly for positive deviations, while the TTF market's responsiveness diminishes, indicating a shift in price correction dynamics between the Asian and European markets over time.

Table 4.3.: Results of symmetric and asymmetric ECM

Subsample	Model	Regime	EAX	TTF	HH	TTF	HH	EAX
First	Symmetric		-0.034 ^a (-5.426)	0.017 ^a (2.699)	-0.028 ^a (-4.220)	0.015 ^b (1.981)	-0.023 ^a (-3.612)	0.025 ^a (3.302)
	Asymmetric	High	-0.003 (-0.476)	0.020 ^b (2.643)	-0.007 (-0.622)	0.007 (0.551)	-0.042 ^b (-2.316)	0.079 ^a (3.684)
		Low	-0.090 ^a (-7.861)	0.020 ^c (1.686)	-0.038 ^a (-4.763)	0.019 ^b (2.029)	-0.023 ^a (-3.348)	0.010 (1.198)
Second	Asymmetric	High	-0.116 ^c (-2.088)	0.105 (1.415)				
		Low	-0.105 ^b (-2.951)	-0.035 (-0.724)				

Note: The first subsample includes data from January 1, 2016, to September 30, 2021, while the second subsample includes data from October 1, 2021, to November 1, 2022. “Symmetric” and “Asymmetric” refer to the Symmetric and Asymmetric ECM. The ECTs in the asymmetric models are estimated separately for two regimes—“High” and “low”—based on the Momentum Threshold Autoregressive (M-TAR) approach outlined in Section 5.4. Specifically, the Heaviside indicator function identifies whether the system is in a high or low regime depending on the threshold value. Additionally, the first difference terms are also estimated separately for the two regimes. For brevity, these results are not presented here but are available upon request. The asterisks a, b, and c attached to the coefficients represent the significance levels at the 1%, 5%, and 10%, respectively.

²⁷The results of diagnostic checks for each estimated ECM (including tests for serial correlation and normality) indicate that the estimated models perform reasonably well. For brevity, we do not report the diagnostic checks here. However, they are available upon request.

4.6. Further results

In the baseline results, we observe that the American gas market price is no longer cointegrated with the European and Asian prices during the second subsample period. This section examines the potential driver of the log spread between HH and TTF prices. Following Luong et al. (2019) and Luong (2023), we apply Toda and Yamamoto (1995), a modified Granger (1969) non-causality test.²⁸ Specifically, we investigate infrastructure congestion as a potential driver, focusing specifically on congestion at LNG import terminals in Northwestern Europe (NWE) and LNG export terminals in the U.S. Our hypothesis is that Granger causality between regional price differentials and LNG infrastructure utilization is bidirectional. Wider regional price differentials can drive higher utilization of connecting infrastructure as traders exploit arbitrage opportunities. Conversely, congestion at LNG terminals, whether at import terminals in NWE or export terminals in the U.S., can widen regional price differentials by restricting LNG flow. We focus on the average utilization rate of U.S. export terminals and the Gate terminal in the Netherlands, which has one of the largest import capacities in NWE. The rationale for using the average utilization rate is that it serves as a comprehensive measure of the infrastructure’s capacity to respond to regional price signals. High average utilization rates signal supply chain bottlenecks, leading to wider price spreads as the market struggles to balance regional supply and demand. Additionally, we investigate the specific impact of congestion at the Gate terminal. We obtain data on the utilization levels of U.S. LNG export terminals from the Energy Information Administration (EIA) (EIA, 2023a). This data is available on a monthly basis, and we assume that each monthly figure represents the average daily utilization rate for all days within that month. For utilization data on the Gate terminal, we use daily data from Gas Infrastructure Europe (GIE) (GIE, 2024). However, no data is available for the utilization rates of corresponding LNG infrastructure in East Asian countries.

Table 4.4 reports the results of the Toda and Yamamoto (1995) Granger causality tests between the HH-TTF spread and two measures of infrastructure congestion: average congestion across the U.S. and NWE, and specific congestion in NWE. In the first subsample, none of the test statistics are statistically significant, indicating no evidence of Granger causality in either direction between infrastructure congestion and the HH-TTF spread. In contrast, in the second subsample, the test statistics for the congestion measures indicate a different pattern. The results show that average congestion across the U.S. and NWE Granger-causes the HH-TTF spread at conventional significance levels, suggesting that increased

²⁸This approach is motivated by the findings of Clarke and Mirza (2006), which show that pretesting for cointegration can result in severe over-rejections of the null hypothesis of non-causality. In contrast, the augmented lag method proposed by Toda and Yamamoto offers better control for Type I error rates, while generally retaining adequate power. Simulation results indicate that this method performs consistently well across various data-generating processes, with robust performance regardless of the stationarity or cointegration properties of the variables.

4. Global natural gas market integration

Table 4.4.: Causality Tests for HH-TTF Spread

	First subsample		Second subsample	
	to spread	from spread	to spread	from spread
Average Congestion (U.S. & NWE)	10.300 (0.110)	6.100 (0.420)	12.300 ^b (0.030)	6.200 (0.280)
Congestion (NWE)	9.200 (0.170)	8.300 (0.220)	11.400 ^b (0.044)	6.900 (0.230)

Note: This table reports Toda and Yamamoto (1995) tests for Granger causality between the log HH-TTF spread and the listed factors. “Average Congestion (U.S. & NWE)” refers to the daily average of LNG export terminal congestion in the U.S. and LNG import terminal congestion in Northwest Europe (NWE). “Congestion (NWE)” represents the congestion level of LNG import infrastructure in NWE only. “to spread” indicates the test for whether a variable does not Granger-cause the spread, and “from spread” is the test for whether the spread does not Granger-cause the infrastructure congestion. The first subsample includes data from January 1, 2016, to September 30, 2021, while the second subsample includes data from October 1, 2021, to November 1, 2022. The χ^2 statistic is reported on the first line, with the asymptotic p-value presented in parentheses on the next line. ^b denotes statistical significance at the 5% level.

congestion is associated with variations in the HH-TTF spread. Similarly, congestion specifically in NWE also shows a statistically significant Granger causal effect on the spread, reinforcing the influence of regional infrastructure constraints on market price differentials. We do not find statistically significant evidence of a bidirectional relationship (i.e., from the HH-TTF spread to congestion), suggesting that infrastructure congestion is more directly determined by physical and logistical constraints than by market price signals. These findings imply that infrastructure congestion, particularly in the second subsample, plays a significant role in driving the price spread between the U.S. and European gas markets, underscoring the importance of infrastructure capacity for market integration.

4.7. Conclusion

This study examines the market integration hypothesis across gas price benchmarks in Europe, the U.S., and Asia over the period from January 2016 to October 2022. We hypothesize that a structural break occurred on October 1, 2021, dividing the sample period into two distinct subsamples. This break coincides with a period of heightened market tightness and supply constraints in the natural gas market, particularly within Europe. During this period, Russia reduced its spot market supply to Europe, fulfilling only long-term contract obligations, which led to increased LNG imports and consequent congestion in European LNG infrastructure. This situation also coincided with congestion in U.S. LNG export infrastructure and relatively lower LNG imports in East Asia, largely due to the economic slowdown in China.

In the first subsample, our findings indicate the presence of both linear and nonlinear cointegration relationships between the regional gas price benchmarks. The presence of nonlinear cointegration suggests that the adjustment process back to equilibrium between these benchmarks may vary depending on the direction or size of shocks, reflecting asymmetric trader responses to positive versus negative deviations in the price spread. This finding is consistent with Chiappini et al. (2019), who documented asymmetric adjustments between the American and European gas markets but found no such relationship between the American and Asian markets over the period 2004–2018. A key development during our sample period is the transition of the U.S. to a net exporter of natural gas, accompanied by a significant expansion in its LNG export capacity. In the second subsample, however, we find evidence of threshold cointegration only between the Asian and European gas prices, with no evidence of cointegration between the American price and the other two prices. The absence of cointegration between the European and American prices is likely attributed to LNG infrastructure congestion during this period. Infrastructure operating at full capacity—including pipelines, transportation fleets, and terminals—limited the ability of arbitrage to restore equilibrium. This supports our hypothesis discussed in Section 4.2 that the efficiency of the arbitrage mechanism and the extent of market integration are critically dependent on the capacity of the infrastructure facilitating commodity trade.

Our analysis yields two main implications. First, the integration between the Asian and European gas markets, despite external shocks, indicates that changes in one market can significantly impact the other. This underscores the importance of considering broader market dynamics when assessing each market’s supply security. Effective management of demand and supply shocks may be achieved through bilateral policies, such as sharing information on LNG trade flows, production levels, and demand forecasts, thereby enhancing coordination and ensuring supply security. Second, our findings suggest that physical infrastructure plays a crucial role in energy market integration, particularly during tight market conditions, which differentiates it from financial markets (see Yang et al. (2003) for a related example). In financial markets, contagion effects often drive integration under stress, while energy markets are constrained by infrastructure bottlenecks, making infrastructure a critical factor to consider in any analysis of energy market integration. Therefore, market participants need to be aware of changing dynamics and the potential breakdown of equilibrium relationships during periods of high physical infrastructure utilization.

5. Decomposing Return and Volatility Connectedness in Northwest European Gas Markets: Evidence from the R^2 connectedness approach

5.1. Introduction

The European Commission has prioritized the creation of an integrated gas market to ensure affordable and stable gas supplies for customers across Europe (Brons et al., 2019). To achieve this, several regulatory reforms, such as Directive 2009/73/EC, have been implemented to remove market barriers, enhance regulatory oversight, and improve market integration and transparency. These measures have facilitated the transition to hub trading and gas-on-gas pricing within the European gas market (Bianco et al., 2015; Garaffa et al., 2019). The observed interdependence in price changes (return connectedness) and the associated risks (volatility connectedness) across these gas hubs underscores the extent of market connectedness (Broadstock et al., 2020). Such interdependence enhances overall welfare by fostering competition, reducing price disparities, and promoting efficient resource allocation (Anderson & Ginsburgh, 1999; Gugler et al., 2018).²⁹

However, recent years have seen extreme external factors, such as the COVID-19 pandemic and the Russian invasion of Ukraine, significantly impacting wholesale prices and trading environments (see Heather (2022, 2024) for a detailed analysis). Previous studies by Chen et al. (2022) and Szafranek et al. (2023) have demonstrated that these shocks also led to reduced market connectedness in terms of price returns between gas hubs. Building on this prior analysis, this paper extends the study of connectedness by addressing the following research questions: *Do European gas markets influence each other's price returns and volatility contemporaneously, or are there delays in this transmission?; How does the timing of connectedness vary between tight and stable market conditions?; How quickly does connectedness recover following major disruptions?*

This paper employs the R^2 decomposition connectedness method, recently introduced by Balli et al. (2023), to analyze return and volatility connectedness

²⁹Note that the costs of increasing market connectedness (e.g., the costs of extending pipeline infrastructure) should be considered when evaluating (net) welfare gains. Furthermore, increasing market connectedness may involve distributional effects. Specifically, price convergence can reduce consumer surplus in regions that initially had lower prices, whereas consumers in previously high-price regions benefit (Finon & Romano, 2009).

among European natural gas benchmarks. Specifically, it focuses on the connectedness of spot prices from four Northwest European (NWE) natural gas hubs: the Title Transfer Facility (TTF) in the Netherlands, the National Balancing Point (NBP) in the United Kingdom, Trading Hub Europe (THE) in Germany, and the Zeebrugge Trading Point (ZTP) in Belgium, over the period from 2020 to 2024.³⁰ In doing so, this study aims to contribute to the literature on European gas market integration, as reviewed in detail in Section 5.2, in three ways:

First, we apply the R^2 connectedness framework to decompose spillover effects among gas benchmarks into contemporaneous and lagged components. While previous studies, such as those by Broadstock et al. (2020) and Chen et al. (2022), have explored transmission mechanisms within European gas markets, they did not differentiate between immediate and delayed spillovers. This distinction in our work provides novel insights, helping market participants determine whether to respond swiftly to shocks or prepare for more gradual impacts, thereby enhancing risk management and optimizing hedging strategies. Additionally, the R^2 decomposition approach enhances interpretability compared to the connectedness methodologies proposed by Diebold and Yilmaz (2012) and Diebold and Yilmaz (2014), as it avoids the associated normalization problem.³¹

Second, by examining the period from 2020 to 2024, we extend existing analyses of market connectedness during the COVID-19 pandemic and the 2021-22 energy crisis by also investigating post-crisis recovery. Therefore, our examination period captures not only the immediate disruptions caused by the COVID-19 pandemic and the Russian invasion of Ukraine but, more importantly, the speed and effectiveness of the subsequent recovery of European gas markets and the re-establishment of market connectedness following these events. This provides a comprehensive understanding of the market's resilience and the pace at which connectedness is restored after major disruptions. Furthermore, we differentiate between spot and futures prices to examine how their connectedness levels vary across periods of market tightness and stability, providing insights into the differing roles of short-term dynamics versus market expectations.

Lastly, we conduct a regression analysis to identify the factors associated with the level of connectedness in the NWE gas markets. Specifically, we assess the relationship between market connectedness and various factors, including physical constraints such as infrastructure congestion between the UK and other NWE countries, market expectations, geopolitical factors, and the 2022 storage mandate implemented during the energy crisis. This analysis helps us understand how these diverse drivers shape the dynamics of gas market connectedness.

The findings of this study can be summarized as follows. In terms of total return connectedness, we observe a slight reduction during the COVID-19 pandemic and

³⁰These four benchmarks are the focus of the analysis as they represent the NWE gas market, which is expected to exhibit closer market fundamentals and shorter transportation distances due to regional proximity.

³¹For further details on how this approach addresses the normalization problem, see Section 5.4.

a sharp decline from the second quarter of 2022, following the Russian invasion of Ukraine, which is consistent with previous studies (Chen et al., 2022; Papi   et al., 2022). Our analysis of the extended sample through 2024 reveals that recovery began in mid-2023, with market connectedness reaching pre-crisis levels by year-end. Total volatility connectedness followed a similar, though slightly less pronounced, trajectory. Our comparative connectedness analysis of spot and futures prices reveals that futures markets exhibited higher connectedness than spot markets during periods of stress, indicating that they were less impacted by physical constraints and more aligned with broader market expectations.

Decomposing the total connectedness index reveals that contemporaneous effects consistently dominate lagged effects for both return and volatility connectedness. This suggests that market participants respond quickly to new information, and price adjustments among gas hubs occur immediately. The persistence of contemporaneous effects during both tight and stable market conditions indicates that the speed of information transmission and market response remains unaffected by shifts in market conditions. This consistent response can be attributed to advanced trading mechanisms and financial instruments, such as virtual trades, locational swaps, and derivatives, which facilitate rapid information flow and immediate price adjustments across varying market conditions (ACER, 2023b).

Our directional analysis shows that the connectedness of NBP and ZTP with TTF and THE dropped significantly during disruptions, with NBP even decoupling completely in late 2022. TTF typically acted as a net transmitter of shocks but became a net receiver from late 2022 to late 2023, while THE transitioned to being a net transmitter during this period, potentially due to increased spot trading linked to Germany’s need to replace Russian gas and the expansion of LNG infrastructure. NBP consistently remained a net receiver. The results also indicate that TTF exhibits a close alignment between contemporaneous and overall net spillover effects, reflecting its immediate influence on other hubs, as its shocks are transmitted to them without delay, often on the same day, likely due to its high liquidity and active trading. This finding is consistent with Liu et al. (2024), suggesting that markets with substantial liquidity tend to be highly influenced by contemporaneous factors.

Finally, our regression analysis reveals significant associations between reduced connectedness and congestion in the pipelines connecting the UK with Belgium and the Netherlands. When combined with futures spreads, the negative association between congestion and connectedness intensifies, suggesting that higher futures spreads exacerbate market decoupling amid congestion. We also find that the EU storage mandate to fill gas storage to 80% capacity is associated with a reduction in market connectedness, indicating that varying storage obligations may have contributed to decreased interdependence among NWE markets. Lastly, higher geopolitical risk is correlated with increased connectedness, likely due to shared market responses to geopolitical events.

The implications of these results are as follows: the dominance of contemporaneous spillovers indicates that these markets adjust almost immediately to shocks. This rapid adjustment requires constant monitoring and quick decision-making by market participants to effectively manage increased volatility risks. The observed decrease in connectedness during crises, along with its association with pipeline congestion, suggests that physical infrastructure constraints can significantly disrupt market integration. However, this effect appears temporary, as connectedness tends to recover once these constraints are alleviated. This implies that, while infrastructure enhancements could increase market efficiency, caution is needed to avoid overinvesting in potentially redundant capacity after markets have recovered.

The rest of the paper is structured as follows: Section 5.2 reviews the literature on European gas market integration. Section 5.3 describes the data used, including their sources, and outlines the dynamics in the NWE gas markets. Section 5.4 discusses the methodology employed in the analysis, while Section 5.5 presents the results of the connectedness analyses. Section 5.6 examines the factors associated with this connectedness. Finally, Section 5.7 concludes the study.

5.2. Literature review

The integration of natural gas markets has been central to European gas market liberalization. The liberalization process began with the First Gas Directive in 1998 (Directive 98/30/EC), which introduced competition and established common rules, including non-discriminatory rights for building new gas infrastructure. This was followed by the Second Gas Directive in 2003 (Directive 2003/55/EC), which mandated the unbundling of gas operators to separate transport networks from production and supply, thereby broadening consumer choice. Despite these reforms, the market continued to face significant hurdles such as concentration, vertical integration, and cross-border trade barriers. This prompted the European Commission to conduct the ‘DG Competition Report on Energy Sector Inquiry’ in 2007, which identified key areas lacking effective competition. In response, the Third Energy Package was enacted in 2009, including Directive 2009/73/EC, which focused on establishing common rules for the internal market in natural gas and repealed Directive 2003/55/EC. This package aimed to further dismantle market barriers, improve regulatory oversight, and enhance market integration and transparency (Bianco et al., 2015; Demir & Demir, 2020). These legislative efforts have gradually reshaped the European natural gas market, promoting a more integrated and competitive environment, which is crucial for the convergence of gas prices across Europe. Such significant changes naturally raise questions about the effectiveness of these liberalization efforts in achieving a truly integrated and competitive market, prompting empirical and academic studies to rigorously examine these issues.

Research on the integration of the European gas market can be categorized into two strands of literature, both primarily utilizing prices from hub-based continental European markets. The first strand focuses on identifying cointegration or convergence among natural gas prices to assess the effectiveness of market integration. The second strand adopts the spillover methodology, also referred to as connectedness, initially developed by Diebold and Yilmaz (2009), which calculates the ‘spillover index’ to quantify how much of the forecast error variance in one market can be explained by shocks in another. This methodology was further extended by Diebold and Yilmaz (2012) to include both a generalized Vector Autoregression (VAR) structure (i.e., invariant to variable ordering) and directional spillovers (i.e., the ‘FROM’ and ‘TO’ analyses).

The connectedness and cointegration approaches differ in both their focus and methodological frameworks for analyzing the integration of European gas markets. The connectedness approach, often based on Vector Autoregression (VAR) models, captures the transmission of shocks between markets by employing forecast error variance decompositions (FEVD). This method measures both total and directional spillovers, quantifying how much of the forecast error variance in one variable is attributed to shocks originating in other variables, in terms of returns or volatility, across different time horizons, depending on the decomposition method used (Baruník & Křehlík, 2018; Diebold & Yilmaz, 2009, 2012; Naeem, Chatziantoniou, et al., 2024). In contrast, the cointegration approach focuses on equilibrium relationships between markets. It examines whether gas prices that do not follow a constant pattern over time tend to have an equilibrium relationship, with deviations from this equilibrium being temporary and corrected over time, typically through price adjustments in response to supply-demand imbalances (Alexander & Wyeth, 1994). In this context, while the connectedness approach provides insights into interdependencies and the flow of volatility or return shocks between European gas markets, the cointegration approach assesses the equilibrium relationship and common trends.

Regarding the first strand of literature, extensive empirical work demonstrates the use of cointegration tests to reveal the degree of market integration. Asche et al. (2002) investigate market integration in the German natural gas market and the impact of long-term take-or-pay contracts. Analyzing 1990–1998 time series data on gas export prices from Norway, the Netherlands, and Russia, the Johansen cointegration test shows proportional price movements, confirming market integration. However, they found that Russian gas prices were systematically lower than Dutch and Norwegian prices, primarily due to differences in volume flexibility, transport costs, and political risk. Growitsch et al. (2015) estimated a time-varying coefficient model to study the convergence path of spot prices in German and Dutch trading hubs. They found improvements in market efficiency and significant price convergence since the introduction of the entry-exit system. Similarly, Neumann and Cullmann (2012) examined price convergence across eight European gas hubs by applying the Kalman filter to estimate time-varying coefficients, which represent the evolution of market integration over time. Their

analysis revealed that only twelve out of twenty-eight possible price pairs exhibited significant integration, with varying degrees of convergence over time. The results also highlighted that market integration fluctuates seasonally, with lower levels of convergence during the winter months, when natural gas prices tend to rise due to higher demand. Accounting for non-linear adjustments between regional European markets, Garaffa et al. (2019) examined price transmission dynamics between the German, Belgian, and Dutch spot markets from April 2013 to December 2014. Their analysis confirmed cointegration and identified significant price asymmetries, particularly in the German market, where transaction costs were evident. Further studies have applied convergence methods to analyze the integration of the European gas market. Robinson (2007) employed convergence tests to analyze annual retail natural gas prices for six EU Member States—Finland, France, Ireland, the Netherlands, Spain, and the UK—from 1978 to 2003. The results indicate some evidence of price convergence according to the β -convergence³² and Bernard-Durlauf tests. Moreover, Bastianin et al. (2019) extended the analysis to fourteen European countries from 1991 to 2017 using natural gas prices for industrial consumers. Their analysis provides evidence of pairwise, σ -convergence³³, and relative price convergence, which is closely linked to the presence of trading hubs and market interconnections.

Moving to the second strand, the focus shifts to the dynamics of price spillovers, exploring how connectedness influences market behavior. Broadstock et al. (2020) employ the spillover methodology, particularly the framework developed by Diebold and Yilmaz (2009), to assess the integration of European natural gas markets by examining the connectedness of price returns and volatilities from key trading hubs (NBP, ZEE³⁴, and TTF). The main findings indicate that while European gas markets show a significant level of integration, with spillover index values between 38% and 69%, complete integration has not yet been achieved. They also find that there has been a notable increase in spillovers since the implementation of the Third Gas Directive in 2009, with TTF emerging as a more dominant hub in terms of both return and volatility spillovers, reflecting its rising importance in the market. Complementing this, Papież et al. (2022) employ the Diebold and Yilmaz (2009) framework combined with a time-varying

³²The *beta*-convergence approach tests whether countries with initially lower gas prices experience faster price growth than those with higher initial prices. The estimate of the rate of convergence, represented by β , indicates how close prices are to converging toward a common level, with a β value close to 1 suggesting absolute convergence.

³³ σ -convergence refers to tracking whether the cross-sectional standard deviation of natural gas prices decreases. In this context, σ represents the cross-sectional standard deviation of log-prices, capturing the degree of dispersion in prices between countries. A decrease in the cross-sectional standard deviation over time indicates σ -convergence, implying that price differences between countries are diminishing.

³⁴ZEE refers to the Zeebrugge Beach gas market, a Belgian gas market that operated alongside the ZTP (Zeebrugge Trading Point). Since 2022, ZEE has experienced a significant decline in trading volumes due to expiring capacity contracts and reduced liquidity, whereas ZTP has attracted more national gas trade (Heather, 2021). To streamline operations, the Belgian regulator approved the merger of the ZEE and ZTP hubs, which took effect on October 1, 2023 (EEX, 2023).

parameters VAR model with stochastic volatility (TVP-VAR-SV). They focus on the connectedness of daily price changes and weekly realized volatility across four key gas hubs: TTF, NBP, NCG, and PSV, analyzing data from November 2013 to January 2022. Their results show a steady rise in the total spillover index, particularly from mid-2017, underscoring a robust co-movement across these markets. However, their analysis shows that when the COVID-19 pandemic hit, the connectedness index decreased substantially by about 15 percentage points from the initial 60% level. This finding was corroborated by Chen et al. (2022), who used a quantile spillover approach to analyze the integration of the European natural gas futures market, particularly during extreme events. They argue that the declining integration during the pandemic was due to increased market instability, a severe imbalance between supply and demand, and significant disruptions to usual market operations. Further, Szafranek et al. (2023) analyzed price dynamics during the turbulent 2021–2022 period using the frequency decomposition method introduced by Baruník and Křehlík (2018) to examine the connectedness of four major European natural gas hubs. The main result reveals that while the connectedness of European gas markets increased significantly before the Russian invasion of Ukraine, it declined markedly afterward.

The findings from both strands of literature reveal a progressive alignment in gas prices across European hubs, indicative of market integration facilitated by regulatory frameworks such as the entry-exit system and successive EU Gas Directives. However, instances of decreased integration often occur, typically linked to significant disruptive events.

The current study contributes to the literature on connectedness analysis in the European gas market by employing a methodological approach that dissects both contemporaneous and lagged spillover effects across gas benchmarks. In doing so, it extends prior research, which primarily focused on immediate spillover effects, often overlooking the potential for lagged interactions to develop over time. Furthermore, the study examines the period from 2020 to 2024 to investigate how different shocks during this time impacted market connectedness and how connectedness evolved during subsequent recovery and stabilization phases.

5.3. Dynamics of gas prices and volatility in NWE

The European natural gas market consists of multiple price hubs. This study focuses on the connectedness of gas price hubs in NWE for three main reasons. First, the NWE region accounts for over half of the EU’s gas consumption, underscoring its central role in the European gas market (Eurostat, 2023). Second, in 2022, the gas-on-gas pricing mechanism dominated the region, comprising approximately 82% of pricing strategies, highlighting the increasing maturity and liquidity of NWE’s gas hubs (IGU, 2022). Finally, gas hubs within the same region are expected to share similar market fundamentals—such as supply sources, demand patterns, and infrastructure—which contribute to price convergence

(Farag & Zaki, 2024; Hulshof et al., 2016). Additionally, the relatively shorter transportation distances between these markets result in lower transportation costs, further supporting price alignment.

For the empirical analysis, this study utilizes settlement prices of day-ahead contracts from four gas hubs: TTF, NBP, THE, and ZTP. Data for TTF, NBP, and THE are sourced from Refinitiv Datastream, while data for ZTP are obtained from the European Energy Exchange AG (EEX). The NBP gas price, originally denominated in GBP/therm, is converted to EUR/MWh to enable direct comparison with the other gas prices, which are measured in EUR/MWh.³⁵ The data cover the period from June 2019 to April 2024. Descriptive statistics for the natural gas price data are provided in Table D.1 in the Appendix. To ensure stationarity, this study uses price returns instead of raw prices for empirical estimations. Daily returns (r_t) are calculated using the standard log-difference formula: $r_t = (\ln p_t - \ln p_{t-1}) \times 100$, where p_t is the price at time t and \ln denotes the natural logarithm. Using price returns captures price fluctuations and growth.

Figure 5.1(a) plots TTF gas prices over the investigated period, while Figures 5.1(b), (c), and (d) show the price ratios between TTF and three other benchmarks. In 2020, TTF prices were relatively low, largely due to reduced economic activity and lower demand resulting from the COVID-19 lockdowns, mild winter temperatures in 2019–2020, and increased wind power generation in Europe (IEA, 2020b). The figure also illustrates an unprecedented rally in prices beginning in March 2021, driven by several converging factors, including the post-pandemic economic recovery, a cold winter in Asia in early 2021, and a sharp decline in European domestic gas production, particularly from the Dutch Groningen field. Consequently, traders withdrew natural gas from storage to meet late winter demand, delaying reinjections (Heather, 2022; ?). From September 2021, Russia reduced daily gas flows to Europe, fulfilling only long-term contracts while halting additional supplies to the spot markets, and underground storage levels remained low (Farag et al., 2023; Fulwood et al., 2022). In 2022, Russia further curtailed gas supplies following its invasion of Ukraine, exacerbating market stress. At the same time, the LNG market tightened due to both planned and unplanned outages, such as the prolonged outage at the Freeport LNG terminal in Texas, U.S., as well as unprecedented increases in charter rates, with global LNG infrastructure operating at maximum capacity (IEA, 2023). In 2023 and 2024, European gas price patterns stabilized after the extreme volatility of previous years, primarily driven by the rapid diversification of supply sources away from Russia through increased LNG imports and reductions in natural gas demand (ACER, 2023a; Ruhnau et al., 2023).

Figure 5.1(b) shows the ratio between THE and TTF. This ratio remained around 1, except during short periods in 2020 and the second half of 2022. Figures 5.1(c) and 5.1(d) depict the ratios of NBP to TTF and ZTP to TTF, respectively.

³⁵To convert the NBP price to EUR/MWh, the spot exchange rate (GBP/EUR) and a conversion factor of 29.3071, reflecting the relationship between therms and MWh, are used.

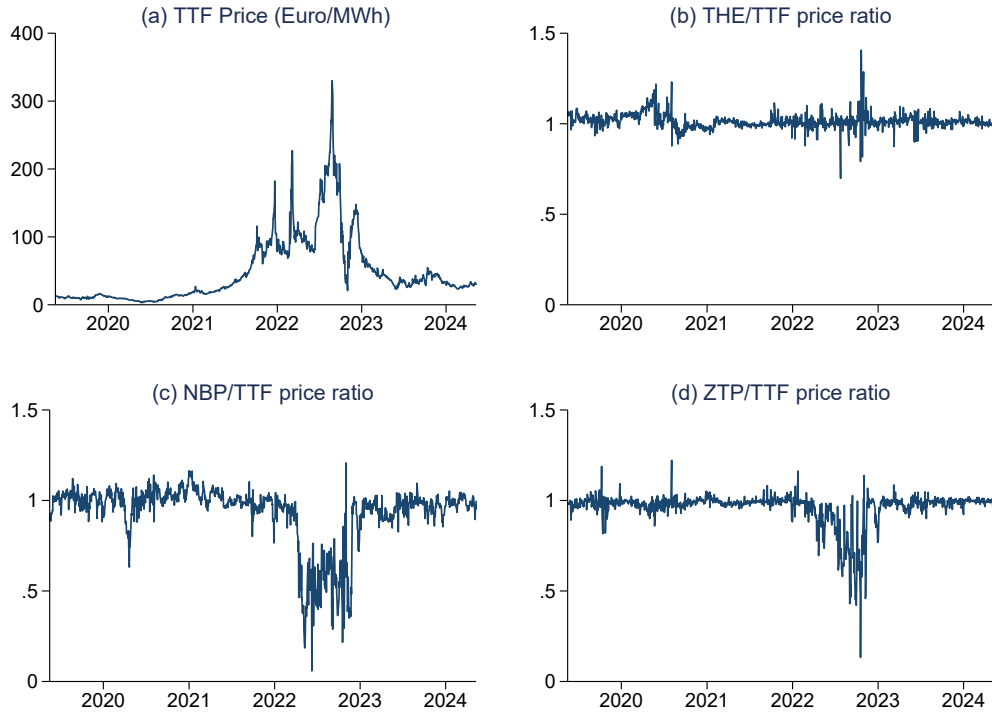


Figure 5.1.: TTF price series and price ratios of THE, NBP, and ZTP to TTF
Note: The top left graph (a) shows the TTF price series (in Euro/MWh). The subsequent graphs display the price ratios: (b) THE/TTF, (c) NBP/TTF, and (d) ZTP/TTF, illustrating the relative price movements of the European gas benchmarks compared to TTF.

These ratios also stayed close to 1, except in 2022 when they dropped to 0.5 or lower. The lower prices in Belgium and the UK during this period can be attributed to larger regasification capacities and the near-full utilization of cross-border pipeline infrastructure connecting these countries with the Netherlands and Germany.

This study uses absolute returns as a proxy for volatility. Defined as the absolute value of daily returns ($|r_t|$), they capture the magnitude of price fluctuations regardless of direction, thereby directly reflecting the intensity of market movements. Previous research has shown that absolute returns exhibit greater persistence than squared return (Ding et al., 1993; Forsberg & Ghysels, 2007). This proxy has also been employed in other studies on volatility connectedness (e.g., Huszár et al., 2023; Jaeck & Lautier, 2016; Khalfaoui et al., 2023). For robustness, we re-run our analysis using realized weekly volatility, estimated with the range volatility approach proposed by Parkinson (1980), in Section D.2 of the Appendix. The conclusions remain consistent with those obtained using absolute returns as a proxy.

Figure 5.2 illustrates the volatility dynamics of European gas markets from May 2019 to May 2024. The TTF volatility series (panel a) shows sharp spikes in

5. Return and Volatility Connectedness in NWE Gas Markets

2022, particularly during the first few months and again in August and September. These spikes coincide with heightened uncertainty about the future of Russian gas supplies and the evolving geopolitical situation in Ukraine, which increased market volatility during these periods. In 2023, TTF volatility began to stabilize, and by 2024, the index exhibited fewer dramatic price swings, suggesting a degree of market rebalancing. The volatility ratios of THE/TTF, NBP/TTF, and ZTP/TTF (panels b, c, and d) demonstrate how the relative volatility of these markets compared to TTF evolved over time. For most of the period, these ratios remained moderate, indicating relatively aligned volatility between these benchmarks and TTF. However, in 2022, the NBP/TTF and ZTP/TTF ratios surged dramatically, signaling that these markets experienced disproportionately higher volatility than TTF during the peak of the crisis.

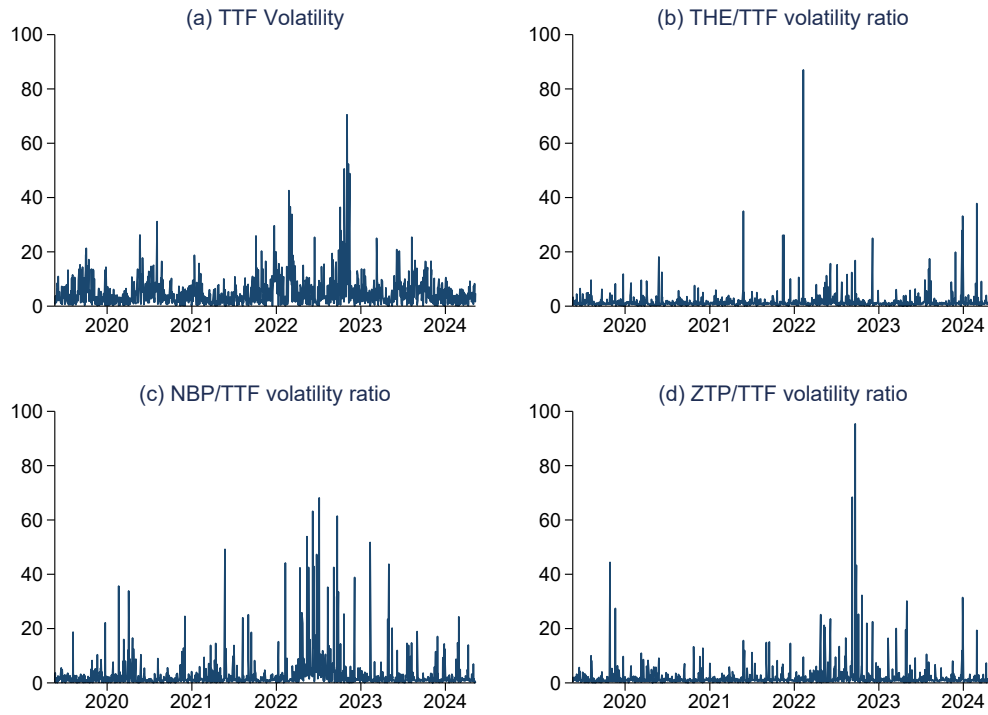


Figure 5.2.: TTF volatility series and volatility ratios of THE, NBP, and ZTP to TTF
Note: The top left graph (a) shows the TTF volatility series, while the subsequent graphs display the volatility ratios: (b) THE/TTF, (c) NBP/TTF, and (d) ZTP/TTF, illustrating the relative volatility movements of the European gas benchmarks compared to TTF. Extreme observations for relative volatility were removed on June 10th, June 16th, and November 27th, 2022, to improve the visualization of graph (c).

Two factors likely explain the higher volatility of NBP and ZTP compared to TTF. The first one is the variation in market liquidity. TTF, Europe's most liquid gas hub, had a churn rate of 63 times in 2022, indicating high trading volumes

and a large number of participants.³⁶ This high liquidity stabilizes prices, as large trades have less impact on the overall market. In contrast, NBP and ZTP had much lower liquidity, with NBP’s churn rate dropping to 6.1 times, and ZTP categorized as a ‘poor’ hub with even lower liquidity. These lower liquidity levels made NBP and ZTP more vulnerable to price swings, as their markets were less able to absorb supply and demand shocks (Heather, 2024). The second factor is related to a substantial increase in LNG imports into both Belgium and the UK during 2022, with volumes rising by 175% year-on-year in Belgium and 70% in the UK. This surge in LNG supply inflated trading volumes relative to domestic demand in both countries, contributing to greater volatility (Heather, 2023).

A key factor examined in relation to the varying levels of connectedness among the NWE gas hubs is the utilization of the physical infrastructure connecting these countries, particularly the interconnectors between the UK and the continent. Both gas interconnectors between the UK and continental Europe—namely, the UK–Netherlands (Figure 5.3(a)) and the UK–Belgium (Figure 5.3(b))—operated near full capacity for much of 2022, as shown in the figures. After Section 5.5 quantifies the level of connectedness, the subsequent section applies regression analysis to examine the relationship between congestion and the estimated connectedness levels.

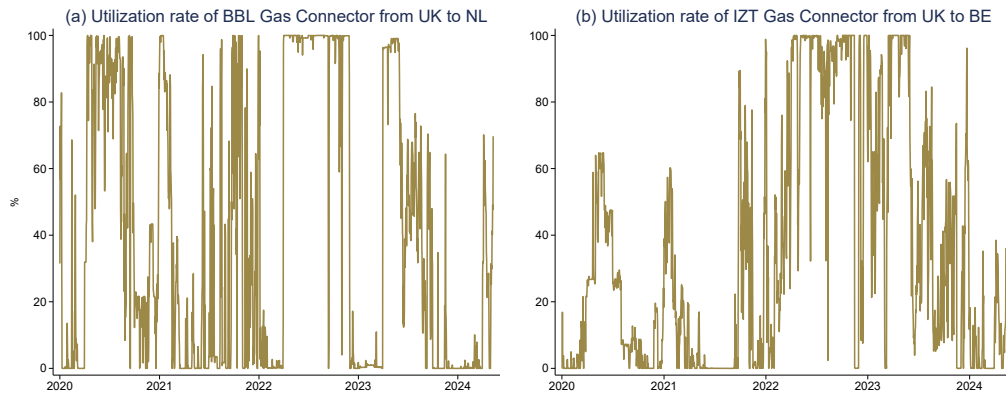


Figure 5.3.: Gas infrastructure utilization in NWE

Note: Data obtained from the ENTSOG Transparency Platform. Country abbreviations: UK (United Kingdom), NL (Netherlands), BE (Belgium).

³⁶The churn rate is a measure of market liquidity, calculated as the ratio of the total volume of trades to the physical demand for gas within a market. A higher churn rate indicates more active trading relative to the volume of gas consumed, with a rate of 10 or more generally considered a benchmark of market maturity. Traders use the churn rate to assess a market’s depth and liquidity, with financial participants often requiring a churn rate above 12 for engagement (IEA, 2020).

5.4. Methodology

This study applies a novel R^2 decomposed connectedness approach developed by Balli et al. (2023) to examine the overall, contemporaneous, and lagged spillover effects within European gas benchmarks. This approach extends the connectedness frameworks established by Diebold and Yilmaz (2012) and Diebold and Yilmaz (2014) by relying on the R^2 decomposition concept of Genizi (1993), allowing for a more accurate and interpretable estimation of connectedness measures by avoiding the associated normalization problem. Specifically, the R^2 value of a multivariate regression model falls between 0 and 1, eliminating the need for scaling to constrain row sums within this range.³⁷ Consequently, this results in more easily interpretable connectedness measures, with the row sums automatically constrained to a functional range (Naeem, Chatziantoniou, et al., 2024).

Consider the following VAR(p) with contemporaneous effects:

$$y_t = \sum_{i=0}^p A_i y_{t-i} + u_t, \quad u_t \sim N(0, \Sigma) \quad (5.1)$$

where y_t , y_{t-i} , and u_t are $N \times 1$ dimensional demeaned vectors in time t , A_i and Σ are $N \times N$ dimensional matrices. Here, $\text{diag}(A_0) = 0$, implying that the left-hand side (LHS) variable is dropped from the right-hand side (RHS) variables. p is the number of lags, with $p = 0$ meaning that the model collapses to the contemporaneous R^2 decomposed connectedness approach of Naeem, Chatziantoniou, et al. (2024). Alternatively, the model presented can be expressed as: $y_{n,t} = a_n x_t + u_{n,t}$ where $x_t = [y'_t, y'_{t-1}, \dots, y'_{t-p}]'$ is an $N(p+1) \times 1$ dimensional vector and a_n is an $1 \times N(p+1)$ dimensional vector with zero on the n th position.

Only if all RHS variables are uncorrelated with each other does the sum of the R^2 contributions, determined through bivariate linear regressions, equal the R^2 goodness-of-fit measure of a multivariate linear regression (MLR). As this is generally not the case, there is a need to find a transformation that converts the correlated series $x_{n,t}$ ³⁸ into an orthogonal series. This can be achieved by using principal component analysis (PCA), where the number of latent factors is equal to the number of RHS variables. Hence, the R^2 decomposition for an MLR can

³⁷The normalization problem arises because the row sums of the GFEVD matrix are not constrained to a fixed range (such as $[0, 1]$) and may exceed unity. The R^2 connectedness approach naturally constrains values within this range, eliminating the need for such normalization. See Naeem, Chatziantoniou, et al. (2024) for a more detailed description of this issue and how the R^2 connectedness framework avoids it.

³⁸ $x_{n,t}$ is equivalent to x_t but excludes the LHS.

be calculated with:

$$R_{xx} = V\Lambda V' = CC' \quad (5.2)$$

$$C = V\Lambda^{1/2}V' \quad (5.3)$$

$$R^{2,d} = C^2(C^{-1}R_{yx})^2 \quad (5.4)$$

Where V , $\Lambda = \text{diag}(\lambda_1, \lambda_2, \dots, \lambda_{N(p+1)-1})$, and R_{xx} represent $[N(p+1)-1] \times [N(p+1)-1]$ eigenvector, eigenvalue, and Pearson correlation matrices, respectively, while R_{yx} and $R^{2,d}$, illustrate the $[N(p+1)-1] \times 1$ Pearson correlation and R^2 contribution vectors, respectively. R_{xx} denotes Pearson correlation coefficients across RHS variables, while R_{xy} is the Pearson correlation coefficient between the LHS and RHS variables. The first $N-1$ values of $R^{2,d}$ denote the contemporaneous R^2 contributions, and the remaining represent the lagged R^2 contributions. Hence, the vector sum of $R^{2,d}$ is equal to the MLR R^2 goodness-of-fit measure. Stacking the $R^{2,d}$ contribution of all N MLRs gives the $N \times N(p+1)$ dimensional $R^{2,d}$ decomposition matrix, $[R_0^{2,d}, \dots, R_i^{2,d}, \dots, R_p^{2,d}]$. $R_0^{2,d}$ ³⁹ can be interpreted as the contemporaneous spillovers ($R_C^{2,d}$), whereas the sum of the lagged values ($R_L^{2,d} = R_1^{2,d} + \dots + R_i^{2,d} + \dots + R_p^{2,d}$) stand for the lagged spillovers.

Based on Diebold and Yilmaz (2012) and Diebold and Yilmaz (2014), $R_C^{2,d}$ and $R_L^{2,d}$ replace the scaled GFEVD matrix. Accordingly, the total connectedness index (TCI) is equal to the average R_n^2 of the N MLRs:

$$TCI = \frac{1}{N} \sum_{n=1}^N R_n^2 \quad (5.5)$$

Here, ‘TCI’ refers to the broader and more systematic relationships and interdependencies among multiple markets. It encompasses the overall structure and dynamics of how these entities are interconnected. Connectedness can be static or dynamic, reflecting how these relationships change over time, especially in response to economic or geopolitical events. As R_n^2 is within zero and unity, TCI is also within the same range, avoiding the connectedness normalization problem, which arises from the need to standardize the GFEVD to ensure that the row sums of the connectedness matrix are equal to one (Naeem, Chatziantoniou, et al., 2024). The contemporaneous and lagged TCI is derived as follows:

$$TCI = \frac{1}{N} \sum_{n=1}^N R_n^2 \quad (5.6)$$

$$= \left(\frac{1}{N} \sum_{n=1}^N \sum_{j=1}^N R_{C,n,j}^{2,d} \right) + \left(\frac{1}{N} \sum_{n=1}^N \sum_{j=1}^N R_{L,n,j}^{2,d} \right) \quad (5.7)$$

$$= TCI^C + TCI^L \quad (5.8)$$

³⁹Note that $\text{diag}(R_0^{2,d}) = 0$

where TCI^C and TCI^L represent the contemporaneous and lagged TCI, respectively.

Furthermore, the ‘TO’, ‘FROM’, and ‘NET’ spillovers are calculated as follows:

$$TO_j = \sum_{n=1}^N R_{C,n,j}^{2,d} + \sum_{n=1}^N R_{L,n,j}^{2,d} \quad (5.9)$$

$$= TO_j^C + TO_j^L \quad (5.10)$$

$$FROM_j = \sum_{n=1}^N R_{C,j,n}^{2,d} + \sum_{n=1}^N R_{L,j,n}^{2,d} \quad (5.11)$$

$$= FROM_j^C + FROM_j^L \quad (5.12)$$

$$NET_j^C = TO_j^C - FROM_j^C \quad (5.13)$$

$$NET_j^L = TO_j^L - FROM_j^L \quad (5.14)$$

$$NET_j = NET_j^C + NET_j^L \quad (5.15)$$

In this context, the TO_j (TO_j^C/TO_j^L) total directional connectedness quantifies the proportion of the overall (contemporaneous/lagged) variance in all LHS variables that is attributable to series j . On the other hand, the $FROM_j$ ($FROM_j^C/FROM_j^L$) total directional connectedness measures the extent to which the combined RHS variables explain the overall (contemporaneous/lagged) variance in series j . This is analogous to the R^2 value in a multivariate linear regression involving n variables. When NET_j is positive (negative), series j acts as a net transmitter (receiver) of shocks, meaning it explains more (less) of the variation in other series than the others explain in it. This interpretation applies equally to both contemporaneous and lagged connectedness measures.

5.5. The connectedness of NWE gas markets

This results section presents the findings of our connectedness analysis in three parts. First, we analyze the connectedness of natural gas price returns, covering both overall and directional dynamics.⁴⁰ Second, we examine volatility connectedness, focusing on similar aspects. Finally, we extend our analysis to futures prices to explore how expectations and forward-looking information are shared among markets.

⁴⁰Our baseline analysis uses a 200-day rolling-window VAR model with Pearson correlation coefficients. Robustness checks using varying window sizes (150 and 250 days) and Spearman correlations show consistent results, confirming the stability and validity of the findings. For brevity, these results are provided in Figures D.1 and D.2 in the Appendix.

5.5.1. Return connectedness results

Figure 5.4 plots the overall connectedness index from 2020 to 2024 for the four gas benchmarks. This index measures the extent to which price movements in one hub are transmitted to others. The figure also shows the decomposition of this index into contemporaneous spillovers (blue line) and lagged spillovers (red line). The results indicate that connectedness in natural gas price returns was around 70% in 2020 and increased to approximately 80% in 2021. It dropped sharply in the second half of 2022, coinciding with market disruptions and supply issues following the Russia-Ukraine invasion and the consequent cuts in Russian gas supply. This finding shows that the dynamic total connectedness index fluctuates over time and is dependent on market events. This is also consistent with Broadstock et al. (2020), Chen et al. (2022), and Papież et al. (2022), who found that various market reforms and external economic and political events influence market connectedness. Our analysis of the extended sample up to 2024 reveals that connectedness began to rise rapidly in the second half of 2023, reaching the highest level observed by the end of the sample, a level previously seen in the second half of 2021. A summary of the averaged connectedness measures among the four return series throughout the sample period is provided in Table D.2 in the Appendix.

Furthermore, Figure 5.4 illustrates that contemporaneous interdependencies, shown in blue, are more prominent than lagged interdependencies, depicted in red. The stronger contemporaneous dependency underscores the dominance of immediate market reactions over delayed responses, suggesting that market participants react swiftly to new information, with price adjustments among the gas hubs occurring almost instantly. This result aligns with the findings of Balli et al. (2023), who also observed the dominance of contemporaneous effects in the connectedness between energy futures prices. Our findings show that this pattern holds for natural gas price hubs before, during, and after the crisis, reflecting the rapid dissemination of the effects of shocks driven by news and events across hubs.

The dominance of contemporaneous effects in the overall connectedness of the NWE gas market, even during periods of infrastructure congestion, can be attributed to the advanced trading mechanisms and financial instruments used in these markets. Specifically, market participants can employ virtual trades and locational swaps,⁴¹ as well as derivatives, to adjust their positions quickly in response to new information. These tools enable the rapid dissemination of price signals across hubs, ensuring that prices adjust promptly, even when physical gas flows are restricted (ACER, 2023b).

Thus far, we have discussed the overall connectedness level, which is of interest but disregards heterogeneity within the connectedness of the gas price hubs as well

⁴¹A locational swap refers to a virtual transaction where a trader exchanges gas between two markets without physically moving the gas. The trader sells gas in one market and simultaneously buys gas in another, profiting from the price difference between the two hubs. This eliminates the need for a physical transportation contract and is considered ‘virtual transport’ (see ACER (2023b) for more details).

5. Return and Volatility Connectedness in NWE Gas Markets

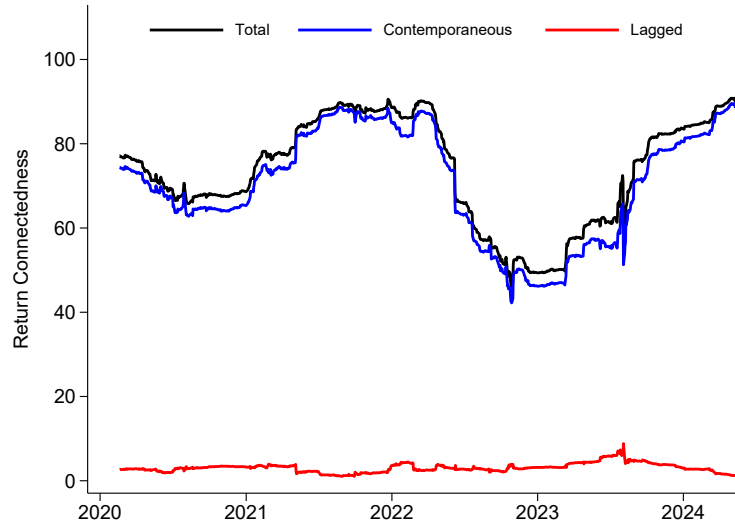


Figure 5.4.: Dynamic total connectedness of return series

Notes: R^2 decomposed measures are based on a 200-day rolling-window VAR model with a lag length of order one (BIC).

as directional information. We now turn to hub-specific directional connectedness measures. The results are depicted in Figure 5.5, which includes three rows: the ‘FROM’ connectedness (first row), measuring how much a particular hub’s price movements are explained by shocks from other hubs; the ‘TO’ connectedness (second row), reflecting how much a hub contributes to price variations in other hubs; and the ‘NET’ connectedness (third row), indicating whether a hub is a net transmitter or net receiver of shocks within the system. Additionally, the figure presents the respective overall R^2 measure of connectedness, along with the contemporaneous and lagged decomposed measures.

The results indicate that the ‘FROM’ and ‘TO’ connectedness indices for the four gas benchmarks generally decreased in the second half of 2020, following the initial impact of the COVID-19 pandemic, and again from the second quarter of 2022 to the first quarter of 2023. However, ZTP’s indices were lower during these subperiods of decreased connectedness, and NBP’s indices dropped even more significantly. This suggests that during times of severe market disruptions, ZTP and NBP became less influential in transmitting and receiving price shocks from other hubs. These findings suggest that local factors and individual market conditions began to dominate price movements rather than shared regional dynamics during tight market conditions. Furthermore, the decomposition of these ‘FROM’ and ‘TO’ connectedness indices reflects the dominance of the contemporaneous effects. This implies that even when NBP and ZTP became less connected overall during periods of market stress, the limited spillovers that persisted were transmitted instantaneously.

The third row of Figure 5.5 shows the time-varying net total directional connectedness of the four gas benchmarks. The results reveal that TTF usually acted as

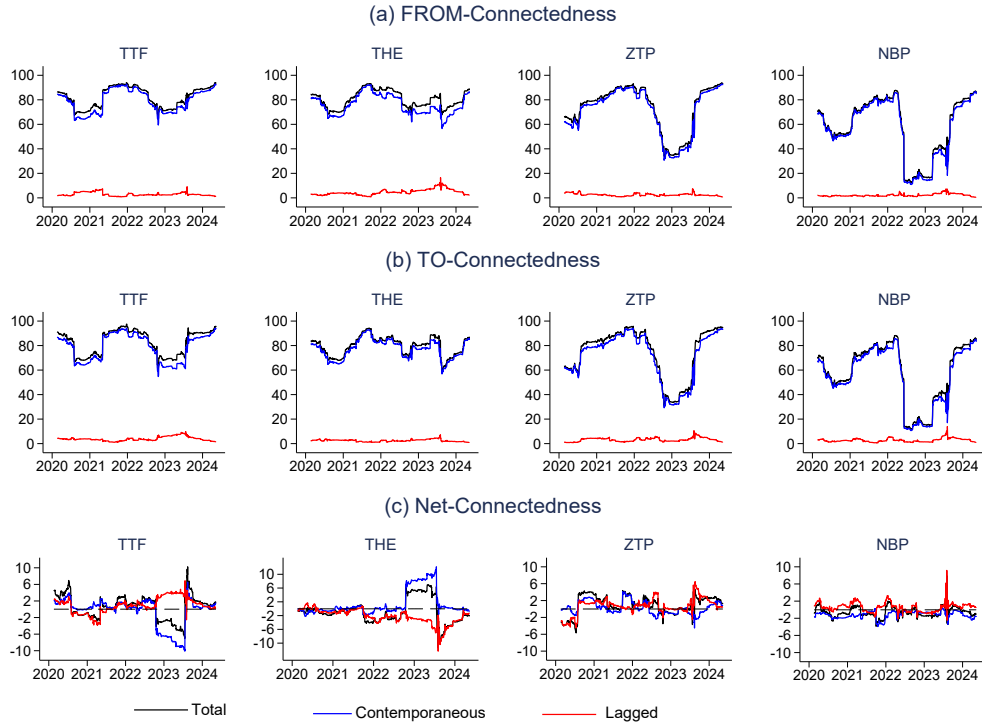


Figure 5.5.: Dynamic directional connectedness of return series

Notes: R^2 decomposed measures are based on a 200-day rolling-window VAR model with a lag length of order one. The black line visualizes the overall dynamic total connectedness, while the dynamic contemporaneous and lagged connectedness are illustrated in blue and red, respectively. The dashed horizontal line in Figure (c) represents the zero value reference line

a net transmitter of shocks, except from late 2022 to late 2023, when it became a net receiver, and THE became a net transmitter. A potential explanation for this shift is Germany's urgent need to replace lost Russian pipeline gas, which led to increased spot trading at THE. Additionally, the construction of new LNG import facilities and Floating Storage Regasification Units (FSRUs) in Germany further solidified THE's role as a key hub for balancing the country's gas needs and managing supply risks during this period of heightened energy insecurity. This argument is supported by Heather (2023), who reported a high market activity score for THE in 2022, ranking it second only to the Dutch TTF.⁴² ZTP exhibited a more varied pattern: initially, it was a net receiver until the first half of 2020, then predominantly a net transmitter, before reverting to a net receiver during the same period as TTF. Lastly, NBP remained a net receiver for most of the analyzed period. The results also reveal that NBP's directional connectedness is primarily driven by contemporaneous effects, indicating that it quickly absorbs

⁴²This score reflects the overall level of market activity at a hub, including the number of active participants, traded products, total traded volumes, the tradability index, and the churn rate. A higher score indicates greater liquidity, a wider diversity of traded products, and a hub's ability to facilitate risk management and portfolio balancing (see Heather (2023) for more details).

and reflects shocks originating from other hubs. For TTF, contemporaneous net spillover effects closely align with the overall net spillover effects throughout the entire sample period, reflecting that its influence on other hubs is immediate. This could be attributed to the high liquidity and significant trading activity of TTF.⁴³ This aligns with the findings of Liu et al. (2024), who reported that markets with a substantial trader base experience a high degree of net connectedness influenced primarily by contemporaneous effects. For THE and ZTP, this higher similarity between contemporaneous net spillover effects and overall net spillover effects only occurs during periods of positive net connectedness.

5.5.2. Volatility connectedness results

Next, we examine the dynamic total connectedness of the volatility series, as shown in Figure 5.6. High volatility connectedness indicates that periods of heightened uncertainty or volatility in one market can influence risk perceptions and price fluctuations in other markets, often through the transmission of market stress or shocks. The results show that the volatility connectedness of these benchmarks ranges between 40% and 70%. The spillover effects reached a high level from the second half of 2021 to the first quarter of 2022, suggesting that interconnectedness among volatility series was high during this period. The peak in the first quarter of 2022, particularly in February 2022, coincides with the Russian invasion of Ukraine. This can be attributed to increased investor caution caused by economic uncertainty and the market reconfiguration following this major news shock (Naeem, Gul, et al., 2024). Following this, the dynamic TCI values for the volatility series gradually declined, reaching the lowest level in early October 2022 at 40%. This decline was potentially due to the aftermath of subsequent shocks, such as the demolition of the Nord Stream 1 and 2 pipelines and the disruption of Russian gas flow to Europe. The results also indicate that throughout the observation period, contemporaneous effects dominated volatility connectedness (approximately 95%), except in the first half of 2023, when lagged effects increased slightly. These findings suggest that news affecting one market can lead to an immediate reassessment of risks in other markets, resulting in contemporaneous volatility spillovers. The slight increase in lagged effects in the first half of 2023 suggests that as markets adjusted to the post-crisis environment, the transmission of volatility may have become slightly more gradual.

Figure 5.7 presents the dynamic directional connectedness results of the volatility series, including 'FROM,' 'TO,' and 'NET' connectedness. Similar to the results obtained for return connectedness, the FROM' and 'TO' volatility connectedness indices for the four gas benchmarks generally decreased in the latter half of 2020 after the initial impact of COVID-19, and again from Q2 2022 to Q1 2023. ZTP and NBP experienced more pronounced declines in their indices during these

⁴³Note that TTF is by far the most liquid hub in the European gas market and has been widely used as the reference price for physical wholesale gas contracts. For a detailed analysis of the liquidity of different European gas benchmarks, refer to Heather (2023).

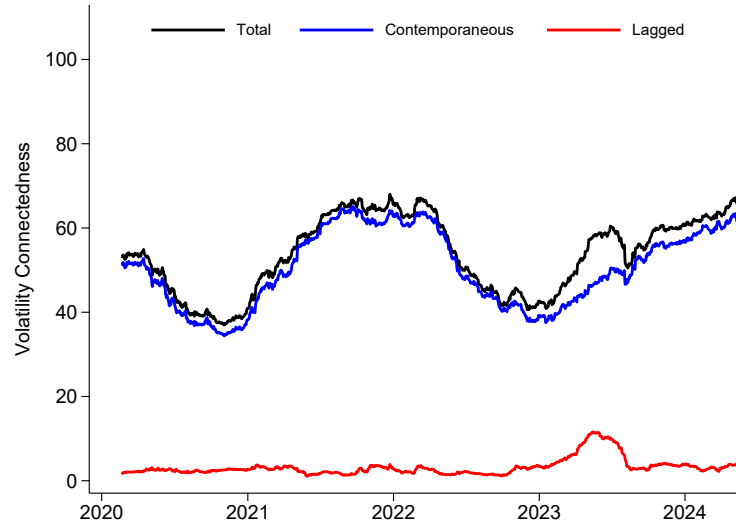


Figure 5.6.: Dynamic total connectedness of volatility series

Notes: R^2 decomposed measures are based on a 200-day rolling-window VAR model with a lag length of order one (BIC). Volatility is measured by the absolute returns and included in the model in log transformation.

periods of market stress, with ZTP showing lower values and NBP experiencing even sharper drops, approaching zero. This indicates that ZTP and NBP were less influenced by the other benchmarks during severe disruptions.

The third row of Figure 5.7 reveals distinct patterns among the gas benchmarks over the observed periods. The TTF benchmark oscillates between being a net transmitter and a net receiver of volatility, highlighting its pivotal role in the NWE gas market, where its influence fluctuates in response to market conditions and external factors. For example, TTF was a net transmitter during the first half of 2020 and throughout 2022, aligning with periods of high market activity or stress, such as the onset of the COVID-19 pandemic and the geopolitical tensions impacting energy supplies. THE was predominantly a net receiver, except from the second half of 2021 to the end of the first half of 2022. ZTP consistently acted as a net receiver, except during the period from 2020 to the first half of 2021, and again in the first half of 2023, when it became a net transmitter. The strong influence of ZTP on other benchmarks may be surprising given its relatively low liquidity, but this could be explained by its central geographic location between the other investigated markets. Conversely, NBP was largely a net receiver, highlighting its reactive nature, with brief periods as a net transmitter at the end of 2021 and in the first half of 2023. These findings indicate that TTF and ZTP play significant roles in market integration and stability, while THE and NBP are more susceptible to external shocks. Moreover, the decomposition of TTF's net connectedness into contemporaneous and lagged effects reveals that contemporaneous effects dominated the directional connectedness for most of the time in the investigated sample. In contrast, for the other three hubs, net

5. Return and Volatility Connectedness in NWE Gas Markets

directional connectedness was mainly driven by lagged effects. This reflects the role of market liquidity; the other three hubs have lower liquidity compared to TTF, causing their influence on other markets to take more time to materialize.

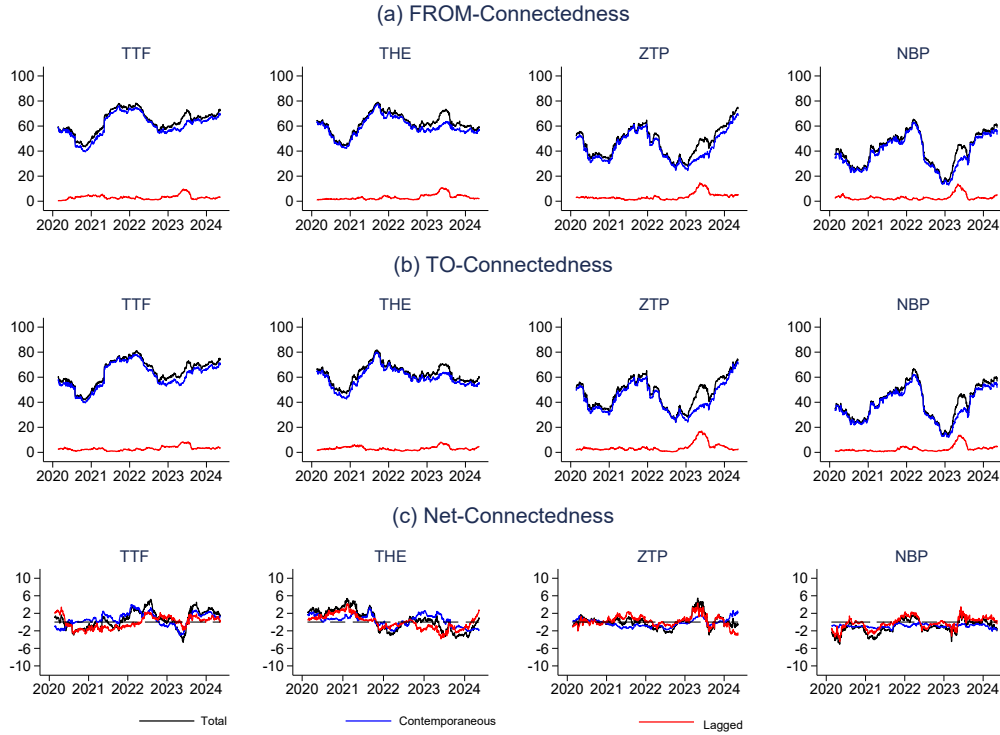


Figure 5.7.: Dynamic directional connectedness of volatility series

Notes: R^2 decomposed measures are based on a 200-day rolling-window VAR model with a lag length of order one. The black line visualizes the overall dynamic total connectedness, while the dynamic contemporaneous and lagged connectedness are illustrated in blue and red, respectively.

For robustness, we also use the range-based volatility measure of Parkinson (1980) to reanalyze the connectedness in the European gas market. The detailed results of this analysis are presented in Figures D.3 and D.4 in the Appendix. The findings are consistent with those of the baseline analysis.

5.5.3. Connectedness analysis using futures prices

This section investigates gas market connectedness based on futures prices, specifically one-month-ahead prices, rather than the spot prices (day-ahead prices) used in the previous subsections. The intuition behind this analysis is that futures prices incorporate traders' anticipations of upcoming supply and demand shifts, geopolitical risks, and macroeconomic factors. A high level of connectedness indicates that market participants across different hubs share similar expectations about the future, leading to synchronized futures price movements. Therefore, we hypothesize that futures prices may exhibit different connectedness patterns com-

pared to spot prices, which are influenced by immediate physical constraints and short-term market dynamics, such as local supply disruptions, weather conditions, and pipeline capacities.

In the following, we focus on the total return connectedness, which is presented in Figure 5.8. Additional results are provided in the Appendix, where Figure D.5 displays the directional connectedness of return series, Figure D.6 presents the total volatility connectedness, and Figure D.7 illustrates the directional connectedness of volatility series. For all figures, spot and futures price results are presented together for easy comparison. The dynamic decomposition of overall connectedness with futures prices leads to similar conclusions as with spot prices, with the contemporaneous effect being the dominant factor.⁴⁴

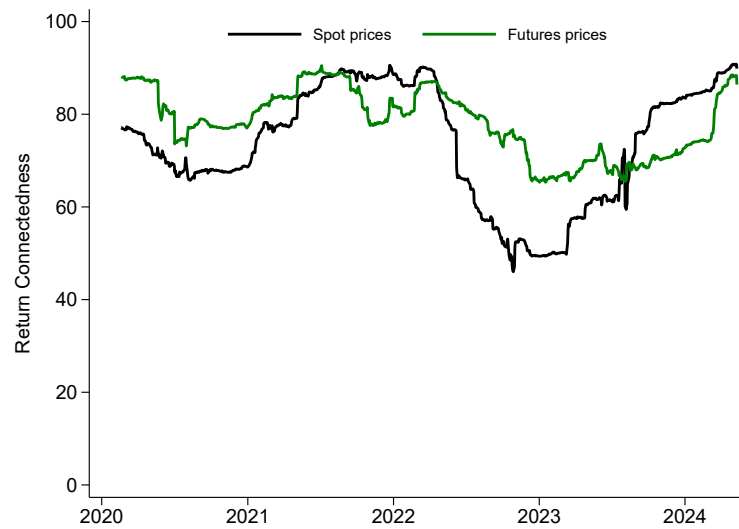


Figure 5.8.: Comparison of return connectedness indices: spot prices vs. futures prices
Notes: R^2 decomposed measures are based on a 200-day rolling-window rolling-window VAR model.

Figure 5.8 indicates that during the initial phase of the COVID-19 pandemic (2020 to early 2021), futures prices exhibited higher connectedness than spot prices. This suggests that market participants shared similar expectations about future market conditions, leading to synchronized futures price movements. As the pandemic's impact eased in the second half of 2021, connectedness among spot prices surpassed that of futures prices, reflecting a resurgence in physical market interdependence and aligned supply-demand dynamics across hubs. From February 2022 until mid-2023, geopolitical tensions stemming from the Russia-Ukraine conflict and associated supply disruptions led to a less pronounced decline in connectedness among futures prices. This suggests that market participants collectively anticipated tighter future markets due to reduced Russian gas supplies and infrastructure constraints, resulting in synchronized futures price movements.

⁴⁴These results are omitted from the figures for brevity but are available upon request from the corresponding author.

Concurrently, physical limitations and localized supply issues caused spot prices to diverge, reducing their connectedness. In the latter half of 2023 and early 2024, as markets stabilized and infrastructure constraints eased, spot prices became more interconnected. The normalization of physical flows allowed spot prices to move more cohesively across hubs, while futures price connectedness slightly diminished as market expectations varied in a less uncertain environment.

Overall, these findings highlight the interplay between physical market conditions and market expectations in shaping the interconnectedness of gas prices. Periods of heightened uncertainty and shared future concerns tend to amplify futures price connectedness, whereas improved physical integration and immediate market alignment enhance spot price connectedness.

5.6. Factors associated with the connectedness of NWE gas markets

The connectedness analysis from the previous section reveals notable fluctuations in connectedness levels. The lowest level occurred at the end of 2022, coinciding with a tight supply situation in Germany and the Netherlands, as these countries had to replace Russian supplies with LNG and increased pipeline supplies from Norway and the UK. Our directional connectedness analysis shows that the decrease in connectedness was mainly due to the decoupling of the NBP benchmark, likely caused by physical congestion at cross-border pipelines. This congestion may have limited the ability to balance gas supply and demand across the regional markets, thereby reducing interdependence and price coherence.

This section examines the relationship between congestion in the pipelines connecting the UK with the other investigated markets and the connectedness of the NWE gas markets. Figures 5.9(a) and 5.9(b) depict the utilization rates of the BBL gas connector from the UK to the Netherlands and the IZT gas connector from the UK to Belgium, respectively. These figures visually support the hypothesis that periods of high utilization in either of the two pipelines correlate with lower connectedness levels, while periods of low utilization are associated with increased connectedness.

To further investigate the effect of pipeline congestion, along with other factors, on connectedness levels, we conduct regression analysis to examine how congestion in the BBL and IZT gas pipelines correlates with the connectedness of the NWE natural gas benchmarks. The dependent variables are total return and volatility connectedness, as obtained from the analysis in the previous section. The main independent variable is 'congestion,' a dummy variable that takes the value of 1 if the BBL or IZT pipeline is congested, defined as having a utilization rate of 80% or higher.

We include a control variable to account for the impact of the EU's 2022 storage mandate, which required member states to fill their gas storage facilities to 80%

5.6. Factors associated with the connectedness of NWE gas markets

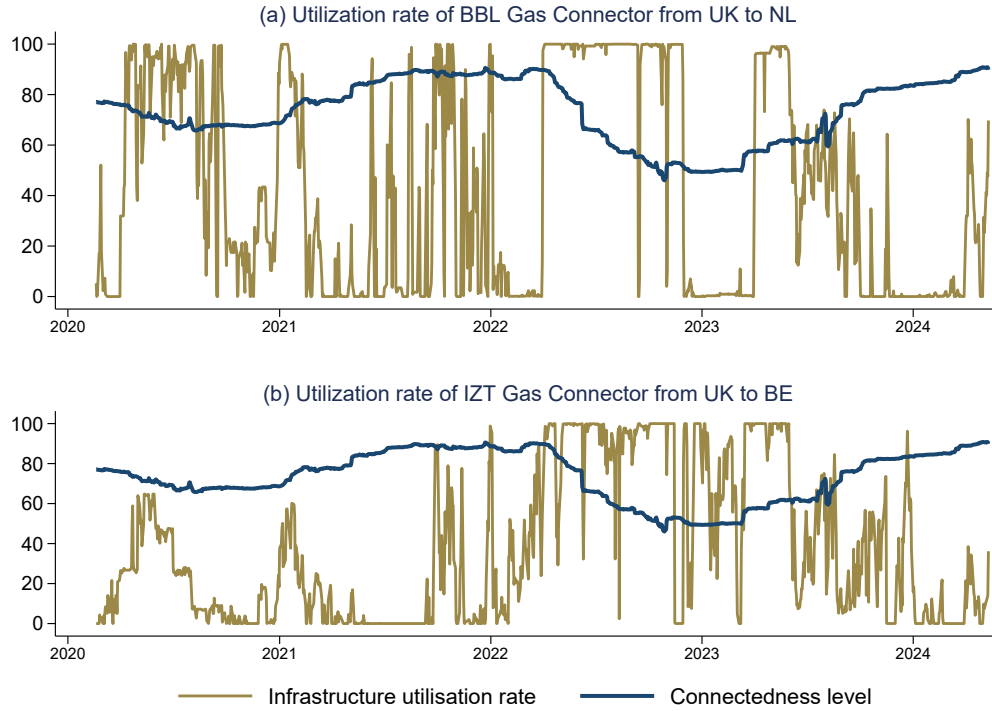


Figure 5.9.: Return connectedness level and utilization rate of BBL and IZT gas pipelines (%)

Notes: Data on utilization rates are obtained from the ENTSOG Transparency Platform. The solid line represents return connectedness between the NWE gas benchmarks, as analyzed in Subsection 5.5.1. Values on the vertical axis are expressed as percentages (%). BBL refers to the Balgzand-Bacton Line pipeline, and IZT refers to the Interconnector Zeebrugge Terminal pipeline. Country abbreviations: UK (United Kingdom), NL (Netherlands), and BE (Belgium).

capacity by November 1, 2022. This mandate was issued by the EU Council on June 27, 2022 (Council of the European Union, 2022). The hypothesis is that this storage mandate created immediate and intense pressure to secure gas supplies across the EU, particularly in Germany, during already tight market conditions, leading to higher prices in the eastern part of the NWE region. To measure this effect, we created a dummy variable that takes the value of 1 starting on June 27, 2022, when the mandate was issued, and ending on August 29, 2022, when the storage target of 80% was reached (Gas Infrastructure Europe, 2022).

We also control for geopolitical risk by including the Geopolitical Risk Index from Caldara and Iacoviello (2022) to isolate and better understand how external political factors influence market integration.⁴⁵ Additionally, we include the futures spreads of TTF and NBP as well as interaction terms between the futures

⁴⁵The index measures adverse geopolitical events based on articles from 10 U.S. newspapers. More details about the index and data can be found on this website: <https://www.matteoiacoviello.com/gpr.htm>.

spreads and the IZT congestion dummy variable.⁴⁶ When the futures spread is positive, it indicates that futures prices are higher than spot prices, suggesting that traders expect gas prices to rise. This can lead to increased gas storage, as market participants prefer to hold onto their inventory in anticipation of higher future prices, impacting overall market dynamics. Therefore, interacting the futures spread with congestion captures the combined effect of infrastructure constraints and market expectations on gas market connectedness, helping us understand how pipeline congestion is influenced by traders' expectations of future gas prices. Lastly, we control for year- and month-fixed effects in all regressions to account for time-specific factors and seasonal variations that could influence gas market connectedness.

The results are presented in Table 5.1, which displays the regression analysis for return connectedness (columns 1–2) and volatility connectedness (columns 3–4). In each set of regressions, the first specification includes only the BBL and IZT variables to capture the effect of pipeline utilization on the connectedness indices. The second specification introduces additional independent variables.

The results indicate that the coefficient for the IZT variable is negative and statistically significant across all specifications, indicating a strong association between IZT pipeline congestion and decreased return connectedness in the NWE gas markets. For example, column (1) shows that IZT congestion is associated with a decrease of 12.817 units in the connectedness index. When control variables are added in the second regression, the effect decreases (in absolute terms) to -9.587 units but remains statistically significant at the 1% level. This suggests that IZT congestion substantially correlates with market connectedness, even after accounting for geopolitical risk, the EU storage mandate, and futures spreads. The BBL variable, however, is not statistically significant in any of the regressions for return connectedness, indicating no significant association between BBL pipeline congestion and return connectedness beyond the extent to which BBL and IZT congestion correlated.⁴⁷ This may be due to the IZT pipeline's more critical role in connecting the NWE gas markets or possible differences in the capacity or usage patterns of the two pipelines.⁴⁸

The results also show that geopolitical risk has a positive coefficient statistically significant at 1%, suggesting that higher geopolitical risk is correlated with increased market connectedness. This implies that geopolitical events may cause

⁴⁶We focus on the TTF and NBP benchmarks because they are the most liquid in the region and focus on IZT congestion because this was found to be more significant (see Table 5.1).

⁴⁷In fact, the Variance Inflation Factor (VIF) values for the BBL and IZT variables were below 5 in all regressions, indicating that multicollinearity is not a concern. The VIF results are available upon request.

⁴⁸The IZT pipeline has a significantly higher capacity for transporting natural gas compared to the BBL pipeline. IZT provides an export capacity of 20 bcm/year (UK to BE) and an import capacity of 25.5 bcm/year (BE to UK), translating to approximately 637 GWh/day and 812 GWh/day, respectively. In contrast, BBL's forward flow (NL to UK) capacity is 432 GWh/day, while its reverse flow (UK to NL) capacity is only 185 GWh/day (Sources: <https://www.fluxys.com/> and <https://bblcompany.com/>).

5.6. Factors associated with the connectedness of NWE gas markets

Table 5.1.: Regression analysis of factors associated with NWE gas markets connectedness

	(1)	(2)	(3)	(4)
	Return connectedness		Volatility connectedness	
BBL	-3.016 (2.598)	-0.631 (1.385)	-1.764 (1.660)	-0.681 (1.477)
IZT	-12.817 ^a (3.385)	-9.587 ^a (3.363)	-7.123 ^a (2.152)	-4.711 ^b (1.975)
Geopolitical Risk		0.049 ^a (0.017)		0.031 ^a (0.010)
EU Storage Mandate		-7.471 ^c (4.447)		-5.647 ^b (2.694)
$Spread_{ttf}$		0.160 (0.161)		0.089 (0.118)
$Spread_{nbp}$		-0.307 ^b (0.143)		-0.113 (0.084)
$IZT \times Spread_{ttf}$		-0.454 ^b (0.179)		-0.205 (0.129)
$IZT \times Spread_{nbp}$		0.217 ^b (0.105)		0.052 (0.075)
Intercept	65.909 ^a (4.408)	59.681 ^a (4.066)	39.169 ^a (4.302)	35.706 ^a (3.919)
No. of observations	1103	1103	1103	1103
Adj. R^2	0.514	0.625	0.518	0.578
Year FE	✓	✓	✓	✓
Month FE	✓	✓	✓	✓

Notes: The dependent variable for columns 1–2 is the return connectedness index, while the dependent variable for columns 3–4 is the volatility connectedness index. The variables “BBL” and “IZT” relate to the “Congestion” of the respective pipeline, which is measured by a dummy set to 1 if the respective pipeline’s utilization rate exceeds 80%. “EU Storage Mandate” is a dummy variable that takes the value of 1 from June 27, 2022, to August 29, 2022. “Spread” is the futures spread (futures - spot) for the TTF and NBP gas benchmarks. Standard errors are reported in parentheses and are computed using the Newey-West heteroskedasticity and autocorrelation consistent estimator. All regressions control for year and month-fixed effects, and their results are available upon request from the corresponding author. ^a, ^b, and ^c represent the 1%, 5%, and 10% significance levels, respectively.

markets to move more in parallel due to shared concerns, thereby increasing connectedness. Regarding the EU storage mandate, the results indicate that this policy may have had a negative effect on connectedness. Column 2 also indicates that the interaction between IZT and the TTF futures spread is negative (-0.454) and statistically significant at the 5% level, suggesting that during congestion, expectations of higher future prices (a positive TTF spread) further reduce current connectedness. This may be due to anticipated supply shortages exacerbating market segmentation. Conversely, the interaction between IZT and the NBP futures spread is positive (0.217) and also significant at the 5% level, indicating that the negative impact of the NBP spread on connectedness is moderated during congestion. However, we do not find a statistically significant effect for these two interaction terms on volatility connectedness.

5.7. Conclusion

This study examines the time-varying connectedness among natural gas prices in the NWE market using the R^2 decomposed connectedness approach, as introduced by Balli et al. (2023). This method decomposes connectedness measures into contemporaneous and lagged components, providing a more nuanced understanding of market dynamics. The analysis is applied to both price returns and volatility.

Our analysis reveals that connectedness within natural gas markets is highly dynamic and varies significantly depending on market conditions, such as external shocks and infrastructure congestion. The findings consistently show that contemporaneous effects dominate lagged effects in both return and volatility connectedness, indicating that immediate market responses are more influential than delayed reactions. This trend is particularly evident during periods of heightened uncertainty, such as the Russia-Ukraine crisis. Furthermore, futures and spot prices exhibit distinct connectedness patterns shaped by different underlying factors. Futures price connectedness tends to increase during periods of uncertainty, driven by shared market expectations of future conditions, whereas spot price connectedness is enhanced by improved physical integration and immediate market alignment. We also find that pipeline congestion is significantly associated with reduced market connectedness, underscoring the impact of infrastructure constraints on the integration of NWE gas markets. The interaction between congestion and market expectations further exacerbates the decline in connectedness, suggesting that infrastructure limitations, combined with expectations of future price increases, can intensify market segmentation. Conversely, heightened geopolitical risk is correlated with increased connectedness, indicating that shared regional responses to geopolitical events can enhance the alignment of market behaviors across hubs.

Our findings have three main implications. First, the dominance of contemporaneous spillovers in both return and volatility connectedness indicates that European gas markets respond quickly to shocks, even during tight market conditions. This suggests that, despite supply constraints or pipeline congestion, information flows and price adjustments are not hindered, driven by trading mechanisms that allow participants to bypass physical bottlenecks through financial instruments and virtual trades. As a result, relying on past shocks to predict future movements is less effective, and market participants need to focus on real-time information and be prepared to act swiftly. However, this also implies that participants have limited time to respond to shocks, potentially increasing their exposure to sudden market volatility. Consequently, constant monitoring and rapid decision-making become critical to mitigate heightened risks.

Second, the decrease in connectedness between European gas markets during crises and tight market conditions underscores the significant impact of physical infrastructure constraints. Unlike financial markets, where crises typically heighten return and volatility spillovers through contagion effects (see, for ex-

ample, Longstaff, 2010; Mensi et al., 2018), our results indicate that congestion in gas pipelines during crisis periods can disrupt market integration, leading to reduced connectedness. This phenomenon is consistent with similar findings in other energy markets, such as the European electricity market (e.g., Gugler et al., 2018). However, once these tight conditions subside, connectedness swiftly returns to normal levels, suggesting that these disruptions are temporary and that the market can restore integration once physical constraints ease.

Lastly, the relationship between pipeline utilization and market connectedness has direct welfare implications. During periods of pipeline congestion, reduced connectedness limits arbitrage opportunities, leading to higher price dispersion across regions and potentially lowering welfare due to inefficient gas allocation. While this generally supports infrastructure enhancements, further expansion of the European natural gas infrastructure should be carefully considered. As we show, connectedness levels had already returned to pre-crisis levels toward the end of our observation period. Further infrastructure investments may, hence, risk becoming stranded assets.

A. Supplementary Material for Chapter 2

A.1. Additional data details

Consumer price index: The real-time, monthly, seasonally adjusted U.S. Consumer Price Index (CPI) for all urban consumers is sourced from the Economic Indicators published by the Council of Economic Advisers and from the macroeconomic real-time database of the Federal Reserve Bank of Philadelphia. The CPI vintages, subject to revision, typically experience a one-month publication delay. Missing CPI observations are nowcasted using that vintage's average historical growth rate from January 1973 (1973M1).

Spot price data: Daily closing prices for all spot prices are used to calculate the monthly average and end-of-month prices. The end-of-month price is the closing price on the last trading day of the month. Following standard practices, monthly average prices are calculated as the simple average of daily closing prices. Spot prices are not subject to revisions and are observed in real time. All spot prices are obtained from Bloomberg, except for crude oil and heating oil, which are sourced from the United States Energy Information Administration (EIA).

Table A.1.: Bloomberg Tickers / Sources for Commodity Spot Prices and Sample Periods

Commodity	Market	Ticker	Source	Sample Start
Energy				
Crude oil	Cushing, OK		EIA	1986.01
Natural Gas	Henry Hub	NGUSHHUB	Bloomberg	1999.01
Heating Oil	New York		EIA	1986.06
Gasoline	New York	RBOB87PM	Bloomberg	2003.11
Ethanol	Chicago	ETHNCHIC	Bloomberg	2007.02
Precious Metals				
Gold		XAUUSD	Bloomberg	1975.01
Silver		XAGUSD	Bloomberg	1973.01
Platinum		XPTUSD	Bloomberg	1987.01
Base Metals				
Aluminum	LME	LMAHDY	Bloomberg	1987.08
Copper	LME	LMCADY	Bloomberg	1986.04
Lead	LME	LMPBDY	Bloomberg	1987.01
Nickel	LME	LMNIDY	Bloomberg	1987.01
Tin	LME	LMSNDY	Bloomberg	1989.06
Zinc	LME	LMZSDY	Bloomberg	1989.01
Agricultural				
Corn	Chicago	CORNCH2Y	Bloomberg	1996.01
Soybeans	Chicago	SOYBCH1Y	Bloomberg	1996.01
Wheat	Chicago	WEATCHEL	Bloomberg	1992.01

A.2. Additional results

Comparison of the no-change benchmarks

We empirically validate the appropriateness of the end-of-month versus average price no-change for monthly average real prices for all primary commodities. We employ two forecast evaluation criteria: the Mean Squared Forecast Error (MSFE) ratio and a measure of directional accuracy, termed success ratios. The MSFE ratio for the h -step-ahead forecast, $MSFE_h^{ratio}$, is computed as the ratio of the MSFE of the end-of-month no-change forecast to the MSFE of the monthly average no-change forecast:

$$MSFE_h^{ratio} = \frac{\sum_{q=1}^Q (\bar{R}_{q+h} - R_{q,n_q})^2}{\sum_{q=1}^Q (\bar{R}_{q+h} - \bar{R}_q)^2}, \quad (\text{A.1})$$

where \bar{R}_q is the monthly average real price in month q , R_{q,n_q} is the real price on the last trading day n_q of month q , \bar{R}_{q+h} is the actual monthly average real price h months ahead, i.e., in month $q+h$, Q is the total number of forecast evaluation periods, and $q = 1, 2, \dots, Q$ indexes the evaluation sample. The null hypothesis, suggesting an equal MSFE of the model-based forecast relative to the no-change

forecast, is tested following the methodology of Diebold and Mariano (1995) and compared against standard normal critical values.

Directional accuracy is evaluated using the mean directional accuracy. This metric describes the fraction of times the forecasting model is able to correctly predict the change in the direction of the real price of a commodity. The calculation is as follows:

$$SR_k = \frac{1}{Q} \sum_{q=1}^Q \mathbb{1} \{ \text{sgn}(\bar{R}_{q+h} - \bar{R}_q) = \text{sgn}(R_{q,n_q} - \bar{R}_q) \}, \quad (\text{A.2})$$

where sgn is a sign function and $\mathbb{1}$ is an indicator function. The test statistic is calculated following Pesaran and Timmermann (2009). The null hypothesis is that the futures-based forecast should be no more successful at predicting the direction of change in the price of the respective commodity, with a success probability of 0.5. Therefore, a success ratio above 0.5 can be interpreted as an improvement over the no-change forecast.

Table A.2.: Real-Time End-of-Month versus Monthly Average No-Change Forecast

	1	3	6	9	12	15	18	21	24
Commodity	MSFE Ratio								
Crude Oil	0.54 (0.000)	0.91 (0.008)	0.97 (0.303)	0.96 (0.058)	0.97 (0.010)	0.97 (0.194)	0.98 (0.205)	0.99 (0.084)	1.00 (0.249)
Natural Gas	0.52 (0.000)	0.88 (0.000)	0.93 (0.044)	0.96 (0.072)	0.92 (0.075)	1.01 (0.276)	1.00 (0.085)	0.97 (0.369)	0.95 (0.534)
Heating Oil	0.60 (0.000)	0.90 (0.009)	0.95 (0.038)	0.96 (0.259)	0.99 (0.155)	0.98 (0.137)	0.99 (0.060)	0.99 (0.223)	1.00 (0.149)
Gasoline	0.60 (0.000)	0.93 (0.002)	1.02 (0.165)	1.03 (0.117)	1.00 (0.152)	0.99 (0.088)	1.00 (0.259)	1.01 (0.294)	1.02 (0.216)
Ethanol	0.91 (0.000)	1.31 (0.225)	1.20 (0.017)	1.13 (0.910)	1.13 (0.101)	1.12 (0.723)	1.13 (0.469)	1.14 (0.213)	1.13 (0.511)
Gold	0.70 (0.000)	0.94 (0.011)	0.94 (0.004)	0.99 (0.112)	0.98 (0.017)	0.99 (0.190)	0.98 (0.317)	0.98 (0.423)	0.99 (0.559)
Silver	0.82 (0.000)	0.95 (0.070)	0.98 (0.060)	1.00 (0.175)	1.01 (0.041)	1.03 (0.362)	1.01 (0.419)	1.00 (0.277)	1.01 (0.345)
Platinum	0.59 (0.000)	0.93 (0.003)	0.98 (0.004)	0.98 (0.190)	0.99 (0.001)	1.01 (0.306)	0.97 (0.038)	0.97 (0.009)	0.97 (0.005)
Aluminum	0.59 (0.000)	0.94 (0.107)	0.97 (0.077)	1.00 (0.435)	1.00 (0.196)	1.04 (0.799)	1.03 (0.854)	1.02 (0.548)	1.03 (0.510)
Copper	0.64 (0.000)	0.91 (0.010)	0.96 (0.163)	0.98 (0.011)	0.99 (0.054)	1.02 (0.129)	1.02 (0.135)	1.01 (0.086)	1.02 (0.305)
Lead	0.70 (0.000)	0.99 (0.001)	0.97 (0.353)	1.00 (0.049)	1.03 (0.329)	1.05 (0.630)	1.05 (0.399)	1.02 (0.549)	1.03 (0.853)
Zinc	0.56 (0.000)	0.91 (0.000)	0.98 (0.258)	1.03 (0.592)	1.02 (0.596)	1.02 (0.782)	1.01 (0.775)	1.00 (0.760)	1.01 (0.897)
Nickel	0.67 (0.000)	0.92 (0.000)	0.98 (0.037)	0.99 (0.300)	0.98 (0.340)	1.02 (0.436)	1.01 (0.151)	1.02 (0.290)	1.02 (0.308)
Tin	0.55 (0.000)	0.86 (0.000)	0.97 (0.027)	1.00 (0.056)	0.99 (0.049)	1.02 (0.259)	1.03 (0.351)	1.03 (0.678)	1.03 (0.667)
Corn	0.67 (0.000)	0.92 (0.002)	0.97 (0.537)	0.99 (0.185)	0.98 (0.108)	1.00 (0.020)	1.00 (0.014)	1.00 (0.050)	1.00 (0.203)
Soybeans	0.59 (0.000)	0.96 (0.000)	1.02 (0.525)	1.04 (0.090)	1.03 (0.217)	1.02 (0.029)	1.01 (0.400)	1.01 (0.270)	1.01 (0.155)
Wheat	0.54 (0.000)	0.90 (0.014)	0.93 (0.205)	0.96 (0.201)	1.02 (0.266)	1.04 (0.298)	1.02 (0.208)	0.99 (0.514)	1.01 (0.772)
	Success Ratio								
Crude Oil	0.74 (0.000)	0.59 (0.008)	0.53 (0.303)	0.57 (0.058)	0.59 (0.010)	0.54 (0.194)	0.54 (0.205)	0.56 (0.084)	0.53 (0.249)
Natural Gas	0.76 (0.000)	0.66 (0.000)	0.56 (0.044)	0.57 (0.072)	0.57 (0.075)	0.53 (0.276)	0.56 (0.085)	0.52 (0.369)	0.50 (0.534)
Heating Oil	0.73 (0.000)	0.58 (0.009)	0.57 (0.038)	0.53 (0.259)	0.54 (0.155)	0.54 (0.137)	0.55 (0.060)	0.52 (0.223)	0.53 (0.149)
Gasoline	0.69 (0.000)	0.60 (0.002)	0.56 (0.165)	0.56 (0.117)	0.55 (0.152)	0.55 (0.088)	0.53 (0.259)	0.52 (0.294)	0.53 (0.216)
Ethanol	0.76 (0.000)	0.53 (0.225)	0.56 (0.017)	0.45 (0.910)	0.54 (0.101)	0.47 (0.723)	0.50 (0.469)	0.52 (0.213)	0.49 (0.511)
Gold	0.73 (0.000)	0.58 (0.011)	0.60 (0.004)	0.55 (0.112)	0.58 (0.017)	0.54 (0.190)	0.52 (0.317)	0.51 (0.423)	0.49 (0.559)
Silver	0.73 (0.000)	0.56 (0.070)	0.58 (0.060)	0.56 (0.175)	0.59 (0.041)	0.54 (0.362)	0.52 (0.419)	0.54 (0.277)	0.53 (0.345)
Platinum	0.75 (0.000)	0.60 (0.003)	0.61 (0.004)	0.54 (0.190)	0.61 (0.001)	0.53 (0.306)	0.58 (0.038)	0.58 (0.009)	0.59 (0.005)
Aluminum	0.70 (0.000)	0.54 (0.107)	0.54 (0.077)	0.50 (0.435)	0.52 (0.196)	0.47 (0.799)	0.45 (0.854)	0.49 (0.548)	0.49 (0.510)
Copper	0.65 (0.000)	0.58 (0.010)	0.53 (0.163)	0.57 (0.011)	0.55 (0.054)	0.53 (0.129)	0.53 (0.135)	0.54 (0.086)	0.51 (0.305)
Lead	0.69 (0.000)	0.60 (0.001)	0.51 (0.353)	0.55 (0.049)	0.51 (0.329)	0.48 (0.630)	0.50 (0.399)	0.49 (0.549)	0.46 (0.853)
Zinc	0.72 (0.000)	0.63 (0.000)	0.52 (0.258)	0.49 (0.592)	0.49 (0.596)	0.46 (0.782)	0.46 (0.775)	0.46 (0.760)	0.44 (0.897)
Nickel	0.72 (0.000)	0.66 (0.000)	0.57 (0.037)	0.52 (0.300)	0.52 (0.340)	0.51 (0.436)	0.54 (0.151)	0.52 (0.290)	0.52 (0.308)
Tin	0.72 (0.000)	0.64 (0.000)	0.58 (0.027)	0.56 (0.056)	0.56 (0.049)	0.52 (0.259)	0.51 (0.351)	0.48 (0.678)	0.48 (0.667)
Corn	0.73 (0.000)	0.60 (0.002)	0.50 (0.537)	0.53 (0.185)	0.55 (0.108)	0.58 (0.020)	0.58 (0.014)	0.57 (0.050)	0.54 (0.203)
Soybeans	0.70 (0.000)	0.62 (0.000)	0.50 (0.525)	0.54 (0.090)	0.53 (0.217)	0.58 (0.029)	0.51 (0.400)	0.52 (0.270)	0.54 (0.155)
Wheat	0.65 (0.000)	0.57 (0.014)	0.53 (0.205)	0.53 (0.201)	0.52 (0.266)	0.52 (0.298)	0.53 (0.208)	0.50 (0.514)	0.47 (0.772)

Notes: See the notes below Table 2.4. This table presents real-time end-of-month forecasts compared to monthly average no-change forecasts for the real price level. Forecasts for ethanol and gasoline start in 2006 due to data limitations.

The no-change forecasts are implemented in real-time; see section 2.4. Across all commodities, the MSFE ratios remain under unity at short-run horizons, and the success ratios exceed 0.5, see Table A.2. Both the magnitude and convergence of forecast criteria closely reflect values for series closely approximated by a random walk. Consistent with the findings for crude oil (Ellwanger & Snudden, 2023a), the forecast gains are significant for both criteria for the majority of commodities up to one year ahead.

These empirical findings reinforce the necessity to test relative to the end-of-period no-change forecast when evaluating period average forecasts of primary commodities. All forecasts in the paper are thus reported and tested against the end-of-month no-change forecast.

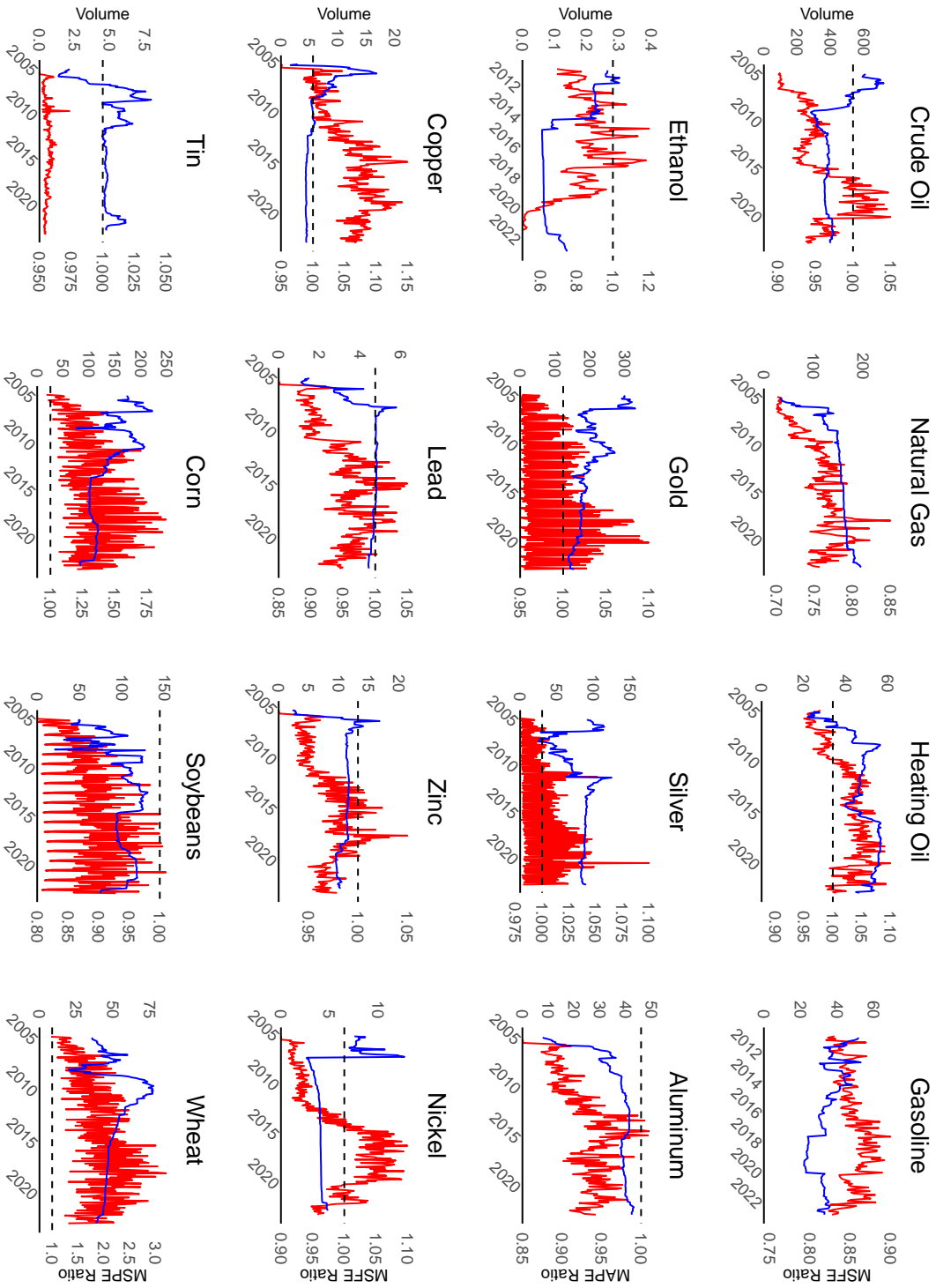
Comparison of contract and horizon alignment assumptions

Table A.3.: Adjustment Variations in First-Month Futures Forecasting, Non-Parametric

	Baseline	No Adjustment	Adjustment (1)	Adjustment (2)	Adjustment (3)	Adjustment (4)
Commodity	MSFE Ratio					
Crude Oil	0.99 (0.313)	0.99 (0.263)	1.00 (0.504)	0.99 (0.159)	1.00 (0.552)	0.99 (0.313)
Natural Gas	1.02 (0.663)	1.18 (0.923)	1.07 (0.829)	1.02 (0.663)	1.27 (0.965)	1.23 (0.922)
Heating Oil	1.04 (0.767)	1.29 (0.954)	1.04 (0.767)	1.06 (0.761)	1.23 (0.961)	1.37 (0.978)
Gasoline	0.81 (0.004)	0.90 (0.058)	0.81 (0.004)	0.92 (0.006)	0.81 (0.022)	0.98 (0.386)
Ethanol	0.72 (0.125)	1.18 (0.663)	0.72 (0.125)	0.80 (0.105)	1.27 (0.717)	1.22 (0.705)
Corn	1.03 (0.580)	1.25 (0.949)	0.93 (0.321)	0.97 (0.339)	1.03 (0.580)	1.49 (0.994)
Soybeans	0.86 (0.125)	0.95 (0.266)	0.83 (0.075)	0.93 (0.036)	0.86 (0.125)	1.12 (0.957)
Wheat	1.10 (0.911)	1.21 (0.985)	1.14 (0.968)	1.01 (0.648)	1.10 (0.911)	1.20 (0.983)
	Success Ratio					
Crude Oil	0.55 (0.091)	0.51 (0.166)	0.51 (0.344)	0.49 (0.195)	0.51 (0.353)	0.55 (0.091)
Natural Gas	0.52 (0.321)	0.53 (0.284)	0.56 (0.081)	0.52 (0.321)	0.51 (0.402)	0.53 (0.203)
Heating Oil	0.52 (0.300)	0.51 (0.470)	0.52 (0.300)	0.52 (0.325)	0.50 (0.566)	0.49 (0.688)
Gasoline	0.62 (0.001)	0.56 (0.029)	0.62 (0.001)	0.60 (0.001)	0.62 (0.000)	0.53 (0.278)
Ethanol	0.55 (0.086)	0.63 (0.001)	0.55 (0.086)	0.64 (0.000)	0.56 (0.033)	0.64 (0.000)
Corn	0.56 (0.028)	0.55 (0.145)	0.58 (0.008)	0.55 (0.088)	0.56 (0.028)	0.55 (0.076)
Soybeans	0.56 (0.051)	0.60 (0.006)	0.54 (0.183)	0.53 (0.269)	0.56 (0.051)	0.56 (0.004)
Wheat	0.55 (0.088)	0.53 (0.164)	0.57 (0.012)	0.56 (0.031)	0.55 (0.088)	0.56 (0.075)

Note: See the notes below Table 2.4. This table presents the performance of futures-based forecasts of nominal monthly prices using the EoM Futures Curve, for one month ahead. “Baseline” refers to the adjustment assumptions detailed in section 2.4.2, used as the baseline in the main tables. “No Adjustment” uses the front-month contract. “Adjustment (1)” omits the front-month contract and averages the spot price with the second-month contract. “Adjustment (2)” assigns the front contract to the two-month-ahead forecast and averages the spot price with the front contract. “Adjustment (3)” calculates the average of the first and second front contracts after aligning them with their corresponding horizons. Lastly, “Adjustment (4)” applies the average curvature from the first 12 contracts to the front contract. This table includes only the commodities for which the front-month contracts do not correspond with the one-month-ahead forecast, in line with the assumptions explained in section 2.4.2.

A. Supplementary Material for Chapter 2



Note: The blue line represents the MSFE Ratio, which measures the performance of futures-based forecasts of real prices using End-of-Month (EoM) futures. The MSFE Ratio compares the forecast accuracy of futures-based models to a random walk (no-change) forecast, where values below 1 indicate that the futures-based forecast is more accurate. The red line represents the trading volume (in thousands) of the corresponding commodity for the front contract.

Table A.4.: Futures-based Forecasts of Monthly Average Real Prices, Non-Parametric, Constructed using Five Day End-of-Month Futures Average

	1	3	6	9	12	15	18	21	24
Commodity	MSFE Ratio								
Crude Oil	1.20 (0.977)	0.95 (0.057)	0.88 (0.027)	0.87 (0.089)	0.83 (0.070)	0.77 (0.026)	0.71 (0.013)	0.66 (0.007)	0.61 (0.003)
Natural Gas	1.19 (0.980)	1.03 (0.657)	0.98 (0.427)	1.07 (0.667)	1.07 (0.669)	0.96 (0.354)	0.96 (0.387)	0.96 (0.378)	0.97 (0.400)
Heating Oil	1.47 (0.997)	1.00 (0.481)	0.97 (0.276)	0.93 (0.059)	0.87 (0.006)	0.86 (0.002)	0.82 (0.000)	0.79 (0.000)	0.74 (0.000)
Gasoline	0.97 (0.394)	0.77 (0.005)	0.70 (0.004)	0.82 (0.048)	0.89 (0.093)	0.83 (0.028)	0.75 (0.010)	0.73 (0.009)	0.70 (0.003)
Ethanol	1.18 (0.646)	0.75 (0.123)	0.84 (0.239)	0.84 (0.181)	0.77 (0.123)	0.70 (0.051)	0.68 (0.046)	0.62 (0.039)	0.57 (0.025)
Gold	0.97 (0.261)	1.01 (0.600)	0.99 (0.450)	0.99 (0.413)	0.98 (0.377)	0.98 (0.336)	0.97 (0.275)	0.95 (0.185)	0.93 (0.125)
Silver	0.99 (0.468)	1.04 (0.857)	1.00 (0.501)	0.98 (0.312)	0.97 (0.188)	0.95 (0.107)	0.92 (0.040)	0.89 (0.022)	0.86 (0.023)
Platinum	1.07 (0.950)	1.02 (0.745)	0.94 (0.088)	0.91 (0.033)	0.88 (0.013)	0.86 (0.003)	0.85 (0.000)	0.84 (0.000)	0.84 (0.000)
Aluminum	1.10 (0.891)	1.00 (0.516)	0.98 (0.297)	0.96 (0.129)	0.94 (0.031)	0.94 (0.049)	0.95 (0.099)	0.95 (0.131)	0.94 (0.121)
Copper	1.00 (0.514)	0.96 (0.166)	0.97 (0.198)	0.94 (0.109)	0.93 (0.079)	0.92 (0.058)	0.89 (0.040)	0.88 (0.040)	0.87 (0.054)
Lead	1.11 (0.923)	0.99 (0.422)	0.96 (0.175)	0.88 (0.043)	0.87 (0.033)	0.87 (0.061)	0.86 (0.066)	0.85 (0.041)	0.82 (0.020)
Zinc	1.15 (0.961)	0.95 (0.119)	0.93 (0.114)	0.89 (0.038)	0.90 (0.068)	0.92 (0.118)	0.93 (0.172)	0.94 (0.227)	0.94 (0.279)
Nickel	1.07 (0.891)	1.01 (0.554)	0.96 (0.147)	0.93 (0.104)	0.92 (0.112)	0.87 (0.036)	0.83 (0.026)	0.80 (0.012)	0.78 (0.009)
Tin	1.08 (0.920)	1.02 (0.601)	1.01 (0.532)	1.00 (0.497)	0.99 (0.429)	0.95 (0.218)	0.94 (0.181)	0.98 (0.323)	0.99 (0.407)
Corn	0.96 (0.365)	0.77 (0.048)	0.69 (0.029)	0.72 (0.052)	0.74 (0.064)	0.68 (0.038)	0.64 (0.034)	0.62 (0.029)	0.58 (0.013)
Soybeans	0.90 (0.120)	0.76 (0.013)	0.73 (0.025)	0.78 (0.047)	0.84 (0.156)	0.78 (0.125)	0.73 (0.085)	0.73 (0.076)	0.68 (0.034)
Wheat	1.12 (0.880)	1.07 (0.734)	1.05 (0.626)	0.99 (0.473)	0.95 (0.380)	0.92 (0.301)	0.93 (0.250)	0.92 (0.197)	0.88 (0.163)
	Success Ratio								
Crude Oil	0.47 (0.709)	0.57 (0.039)	0.57 (0.060)	0.58 (0.069)	0.68 (0.000)	0.71 (0.000)	0.66 (0.001)	0.65 (0.002)	0.76 (0.000)
Natural Gas	0.53 (0.249)	0.56 (0.064)	0.60 (0.002)	0.61 (0.011)	0.66 (0.002)	0.64 (0.005)	0.65 (0.007)	0.63 (0.009)	0.62 (0.018)
Heating Oil	0.53 (0.182)	0.57 (0.057)	0.66 (0.000)	0.66 (0.002)	0.75 (0.000)	0.82 (0.000)	0.81 (0.000)	0.80 (0.000)	0.77 (0.000)
Gasoline	0.56 (0.051)	0.60 (0.019)	0.72 (0.000)	0.64 (0.001)	0.62 (0.001)	0.63 (0.000)	0.63 (0.007)	0.71 (0.000)	0.70 (0.000)
Ethanol	0.58 (0.009)	0.60 (0.012)	0.63 (0.000)	0.61 (0.012)	0.64 (0.018)	0.68 (0.000)	0.65 (0.001)	0.67 (0.000)	0.73 (0.000)
Gold	0.56 (0.033)	0.47 (0.882)	0.53 (0.052)	0.57 (0.097)	0.55 (0.262)	0.61 (0.000)	0.60 (0.000)	0.60 (0.000)	0.53 (0.000)
Silver	0.55 (0.100)	0.53 (0.295)	0.58 (0.155)	0.62 (0.140)	0.59 (0.395)	0.62 (0.132)	0.68 (0.000)	0.67 (0.000)	0.64 (0.001)
Platinum	0.47 (0.707)	0.47 (0.851)	0.60 (0.096)	0.62 (0.162)	0.68 (0.075)	0.73 (0.023)	0.74 (0.006)	0.77 (0.001)	0.77 (0.008)
Aluminum	0.55 (0.079)	0.52 (0.292)	0.49 (0.539)	0.50 (0.452)	0.53 (0.252)	0.54 (0.219)	0.53 (0.293)	0.58 (0.062)	0.56 (0.116)
Copper	0.55 (0.118)	0.53 (0.348)	0.60 (0.163)	0.59 (0.522)	0.64 (0.145)	0.63 (0.317)	0.61 (0.160)	0.59 (1.000)	0.59 (1.000)
Lead	0.51 (0.430)	0.52 (0.352)	0.52 (0.466)	0.58 (0.087)	0.57 (0.064)	0.61 (0.138)	0.63 (0.202)	0.63 (0.289)	0.65 (0.298)
Zinc	0.51 (0.581)	0.53 (0.252)	0.58 (0.018)	0.57 (0.019)	0.61 (0.002)	0.62 (0.004)	0.60 (0.019)	0.57 (0.034)	0.58 (0.122)
Nickel	0.50 (0.500)	0.49 (0.541)	0.48 (0.635)	0.53 (0.159)	0.56 (0.009)	0.53 (0.130)	0.52 (0.152)	0.60 (0.014)	0.62 (0.000)
Tin	0.47 (0.843)	0.51 (0.417)	0.52 (0.101)	0.55 (0.007)	0.56 (0.000)	0.55 (0.000)	0.60 (0.000)	0.59 (0.000)	0.56 (0.000)
Corn	0.59 (0.009)	0.62 (0.001)	0.66 (0.001)	0.58 (0.050)	0.51 (0.443)	0.51 (0.441)	0.57 (0.117)	0.57 (0.063)	0.58 (0.035)
Soybeans	0.58 (0.015)	0.60 (0.012)	0.62 (0.011)	0.64 (0.007)	0.61 (0.023)	0.59 (0.110)	0.57 (0.083)	0.60 (0.041)	0.63 (0.002)
Wheat	0.61 (0.000)	0.64 (0.001)	0.59 (0.023)	0.52 (0.547)	0.48 (0.870)	0.48 (0.758)	0.53 (0.437)	0.54 (0.462)	0.56 (0.269)

Notes: See the notes below Table 2.4. This table presents the performance of futures-based forecasts of monthly average spot prices using the five-day end-of-month average of futures prices. Bold values represent improvements over the baseline results in Table 2.4.

Parametric models

Table A.5.: MSFE Precision of Futures-based Forecasts of Monthly Real Prices, Parametric

Commodity	Model	1	3	6	12	15	18	24
		MSFE Ratio						
Crude Oil	$\hat{\alpha}$	27.89 (1.000)	4.29 (1.000)	2.15 (0.997)	1.31 (0.825)	1.03 (0.540)	0.83 (0.256)	0.64 (0.049)
	$\hat{\beta}$	1.00 (0.147)	1.00 (0.009)	0.98 (0.014)	0.95 (0.027)	0.91 (0.010)	0.88 (0.007)	0.82 (0.002)
	$\hat{\alpha}, \hat{\beta}$	1.00 (0.577)	1.05 (0.939)	1.06 (0.922)	1.17 (0.986)	1.09 (0.951)	1.09 (0.971)	1.17 (0.981)
Natural Gas	$\hat{\alpha}$	4.41 (1.000)	1.63 (0.969)	1.38 (0.891)	1.31 (0.844)	1.13 (0.753)	1.12 (0.748)	1.10 (0.717)
	$\hat{\beta}$	1.00 (0.166)	0.97 (0.036)	0.95 (0.190)	1.06 (0.684)	1.03 (0.582)	1.07 (0.662)	1.12 (0.738)
	$\hat{\alpha}, \hat{\beta}$	1.11 (0.970)	1.07 (0.717)	1.27 (0.879)	1.60 (0.923)	1.29 (0.874)	1.22 (0.857)	1.19 (0.836)
Heating Oil	$\hat{\alpha}$	24.26 (1.000)	4.78 (1.000)	2.58 (1.000)	1.29 (0.900)	1.06 (0.635)	0.91 (0.279)	0.73 (0.025)
	$\hat{\beta}$	1.00 (0.184)	0.99 (0.096)	0.99 (0.037)	0.96 (0.003)	0.94 (0.001)	0.92 (0.000)	0.86 (0.000)
	$\hat{\alpha}, \hat{\beta}$	1.01 (0.856)	1.02 (0.926)	1.05 (0.940)	1.09 (0.969)	1.06 (0.884)	1.02 (0.713)	1.03 (0.695)
Gasoline	$\hat{\alpha}$	3.84 (1.000)	1.12 (0.743)	0.84 (0.171)	1.04 (0.600)	0.96 (0.382)	0.85 (0.102)	0.83 (0.070)
	$\hat{\beta}$	0.98 (0.004)	0.82 (0.001)	0.75 (0.014)	0.90 (0.104)	0.87 (0.137)	0.81 (0.140)	0.71 (0.040)
	$\hat{\alpha}, \hat{\beta}$	1.06 (0.770)	1.25 (0.898)	1.18 (0.760)	1.49 (0.958)	1.80 (0.991)	1.62 (0.959)	1.77 (0.956)
Ethanol	$\hat{\alpha}$	2.11 (0.963)	1.17 (0.709)	1.12 (0.640)	0.81 (0.254)	0.74 (0.158)	0.72 (0.132)	0.67 (0.103)
	$\hat{\beta}$	0.87 (0.036)	0.69 (0.021)	0.98 (0.481)	0.90 (0.369)	0.69 (0.087)	0.65 (0.055)	0.81 (0.115)
	$\hat{\alpha}, \hat{\beta}$	0.85 (0.122)	0.75 (0.079)	1.19 (0.667)	0.96 (0.447)	0.78 (0.189)	0.82 (0.232)	0.99 (0.483)
Gold	$\hat{\alpha}$	113.54 (1.000)	22.41 (1.000)	10.77 (1.000)	5.41 (1.000)	4.30 (1.000)	3.61 (1.000)	2.85 (1.000)
	$\hat{\beta}$	1.00 (0.644)	1.00 (0.333)	1.00 (0.124)	1.00 (0.010)	1.00 (0.001)	1.00 (0.001)	0.99 (0.007)
	$\hat{\alpha}, \hat{\beta}$	1.02 (0.777)	1.20 (0.940)	1.54 (0.969)	2.45 (0.993)	3.00 (0.996)	3.66 (0.997)	5.68 (0.999)
Silver	$\hat{\alpha}$	17.30 (1.000)	4.50 (1.000)	2.38 (1.000)	1.42 (0.942)	1.25 (0.846)	1.14 (0.714)	0.91 (0.363)
	$\hat{\beta}$	1.00 (0.375)	1.00 (0.178)	1.00 (0.048)	1.00 (0.022)	1.00 (0.017)	0.99 (0.007)	0.98 (0.007)
	$\hat{\alpha}, \hat{\beta}$	1.03 (0.890)	1.17 (0.931)	1.45 (0.954)	2.03 (0.989)	2.42 (0.995)	3.27 (0.997)	4.92 (0.998)
Platinum	$\hat{\alpha}$	61.05 (1.000)	11.37 (1.000)	5.82 (1.000)	2.36 (0.997)	1.70 (0.951)	1.27 (0.762)	0.74 (0.197)
	$\hat{\beta}$	1.00 (0.718)	1.00 (0.011)	1.00 (0.001)	1.00 (0.000)	0.99 (0.000)	0.99 (0.000)	0.98 (0.000)
	$\hat{\alpha}, \hat{\beta}$	1.02 (0.807)	1.23 (0.986)	1.79 (0.998)	1.77 (0.999)	2.13 (1.000)	2.36 (1.000)	2.91 (1.000)
Aluminum	$\hat{\alpha}$	32.48 (1.000)	5.84 (1.000)	2.95 (1.000)	1.93 (0.994)	1.69 (0.982)	1.56 (0.967)	1.34 (0.898)
	$\hat{\beta}$	1.00 (0.751)	1.00 (0.700)	1.00 (0.238)	1.00 (0.073)	1.00 (0.166)	1.00 (0.273)	1.00 (0.361)
	$\hat{\alpha}, \hat{\beta}$	1.01 (0.844)	1.06 (0.951)	1.13 (0.974)	1.20 (0.997)	1.21 (0.997)	1.20 (0.995)	1.13 (0.893)
Copper	$\hat{\alpha}$	28.93 (1.000)	4.96 (1.000)	2.18 (0.999)	1.21 (0.849)	1.14 (0.801)	1.15 (0.882)	1.44 (1.000)
	$\hat{\beta}$	1.00 (0.950)	1.00 (0.048)	1.00 (0.042)	0.98 (0.019)	0.97 (0.019)	0.96 (0.015)	0.93 (0.033)
	$\hat{\alpha}, \hat{\beta}$	1.03 (0.929)	1.23 (0.958)	1.62 (0.984)	2.47 (0.999)	2.84 (1.000)	3.24 (1.000)	4.23 (1.000)
Lead	$\hat{\alpha}$	21.28 (1.000)	4.55 (1.000)	2.16 (1.000)	1.07 (0.645)	1.00 (0.505)	1.02 (0.566)	1.12 (0.846)
	$\hat{\beta}$	1.00 (0.995)	1.00 (0.001)	0.99 (0.006)	0.96 (0.007)	0.94 (0.017)	0.92 (0.024)	0.86 (0.007)
	$\hat{\alpha}, \hat{\beta}$	1.03 (0.909)	1.25 (0.969)	1.71 (0.981)	2.81 (0.997)	3.21 (0.999)	4.11 (1.000)	6.17 (1.000)
Zinc	$\hat{\alpha}$	22.68 (1.000)	4.86 (1.000)	2.49 (1.000)	1.62 (0.985)	1.43 (0.964)	1.28 (0.920)	1.12 (0.788)
	$\hat{\beta}$	1.00 (0.971)	1.00 (0.043)	0.99 (0.043)	0.97 (0.029)	0.96 (0.052)	0.95 (0.069)	0.93 (0.161)
	$\hat{\alpha}, \hat{\beta}$	1.00 (0.422)	1.08 (0.992)	1.19 (0.989)	1.35 (0.998)	1.36 (0.999)	1.30 (0.999)	1.14 (0.965)
Nickel	$\hat{\alpha}$	9.79 (1.000)	2.25 (1.000)	1.39 (0.935)	1.25 (0.991)	1.40 (0.999)	1.58 (0.999)	1.82 (0.999)
	$\hat{\beta}$	1.00 (0.283)	1.00 (0.304)	0.99 (0.094)	0.93 (0.067)	0.84 (0.037)	0.76 (0.020)	0.69 (0.007)
	$\hat{\alpha}, \hat{\beta}$	1.01 (0.734)	1.07 (0.958)	1.16 (0.944)	1.36 (0.993)	1.45 (0.999)	1.56 (1.000)	1.74 (1.000)
Tin	$\hat{\alpha}$	17.68 (1.000)	2.85 (0.999)	1.41 (0.858)	1.17 (0.785)	1.11 (0.770)	1.10 (0.805)	1.18 (0.979)
	$\hat{\beta}$	1.00 (0.228)	1.00 (0.577)	1.00 (0.512)	0.99 (0.302)	0.98 (0.154)	0.97 (0.131)	0.99 (0.284)
	$\hat{\alpha}, \hat{\beta}$	1.05 (0.891)	1.16 (0.919)	1.33 (0.957)	1.66 (0.990)	1.85 (0.994)	2.23 (0.997)	3.18 (0.999)
Corn	$\hat{\alpha}$	17.98 (1.000)	3.89 (1.000)	2.21 (0.998)	1.82 (0.985)	1.62 (0.951)	1.47 (0.881)	1.02 (0.520)
	$\hat{\beta}$	1.00 (0.090)	0.98 (0.014)	0.95 (0.015)	0.94 (0.030)	0.90 (0.017)	0.85 (0.011)	0.77 (0.008)
	$\hat{\alpha}, \hat{\beta}$	1.01 (0.740)	1.03 (0.821)	1.05 (0.783)	1.15 (0.997)	1.14 (0.935)	1.15 (0.803)	1.02 (0.530)
Soybeans	$\hat{\alpha}$	32.66 (1.000)	4.78 (1.000)	2.53 (1.000)	2.26 (1.000)	2.01 (0.995)	1.69 (0.973)	1.21 (0.776)
	$\hat{\beta}$	1.00 (0.022)	0.98 (0.016)	0.95 (0.017)	0.91 (0.018)	0.87 (0.017)	0.84 (0.012)	0.78 (0.011)
	$\hat{\alpha}, \hat{\beta}$	1.00 (0.483)	1.02 (0.730)	1.01 (0.564)	1.04 (0.756)	1.08 (0.814)	1.10 (0.865)	1.05 (0.661)
Wheat	$\hat{\alpha}$	29.41 (1.000)	6.58 (1.000)	4.03 (1.000)	2.57 (1.000)	2.35 (0.998)	2.13 (0.990)	1.49 (0.885)
	$\hat{\beta}$	1.00 (0.086)	1.00 (0.210)	0.99 (0.234)	0.97 (0.138)	0.95 (0.086)	0.94 (0.030)	0.91 (0.037)
	$\hat{\alpha}, \hat{\beta}$	1.02 (0.979)	1.04 (0.994)	1.08 (0.997)	1.05 (0.778)	1.14 (0.776)	1.28 (0.844)	1.28 (0.790)

Notes: See the notes below Table 2.4. This table presents the performance of futures-based forecasts using the futures-spot spread model, specified in Equation 2.7. Bold values represent improvements over the baseline results in Table 2.4.

Table A.6.: Directional Accuracy of Futures-based Forecasts of Monthly Real Prices, Parametric

Commodity	Model	1	3	6	12	15	18	24
		Success Ratio						
Crude Oil	$\hat{\alpha}$	0.47 (1.000)	0.46 (1.000)	0.46 (0.100)	0.48 (0.100)	0.51 (0.252)	0.49 (0.281)	0.59 (0.000)
	$\hat{\beta}$	0.55 (0.091)	0.52 (0.208)	0.58 (0.093)	0.68 (0.002)	0.69 (0.000)	0.66 (0.002)	0.75 (0.000)
	$\hat{\alpha}, \hat{\beta}$	0.46 (0.934)	0.48 (0.673)	0.49 (0.532)	0.46 (0.732)	0.49 (0.535)	0.41 (0.892)	0.41 (0.873)
Natural Gas	$\hat{\alpha}$	0.50 (0.100)	0.54 (0.000)	0.64 (0.000)	0.61 (0.025)	0.60 (0.102)	0.60 (0.103)	0.56 (0.269)
	$\hat{\beta}$	0.52 (0.321)	0.54 (0.169)	0.61 (0.000)	0.64 (0.006)	0.66 (0.003)	0.63 (0.017)	0.62 (0.021)
	$\hat{\alpha}, \hat{\beta}$	0.50 (0.000)	0.54 (0.000)	0.62 (0.000)	0.64 (0.001)	0.63 (0.026)	0.60 (0.123)	0.60 (0.140)
Heating Oil	$\hat{\alpha}$	0.49 (1.000)	0.47 (1.000)	0.50 (0.100)	0.50 (0.100)	0.55 (0.000)	0.61 (0.000)	0.60 (0.008)
	$\hat{\beta}$	0.52 (0.300)	0.56 (0.072)	0.61 (0.019)	0.77 (0.000)	0.82 (0.000)	0.81 (0.000)	0.81 (0.000)
	$\hat{\alpha}, \hat{\beta}$	0.48 (0.668)	0.42 (0.924)	0.36 (0.991)	0.40 (0.916)	0.43 (0.827)	0.43 (0.797)	0.43 (0.790)
Gasoline	$\hat{\alpha}$	0.51 (0.000)	0.58 (0.003)	0.64 (0.000)	0.56 (0.014)	0.56 (0.014)	0.58 (0.033)	0.58 (0.000)
	$\hat{\beta}$	0.62 (0.001)	0.62 (0.004)	0.71 (0.000)	0.62 (0.001)	0.62 (0.001)	0.65 (0.002)	0.70 (0.000)
	$\hat{\alpha}, \hat{\beta}$	0.51 (0.000)	0.58 (0.002)	0.59 (0.000)	0.55 (0.050)	0.53 (0.105)	0.55 (0.098)	0.59 (0.000)
Ethanol	$\hat{\alpha}$	0.52 (1.000)	0.57 (0.062)	0.63 (0.000)	0.65 (0.043)	0.65 (0.000)	0.57 (0.397)	0.67 (0.000)
	$\hat{\beta}$	0.54 (0.207)	0.60 (0.024)	0.68 (0.000)	0.63 (0.129)	0.67 (0.000)	0.62 (0.024)	0.73 (0.000)
	$\hat{\alpha}, \hat{\beta}$	0.52 (1.000)	0.56 (0.116)	0.61 (0.000)	0.63 (0.210)	0.65 (0.000)	0.57 (0.397)	0.67 (0.000)
Gold	$\hat{\alpha}$	0.46 (1.000)	0.52 (1.000)	0.46 (1.000)	0.53 (1.000)	0.53 (1.000)	0.50 (1.000)	0.45 (1.000)
	$\hat{\beta}$	0.53 (0.556)	0.47 (0.630)	0.52 (0.422)	0.58 (0.155)	0.70 (0.000)	0.67 (0.000)	0.50 (0.100)
	$\hat{\alpha}, \hat{\beta}$	0.55 (1.000)	0.48 (1.000)	0.54 (1.000)	0.47 (1.000)	0.47 (1.000)	0.50 (1.000)	0.55 (1.000)
Silver	$\hat{\alpha}$	0.48 (1.000)	0.53 (1.000)	0.60 (1.000)	0.65 (1.000)	0.61 (1.000)	0.58 (1.000)	0.56 (1.000)
	$\hat{\beta}$	0.49 (0.535)	0.50 (0.779)	0.59 (0.353)	0.67 (0.037)	0.66 (0.004)	0.67 (0.000)	0.63 (0.009)
	$\hat{\alpha}, \hat{\beta}$	0.52 (1.000)	0.47 (1.000)	0.40 (1.000)	0.35 (1.000)	0.39 (1.000)	0.42 (1.000)	0.44 (1.000)
Platinum	$\hat{\alpha}$	0.47 (1.000)	0.55 (1.000)	0.62 (1.000)	0.69 (1.000)	0.73 (1.000)	0.73 (1.000)	0.79 (1.000)
	$\hat{\beta}$	0.49 (0.370)	0.56 (0.238)	0.66 (0.016)	0.72 (0.011)	0.76 (0.002)	0.79 (0.000)	0.84 (0.000)
	$\hat{\alpha}, \hat{\beta}$	0.44 (1.000)	0.45 (1.000)	0.38 (1.000)	0.31 (1.000)	0.27 (1.000)	0.27 (1.000)	0.21 (1.000)
Aluminum	$\hat{\alpha}$	0.56 (1.000)	0.53 (1.000)	0.54 (1.000)	0.54 (1.000)	0.56 (1.000)	0.58 (1.000)	0.62 (1.000)
	$\hat{\beta}$	0.53 (0.351)	0.55 (0.138)	0.46 (0.682)	0.50 (0.466)	0.49 (0.504)	0.53 (0.235)	0.56 (0.064)
	$\hat{\alpha}, \hat{\beta}$	0.53 (0.777)	0.49 (0.615)	0.45 (0.819)	0.40 (0.982)	0.38 (0.999)	0.38 (1.000)	0.50 (0.987)
Copper	$\hat{\alpha}$	0.52 (1.000)	0.53 (1.000)	0.60 (1.000)	0.63 (1.000)	0.63 (0.579)	0.49 (0.901)	0.23 (1.000)
	$\hat{\beta}$	0.47 (0.976)	0.53 (0.000)	0.60 (1.000)	0.63 (1.000)	0.63 (1.000)	0.60 (1.000)	0.59 (1.000)
	$\hat{\alpha}, \hat{\beta}$	0.44 (0.954)	0.46 (1.000)	0.40 (1.000)	0.37 (1.000)	0.37 (1.000)	0.40 (1.000)	0.41 (1.000)
Lead	$\hat{\alpha}$	0.49 (1.000)	0.52 (1.000)	0.54 (1.000)	0.55 (0.000)	0.63 (0.105)	0.63 (0.212)	0.41 (0.974)
	$\hat{\beta}$	0.44 (0.940)	0.61 (0.005)	0.60 (0.057)	0.58 (0.011)	0.65 (0.009)	0.66 (0.144)	0.67 (0.061)
	$\hat{\alpha}, \hat{\beta}$	0.42 (0.971)	0.48 (0.541)	0.46 (1.000)	0.48 (1.000)	0.39 (1.000)	0.35 (1.000)	0.34 (1.000)
Zinc	$\hat{\alpha}$	0.56 (1.000)	0.51 (1.000)	0.49 (1.000)	0.50 (1.000)	0.53 (1.000)	0.53 (1.000)	0.46 (0.818)
	$\hat{\beta}$	0.46 (0.547)	0.51 (0.506)	0.52 (0.346)	0.57 (0.086)	0.61 (0.021)	0.60 (0.020)	0.58 (0.120)
	$\hat{\alpha}, \hat{\beta}$	0.56 (0.830)	0.46 (0.763)	0.46 (1.000)	0.49 (1.000)	0.40 (0.995)	0.37 (0.986)	0.42 (0.881)
Nickel	$\hat{\alpha}$	0.50 (1.000)	0.49 (1.000)	0.49 (1.000)	0.38 (0.980)	0.24 (1.000)	0.23 (1.000)	0.34 (1.000)
	$\hat{\beta}$	0.50 (1.000)	0.49 (0.290)	0.50 (0.569)	0.50 (1.000)	0.50 (1.000)	0.49 (1.000)	0.55 (0.000)
	$\hat{\alpha}, \hat{\beta}$	0.51 (0.321)	0.45 (0.814)	0.34 (0.998)	0.35 (0.990)	0.28 (1.000)	0.32 (0.995)	0.16 (1.000)
Tin	$\hat{\alpha}$	0.53 (1.000)	0.50 (1.000)	0.48 (1.000)	0.52 (1.000)	0.54 (1.000)	0.55 (0.950)	0.47 (0.736)
	$\hat{\beta}$	0.53 (1.000)	0.50 (1.000)	0.48 (1.000)	0.52 (1.000)	0.54 (1.000)	0.58 (1.000)	0.54 (1.000)
	$\hat{\alpha}, \hat{\beta}$	0.44 (0.937)	0.49 (1.000)	0.52 (1.000)	0.48 (1.000)	0.47 (1.000)	0.42 (1.000)	0.46 (1.000)
Corn	$\hat{\alpha}$	0.48 (1.000)	0.48 (1.000)	0.48 (1.000)	0.50 (1.000)	0.51 (1.000)	0.53 (1.000)	0.58 (1.000)
	$\hat{\beta}$	0.55 (0.127)	0.64 (0.000)	0.65 (0.001)	0.52 (0.404)	0.50 (0.486)	0.55 (0.177)	0.58 (0.035)
	$\hat{\alpha}, \hat{\beta}$	0.42 (0.999)	0.44 (0.994)	0.47 (0.851)	0.44 (0.827)	0.49 (1.000)	0.52 (1.000)	0.59 (0.000)
Soybeans	$\hat{\alpha}$	0.51 (1.000)	0.46 (1.000)	0.49 (1.000)	0.50 (1.000)	0.53 (1.000)	0.49 (1.000)	0.53 (1.000)
	$\hat{\beta}$	0.55 (0.147)	0.53 (0.251)	0.60 (0.023)	0.57 (0.091)	0.58 (0.150)	0.56 (0.117)	0.61 (0.034)
	$\hat{\alpha}, \hat{\beta}$	0.48 (0.991)	0.45 (0.923)	0.48 (0.751)	0.49 (0.559)	0.53 (0.453)	0.48 (0.585)	0.53 (0.000)
Wheat	$\hat{\alpha}$	0.51 (1.000)	0.50 (1.000)	0.48 (1.000)	0.45 (1.000)	0.49 (1.000)	0.47 (1.000)	0.50 (1.000)
	$\hat{\beta}$	0.55 (0.069)	0.57 (0.057)	0.58 (0.033)	0.50 (0.774)	0.49 (0.659)	0.53 (0.441)	0.56 (0.269)
	$\hat{\alpha}, \hat{\beta}$	0.45 (0.937)	0.42 (0.956)	0.34 (1.000)	0.46 (1.000)	0.49 (0.100)	0.49 (1.000)	0.50 (1.000)

Notes: See the notes below Table 2.4. This table presents the performance of futures-based forecasts using the futures-spot spread model, specified in Equation 2.7. Bold values represent improvements over the baseline results in Table 2.4.

Robustness over time

Table A.7.: Futures-based Forecasts of Monthly Average Real Prices,
Non-Parametric, Sample Starting 2000

	1	3	6	9	12	15	18	21	24
Commodity	MSPE								
Crude Oil	0.97 (0.102)	0.97 (0.046)	0.95 (0.100)	0.94 (0.139)	0.89 (0.053)	0.84 (0.024)	0.83 (0.031)	0.83 (0.052)	0.83 (0.069)
Natural Gas	0.81 (0.106)	0.90 (0.166)	0.82 (0.041)	0.76 (0.041)	0.75 (0.024)	0.81 (0.049)	0.84 (0.088)	0.86 (0.153)	0.86 (0.158)
Heating Oil	1.05 (0.887)	1.02 (0.667)	1.03 (0.794)	0.99 (0.353)	0.91 (0.025)	0.88 (0.011)	0.87 (0.011)	0.84 (0.006)	0.80 (0.002)
Gasoline	0.82 (0.000)	0.75 (0.000)	0.72 (0.000)	0.83 (0.009)	0.91 (0.079)	0.82 (0.005)	0.71 (0.000)	0.70 (0.000)	0.70 (0.000)
Ethanol	0.74 (0.121)	0.77 (0.097)	0.85 (0.176)	0.86 (0.158)	0.83 (0.157)	0.76 (0.079)	0.70 (0.039)	0.67 (0.035)	0.66 (0.021)
Gold	1.01 (0.808)	1.01 (0.603)	1.01 (0.593)	1.00 (0.509)	1.00 (0.495)	0.99 (0.445)	0.99 (0.396)	0.98 (0.342)	0.98 (0.304)
Silver	1.04 (0.904)	1.00 (0.571)	0.99 (0.328)	0.98 (0.219)	0.98 (0.225)	0.98 (0.214)	0.97 (0.206)	0.97 (0.195)	0.96 (0.177)
Aluminum	0.99 (0.264)	1.01 (0.643)	1.00 (0.541)	1.00 (0.448)	1.03 (0.776)	1.08 (0.911)	1.07 (0.857)	1.03 (0.613)	0.98 (0.451)
Copper	0.99 (0.168)	0.99 (0.423)	1.00 (0.509)	1.03 (0.645)	1.08 (0.803)	1.09 (0.818)	1.10 (0.811)	1.14 (0.863)	1.16 (0.895)
Lead	0.99 (0.154)	0.99 (0.232)	1.01 (0.572)	1.01 (0.554)	1.00 (0.485)	0.97 (0.396)	0.97 (0.382)	0.98 (0.406)	1.00 (0.475)
Zinc	0.98 (0.032)	0.96 (0.019)	0.97 (0.193)	0.93 (0.088)	0.91 (0.114)	0.88 (0.090)	0.85 (0.071)	0.82 (0.067)	0.79 (0.069)
Nickel	0.97 (0.287)	1.01 (0.532)	1.00 (0.485)	0.99 (0.484)	0.95 (0.322)	0.91 (0.238)	0.87 (0.225)	0.84 (0.222)	0.83 (0.232)
Tin	1.00 (0.579)	1.02 (0.710)	1.03 (0.676)	1.02 (0.619)	1.02 (0.615)	1.01 (0.589)	1.02 (0.649)	1.05 (0.857)	1.05 (0.913)
Corn	1.24 (0.936)	0.91 (0.254)	0.83 (0.114)	0.82 (0.110)	0.82 (0.111)	0.76 (0.044)	0.69 (0.015)	0.66 (0.006)	0.62 (0.001)
Soybeans	0.90 (0.090)	0.77 (0.004)	0.73 (0.007)	0.75 (0.010)	0.79 (0.030)	0.79 (0.035)	0.80 (0.058)	0.81 (0.060)	0.77 (0.022)
Wheat	1.86 (0.983)	1.29 (0.927)	1.15 (0.790)	1.02 (0.567)	0.94 (0.331)	0.86 (0.144)	0.79 (0.052)	0.76 (0.019)	0.72 (0.004)
	Success Ratio								
Crude Oil	0.57 (0.005)	0.51 (0.150)	0.54 (0.126)	0.56 (0.052)	0.61 (0.004)	0.63 (0.000)	0.60 (0.000)	0.56 (0.010)	0.60 (0.001)
Natural Gas	0.56 (0.027)	0.54 (0.066)	0.60 (0.002)	0.62 (0.002)	0.63 (0.005)	0.66 (0.001)	0.61 (0.014)	0.63 (0.006)	0.59 (0.032)
Heating Oil	0.51 (0.393)	0.54 (0.291)	0.59 (0.090)	0.62 (0.018)	0.66 (0.000)	0.69 (0.000)	0.70 (0.000)	0.70 (0.000)	0.68 (0.000)
Gasoline	0.62 (0.000)	0.66 (0.000)	0.73 (0.000)	0.63 (0.001)	0.64 (0.000)	0.65 (0.000)	0.67 (0.000)	0.73 (0.000)	0.71 (0.000)
Ethanol	0.57 (0.017)	0.61 (0.001)	0.67 (0.000)	0.68 (0.000)	0.65 (0.000)	0.69 (0.000)	0.68 (0.000)	0.71 (0.000)	0.73 (0.000)
Gold	0.46 (0.815)	0.46 (0.525)	0.44 (0.534)	0.46 (0.224)	0.44 (0.281)	0.47 (0.071)	0.48 (0.026)	0.48 (0.006)	0.47 (0.001)
Silver	0.45 (0.954)	0.44 (0.944)	0.48 (0.724)	0.52 (0.304)	0.52 (0.315)	0.49 (0.370)	0.48 (0.305)	0.46 (0.337)	0.44 (0.416)
Palladium	0.46 (0.685)	0.50 (0.114)	0.47 (0.482)	0.47 (0.375)	0.46 (0.424)	0.42 (0.690)	0.44 (0.672)	0.45 (0.654)	0.45 (0.601)
Platinum	0.48 (0.314)	0.47 (0.282)	0.49 (0.123)	0.48 (0.237)	0.53 (0.106)	0.54 (0.221)	0.58 (0.023)	0.59 (0.032)	0.59 (0.043)
Aluminum	0.50 (0.429)	0.47 (0.756)	0.49 (0.583)	0.47 (0.728)	0.46 (0.769)	0.48 (0.637)	0.51 (0.406)	0.54 (0.274)	0.53 (0.300)
Copper	0.49 (0.757)	0.50 (0.337)	0.51 (0.212)	0.53 (0.023)	0.53 (0.193)	0.52 (0.248)	0.52 (0.105)	0.51 (0.010)	0.51 (0.022)
Lead	0.49 (0.635)	0.56 (0.047)	0.55 (0.079)	0.55 (0.036)	0.51 (0.140)	0.55 (0.037)	0.54 (0.102)	0.54 (0.117)	0.56 (0.042)
Zinc	0.50 (0.618)	0.52 (0.344)	0.56 (0.091)	0.54 (0.191)	0.57 (0.054)	0.58 (0.022)	0.60 (0.012)	0.61 (0.001)	0.62 (0.001)
Nickel	0.49 (1.000)	0.47 (0.834)	0.49 (1.024)	0.48 (0.822)	0.48 (0.500)	0.45 (0.500)	0.46 (0.500)	0.47 (0.000)	0.47 (0.000)
Tin	0.50 (0.808)	0.46 (0.859)	0.45 (0.663)	0.46 (0.669)	0.47 (0.222)	0.49 (0.000)	0.52 (0.000)	0.52 (0.000)	0.48 (0.000)
Corn	0.56 (0.025)	0.62 (0.000)	0.60 (0.002)	0.55 (0.093)	0.56 (0.205)	0.57 (0.067)	0.62 (0.012)	0.66 (0.000)	0.70 (0.000)
Soybeans	0.53 (0.170)	0.58 (0.020)	0.60 (0.012)	0.61 (0.011)	0.60 (0.013)	0.63 (0.008)	0.59 (0.016)	0.60 (0.004)	0.66 (0.000)
Wheat	0.53 (0.048)	0.56 (0.042)	0.61 (0.001)	0.59 (0.097)	0.59 (0.239)	0.62 (0.046)	0.68 (0.001)	0.69 (0.001)	0.70 (0.000)

Note: See the notes below Table 2.4. This table presents the performance of futures-based forecasts of monthly average spot prices using end-of-month (EOM) futures prices, with the forecast evaluation sample covering January 2000–2023. The exception is gasoline and ethanol, which begin in January 2008. Bold values represent improvements over the baseline results in Table 2.4.

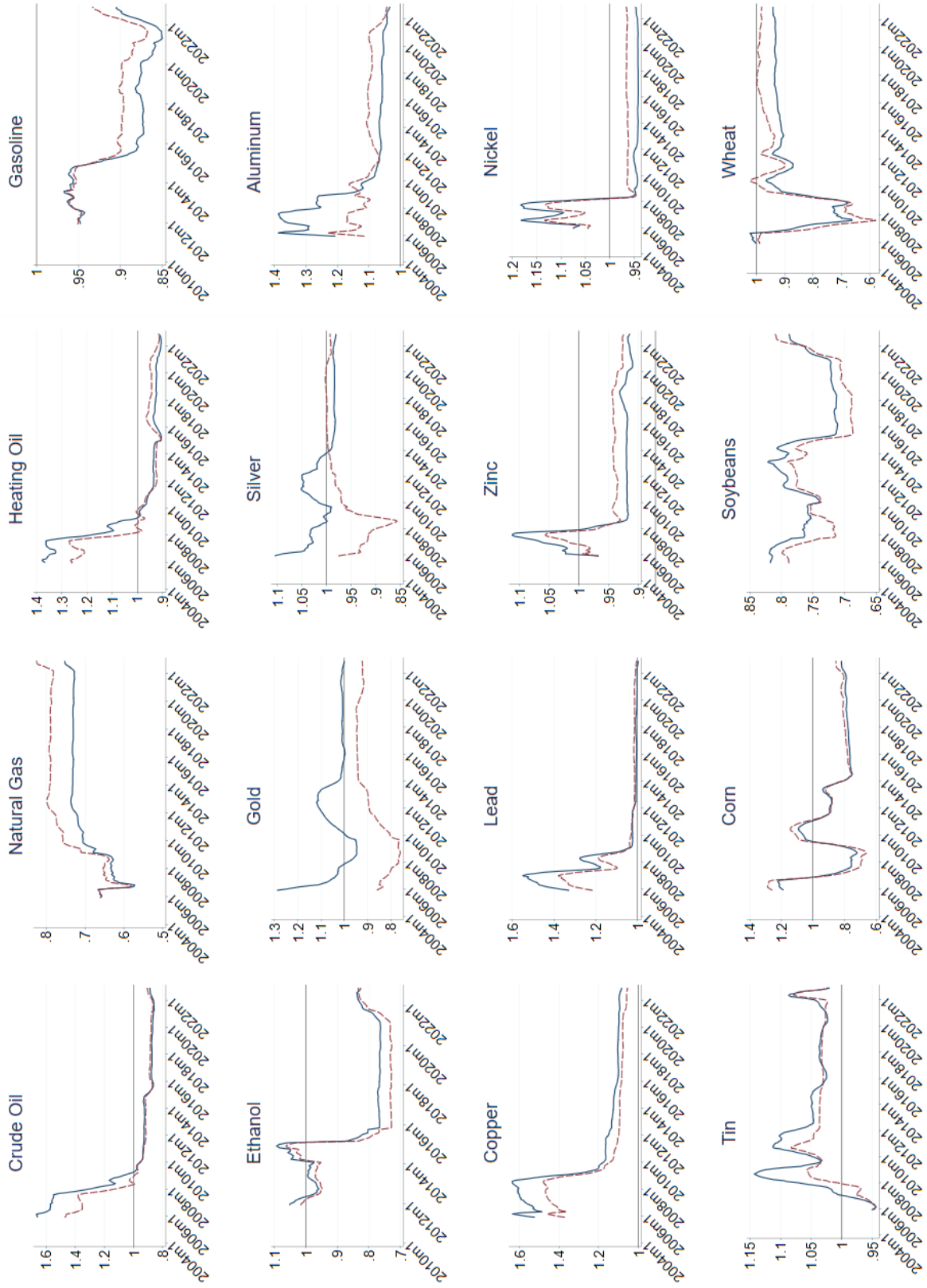


Figure A.2.: Evolution of MSFEs Criteria For Futures-Based Forecasts, One-Year Ahead.

Note: The blue line represents the performance of futures-based forecasts of real prices using End-of-Month (EoM) futures, while the red line illustrates the performance of futures-based forecasts of nominal prices using EoM. A horizontal reference line is drawn at the value of 1 to serve as a benchmark for evaluating MSFE values, which are reported relative to the average price of a no-change forecast.

A. Supplementary Material for Chapter 2

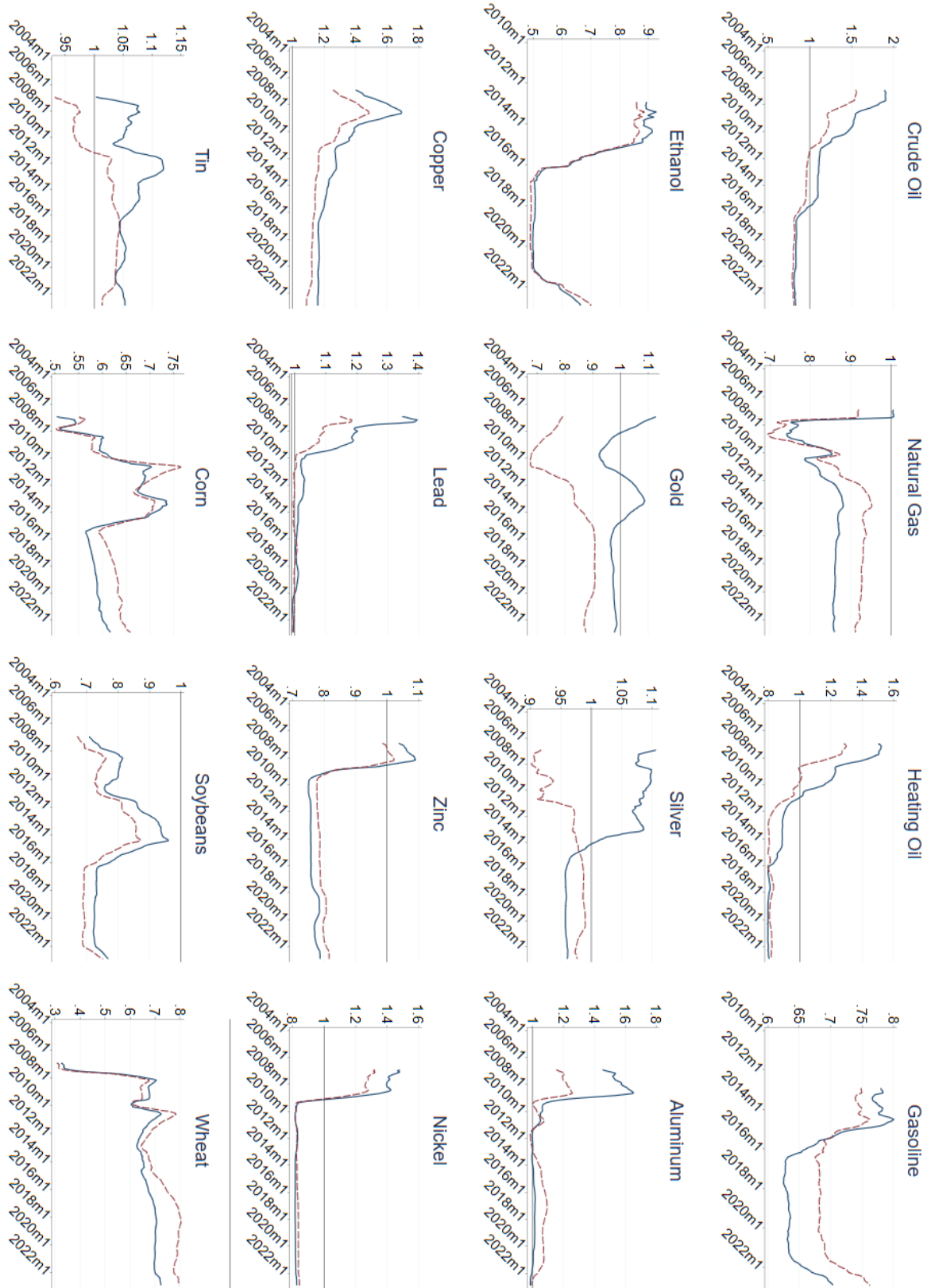


Figure A.3.: Evolution of MSFEs Criteria For Futures-Based Forecasts, Two-Year Ahead.

Note: The blue line represents the performance of futures-based forecasts of real prices using End-of-Month (EoM) futures, while the red line illustrates the performance of futures-based forecasts of nominal prices using EoM. A horizontal reference line is drawn at the value of 1 to serve as a benchmark for evaluating MSFE values, which are reported relative to the average price of a no-change forecast.

B. Supplementary Material for Chapter 3

B.1. Detailed Bayesian identification and estimation of the SVAR model

Consider the following SVAR specification for a n -dimensional time series vector y_t :

$$\mathbf{A}y_t = \mathbf{B}x_{t-1} + u_t \quad (\text{B.1})$$

where y_t is an $n \times 1$ vector of endogenous variables, \mathbf{A} is an $(n \times n)$ matrix summarizing their contemporaneous structural relations, x_{t-1} is a $(k \times 1)$ vector (with $k = mn+1$) containing a constant and m lags of y ($x_{t-1} = (y'_{t-1}, y'_{t-2}, \dots, y'_{t-m}, 1)'$), and u_t is an $(n \times 1)$ vector of structural disturbances assumed to be independent and identically distributed (i.i.d.) $\mathcal{N}(0, \mathbf{D})$ and mutually uncorrelated (\mathbf{D} is diagonal).⁴⁹ Following Baumeister and Hamilton (2019) and Braun (2023), the model includes $m = 12$ lags.

The reduced-form VAR associated with this structural model is represented as follows:

$$y_t = \Phi x_{t-1} + \varepsilon_t, \quad (\text{B.2})$$

$$\Phi = \mathbf{A}^{-1}\mathbf{B}, \quad (\text{B.3})$$

$$\varepsilon_t = \mathbf{A}^{-1}u_t, \quad (\text{B.4})$$

$$E(\varepsilon_t \varepsilon_t') = \mathbf{\Omega} = \mathbf{A}^{-1}\mathbf{D}(\mathbf{A}^{-1})', \quad (\text{B.5})$$

This study follows the identification and estimation strategy introduced by Baumeister and Hamilton (2015) and further developed by Baumeister and Hamilton (2019) to construct a specific four-variable oil market model, which was later applied to the U.S. natural gas market by Rubaszek et al. (2021). This strategy yields a set-identified SVAR model through two primary steps. The first step involves specifying informative prior beliefs about the values of the structural parameters represented by a density $p(\mathbf{A}, \mathbf{D}, \mathbf{B})$. The second step generates draws from the posterior distribution of the structural coefficients to assess how the data influences the prior beliefs.

Prior information about \mathbf{A} is expressed in the form of an arbitrary prior distribution $p(\mathbf{A})$. Higher values of $p(\mathbf{A})$ correspond to more plausible values of

⁴⁹This section follows the notation introduced by Baumeister and Hamilton (2019), retaining the same symbols for variables and parameters to maintain consistency with the original framework.

\mathbf{A} , while $p(\mathbf{A}) = 0$ is associated with any values of \mathbf{A} that are entirely excluded. This prior can incorporate a mix of exclusion restrictions, sign restrictions, and informative assumptions about the elements of \mathbf{A} . To represent prior information about the other parameters, this identification approach employs natural conjugate distributions that facilitate the analytical characterization of results and allow for straightforward analytical solutions.

The prior for the inverse of the structural variances is assumed to follow a gamma distribution, $\Gamma(\kappa_i, \tau_i)$:

$$p(\mathbf{D} | \mathbf{A}) = \prod_{i=1}^n p(d_{ii} | \mathbf{A}), \quad (\text{B.6})$$

$$p(d_{ii}^{-1} | \mathbf{A}) = \begin{cases} \frac{\tau_i^{\kappa_i}}{\Gamma(\kappa_i)} (d_{ii}^{-1})^{\kappa_i-1} \exp(-\tau_i d_{ii}^{-1}) & \text{for } d_{ii}^{-1} \geq 0, \\ 0 & \text{otherwise,} \end{cases} \quad (\text{B.7})$$

where d_{ii} denotes the row i , column i element of \mathbf{D} . The ratio κ_i/τ_i represents the expected value of d_{ii}^{-1} before learning from the data, whereas κ_i/τ_i^2 is the variance of this prior distribution. A stronger belief in these prior values is indicated by large κ_i and τ_i , leading to a more concentrated prior distribution around κ_i/τ_i . Following Baumeister and Hamilton (2019), this study sets $\kappa_i = 2$, which gives the priors a weight equivalent to four observations of data, and allows τ_i to depend on \mathbf{A} .

Prior information about the lagged structural parameters \mathbf{B} is represented with a conditional normal distribution, $\mathbf{b}_i | \mathbf{A}, \mathbf{D} \sim \mathcal{N}(\mathbf{m}_i, d_{ii} \mathbf{M}_i)$:

$$p(\mathbf{B} | \mathbf{D}, \mathbf{A}) = \prod_{i=1}^n p(\mathbf{b}_i | \mathbf{D}, \mathbf{A}), \quad (\text{B.8})$$

$$p(\mathbf{b}_i | \mathbf{D}, \mathbf{A}) = \frac{1}{(2\pi)^{k/2} |d_{ii} \mathbf{M}_i|^{1/2}} \exp \left(-\frac{1}{2} (\mathbf{b}_i - \mathbf{m}_i)' (d_{ii} \mathbf{M}_i)^{-1} (\mathbf{b}_i - \mathbf{m}_i) \right), \quad (\text{B.9})$$

where \mathbf{b}_i' denotes the i th row of \mathbf{B} , \mathbf{m}_i represents the prior mean for \mathbf{b}_i , and $d_{ii} \mathbf{M}_i$ is the variance associated with this prior. Thus, the matrix \mathbf{M}_i reflects the confidence level in this prior information, with greater variances signifying higher uncertainty. Conversely, a scenario with minimal valuable prior knowledge is akin to the scenario where \mathbf{M}_i^{-1} approaches zero. This study assumes that the prior expected value for these coefficients, \mathbf{m}_i , is zero, implying that changes in the underlying variables are difficult to forecast, and that the prior variance is $100 \times \mathbf{I}$. The overall prior distribution is

$$p(\mathbf{A}, \mathbf{D}, \mathbf{B}) = p(\mathbf{A}) \prod_{i=1}^n [p(d_{ii} | \mathbf{A}) p(\mathbf{b}_i | \mathbf{D}, \mathbf{A})] \quad (\text{B.10})$$

The second step includes describing how the data $Y_T = (y'_1, y'_2, \dots, y'_T)'$ affects the prior beliefs about the unknown parameters \mathbf{B} , \mathbf{A} , and \mathbf{D} . The posterior distribution is decomposed as follows:

$$p(\mathbf{A}, \mathbf{D}, \mathbf{B} | Y_T) = p(\mathbf{A} | Y_T) p(\mathbf{D} | \mathbf{A}, Y_T) p(\mathbf{B} | \mathbf{A}, \mathbf{D}, Y_T) \quad (\text{B.11})$$

The posterior distribution for the covariance matrix is represented as:

$$p(\mathbf{D} | \mathbf{A}, \mathbf{Y}_T) = \prod_{i=1}^n \gamma(d_{ii}^{-1}; \kappa_i^*, \tau_i^*(\mathbf{A})) \quad (\text{B.12})$$

where:

$$\kappa_i^* = \kappa_i + T/2 \quad (\text{B.13})$$

$$\tau_i^*(\mathbf{A}) = \tau_i(\mathbf{A}) + (1/2)\zeta_i^*(\mathbf{A}) \quad (\text{B.14})$$

The value of $\zeta_i^*(\mathbf{A})$ is the sum of squared residuals obtained from regressing $\tilde{Y}_i(\mathbf{A})$ on $\tilde{\mathbf{X}}_i$:

$$\zeta_i^*(\mathbf{A}) = (\tilde{Y}_i'(\mathbf{A})\tilde{Y}_i(\mathbf{A})) - (\tilde{Y}_i'(\mathbf{A})\tilde{\mathbf{X}}_i)(\tilde{\mathbf{X}}_i'\tilde{\mathbf{X}}_i)^{-1}(\tilde{\mathbf{X}}_i'\tilde{Y}_i(\mathbf{A})), \quad (\text{B.15})$$

$$\tilde{Y}_i(\mathbf{A}) = [\mathbf{a}'_i y_1 \dots \mathbf{a}'_i y_T \mathbf{m}_i(\mathbf{A})' \mathbf{P}_i']', \quad (\text{B.16})$$

$$\tilde{\mathbf{X}}_i = [\mathbf{x}'_0 \dots \mathbf{x}'_{T-1} \mathbf{P}_i']'. \quad (\text{B.17})$$

with \mathbf{P}_i being the Chelosky factor of $\mathbf{M}_i^{-1} = \mathbf{P}_i \mathbf{P}_i'$

The posterior distribution for the lagged structural coefficients \mathbf{B} can be written as $p(\mathbf{B} | \mathbf{A}, \mathbf{D}, \mathbf{Y}_T) = \prod_{i=1}^n \phi(\mathbf{b}_i; m_i^*, d_{ii} M_i^*)$, where

$$\mathbf{m}_i^*(\mathbf{A}) = (\tilde{\mathbf{X}}_i' \tilde{\mathbf{X}}_i)^{-1} (\tilde{\mathbf{X}}_i' \tilde{Y}_i(\mathbf{A})), \quad (\text{B.18})$$

$$\mathbf{M}_i^* = (\tilde{\mathbf{X}}_i' \tilde{\mathbf{X}}_i)^{-1}. \quad (\text{B.19})$$

The posterior marginal distribution for \mathbf{A} is given by

$$p(\mathbf{A} | Y_T) = \frac{k_T p(\mathbf{A}) \left[\det(\mathbf{A} \hat{\mathbf{\Omega}}_T \mathbf{A}') \right]^{T/2}}{\prod_{i=1}^n [(2/T) \tau_i^*(\mathbf{A})]^{\kappa_i^*}} \prod_{i=1}^n \tau_i(\mathbf{A})^{\kappa_i}. \quad (\text{B.20})$$

where $p(\mathbf{A})$ refers to the original prior density for \mathbf{A} , and $\hat{\mathbf{\Omega}}_T$ is the sample variance matrix that is calculated with the reduced-form VAR model.

B.2. Additional results: posterior distributions and historical decompositions

Posteriors for contemporaneous relations in matrix **A**

Table B.1.: Summary statistics for the contemporaneous coefficients in **A**

Parameter	Baseline	S1	S2	S3	S4	S5
α_{qp}	0.019 (0.009, 0.033)	0.021 (0.009, 0.037)	0.022 (0.010, 0.037)	0.024 (0.010, 0.042)	0.020 (0.009, 0.034)	0.007 (0.002, 0.015)
α_{yp}	-0.005 (-0.008, -0.002)	-0.004 (-0.008, -0.001)	-0.008 (-0.015, -0.003)	-0.010 (-0.016, -0.005)	-0.005 (-0.009, -0.002)	-0.004 (-0.009, -0.002)
β_{qy}	0.741 (0.398, 1.187)	0.788 (0.461, 1.322)	0.807 (0.517, 1.262)	0.786 (0.430, 1.379)	0.730 (0.496, 1.183)	0.908 (0.526, 1.80)
β_{qp}	-0.177 (-0.300, -0.088)	-0.184 (-0.323, -0.088)	-0.145 (-0.256, -0.065)	-0.130 (-0.265, -0.046)	-0.166 (-0.299, -0.079)	-0.219 (-0.365, -0.126)
ψ_1	-0.482 (-0.881, -0.209)	-0.484 (-0.914, -0.181)	-0.575 (-1.013, -0.269)	-0.563 (-1.017, -0.204)	-0.510 (-0.929, -0.220)	-0.305 (-0.537, -0.111)
ψ_2	1.550 (0.908, 2.344)	1.465 (0.781, 2.325)	0.646 (0.252, 1.146)	1.599 (0.545, 3.034)	1.581 (0.924, 2.404)	1.487 (0.866, 2.311)
ψ_3	-0.362 (-0.422, -0.311)	-0.393 (-0.466, -0.333)	-0.374 (-0.438, -0.320)	-0.348 (-0.410, -0.297)	-0.368 (-0.430, -0.312)	-0.343 (-0.398, -0.291)
λ_1	0.008 (-0.006, 0.023)	0.022 (0.011, 0.022)	0.045 (0.032, 0.060)	-0.001 (-0.039, 0.042)	0.008 (-0.006, 0.023)	0.018 (0.008, 0.028)
λ_2	0.010 (-0.030, 0.049)	-0.009 (-0.039, 0.022)	0.043 (0.020, 0.067)	0.155 (0.033, 0.278)	0.010 (0.030, 0.050)	0.000 (-0.027, 0.028)
λ_3	-0.002 (-0.004, 0.000)	-0.001 (-0.003, 0.000)	-0.003 (-0.005, -0.001)	-0.005 (-0.010, 0.003)	-0.002 (-0.003, 0.000)	-0.002 (-0.002, 0.001)
λ_4	0.006 (0.000, 0.012)	0.004 (0.000, 0.008)	0.010 (0.004, 0.016)	0.002 (-0.016, 0.020)	0.005 (-0.000, 0.011)	0.004 (0.001, 0.008)

Notes: This table presents the posterior medians (in bold) and 68 percent credibility regions (in parentheses) for the structural parameters of matrix **A**, used in our SVAR model. The “Baseline” column contains results from the baseline model estimation, while columns “S1” to “S5” correspond to various sensitivity analyses described in Section 3.6. Specifically, “S1” re-estimates the baseline model using data until December 2019 (2019:M12). “S2” uses the full dataset from January 1992 to October 2023 (1992:M1 to 2023:M10), including pandemic data. “S3” estimates the model from January 2009, assessing the effect of the shale gas revolution. “S4” evaluates the impact of employing less informative priors on the short-run supply and demand elasticities. “S5” leverages non-Gaussianity as an additional source of identifying information. For definitions of each parameter, please refer to Table 3.2.

B.2. Additional results: posterior distributions and historical decompositions

Detailed forecast error variance decompositions with credibility intervals

Table B.2.: Percent contribution of shocks to the overall variability of each variable (with credibility sets)

Horizon	Natural gas supply					Economic activity				
	u_t^s	u_t^{ea}	u_t^{cd}	u_t^{id}	u_t^{exd}	u_t^s	u_t^{ea}	u_t^{cd}	u_t^{id}	u_t^{exd}
1	94.29 (85.01, 98.12)	1.24 (0.11, 3.91)	1.77 (0.26, 5.40)	1.76 (0.18, 7.20)	0.34 (0.01, 2.02)	0.45 (0.04, 1.88)	95.97 (90.27, 98.68)	1.62 (0.29, 4.55)	1.30 (0.14, 4.56)	0.16 (0.01, 1.31)
2	92.33 (83.04, 96.74)	1.52 (0.27, 4.41)	2.04 (0.42, 5.70)	2.13 (0.39, 7.42)	1.18 (0.1, 4.31)	0.75 (0.11, 2.65)	94.21 (88.19, 97.35)	2.03 (0.53, 5.05)	1.65 (0.31, 4.88)	0.80 (0.08, 2.81)
3	90.96 (81.67, 95.61)	1.86 (0.45, 4.96)	2.33 (0.60, 6.05)	2.40 (0.56, 7.67)	1.67 (0.29, 4.77)	2.06 (0.50, 5.33)	91.53 (84.95, 95.52)	2.55 (0.76, 5.87)	1.99 (0.5, 5.36)	1.12 (0.18, 3.55)
6	85.88 (76.85, 91.45)	3.04 (1.17, 6.39)	3.12 (1.07, 6.95)	3.96 (1.45, 9.31)	3.28 (1.14, 7.01)	3.69 (1.27, 7.89)	87.17 (80.13, 92.07)	3.26 (1.32, 6.7)	2.88 (0.99, 6.64)	2.14 (0.65, 5.10)
12	76.3 (67.64, 82.96)	4.99 (2.47, 8.89)	5.80 (2.84, 10.31)	6.70 (3.35, 11.96)	5.37 (2.59, 9.84)	6.88 (3.31, 12.03)	77.74 (70.31, 84.05)	4.99 (2.56, 8.93)	4.80 (2.27, 8.95)	4.70 (2.19, 8.82)
16	74.57 (65.87, 81.51)	5.54 (2.88, 9.52)	6.13 (3.16, 10.63)	7.11 (3.67, 12.37)	5.81 (2.92, 10.39)	7.38 (3.69, 12.73)	76.01 (68.30, 82.65)	5.40 (2.87, 9.54)	5.10 (2.51, 9.39)	5.16 (2.50, 9.50)

Horizon	Real natural gas price					Natural gas inventories				
	u_t^s	u_t^{ea}	u_t^{cd}	u_t^{id}	u_t^{exd}	u_t^s	u_t^{ea}	u_t^{cd}	u_t^{id}	u_t^{exd}
1	8.48 (5.00, 14.10)	3.61 (1.79, 6.45)	54.06 (41.05, 66.45)	31.54 (23.33, 39.2)	0.73 (0.26, 1.79)	3.16 (0.91, 7.04)	1.22 (0.11, 4.02)	76.90 (61.8, 85.60)	16.62 (5.6, 33.43)	1.36 (0.31, 3.94)
2	8.82 (5.49, 14.07)	4.67 (2.69, 7.43)	52.45 (39.88, 64.29)	31.09 (22.88, 38.66)	1.65 (0.71, 3.10)	3.47 (1.13, 7.21)	2.51 (0.71, 5.60)	75.20 (60.43, 83.90)	16.47 (5.85, 32.78)	1.70 (0.43, 4.57)
3	8.86 (5.62, 13.96)	5.23 (3.17, 8.07)	51.19 (39.04, 62.88)	31.41 (23.32, 38.84)	2.00 (0.98, 3.49)	4.27 (1.59, 8.44)	3.29 (1.07, 7.05)	73.27 (59.07, 81.88)	15.98 (5.79, 31.65)	2.38 (0.7, 5.67)
6	10.04 (6.67, 14.98)	6.87 (4.59, 9.83)	48.27 (36.96, 59.26)	29.92 (22.37, 36.8)	3.75 (2.24, 5.73)	6.07 (2.81, 10.61)	5.44 (2.29, 10.41)	68.79 (55.45, 77.64)	15.60 (6.12, 30.26)	3.16 (1.19, 6.67)
12	10.54 (7.47, 14.98)	7.63 (5.52, 10.40)	46.16 (35.93, 55.87)	28.56 (21.59, 35)	6.15 (4.32, 8.40)	7.44 (4.02, 12.24)	7.22 (3.69, 12.26)	63.57 (51.29, 72.24)	15.71 (7.18, 28.90)	5.04 (2.55, 8.91)
16	10.71 (7.65, 15.02)	7.95 (5.83, 10.71)	45.60 (35.81, 55.01)	27.92 (21.22, 34.05)	6.81 (4.83, 9.22)	7.82 (4.33, 12.60)	7.48 (3.96, 12.56)	62.34 (50.35, 71.12)	15.91 (7.46, 28.87)	5.43 (2.87, 9.45)

Horizon	Natural gas exports				
	u_t^s	u_t^{ea}	u_t^{cd}	u_t^{id}	u_t^{exd}
1	1.01 (0.09, 0.05)	0.67 (0.45, 0.03)	2.16 (90.83, 3.34)	0.47 (2.76, 5.38)	94.94 (2.08, 97.71)
2	1.59 (0.31, 0.18)	1.18 (0.91, 0.11)	2.99 (88.03, 4.26)	0.78 (3.69, 6.50)	92.67 (2.60, 96.10)
3	2.54 (0.74, 0.32)	1.47 (1.40, 0.42)	3.75 (84.45, 5.64)	1.83 (4.07, 7.52)	89.59 (4.65, 93.68)
6	4.62 (1.96, 1.38)	3.62 (2.00, 1.01)	4.59 (77.64, 8.49)	2.83 (7.19, 8.56)	83.50 (6.07, 88.6)
12	7.19 (3.85, 3.04)	5.96 (2.99, 2.62)	5.74 (68.67, 11.92)	5.12 (10.43, 9.78)	75.14 (8.85, 81.01)
16	7.92 (4.34, 3.39)	6.44 (3.27, 3.15)	6.11 (65.88, 12.96)	5.89 (11.04, 10.23)	72.73 (9.91, 79.08)

Note: This table provides posterior median estimates of the contribution of each shock to the forecast error variance of each variable. Values in brackets indicate corresponding 68% posterior credibility sets. Horizons are expressed in months. The terms u_t^s , u_t^{ea} , u_t^{cd} , u_t^{id} , and u_t^{exd} refer to supply, economic activity, consumption demand, inventory demand, and exports demand shocks, respectively. Estimates are based on the model specified in Section 3.3.2.

Historical decomposition of U.S. natural gas prices during Hurricanes Katrina and Rita

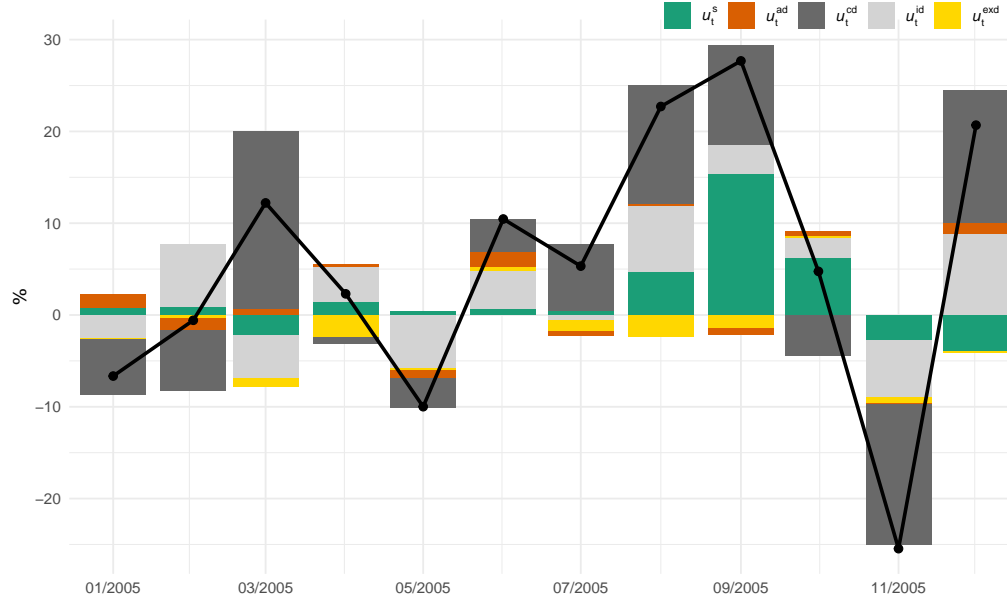


Figure B.1.: Historical decomposition of U.S. real natural gas price movements from January 2005 to December 2005

Note: Each bar in the graph represents the median estimate of historical contribution of separate shocks—supply (u_t^s), aggregate demand (u_t^{ad}), consumption demand (u_t^{cd}), inventory demand (u_t^{id}), and export demand (u_t^{exd})—for each month during the specified period. The colors correspond to these specific shocks, as labeled directly on the figure. The solid black line represents the logarithmic changes in the real prices of U.S. natural gas. Estimates are based on the model specified in Section 3.3.2, using monthly data from 1992 to 2023.

Historical decomposition of U.S. natural gas prices from 2015 to 2017

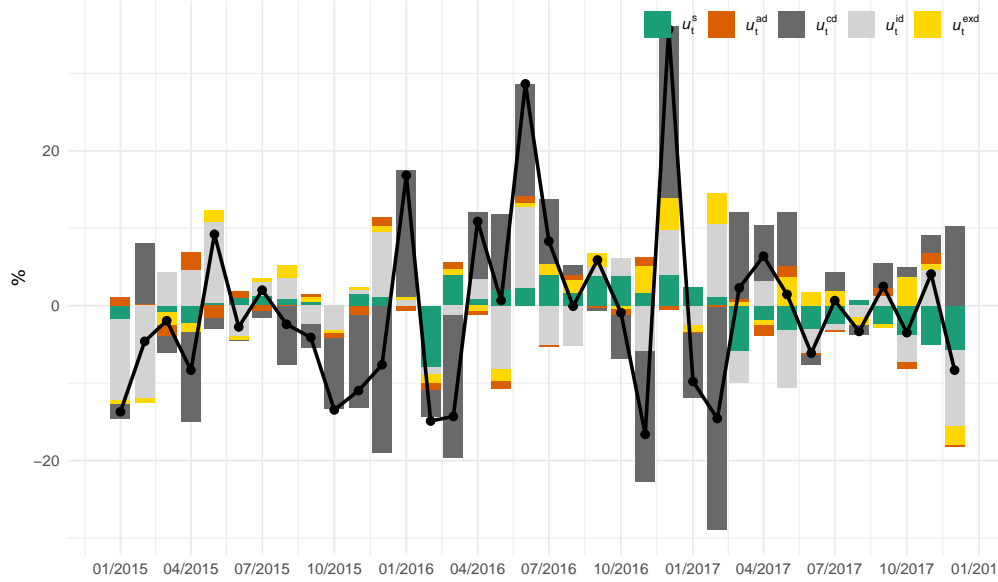


Figure B.2.: Historical decomposition of U.S. real natural gas price movements from January 2015 to December 2017

Note: Each bar in the graph represents the median estimate of historical contribution of separate shocks—supply (u_t^s), aggregate demand (u_t^{ad}), consumption demand (u_t^{cd}), inventory demand (u_t^{id}), and export demand (u_t^{exd})—for each month during the specified period. The colors correspond to these specific shocks, as labeled directly on the figure. The solid black line represents the logarithmic changes in the real prices of U.S. natural gas. Estimates are based on the model specified in Section 3.3.2, using monthly data from 1992 to 2023.

B.3. Detailed results of the sensitivity analyses

Results of pre-pandemic analysis (through 2019)

This analysis investigates the stability and consistency of the baseline model's IRFs, using data exclusively from the period prior to the COVID-19 pandemic, ending in December 2019. By isolating the pre-pandemic period, this exercise aims to establish a baseline understanding of market dynamics unaffected by the extraordinary economic disruptions caused by the pandemic.

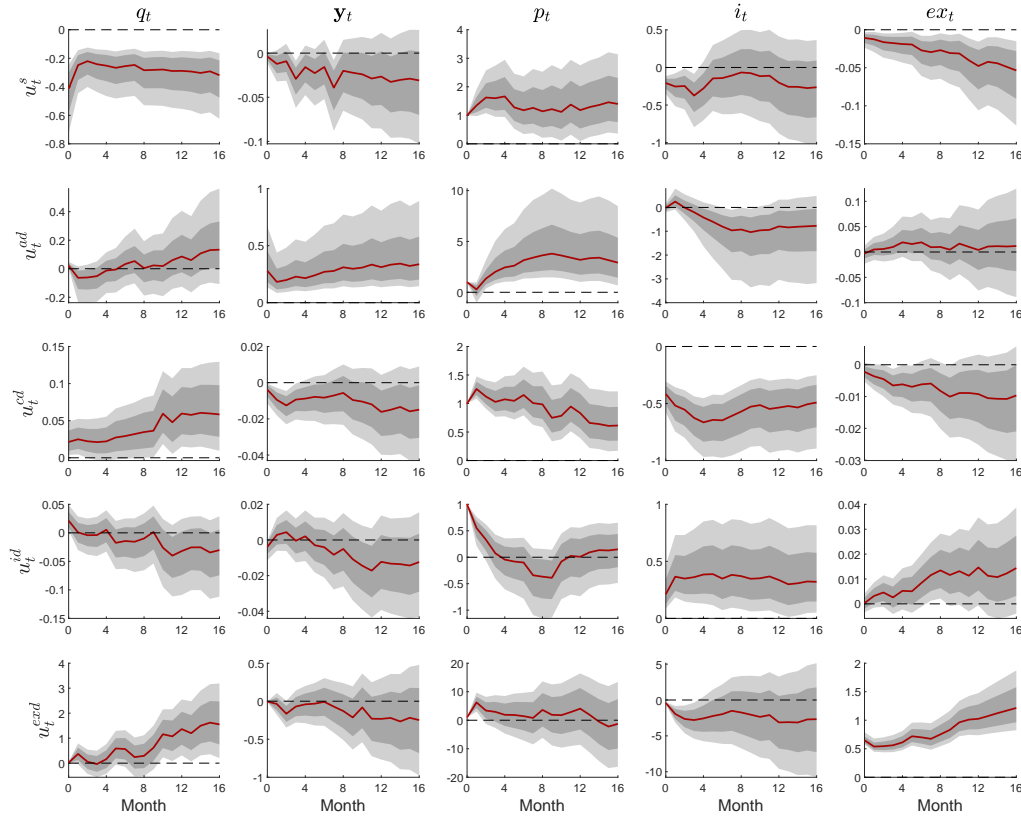


Figure B.3.: Impulse response functions for the model estimated from January 1992 to December 2019

Note: The rows represent the responses to different shocks, denoted as u_t^s (supply shock), u_t^{ea} (economic activity shock), u_t^{cd} (consumption demand shock), u_t^{id} (inventory demand shock), and u_t^{exd} (export demand shock). The columns represent the variables: q_t (total U.S. natural gas supply), y_t (real U.S. GDP), p_t (real gas price), i_t (U.S. gas inventories), and ex_t (U.S. gas exports). The red solid lines represent the Bayesian posterior median, while the dark- and light-shaded grey areas denote the 68% and 90% posterior credible regions, respectively.

Results of full sample analysis including the Covid-19 pandemic period

This section presents the results of an analysis incorporating the entire dataset spanning January 1992 to October 2023. It examines the extent to which the inclusion of COVID-19-related data affects the estimation of the IRFs.

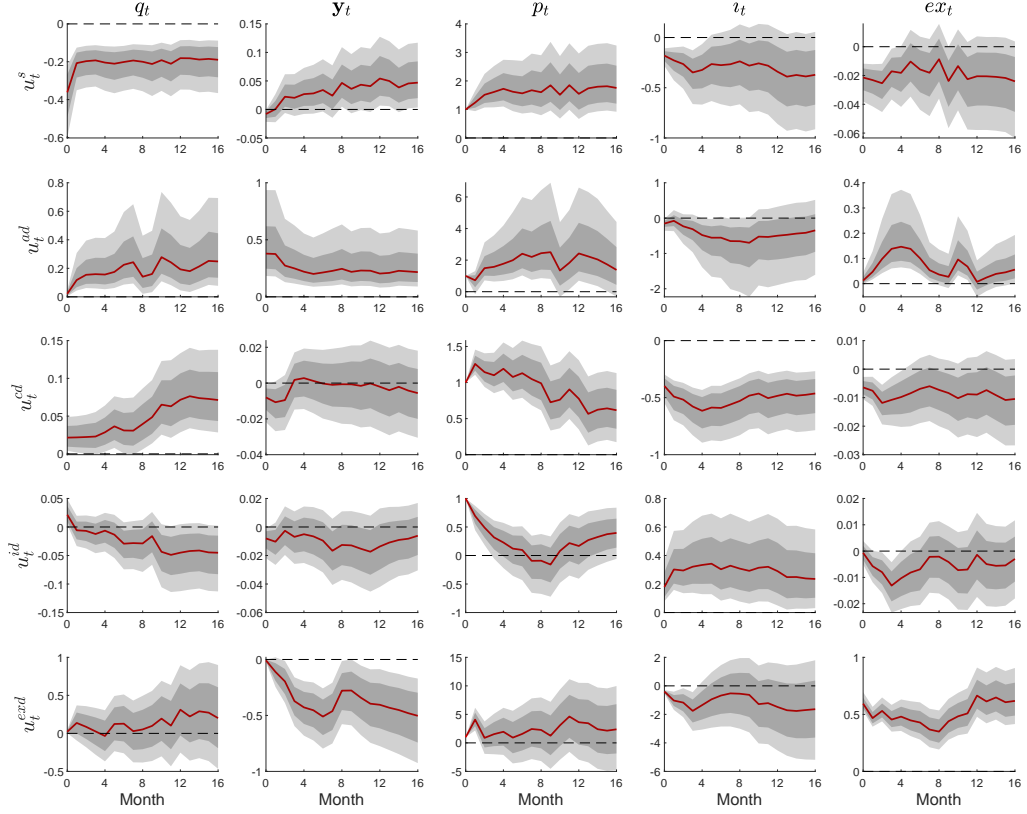


Figure B.4.: Impulse response functions for the model estimated using the entire sample from January 1992 to October 2023, including observations during the COVID-19 pandemic.

Note: The rows represent the responses to different shocks, denoted as u_t^s (supply shock), u_t^{ea} (economic activity shock), u_t^{cd} (consumption demand shock), u_t^{id} (inventory demand shock), and u_t^{exd} (export demand shock). The columns represent the variables: q_t (total U.S. natural gas supply), y_t (real U.S. GDP), p_t (real gas price), i_t (U.S. gas inventories), and ex_t (U.S. gas exports). The red solid lines represent the Bayesian posterior median, while the dark- and light-shaded grey areas denote the 68% and 90% posterior credible regions, respectively.

Results of sensitivity analysis from 2009 onward

This section presents the results of sensitivity analyses focusing on the impact of the shale gas revolution from January 2009 to October 2023, while explicitly excluding data from the COVID-19 pandemic period. The analysis explores how shifts in market dynamics, driven by technological and infrastructural advancements, have influenced the structural dynamics within the U.S. gas market.

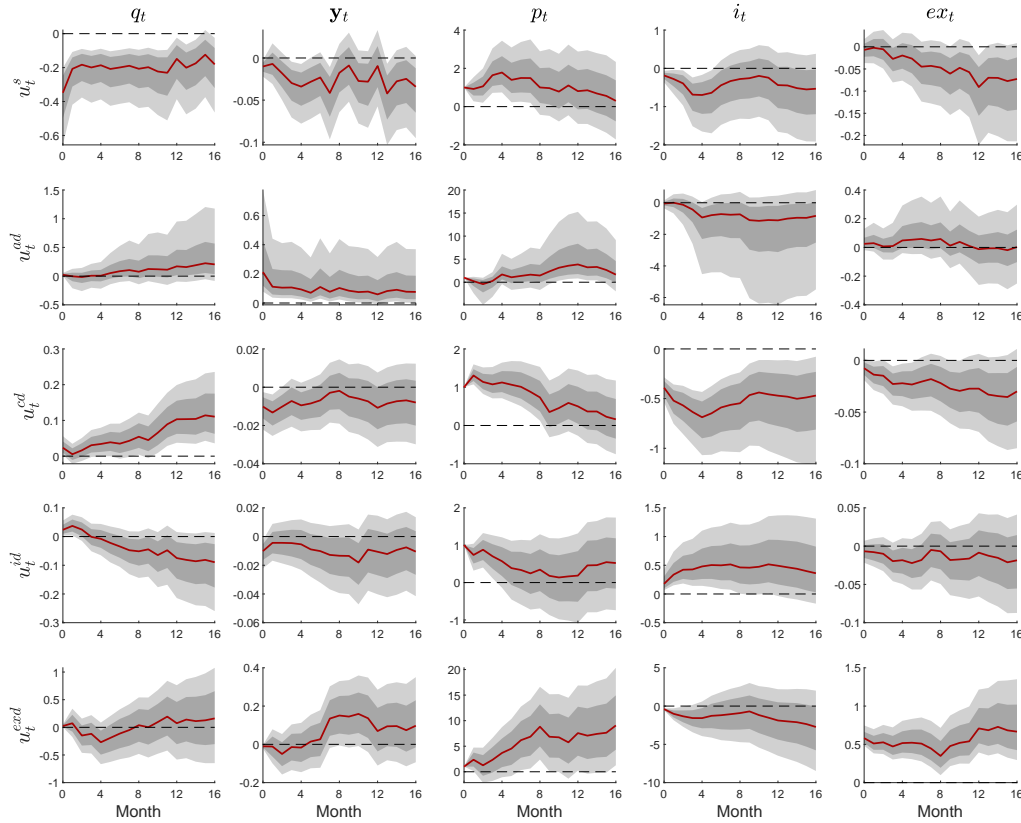


Figure B.5.: Impulse response functions for the model estimated from January 2009 to October 2023, excluding the COVID-19 pandemic period from March 2020 to February 2021.

Note: The rows represent the responses to different shocks, denoted as u_t^s (supply shock), u_t^{ea} (economic activity shock), u_t^{cd} (consumption demand shock), u_t^{id} (inventory demand shock), and u_t^{exd} (export demand shock). The columns represent the variables: q_t (total U.S. natural gas supply), y_t (real U.S. GDP), p_t (real gas price), i_t (U.S. gas inventories), and ex_t (U.S. gas exports). The red solid lines represent the Bayesian posterior median, while the dark- and light-shaded grey areas denote the 68% and 90% posterior credible regions, respectively.

Results of sensitivity analysis with weaker priors on supply and demand elasticities

This section presents impulse response functions from sensitivity analyses where weaker priors were applied to supply and demand elasticities. The model covers data from January 1992 to December 2023, excluding the pandemic-related period from March 2020 to February 2021, and explores how weaker priors affect the estimation of these elasticities.

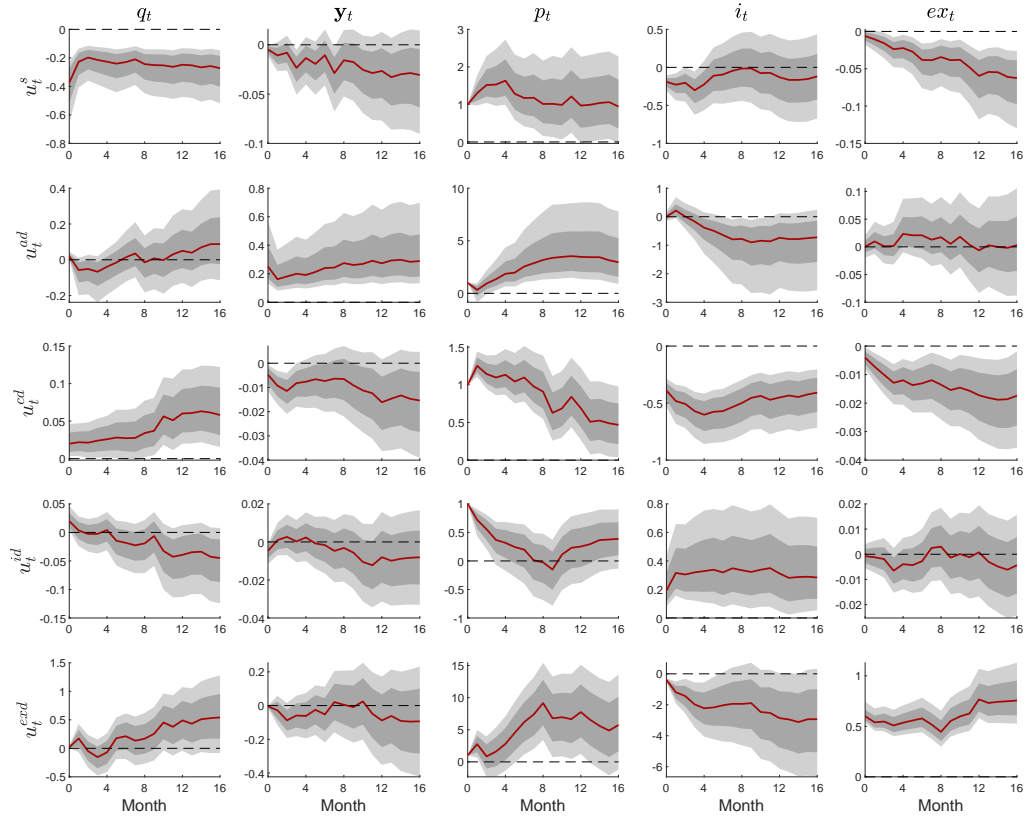


Figure B.6.: Impulse response functions from the model estimated using the full dataset from January 1992 to December 2023, excluding the period from March 2020 to February 2021, with weaker priors for supply and demand elasticities.

Note: The rows represent the responses to different shocks, denoted as u_t^s (supply shock), u_t^{ea} (economic activity shock), u_t^{cd} (consumption demand shock), u_t^{id} (inventory demand shock), and u_t^{exd} (export demand shock). The columns represent the variables: q_t (total U.S. natural gas supply), y_t (real U.S. GDP), p_t (real gas price), i_t (U.S. gas inventories), and ex_t (U.S. gas exports). The red solid lines represent the Bayesian posterior median, while the dark- and light-shaded grey areas denote the 68% and 90% posterior credible regions, respectively.

Results of incorporating non-Gaussianity for structural shock identification

This exercise introduces non-Gaussianity as an additional source of identifying information. The analysis employs a novel identification strategy proposed by Braun (2023), which combines economically motivated prior distributions, as introduced by Baumeister and Hamilton (2019), with identification by non-Gaussianity. This approach ensures that economic interpretations remain relevant throughout the analysis.

To model non-Gaussianity, the distribution of each structural error is approximated using a nonparametric Dirichlet process mixture model (DPMM). This nonparametric approach offers two key advantages. First, it allows for flexible modeling of the unknown density functions of structural shocks, enhancing the model's robustness against error-term misspecification and potentially improving estimation efficiency by adapting to the actual distribution of shocks. Second, the DPMM framework enables a straightforward assessment of non-Gaussianity in the data by comparing the posterior predictive density to the kernel of a standard normal distribution, as detailed by Braun (2023). Such comparisons provide insights into the identifying information derivable from the statistical properties of each shock. A detailed description of the SVAR-DPMM model is available in the source article.

Before presenting the results of the non-Gaussian SVAR model, it is essential to assess the empirical validity of the assumptions regarding non-Gaussianity and mutual independence in the U.S. natural gas market. This validation occurs in two steps.

The first step involves examining the deviation of structural shocks from Gaussianity. Figure B.7 presents the posterior median estimates of predictive densities for standardized structural shocks, with 68% posterior confidence intervals (shaded areas), compared against the density of a standard normal distribution (gray line). This figure reveals significant degrees of non-Gaussianity in the structural shocks, particularly in supply, economic activity, and export shocks. These distributional characteristics underscore the potential for leveraging non-Gaussian distributions to identify structural shocks in the U.S. gas market.

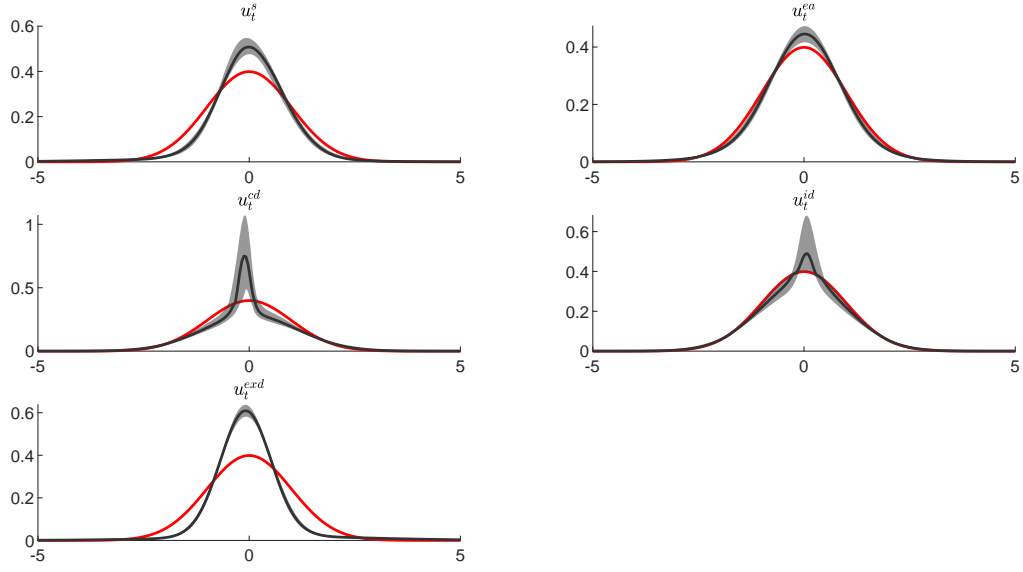


Figure B.7.: Posterior predictive densities of standardized structural shocks

Note: Posterior predictive densities of standardized structural shocks $\hat{u}_{i,T+1} = \sigma_i^{-\frac{1}{2}}(\hat{u}_{i,T+1} - \mu_i)$, showcased with a 68% credible interval. The black line refers to the density of a standard normal distribution.

The second step assesses the mutual independence of the structural shocks. Figure B.8 presents the posterior of the test statistic from the test introduced by Matteson and Tsay (2017). For comparison, the figure also overlays the distribution of this test statistic with that of the same statistic computed for randomly permuted shocks, denoted as $U_0(\mathbf{E})$. In accordance with the principle of mutual independence, each shock $\hat{u}_{j,t}$ is resampled independently from the other shocks, rather than resampling all components in the vector u_{ij} together. This process is repeated at each iteration of the posterior inference algorithm. The comparison, as illustrated in Figure B.8, demonstrates a close match between the distributions of $U(\mathbf{E})$ and $U_0(\mathbf{E})$, indicating no significant evidence against the mutual independence of the shocks.

B. Supplementary Material for Chapter 3

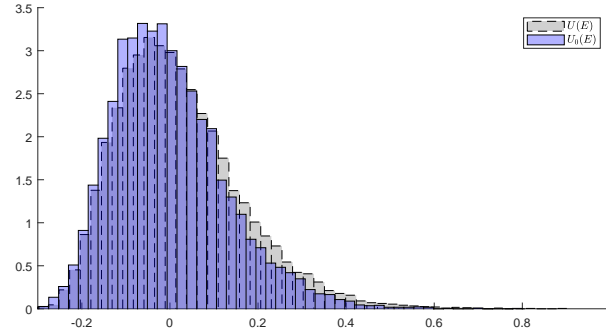


Figure B.8.: Posterior distributions of the mutual independence test statistics $U(E)$, as per Matteson and Tsay (2017).

Note: The distributions of test statistics based on actual data are compared with those obtained from randomly repermuted shocks, denoted as $U_0(E)$, to assess the empirical plausibility of the mutual independence assumption. A close resemblance between the distributions of $U(E)$ and $U_0(E)$ indicates no substantial evidence against the mutual independence of shocks in the non-Gaussian model.

Given the large deviations from Gaussianity characterizing many natural gas market shocks, and their established mutual independence, non-Gaussianity can be exploited as an additional source of identifying information. The results of the IRFs are presented in Figure B.9. These results show no significant difference between the IRFs obtained by leveraging non-Gaussianity and those from the baseline model.

B.3. Detailed results of the sensitivity analyses

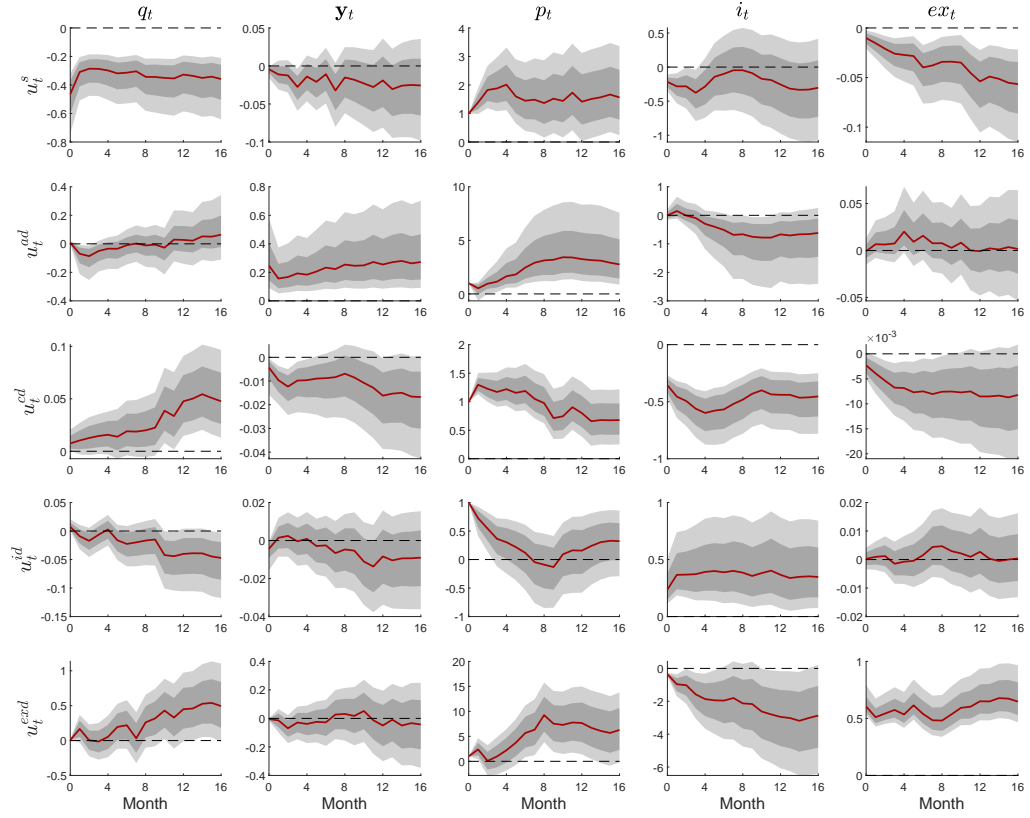


Figure B.9.: Impulse response functions with Non-Gaussianity as an additional source of identification.

Note: The rows represent the responses to different shocks, denoted as u_t^s (supply shock), u_t^{ea} (economic activity shock), u_t^{cd} (consumption demand shock), u_t^{id} (inventory demand shock), and u_t^{exd} (export demand shock). The columns represent the variables: q_t (total U.S. natural gas supply), y_t (real U.S. GDP), p_t (real gas price), i_t (U.S. gas inventories), and ex_t (U.S. gas exports). The red solid lines represent the Bayesian posterior median, while the dark- and light-shaded grey areas denote the 68% and 90% posterior credible regions, respectively.

B. Supplementary Material for Chapter 3

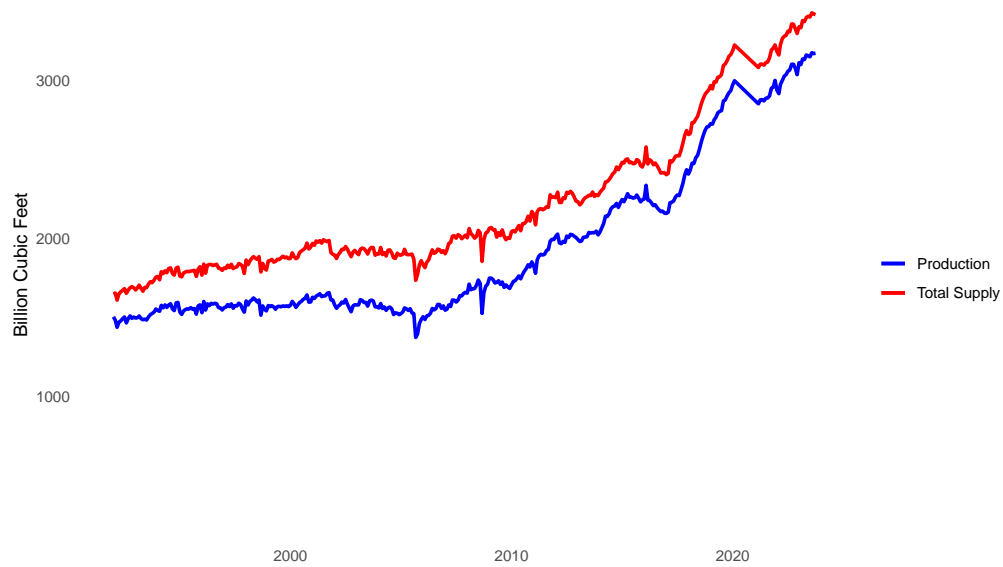


Figure B.10.: Monthly U.S. domestic natural gas production and total supply (in billion cubic feet) from 1992 to 2023.

Note: The data are sourced from the U.S. Energy Information Administration (EIA) and are seasonally adjusted. Total supply is calculated as the sum of domestic production and imports.

C. Supplementary Material for Chapter 4

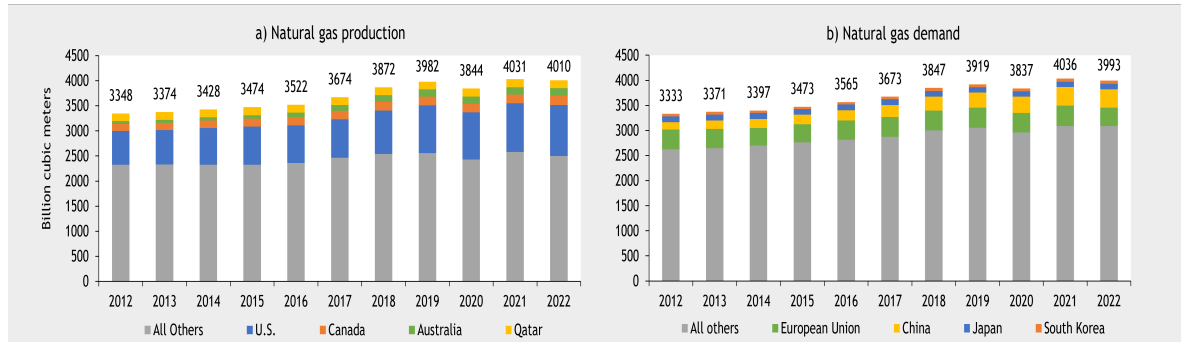


Figure C.1.: Worldwide and regional developments of natural gas a) production and b) demand from 2012 to 2022 (Billion cubic meters).

Source: Own construction based on Rystad Energy (2023).

Table C.1 presents the summary statistics for the EAX, TTF, and HH gas prices across two distinct subsamples, delineated by data before and after October 1, 2021. In the first subsample, the mean prices are 7.246 USD/MMBtu for EAX, 5.914 USD/MMBtu for TTF, and 2.748 USD/MMBtu for HH, with standard deviations of 3.715, 3.147, and 0.618, respectively. These values indicate that the HH market had the lowest price level and volatility during this period. In the second subsample, there is a significant increase in mean prices, with EAX rising to 34.920 USD/MMBtu, TTF to 39.209 USD/MMBtu, and HH to 6.177 USD/MMBtu, accompanied by higher standard deviations, particularly for TTF. The minimum and maximum values also reflect increased price ranges in the second period. The kurtosis values indicate more extreme price movements for TTF and EAX in the first subsample, while skewness values show that all three price series exhibit a right-skewed distribution, becoming more pronounced in the second subsample for TTF and EAX. Overall, these statistics suggest a shift toward higher prices and greater variability in the gas markets post-September 2021, reflecting possible market changes or external shocks affecting supply and demand dynamics.

A necessary condition for conducting cointegration analysis is the presence of a unit root, which indicates that the price series are integrated of order I (1). To ensure reliable outcomes, we conducted three unit root tests: the Augmented Dickey-Fuller (ADF), Phillips-Perron (PP), and Kwiatkowski-Phillips-Schmidt-Shin (KPSS). The null hypothesis for ADF and PP states that the data series has a unit root, with the alternative being that it is stationary. Conversely, the null hypothesis for KPSS indicates that the variable is stationary. Table C.2

summarizes the results of the tests for the log level and first differences of the three price series in each sub-period. The results indicate that the three price series are not stationary in levels but are stationary in first differences at the 1% significance level. Thus, it is concluded that the three gas prices are I(1).

Table C.1.: Summary statistics of gas price series across different periods

Variable	Subsample	Mean		SD		Minimum		Maximum		Kurtosis		Skewness	
		Level	Log	Level	Log	Level	Log	Level	Log	Level	Log	Level	Log
EAX	First	7.246	1.868	3.715	0.474	1.750	0.560	33.000	3.499	9.531	3.508	1.878	-0.156
	Second	34.920	3.515	9.974	0.269	20.050	2.998	72.150	4.279	4.622	2.878	1.135	0.355
TTF	First	5.914	1.666	3.147	0.461	1.147	0.137	30.529	3.418	14.305	4.48	2.593	-0.172
	Second	39.209	3.608	14.785	0.336	21.599	3.073	93.917	4.542	4.259	2.525	1.303	0.726
HH	First	2.748	0.986	0.618	0.221	1.482	0.393	5.880	1.771	4.917	3.383	0.748	-0.141
	Second	6.177	1.782	1.695	0.277	3.561	1.270	9.680	2.270	1.928	1.859	0.333	-0.010

Note: SD stands for Standard Deviation, measuring data dispersion around the mean. Prices are in \$/MMBTU. The first subsample includes data from January 1, 2016, to September 30, 2021, while the second subsample includes data from October 1, 2021, to November 1, 2022.

Table C.2.: Time series properties of the data

Variable	Subsample	Log level			First difference of log level		
		ADF	PP	KPSS	ADF	PP	KPSS
EAX	First	-1.093	-0.552	1.413 ^a	-6.390 ^a	-29.664 ^a	0.066
	Second	-2.400	-2.645	0.315 ^a	-11.425 ^a	-14.516 ^a	0.043
TTF	First	-0.192	0.879	1.494 ^a	-4.860 ^a	-38.976 ^a	0.129
	Second	-2.276	-2.140	0.239 ^a	-6.544 ^a	-15.663 ^a	0.067
HH	First	-1.587	-1.551	1.355 ^a	-22.433 ^a	-40.623 ^a	0.056
	Second	-2.222	-2.140	0.408 ^a	-17.781 ^a	-17.810 ^a	0.119

Note: The lag selection for ADF and KPSS tests is based on Akaike Information Criteria (AIC). The test equations are estimated, including an intercept and trend for the variables in levels, whereas they include only an intercept for the first differences. ^a represents the 1% significance level. The three series are expressed in logarithms. The Critical values are obtained from MacKinnon (2010). The dataset is split based on the date October 1, 2021: data before this date is labeled “First,” and data from this date onwards is labeled “Second.” The full sample period covers January 1, 2016, to November 1, 2022.

D. Supplementary Material for Chapter 5

D.1. Additional data details

Table D.1 presents descriptive statistics for the natural gas price data. The mean prices of the gas benchmarks are relatively close, with THE having the highest mean price and NBP the lowest. The standard deviations reveal significant volatility across all series, with THE exhibiting the highest volatility and NBP the lowest. Results of the Augmented Dickey-Fuller (ADF) unit root test indicate that none of the series is stationary. The minimum and maximum values show that TTF has the broadest price range, while ZTP has the narrowest.

Table D.1.: Descriptive statistics for NWE gas benchmarks

	TTF	THE	NBP	ZTP
Mean	47.590	47.948	39.063	43.285
SD	49.909	50.006	35.444	41.148
Minimum	3.100	3.670	3.251	2.904
Maximum	330	315.130	227.796	249.116
Skewness	2.013 ^a (0.000)	1.981 ^a (0.000)	1.828 ^a (0.000)	1.701 ^a (0.000)
kurtosis	7.612 ^a (0.000)	7.347 ^a (0.000)	6.981 ^a (0.000)	6.197 ^a (0.000)
JB	2031.977 ^a (0.000)	1874.907 ^a (0.000)	1583.369 ^a (0.000)	1181.495 ^a (0.000)
ADF	-2.365	-2.380	-3.140	-2.605

Note: The Mean represents the average value of the four gas benchmarks in levels (Euro/MWh). The other descriptive statistics are based on the return series of these price series. Skewness and Kurtosis are based on the tests by D'Agostino (1970) and Anscombe and Glynn (1983), respectively. JB refers to the Jarque-Bera normality test (Jarque & Bera, 1980). ADF is the Augmented Dickey-Fuller unit root test. ^a denotes significance at the one percent level, with values in parentheses representing p-values.

D.2. Additional results

Averaged return connectedness measures

Table D.2 presents the averaged connectedness measures among the four return series throughout the sample period. Specifically, the table provides the overall R^2 decomposed measures, with the values in parentheses specifying contemporaneous and lagged R^2 decomposed measures, respectively. The ‘FROM’ column represents the total directional connectedness ‘from’ other variables in the system to the specific variable, measuring the extent to which a variable is influenced by shocks from all other variables. Similarly, the ‘TO’ row represents the total directional connectedness to other variables from the specific variables, indicating the influence of one benchmark on the rest of the variables in the system. The ‘NET’ row represents net connectedness, calculated as the difference between ‘TO’ and ‘FROM’ for each variable. Therefore, positive NET values indicate that the variable is a net transmitter of shocks (i.e., it influences other variables more than it is influenced), whereas negative NET values indicate that the variable is a net receiver of shocks (i.e., it is influenced more by other variables than it influences them). Finally, the ‘TCI’ value at the bottom of the last column represents the total connectedness in this network, with higher values suggesting a higher level of interconnectedness among the variables.

Table D.2.: Averaged connectedness of return series

	TTF	THE	ZTP	NBP	FROM
TTF	2.17 [0.00, 2.17]	36.72 [35.63, 1.09]	27.25 [26.24, 1.01]	18.26 [17.44, 0.82]	82.23 [79.32, 2.91]
THE	36.99 [34.83, 2.16]	2.21 [0.00, 2.21]	25.20 [23.91, 1.30]	18.24 [17.02, 1.22]	80.44 [75.75, 4.68]
ZTP	27.35 [26.35, 1.00]	24.92 [24.13, 0.79]	1.10 [0.00, 1.10]	20.91 [20.21, 0.71]	73.18 [70.69, 2.50]
NBP	18.38 [17.65, 0.72]	17.95 [17.37, 0.58]	21.68 [20.79, 0.89]	1.76 [0.00, 1.76]	58.00 [55.81, 2.19]
TO	82.73 [78.84, 3.89]	79.58 [77.13, 2.45]	74.13 [70.93, 3.20]	57.41 [54.66, 2.75]	TCI [TCI ^c , TCI ^l]
NET	0.50 [-0.48, 0.97]	-0.85 [1.38, -2.23]	0.95 [0.25, 0.70]	-0.59 [-1.15, 0.56]	73.46 [70.39, 3.07]

Notes: R^2 decomposed measures are based on a 200-day rolling-window VAR model with a lag length of order one (BIC). Values in parentheses represent contemporaneous and lagged effects, respectively.

The results reveal that the TCI is 73.46%, indicating that, on average, 73.90% of the variance in each gas benchmark’s returns can be explained by changes in the returns of other benchmarks within the network. A decomposition of contemporaneous and lagged components shows that contemporaneous interactions are the dominant factor, contributing 70.39%, while lagged interactions account for only 3.07%. This decomposition highlights that immediate temporal dynamics are

the primary drivers of overall connectedness, while the impact of lagged effects is minor. Similarly, all contemporaneous ‘FROM’ and ‘TO’ connectedness measures are substantially higher than their lagged counterparts. Also, the ‘FROM’ column reveals that NBP has the lowest value at 58.00%, implying it receives the least amount of shocks from other benchmarks. Likewise, the ‘TO’ row indicates that NBP also has the lowest spillover contribution to others at 57.41%, underscoring its relatively isolated position within the network of benchmarks. Lastly, the ‘NET’ row shows that both THE and NBP are net receivers of return spillovers, with net connectedness values of -0.85% and -0.59%, respectively. This contrasts with TTF and ZTP, which exhibit positive net connectedness, indicating that these benchmarks are net transmitters of shocks.

Averaged volatility connectedness measures

Similar to the previous subsection, Table D.3 presents averaged connectedness measures for volatility. The TCI is 53.62%, implying that the explanatory power of the TCI accounts for 53.62% of the variance in each gas benchmark’s volatility within the network. By decomposing this metric into its contemporaneous and lagged components, we observe that about 50.38% is caused by contemporaneous dynamics while only 3.24% is related to lagged interdependencies. The results also show that NBP exhibits the highest own volatility contribution at 2.38%, indicating that a significant portion of its volatility is self-explained. In contrast, the own volatility contributions for TTF and THE are much smaller (0.78% and 0.87%, respectively), indicating that these benchmarks’ volatility is largely influenced by spillovers from each other. Analyzing the ‘FROM’ column and ‘TO’ row shows that NBP has the lowest values at 41.19% and 40.13%, respectively, highlighting its relatively isolated position within the network of benchmarks. Lastly, the ‘NET’ row shows that NBP is a net receiver of volatility spillovers, with a net connectedness value of -1.07%. This negative value contrasts with TTF, ZTP, and THE, which either exhibit positive net connectedness or are closer to zero, indicating that these benchmarks are net transmitters or more balanced in their spillover dynamics. Overall, from a static perspective, the analysis underscores NBP’s unique position as a relatively self-contained benchmark with minimal influence on, and from, the other gas benchmarks.

This section presents robustness checks to validate the baseline analysis. Specifically, three exercises are performed: first, using different rolling window sizes; second, replacing Pearson correlation coefficients with Spearman correlation coefficients; and finally, employing the range volatility measure of Parkinson (1980) as a proxy for volatility, instead of using absolute returns.

Robustness of connectedness measures to rolling window sizes

This subsection assesses the sensitivity of the connectedness measures to varying rolling window sizes. Specifically, we investigate the time-varying total return and

Table D.3.: Averaged connectedness of volatility series

	TTF	THE	ZTP	NBP	FROM
TTF	0.78 [0.00, 0.78]	32.78 [31.73, 1.05]	17.91 [16.67, 1.25]	12.95 [12.13, 0.82]	63.64 [60.53, 3.11]
THE	32.88 [31.83, 1.06]	0.87 [0.00, 0.87]	15.71 [14.33, 1.38]	13.82 [13.10, 0.71]	62.41 [59.26, 3.15]
ZTP	18.19 [17.03, 1.16]	15.67 [14.40, 1.27]	2.25 [0.00, 2.25]	13.36 [12.09, 1.27]	47.22 [43.52, 3.70]
NBP	13.20 [12.36, 0.84]	14.34 [13.51, 0.82]	13.66 [12.33, 1.33]	2.38 [0.00, 2.38]	41.19 [38.20, 2.99]
TO	64.27 [61.22, 3.05]	62.79 [59.64, 3.15]	47.29 [43.34, 3.95]	40.13 [37.33, 2.80]	TCI [TCI ^c , TCI ^l]
NET	0.63 [0.68, -0.06]	0.37 [0.37, 0.00]	0.07 [-0.18, 0.25]	-1.07 [-0.87, -0.19]	53.62 [50.38, 3.24]

Notes: R^2 decomposed measures are based on a 200-day rolling-window VAR model with a lag length of order one (BIC). Values in parentheses represent contemporaneous and lagged effects, respectively.

volatility spillover indices using the R^2 decomposed connectedness approach for three different rolling window lengths (150, 200, and 250 days), with 200 days being the window size used in the baseline analysis. Figures D.1(a) and D.1(b) indicate that the estimates of the time-varying total spillover indices remain both qualitatively and quantitatively stable across different window sizes, reinforcing the validity of our initial empirical results.

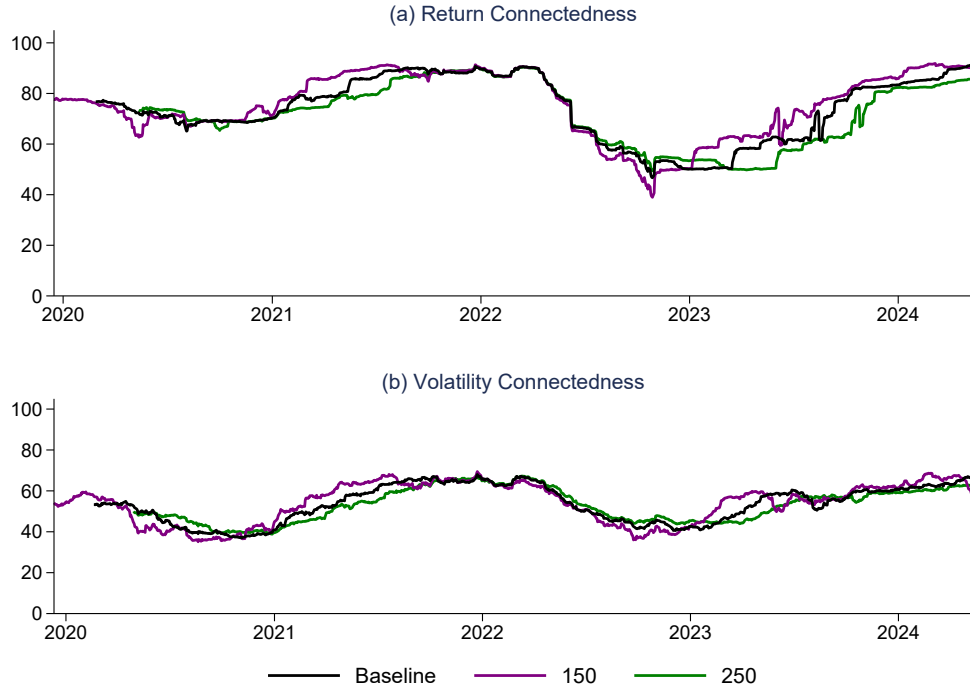


Figure D.1.: Connectedness with different rolling window sizes (150, 200, 250) for return and volatility series

Notes: R^2 decomposed measures are based on a 150, 200, and 250-day rolling-window VAR model with a lag length of order one (BIC).

Robustness of connectedness measures to correlation coefficients

This subsection replaces the Pearson correlation coefficients with Spearman correlation coefficients. The Spearman correlation is a non-parametric measure, less sensitive to outliers. The results, presented in Figures D.2(a) for return series and D.2(b) for volatility series, indicate that the findings are quantitatively similar to the baseline results, demonstrating robustness to the choice of correlation measure.

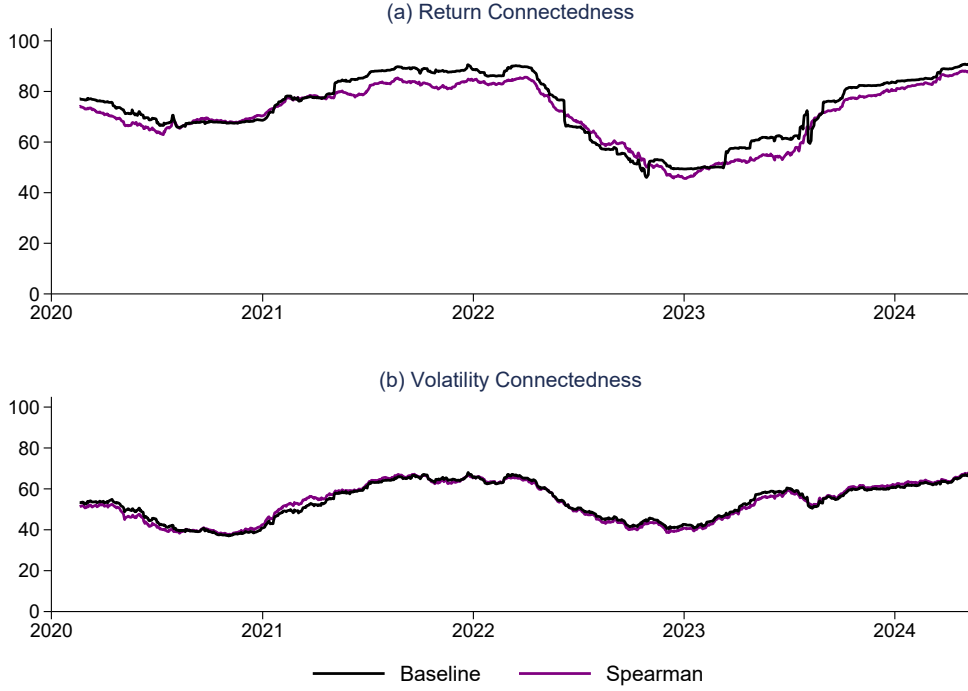


Figure D.2.: Connectedness using Spearman correlation coefficient for return and volatility series

Notes: R^2 decomposed measures are based on a 200-day rolling-window VAR model with a lag length of order one (BIC).

Robustness of volatility connectedness to a different volatility measure

This subsection analyzes volatility connectedness using the range volatility measure as proposed by Parkinson (1980). Following Alizadeh et al. (2002) and Diebold and Yilmaz (2012), weekly range volatility is calculated by:

$$Volatility_{Range} = 0.361 \times [\ln(P_t^{\max}) - \ln(P_t^{\min})]^2 \quad (D.1)$$

where P_t^{\max} is the maximum price in week t , and P_t^{\min} is the minimum price.

The intuition behind this approach is to examine the robustness of the conclusion regarding the dominance of contemporaneous effects on volatility connectedness, as found in the baseline analysis that uses absolute returns as a proxy for volatility. Additionally, this approach allows us to assess the robustness of the overall patterns of volatility connectedness during the examined shocks.

The results of the overall volatility index and its decomposition are presented in Figure D.3, while the results of the directional connectedness are presented in Figure D.4. Overall, the conclusions from this analysis, using this realized volatility measure, are consistent with those obtained in the baseline analysis of volatility connectedness.

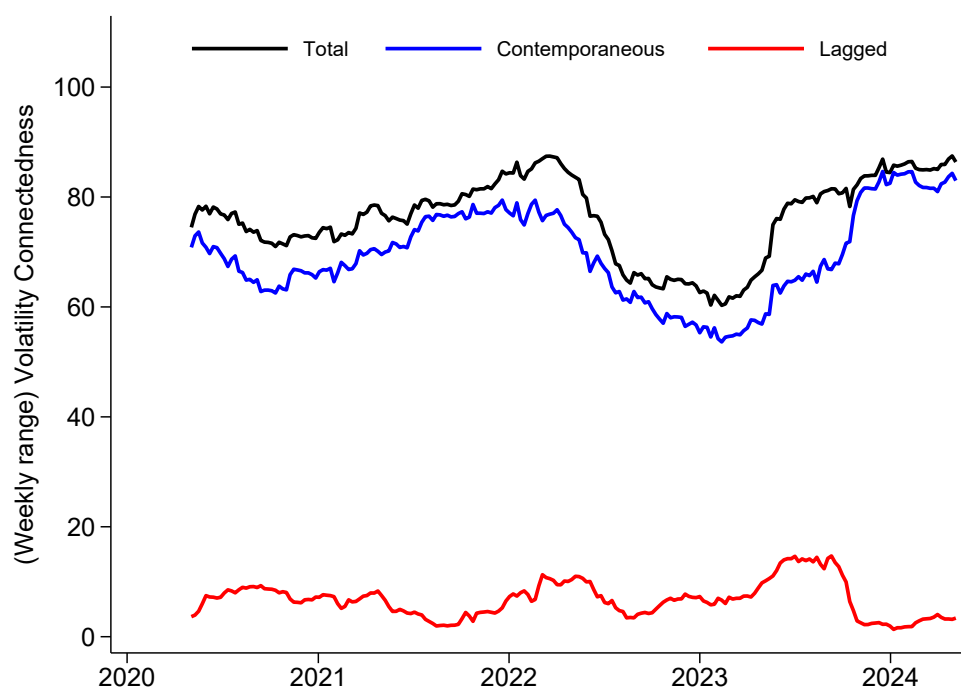


Figure D.3.: Dynamic total connectedness of realized weekly volatility series
 Notes: R^2 decomposed measures are based on a 52-week (one year) rolling-window rolling-window VAR model with a lag length of order one.

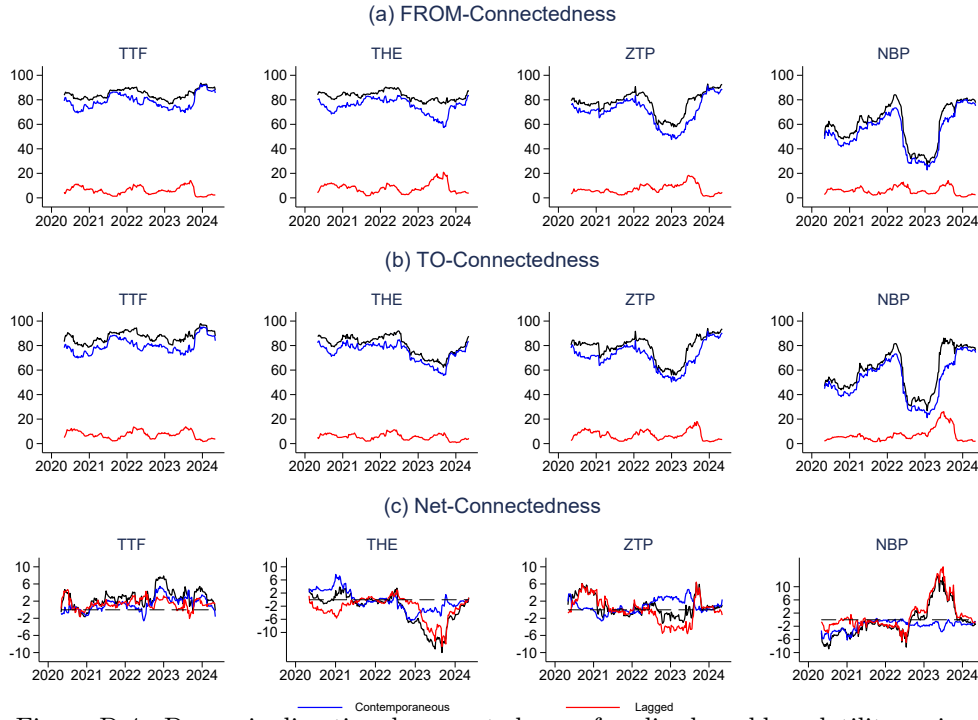


Figure D.4.: Dynamic directional connectedness of realized weekly volatility series
Notes: R^2 decomposed measures are based on a 52-week (one year) rolling-window rolling-window VAR model with a lag length of order one.

Connectedness analysis of NWE gas benchmarks using futures prices

The ‘From’ and ‘To’ directional connectedness for return and volatility series for futures prices are presented in Figures D.5 and D.7 respectively. The results indicate that spot and futures prices exhibit similar connectedness levels for these indices, except for NBP, where the ‘From’ and ‘To’ connectedness values for futures are relatively higher and more stable compared to those of spot prices throughout the entire period. This seems plausible, as our previous analyses show that the decoupling of NBP drives the low connectedness of spot prices across NWE. The net total directional connectedness analysis (Figures D.5(c) for return series) shows that for THE and TTF, spot and futures prices generally share the same connectedness direction, except from the second half of 2022 to the first half of 2023. During this period, TTF futures are positive (transmitting shocks), while spot prices are negative (receiving shocks). Conversely, for THE, spot prices are positive while futures are negative. This highlights the different roles and reactions of futures and spot markets for these two benchmarks during stress periods. For ZTP, spot and futures net connectedness align except from the second half of 2021 to the second half of 2022. NBP also shows consistent net connectedness direction for both spot and futures prices except during the second half of 2020 and the first half of 2023. On the other hand, the net total directional connectedness analysis (Figures D.7(c) for volatility series) shows that net connectedness estimated with

spot and futures prices has the same sign throughout the entire investigated period. This suggests that both spot and futures markets for these benchmarks respond to and transmit volatility, driven by market uncertainty and risk, in the same manner through both stable and volatile periods.

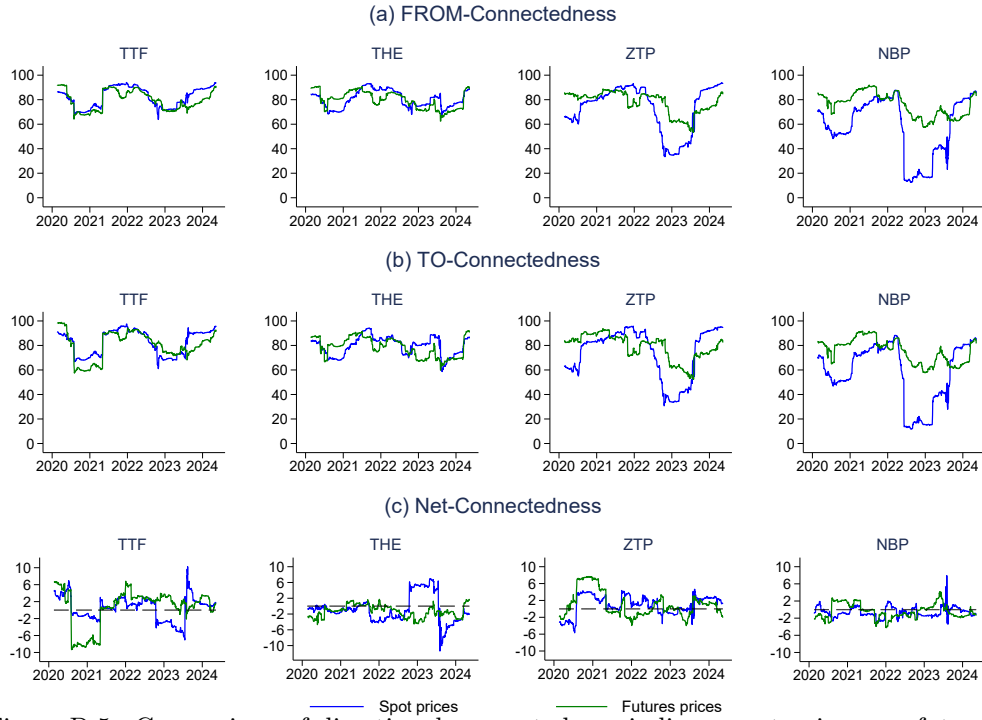


Figure D.5.: Comparison of directional connectedness indices: spot prices vs. futures prices

Notes: R^2 decomposed measures are based on a 200-day rolling-window rolling-window VAR model with a lag length of order one. These lines represent the total connectedness index. The contemporaneous and lagged connectedness are removed to facilitate comparison, but they show the same pattern as observed in the baseline results.

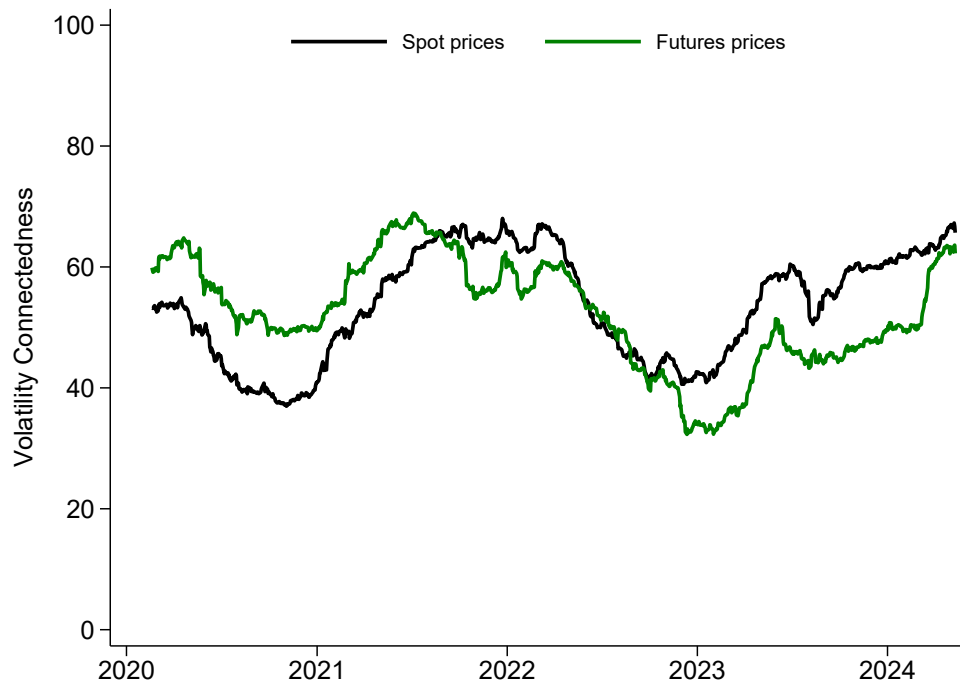


Figure D.6.: Dynamic total connectedness of volatility series using futures prices

Notes: R^2 decomposed measures are based on a 200-day rolling-window rolling-window VAR model with a lag length of order one. These lines represent the overall connectedness index. The contemporaneous and lagged connectedness are removed to facilitate comparison, but they show the same pattern as observed in the baseline results.

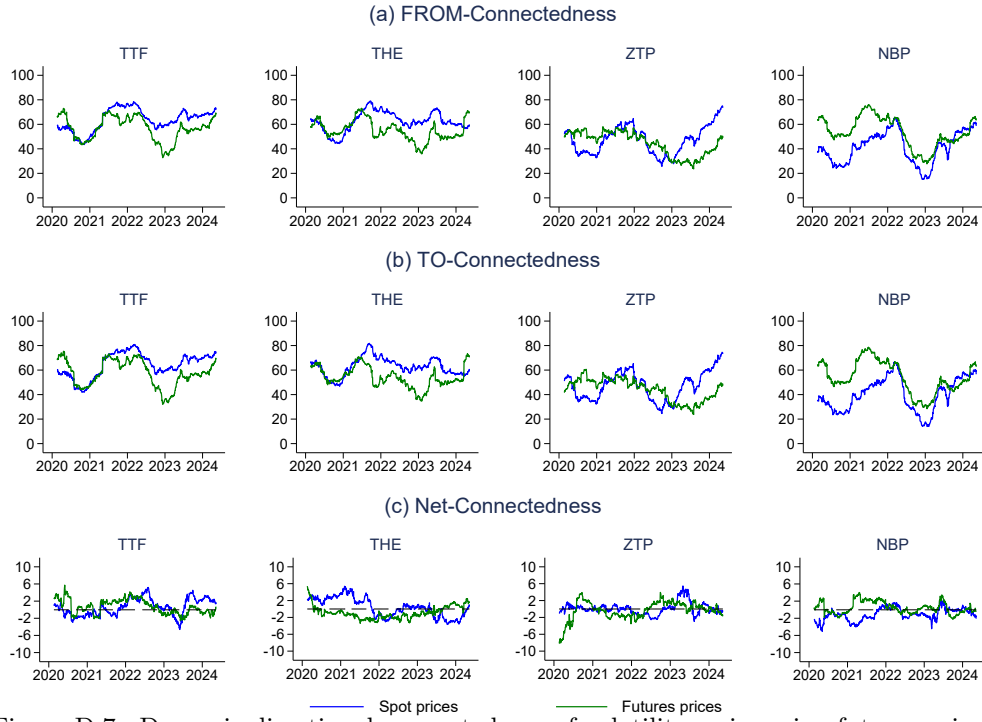


Figure D.7.: Dynamic directional connectedness of volatility series using futures prices

Notes: R^2 decomposed measures are based on a 200-day rolling-window rolling-window VAR model with a lag length of order one. These lines represent the total connectedness index. The contemporaneous and lagged connectedness are removed to facilitate comparison, but they show the same pattern as observed in the baseline results.

The relationship between infrastructure congestion and gas market volatility connectedness in NWE

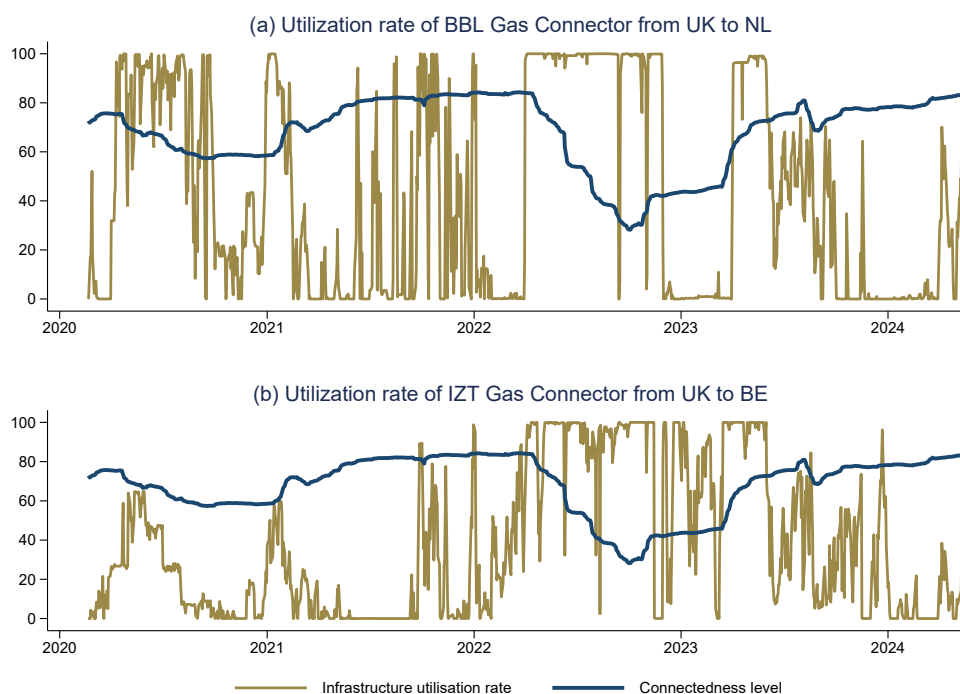


Figure D.8.: volatility connectedness level and utilization rate of BBL and IZT gas pipelines

Notes: Data on the utilization rates are obtained from the ENTSOG Transparency Platform. The solid line represents the volatility connectedness between the NWE gas benchmarks, as analyzed in Subsection 5.5.2. Values on the vertical axis are expressed as percentages (%). BBL refers to the Balgzand-Bacton Line pipeline, and IZT refers to the Interconnector Zeebrugge Terminal pipeline. Country abbreviations: UK (United Kingdom), NL (Netherlands), and BE (Belgium).

Bibliography

- Abosedra, S., & Baghestani, H. (2004). On the predictive accuracy of crude oil futures prices. *Energy Policy*, 32(12), 1389–1393.
- Acaravci, A., Ozturk, I., & Kandir, S. Y. (2012). Natural gas prices and stock prices: Evidence from eu-15 countries. *Economic Modelling*, 29(5), 1646–1654.
- ACER. (2023a). *Addressing congestion in north-west european gas markets*. Retrieved from https://acer.europa.eu/sites/default/files/documents/Publications/ACER_Special_Report_Congestion2023.pdf (Accessed: 2024-06-12)
- ACER. (2023b). *European gas market trends and price drivers - 2023 market monitoring report*. Retrieved from https://www.acer.europa.eu/sites/default/files/documents/Publications/ACER_MMR_2023_Gas_market_trends_price_drivers.pdf (Accessed: 2024-09-22)
- Aitken, C., & Ersoy, E. (2023). War in ukraine: The options for europe’s energy supply. *The World Economy*, 46(4), 887–896.
- Alexander, C., & Wyeth, J. (1994). Cointegration and market integration: An application to the indonesian rice market. *The Journal of Development Studies*, 30(2), 303–334.
- Alexeev, M., & Chih, Y.-Y. (2021). Energy price shocks and economic growth in the us: A state-level analysis. *Energy Economics*, 98, 105242.
- Alizadeh, S., Brandt, M. W., & Diebold, F. X. (2002). Range-based estimation of stochastic volatility models. *The Journal of Finance*, 57(3), 1047–1091.
- Alquist, R., & Kilian, L. (2010). What do we learn from the price of crude oil futures? *Journal of Applied Econometrics*, 25(4), 539–573.
- Alquist, R., Kilian, L., & Vigfusson, R. (2013). Forecasting the price of oil. In G. Elliott, C. Granger, & A. Timmermann (Eds.), *Handbook of economic forecasting* (1st ed., Vol. 2, pp. 427–507). Elsevier.

Bibliography

- Al-Sahlawi, M. A. (1989). Research reports the demand for natural gas: A survey of price and income elasticities. *The Energy Journal*, 10(1), 77–90.
- Amemiya, T., & Wu, R. Y. (1972). The effect of aggregation on prediction in the autoregressive model. *Journal of the American Statistical Association*, 67(339), 628–632.
- Anderson, S. P., & Ginsburgh, V. A. (1999). International pricing with costly consumer arbitrage. *Review of International Economics*, 7(1), 126–139.
- Anscombe, F. J., & Glynn, W. J. (1983). Distribution of the kurtosis statistic b₂ for normal samples. *Biometrika*, 70(1), 227–234.
- Arora, V. (2014). Estimates of the price elasticities of natural gas supply and demand in the united states.
- Arora, V., & Lieskovsky, J. (2014). Natural gas and us economic activity. *The Energy Journal*, 35(3).
- Asche, F., Osmundsen, P., & Tveterås, R. (2002). European market integration for gas? volume flexibility and political risk. *Energy Economics*, 24(3), 249–265.
- Bachmeier, L., & Griffin, J. (2006). Testing for market integration: crude oil, coal, and natural gas. *Energy Journal*, 27, 55–71.
- Balli, F., Balli, H. O., Dang, T. H. N., & Gabauer, D. (2023). Contemporaneous and lagged r² decomposed connectedness approach: New evidence from the energy futures market. *Finance Research Letters*, 57, 104168.
- Bank of Japan. (2024, January). *Outlook for economic activity and prices*. Retrieved from <https://www.boj.or.jp/en/mopo/outlook/gor2401b.pdf> ()
- Barnes, R., & Bosworth, R. (2015). Lng is linking regional natural gas markets: Evidence from the gravity model. *Energy Economics*, 47, 11–17.
- Barret, C. (1992). Us natural gas market: a disequilibrium approach. In *Coping with the energy future: markets and regulations. volume 2*.
- Baruník, J., & Křehlík, T. (2018). Measuring the frequency dynamics of financial connectedness and systemic risk. *Journal of Financial Econometrics*, 16(2), 271–296.

- Bastianin, A., Galeotti, M., & Polo, M. (2019). Convergence of european natural gas prices. *Energy Economics*, 81, 793–811.
- Baumeister, C. (2023). *Pandemic, war, inflation: Oil markets at a crossroads?* (Tech. Rep.). National Bureau of Economic Research.
- Baumeister, C., Guérin, P., & Kilian, L. (2015). Do high-frequency financial data help forecast oil prices? the midas touch at work. *International Journal of Forecasting*, 31(2), 238–252.
- Baumeister, C., & Hamilton, J. D. (2015). Sign restrictions, structural vector autoregressions, and useful prior information. *Econometrica*, 83(5), 1963–1999.
- Baumeister, C., & Hamilton, J. D. (2018). Inference in structural vector autoregressions when the identifying assumptions are not fully believed: Re-evaluating the role of monetary policy in economic fluctuations. *Journal of Monetary Economics*, 100, 48–65.
- Baumeister, C., & Hamilton, J. D. (2019). Structural interpretation of vector autoregressions with incomplete identification: Revisiting the role of oil supply and demand shocks. *American Economic Review*, 109(5), 1873–1910.
- Baumeister, C., & Hamilton, J. D. (2024). Uncovering disaggregated oil market dynamics: A full-information approach to granular instrumental variables.
- Baumeister, C., & Kilian, L. (2012). Real-time forecasts of the real price of oil. *Journal of Business & Economic Statistics*, 30(2), 326–336.
- Baumeister, C., & Kilian, L. (2014). What central bankers need to know about forecasting oil prices. *International Economic Review*, 55(3), 869–889.
- Baumeister, C., & Kilian, L. (2015). Forecasting the real price of oil in a changing world: A forecast combination approach. *Journal of Business & Economic Statistics*, 33(3), 338–351.
- Baumeister, C., Kilian, L., & Lee, T. K. (2017). Inside the crystal ball: New approaches to predicting the gasoline price at the pump. *Journal of Applied Econometrics*, 32(2), 275–295.
- Baumeister, C., & Peersman, G. (2013). The role of time-varying price elasticities in accounting for volatility changes in the crude oil market. *Journal of applied econometrics*, 28(7), 1087–1109.

Bibliography

- Bazilian, M. D., Clough, G., Akamboe, J., Malone, A., Amoah, M., Lange, I., . . . Copan, W. (2023). *The state of critical minerals report 2023* (Tech. Rep.). The Payne Institute for Public Policy.
- Beetsma, R., Giuliadori, M., & Klaassen, F. (2009). Temporal aggregation and svar identification, with an application to fiscal policy. *Economics Letters*, 105(3), 253–255.
- Bernstein, P., Tuladhar, S. D., & Yuan, M. (2016). Economics of us natural gas exports: Should regulators limit us lng exports? *Energy Economics*, 60, 427–437.
- Bernstein, R., & Madlener, R. (2011). Residential natural gas demand elasticities in oecd countries: an ardl bounds testing approach.
- Bianco, V., Scarpa, F., & Tagliafico, L. A. (2015). Current situation and future perspectives of european natural gas sector. *Frontiers in Energy*, 9, 1–6.
- Bohl, M. T., Irwin, S. H., Pütz, A., & Sulewski, C. (2023). The impact of financialization on the efficiency of commodity futures markets. *Journal of Commodity Markets*, 31, 100330.
- Bork, L., Kaltwasser, P. R., & Sercu, P. (2022). Aggregation bias in tests of the commodity currency hypothesis. *Journal of Banking & Finance*, 135, 106392.
- Bowman, C., & Husain, A. M. (2006). Forecasting commodity prices: futures versus judgment. In A. Sarris & D. Hallam (Eds.), *Agricultural commodity markets and trade: New approaches to analyzing market structure and instability* (p. 61-82). Edward Elgar Publishing.
- Braun, R. (2023). The importance of supply and demand for oil prices: Evidence from non-gaussianity. *Quantitative Economics*, 14(4), 1163–1198.
- Brennan, M. J. (1976). The supply of storage. *The economics of futures trading*, 100–107.
- Broadstock, D. C., Li, R., & Wang, L. (2020). Integration reforms in the european natural gas market: A rolling-window spillover analysis. *Energy Economics*, 92, 104939.
- Brons, M., Kalantzis, F., & Vergano, L. (2019). *Market functioning and market integration in EU network industries: Telecommunications, energy and transport* (Tech. Rep.). Directorate General Economic and Financial Affairs (DG ECFIN), European Commission.

- Brown, S. P., & Yttcel, M. K. (2008). What drives natural gas prices? *The Energy Journal*, 29(2), 1–16.
- Burke, P. J., & Yang, H. (2016). The price and income elasticities of natural gas demand: International evidence. *Energy Economics*, 59, 466–474.
- Büyük şahin, B., Lee, T. K., Moser, J. T., & Robe, M. A. (2013). Physical markets, paper markets and the wti-brent spread. *The Energy Journal*, 34(3), 129–152.
- Caldara, D., & Iacoviello, M. (2022). Measuring geopolitical risk. *American Economic Review*, 112(4), 1194–1225.
- Carriero, A., Clark, T. E., Marcellino, M., & Mertens, E. (2022). Addressing covid-19 outliers in bvars with stochastic volatility. *Review of Economics and Statistics*, 1–38.
- Cavalcanti, T., & Jalles, J. T. (2013). Macroeconomic effects of oil price shocks in brazil and in the united states. *Applied Energy*, 104, 475–486.
- Chan, K.-S. (1993). Consistency and limiting distribution of the least squares estimator of a threshold autoregressive model. *The annals of statistics*, 520–533.
- Chang, C.-L., Chen, L.-H., Hammoudeh, S., & McAleer, M. (2012). Asymmetric adjustments in the ethanol and grains markets. *Energy economics*, 34(6), 1990–2002.
- Chen, Y., Wang, C., & Zhu, Z. (2022). Toward the integration of european gas futures market under covid-19 shock: A quantile connectedness approach. *Energy Economics*, 114, 106288.
- Chernenko, S., Schwarz, K., & Wright, J. H. (2004). The information content of forward and futures prices: Market expectations and the price of risk. *FRB International Finance Discussion Papers*(808).
- Chiappini, R., Jégourel, Y., & Raymond, P. (2019). Towards a worldwide integrated market? new evidence on the dynamics of us, european and asian natural gas prices. *Energy Economics*, 81, 545–565.
- Chinn, M. D., & Coibion, O. (2014). The predictive content of commodity futures. *Journal of Futures Markets*, 34(7), 607–636.

Bibliography

- Chinn, M. D., LeBlanc, M., & Coibion, O. (2005). The predictive content of energy futures: an update on petroleum, natural gas, heating oil and gasoline. *NBER Working Paper No. 11033*.
- Chow, G. C. (1960). Tests of equality between sets of coefficients in two linear regressions. *Econometrica: Journal of the Econometric Society*, 591–605.
- Chu, P. K., Hoff, K., Molnár, P., & Olsvik, M. (2022). Crude oil: Does the futures price predict the spot price? *Research in International Business and Finance*, 60(101611), 1–7.
- Clarke, J. A., & Mirza, S. (2006). A comparison of some common methods for detecting granger noncausality. *Journal of Statistical Computation and Simulation*, 76(3), 207–231.
- Conlon, T., Cotter, J., & Eyiah-Donkor, E. (2022). The illusion of oil return predictability: The choice of data matters! *Journal of Banking & Finance*, 134, 106331.
- Council of the European Union. (2022). *Council adopts regulation on gas storage*. Retrieved from <https://www.consilium.europa.eu/en/press/press-releases/2022/06/27/council-adopts-regulation-gas-storage/#:~:text=The%20regulation%20provides%20that%20underground,before%20the%20following%20winter%20periods>. (Accessed: 2024-06-13)
- Cournot, A. A. (1838). *Recherches sur les principes mathématiques de la théorie des richesses*. L. Hachette.
- Cunado, J., & De Gracia, F. P. (2005). Oil prices, economic activity and inflation: evidence for some asian countries. *The Quarterly Review of Economics and Finance*, 45(1), 65–83.
- D’Agostino, R. B. (1970). Transformation to normality of the null distribution of g_1 . *Biometrika*, 679–681.
- Demir, O., & Demir, O. (2020). Natural gas market liberalisation in the context of the eu. *Liberalisation of Natural Gas Markets: Potential and Challenges of Integrating Turkey into the EU Market*, 63–102.
- Diebold, F. X., & Mariano, R. S. (1995). Comparing predictive accuracy. *Journal of Business & Economic Statistics*, 13(3), 253–263.
- Diebold, F. X., & Yilmaz, K. (2009). Measuring financial asset return and volatility spillovers, with application to global equity markets. *The Economic Journal*, 119(534), 158–171.

- Diebold, F. X., & Yilmaz, K. (2012). Better to give than to receive: Predictive directional measurement of volatility spillovers. *International Journal of forecasting*, 28(1), 57–66.
- Diebold, F. X., & Yilmaz, K. (2014). On the network topology of variance decompositions: Measuring the connectedness of financial firms. *Journal of econometrics*, 182(1), 119–134.
- Ding, Z., Granger, C. W., & Engle, R. F. (1993). A long memory property of stock market returns and a new model. *Journal of empirical finance*, 1(1), 83–106.
- Drachal, K. (2016). Forecasting spot oil price in a dynamic model averaging framework—have the determinants changed over time? *Energy Economics*, 60, 35–46.
- Duarte, A. M., Gaglianone, W. P., de Carvalho Guillén, O. T., & Issler, J. V. (2021). Commodity prices and global economic activity: a derived-demand approach. *Energy Economics*, 96, 105120.
- Dukhanina, E., & Massol, O. (2018). Spatial integration of natural gas markets: A literature review. *Current Sustainable/Renewable Energy Reports*, 5(2), 129–137.
- Ebinger, C., Massy, K., & Avasarala, G. (2012). Liquid markets: Assessing the case for us exports of liquefied natural gas. *Policy*.
- ECB. (2024, March). *Eurosystem staff macroeconomic projections for the euro area*. Retrieved from https://www.ecb.europa.eu/pub/pdf/other/ecb_projections202403_ecbstaff~f2f2d34d5a.en.pdf (European Central Bank (ECB))
- Economides, M. J., & Wood, D. A. (2009). The state of natural gas. *Journal of Natural Gas Science and Engineering*, 1(1-2), 1–13.
- EEX. (2023). *European energy exchange newsroom*. Retrieved from https://www.eex.com/en/newsroom/detail?tx_news_pi1%5Baction%5D=detail&tx_news_pi1%5Bcontroller%5D=News&tx_news_pi1%5Bnews%5D=7321&cHash=8601dc6293eaae322feaea70e61ef96e (Accessed: 2023-06-17)
- Egging, R., & Holz, F. (2016). Risks in global natural gas markets: investment, hedging and trade. *Energy Policy*, 94, 468–479.

Bibliography

- EIA, . (2023a). AEO2023 Issues in Focus: Effects of Liquefied Natural Gas Exports on the U.S. Natural Gas Market. Retrieved from https://www.eia.gov/outlooks/aeo/IIF_LNG/pdf/LNG_Issue_in_Focus.pdf (Accessed: 2024-02-11)
- EIA, . (2023b). US Energy Information Administration (EIA): 2023 Edition US annual energy outlook report (AEO2023). Retrieved from https://www.eia.gov/outlooks/aeo/pdf/AEO2023_Narrative.pdf (Accessed: 2024-04-10)
- EIA. (2024, September). *Appendix B: Metric and Thermal Conversion Factors*. Natural Gas Monthly, September 2024. (Available: https://www.eia.gov/naturalgas/monthly/pdf/appendix_b.pdf)
- Ellwanger, R., & Snudden, S. (2023a). Forecasts of the real price of oil revisited: Do they beat the random walk? *Journal of Banking and Finance*, 154, 1–8.
- Ellwanger, R., & Snudden, S. (2023b). Futures prices are useful predictors of the spot price of crude oil. *The Energy Journal*, 44(4), 65–82.
- Ellwanger, R., Snudden, S., & Arango-Castillo, L. (2023). Seize the last day: Period-end-price sampling for forecasts of temporally aggregated data. *LCERPA Working Paper*, 2023-6.
- Enders, W., & Siklos, P. L. (2001). Cointegration and threshold adjustment. *Journal of Business & Economic Statistics*, 19(2), 166–176.
- Engle, R. F., & Granger, C. W. (1987). Co-integration and error correction: representation, estimation, and testing. *Econometrica: journal of the Econometric Society*, 251–276.
- Enke, S. (1951). Equilibrium among spatially separated markets: Solution by electric analogue. *Econometrica: Journal of the Econometric Society*, 40–47.
- ENTSOG. (2023). *Transparency platform*. The European Network of Transmission System Operators for Gas (ENTSOG). Retrieved from <https://transparency.entsog.eu/#/map>
- Erdős, P., & Ormos, M. (2012). Natural gas prices on three continents. *Energies*, 5(10), 4040–4056.
- European Central Bank. (2024, September). *Eurosystem staff macroeconomic projections for the euro area*. Retrieved from <https://www.ecb.europa.eu/>

pub/pdf/other/ecb.projections202409_ecbstaff~9c88364c57.en.pdf
()

- Eurostat. (2023). *Natural gas consumption statistics*. Retrieved from https://ec.europa.eu/eurostat/databrowser/view/nrg_cb_gas/default/table?lang=en&category=nrg.nrg_quant.nrg_quanta.nrg_cb (Accessed: 2023-06-09)
- EVA, . (2023). Impact Analysis of U.S. Natural Gas Exports on Domestic Natural Gas Pricing. Retrieved from <https://www.api.org/~media/files/news/2024/03/18/api-eva-lng-price-full-report> (Accessed: 2024-04-20)
- Fackler, P. L., & Goodwin, B. K. (2001). Spatial price analysis. *Handbook of agricultural economics*, 1, 971–1024.
- Fama, E. F., & French, K. R. (1987). Commodity futures prices: Some evidence on forecast power, premiums, and the theory of storage. *The Journal of Business*, 60(1), 55–73.
- Farag, M. (2024). *Revisiting the dynamics and elasticities of the us natural gas market* (Tech. Rep.). EWI Working Paper.
- Farag, M., Jeddi, S., & Kopp, J. H. (2023). *Global natural gas market integration in the face of shocks: Evidence from the dynamics of european, asian, and us gas futures prices* (Tech. Rep.). Energiewirtschaftliches Institut an der Universitaet zu Koeln (EWI).
- Farag, M., & Ruhnau, O. (2024). *Decomposing return and volatility connectedness in northwest european gas markets: Evidence from the r2 connectedness approach* (Tech. Rep.). Technical Report. Energiewirtschaftliches Institut an der Universitaet zu
- Farag, M., & Zaki, C. (2021a). *On the determinants of trade in natural gas: A political economy approach* (Tech. Rep.). EWI Working Paper.
- Farag, M., & Zaki, C. (2021b). Price and income elasticities of natural gas demand in egypt: A bound test approach. *Review of Middle East Economics and Finance*, 17(1), 27–55.
- Farag, M., & Zaki, C. (2024). On the economic and political determinants of trade in natural gas. *The World Economy*, 47(2), 806–836.
- Finon, D., & Romano, E. (2009). Electricity market integration: Redistribution effect versus resource reallocation. *Energy Policy*, 37(8), 2977–2985.

Bibliography

- Fleury, K. (2024, 4). *U.s. henry hub natural gas prices in 2023 were the lowest since mid-2020*. U.S. Energy Information Administration. Retrieved from <https://www.eia.gov/todayinenergy/detail.php?id=61183#:~:text=January%20%2C%202024-,U.S.%20Henry%20Hub%20natural%20gas%20prices%20in,the%20lowest%20since%20mid%2D2020&text=The%20U.S.%20benchmark%20Henry%20Hub,to%20data%20from%20Refinitiv%20Eikon>.
- Forsberg, L., & Ghysels, E. (2007). Why do absolute returns predict volatility so well? *Journal of Financial Econometrics*, 5(1), 31–67.
- Fulwood, M., Sharples, J., & Henderson, J. (2022). *Ukraine invasion: What this means for the european gas market*. The Oxford Institute for Energy Studies.
- Funk, C. (2018). Forecasting the real price of oil-time-variation and forecast combination. *Energy Economics*, 76, 288–302.
- Garaffa, R., Szklo, A., Lucena, A. F., & Féres, J. G. (2019). Price adjustments and transaction costs in the european natural gas market. *The Energy Journal*, 40(1), 171–188.
- Gas Infrastructure Europe. (2022). *Aggregated Gas Storage Inventory (AGSI+)*. <https://agsi.gie.eu/data-overview/DE>.
- Gautam, T. K., & Paudel, K. P. (2018). The demand for natural gas in the northeastern united states. *Energy*, 158, 890–898.
- Gelos, G., & Ustyugova, Y. (2017). Inflation responses to commodity price shocks—how and why do countries differ? *Journal of International Money and Finance*, 72, 28–47.
- Geng, J.-B., Ji, Q., & Fan, Y. (2014). A dynamic analysis on global natural gas trade network. *Applied Energy*, 132, 23–33.
- Geng, J.-B., Ji, Q., & Fan, Y. (2016a). How regional natural gas markets have reacted to oil price shocks before and since the shale gas revolution: A multi-scale perspective. *Journal of Natural Gas Science and Engineering*, 36, 734–746.
- Geng, J.-B., Ji, Q., & Fan, Y. (2016b). The impact of the north american shale gas revolution on regional natural gas markets: Evidence from the regime-switching model. *Energy Policy*, 96, 167–178.

- Genizi, A. (1993). Decomposition of r^2 in multiple regression with correlated regressors. *Statistica Sinica*, 407–420.
- GIE. (2024). *Aggregated lng system inventory*. Gas Infrastructure Europe (GIE). Retrieved from <https://alsi.gie.eu/>
- GIIGNL, I. G. o. L. N. G. I. G. (2022). *The lng industry giignl 2022 annual report* (Tech. Rep.). GIIGNL - International Group of Liquefied Natural Gas Importers.
- Golding, G. (2019). *Don't expect u.s. shale producers to respond quickly to geopolitical supply disruption*. (<https://www.dallasfed.org/research/economics/2019/1003>)
- Granger, C. W. (1969). Investigating causal relations by econometric models and cross-spectral methods. *Econometrica: journal of the Econometric Society*, 424–438.
- Growitsch, C., Nepal, R., & Stronzik, M. (2015). Price convergence and information efficiency in german natural gas markets. *German Economic Review*, 16(1), 87–103.
- Gugler, K., Haxhimusa, A., & Liebensteiner, M. (2018). Integration of european electricity markets: Evidence from spot prices. *The Energy Journal*, 39(2_suppl), 41–66.
- Hailemariam, A., & Smyth, R. (2019). What drives volatility in natural gas prices? *Energy Economics*, 80, 731–742.
- Hailemariam, A., Smyth, R., & Zhang, X. (2019). Oil prices and economic policy uncertainty: Evidence from a nonparametric panel data model. *Energy economics*, 83, 40–51.
- Hamilton, J. D., & Wu, J. C. (2014). Risk premia in crude oil futures prices. *Journal of International Money and Finance*, 42, 9–37.
- Hammoudeh, S. M., Ewing, B. T., & Thompson, M. A. (2008). Threshold cointegration analysis of crude oil benchmarks. *The Energy Journal*, 29(4).
- Hanly, J. (2017). Managing energy price risk using futures contracts: A comparative analysis. *The Energy Journal*, 38(3), 93–112.
- He, Y., Wang, S., & Lai, K. K. (2010). Global economic activity and crude oil prices: A cointegration analysis. *Energy Economics*, 32(4), 868–876.

Bibliography

- Heather, P. (2021). *European traded gas hubs: German hubs about to merge* (No. 170). OIES Paper: NG.
- Heather, P. (2022). A series of unfortunate events: Explaining european gas prices in 2021—the role of the traded gas hubs. *Oxford Institute for Energy Studies, March*.
- Heather, P. (2023). *European traded gas hubs: Their continued relevance* (No. 183). OIES Paper: NG.
- Heather, P. (2024). *European traded gas hubs: the markets have rebalanced* (Tech. Rep.). OIES Paper: NG.
- Hinchey, N. (2018). The impact of securing alternative energy sources on russian-european natural gas pricing. *The Energy Journal*, 39(2).
- Hou, C., & Nguyen, B. H. (2018). Understanding the us natural gas market: A markov switching var approach. *Energy Economics*, 75, 42–53.
- Hu, H., Wei, W., & Chang, C.-P. (2020). The relationship between shale gas production and natural gas prices: An environmental investigation using structural breaks. *Science of the total environment*, 713, 136545.
- Hull, J. C., & Basu, S. (2016). *Options, futures, and other derivatives*. Pearson Education India.
- Hulshof, D., Van Der Maat, J.-P., & Mulder, M. (2016). Market fundamentals, competition and natural-gas prices. *Energy policy*, 94, 480–491.
- Huszár, Z. R., Kotró, B. B., & Tan, R. S. (2023). Dynamic volatility transfer in the european oil and gas industry. *Energy Economics*, 127, 107052.
- IEA. (2020). *Fast-tracking gas market reforms*. Retrieved from <https://www.iea.org/commentaries/fast-tracking-gas-market-reforms> (International Energy Agency. Accessed: September 21, 2024)
- IEA. (2020a). Gas 2020. IEA: <https://www.iea.org/reports/gas-2020>.
- IEA. (2020b). *Gas 2020*. Retrieved from <https://www.oecd-ilibrary.org/content/publication/df4b275f-en> doi: <https://doi.org/https://doi.org/10.1787/df4b275f-en>
- IEA. (2023). *Gas market report q1 2023*. Retrieved from <https://www.iea.org/reports/gas-market-report-q1-2023>

- IGU, I. G. U. (2021). *Wholesale gas price survey 2021 edition - international gas union* (Tech. Rep.). IGU - International Gas Union.
- IGU, I. G. U. (2022). *Wholesale gas price survey 2023 edition - international gas union*.
- Ihle, R., & von Cramon-Taubadel, S. (2008). *A comparison of threshold cointegration and markov-switching vector error correction models in price transmission analysis* (Tech. Rep.).
- IHS Markit. (2022). *Us monthly gdp (mgdp) index*. <https://ihsmarkit.com/products/us-monthly-gdp-index.html>. (Retrieved on September 20, 2022)
- IMF. (2024, January). *World economic outlook update: Moderating inflation and steady growth open path to soft landing*. Retrieved from <https://www.imf.org/en/Publications/WE0/Issues/2024/01/30/world-economic-outlook-update-january-2024> (International Monetary Fund (IMF))
- Jaeck, E., & Lautier, D. (2016). Volatility in electricity derivative markets: The samuelson effect revisited. *Energy Economics*, 59, 300–313.
- Jarque, C. M., & Bera, A. K. (1980). Efficient tests for normality, homoscedasticity and serial independence of regression residuals. *Economics letters*, 6(3), 255–259.
- Ji, Q., Zhang, D., & Kutan, A. M. (2020). *Energy financialization, risk and challenges* (Vol. 68). Elsevier.
- Jin, X. (2017). Do futures prices help forecast the spot price? *Journal of Futures Markets*, 37(12), 1205–1225.
- JODI. (2024). *Gas world database*. Joint Organizations Data Initiative (JODI). Retrieved from <https://www.jodidata.org/gas/database/overview.aspx>
- Joshi, J. (2021). Sectoral and temporal changes in natural gas demand in the united states. *Journal of Natural Gas Science and Engineering*, 96, 104245.
- Joskow, P. L. (2013). Natural gas: from shortages to abundance in the united states. *American Economic Review*, 103(3), 338–343.
- Joutz, F., et al. (2009). Estimating regional short-run and long-run price elasticities of residential natural gas demand in the u.s. *SSRN Electronic Journal*. Retrieved from <http://dx.doi.org/10.2139/ssrn.1444927> (WP 09-021)

Bibliography

- Kaminski, V. (2012). *Energy markets*. London: Risk Books, a Division of Incisive Media Investments Ltd. (Copy-edited by Laurie Donaldson, Typeset by Mark Heslington Ltd, Printed and bound in the UK by Berforts Group Ltd)
- Khalfaoui, R., Hammoudeh, S., & Rehman, M. Z. (2023). Spillovers and connectedness among brics stock markets, cryptocurrencies, and uncertainty: Evidence from the quantile vector autoregression network. *Emerging Markets Review*, 54, 101002.
- Kilian, L. (2008). The economic effects of energy price shocks. *Journal of economic literature*, 46(4), 871–909.
- Kilian, L. (2009). Not all oil price shocks are alike: Disentangling demand and supply shocks in the crude oil market. *American economic review*, 99(3), 1053–1069.
- Kilian, L., & Lütkepohl, H. (2017). *Structural vector autoregressive analysis*. Cambridge University Press.
- Kilian, L., & Murphy, D. P. (2012). Why agnostic sign restrictions are not enough: understanding the dynamics of oil market var models. *Journal of the European Economic Association*, 10(5), 1166–1188.
- Kilian, L., & Murphy, D. P. (2014). The role of inventories and speculative trading in the global market for crude oil. *Journal of Applied econometrics*, 29(3), 454–478.
- Kim, A., Ryu, D., & Webb, R. I. (2024). Evolving roles of energy futures markets: A survey. *Borsa Istanbul Review*.
- Kumar, M. S. (1992). The forecasting accuracy of crude oil futures prices. *IMF Staff Papers*, 39(2), 432–461.
- Kuper, G. H., & Mulder, M. (2016). Cross-border constraints, institutional changes and integration of the dutch–german gas market. *Energy Economics*, 53, 182–192.
- Kwas, M., & Rubaszek, M. (2021). Forecasting commodity prices: Looking for a benchmark. *Forecasting*, 3(2), 447–459.
- Labandeira, X., Labeaga, J. M., & López-Otero, X. (2017). A meta-analysis on the price elasticity of energy demand. *Energy policy*, 102, 549–568.

- Lenza, M., & Primiceri, G. E. (2022). How to estimate a vector autoregression after march 2020. *Journal of Applied Econometrics*, 37(4), 688–699.
- Li, R., Joyeux, R., & Ripple, R. D. (2014). International natural gas market integration. *The Energy Journal*, 35(4).
- Liu, J., Julaiti, J., & Gou, S. (2024). Decomposing interconnectedness: A study of cryptocurrency spillover effects in global financial markets. *Finance Research Letters*, 61, 104950.
- Longstaff, F. A. (2010). The subprime credit crisis and contagion in financial markets. *Journal of financial economics*, 97(3), 436–450.
- Luong, P. V. (2023). Crude oil pipeline constraints: A tale of two shales. *Resources Policy*, 80, 103203.
- Luong, P. V., Mizrach, B., & Otsubo, Y. (2019). Location basis differentials in crude oil prices. *The Energy Journal*, 40(2_suppl), 41–58.
- MacKinnon, J. G. (2010). *Critical values for cointegration tests* (Tech. Rep.). Queen’s Economics Department Working Paper.
- Makholm, J. (2010). Seeking competition and supply security in natural gas: the us experience and european challenge. In *Security of energy supply in europe*. Edward Elgar Publishing.
- Manescu, C. B., & Van Robays, I. (2016). Forecasting the brent oil price: Addressing time-variation in forecast performance. *CESifo Working Paper No. 6242*.
- Marcellino, M. (1999). Some consequences of temporal aggregation in empirical analysis. *Journal of Business & Economic Statistics*, 17(1), 129–136.
- Mason, C. F., Muehlenbachs, L. A., & Olmstead, S. M. (2015). The economics of shale gas development. *Annu. Rev. Resour. Econ.*, 7(1), 269–289.
- Mason, C. F., & Roberts, G. (2018). Price elasticity of supply and productivity: an analysis of natural gas wells in wyoming. *The Energy Journal*, 39(1_suppl), 79–100.
- Matteson, D. S., & Tsay, R. S. (2017). Independent component analysis via distance covariance. *Journal of the American Statistical Association*, 112(518), 623–637.

Bibliography

- McNew, K., & Fackler, P. L. (1997). Testing market equilibrium: Is cointegration informative? *Journal of Agricultural and Resource Economics*, 191–207.
- McWilliams, B., Sgaravatti, G., Tagliapietra, S., & Zachmann, G. (2023). Can europe live without russian natural gas? *The World Economy*, 46(4), 897–905.
- Melamid, A. (1994). International trade in natural gas. *Geographical Review*, 84(2), 216–221.
- Melikoglu, M. (2014). Shale gas: Analysis of its role in the global energy market. *Renewable and Sustainable Energy Reviews*, 37, 460–468.
- Mensi, W., Boubaker, F. Z., Al-Yahyaee, K. H., & Kang, S. H. (2018). Dynamic volatility spillovers and connectedness between global, regional, and gipsi stock markets. *Finance Research Letters*, 25, 230–238.
- Miao, H., Ramchander, S., Wang, T., & Yang, D. (2017). Influential factors in crude oil price forecasting. *Energy Economics*, 68, 77–88.
- Naeem, M. A., Chatziantoniou, I., Gabauer, D., & Karim, S. (2024). Measuring the g20 stock market return transmission mechanism: Evidence from the r2 connectedness approach. *International Review of Financial Analysis*, 91, 102986.
- Naeem, M. A., Gul, R., Shafiullah, M., Karim, S., & Lucey, B. M. (2024). Tail risk spillovers between shanghai oil and other markets. *Energy Economics*, 130, 107182.
- Neukirchen, D., Köchling, G., & Posch, P. N. (2023). Enforcement of corporate misconduct during democratic and republican administrations. *Finance Research Letters*, 55, 103921.
- Neumann, A. (2009). Linking natural gas markets-is lng doing its job? *The Energy Journal*, 30(Special Issue).
- Neumann, A., & Cullmann, A. (2012). What's the story with natural gas markets in europe? empirical evidence from spot trade data. In *2012 9th international conference on the european energy market* (pp. 1–6).
- Newey, W. K., & West, K. D. (1987). Hypothesis testing with efficient method of moments estimation. *International Economic Review*, 777–787.
- Ng, S. (2021). *Modeling macroeconomic variations after covid-19* (Tech. Rep.). National Bureau of Economic Research.

- NGI. (2017). *Gulf coast facilities recovering from harvey, but impact far-reaching*. Retrieved from <https://www.naturalgasintel.com/gulf-coast-facilities-recovering-from-harvey-but-impact-far-reaching/> (Accessed: 2024-05-25)
- Nguyen, B. H., & Okimoto, T. (2019). Asymmetric reactions of the us natural gas market and economic activity. *Energy Economics*, 80, 86–99.
- Nick, S., & Tischler, B. (2014). *The law of one price in global natural gas markets: A threshold cointegration analysis* (Tech. Rep.). EWI Working Paper.
- Nyga-Łukaszewska, H., & Aruga, K. (2020). Energy prices and covid-immunity: The case of crude oil and natural gas prices in the us and japan. *Energies*, 13(23), 6300.
- Ogbonna, A. E., Farag, M., Akintande, O. J., Yaya, O. S., & Olubusoye, O. E. (2024). Re-validating the phillips curve hypothesis in africa and the role of oil prices: A mixed-frequency approach. *Energy*, 303, 131862.
- Pagano, P., & Pisani, M. (2009). Risk-adjusted forecasts of oil prices. *The BE Journal of Macroeconomics*, 9(1), 1–26.
- Papież, M., Rubaszek, M., Szafranek, K., & Śmiech, S. (2022). Are european natural gas markets connected? a time-varying spillovers analysis. *Resources Policy*, 79, 103029.
- Parkinson, M. (1980). The extreme value method for estimating the variance of the rate of return. *Journal of business*, 61–65.
- Pesaran, M. H., & Timmermann, A. (2009). Testing dependence among serially correlated multicategory variables. *Journal of the American Statistical Association*, 104(485), 325–337.
- Phillips, P. C., & Sul, D. (2007). Transition modeling and econometric convergence tests. *Econometrica*, 75(6), 1771–1855.
- Pindyck, R. S. (2001). The dynamics of commodity spot and futures markets: a primer. *The energy journal*, 22(3).
- Ponce, M., & Neumann, A. (2014). Elasticities of supply for the us natural gas market.
- Reeve, T. A., & Vigfusson, R. J. (2011). Evaluating the forecasting performance of commodity futures prices. *FRB International Finance Discussion Paper*(1025).

Bibliography

- Rehman, M. U., & Vo, X. V. (2021). Energy commodities, precious metals and industrial metal markets: A nexus across different investment horizons and market conditions. *Resources Policy*, 70, 101843.
- Reichsfeld, M. D. A., & Roache, M. S. K. (2011). Do commodity futures help forecast spot prices? *IMF Working Paper*, No. 2011/254.
- Ritz, R. A. (2019). A strategic perspective on competition between pipeline gas and lng. *The Energy Journal*, 40(5).
- Robinson, T. (2007). Have european gas prices converged? *Energy Policy*, 35(4), 2347–2351.
- Roman, M., & Žáková Kroupová, Z. (2022). Spatial market integration: A case study of the polish–czech milk market. *Economies*, 10(1), 25.
- Rubaszek, M., Szafranek, K., & Uddin, G. S. (2021). The dynamics and elasticities on the us natural gas market. a bayesian structural var analysis. *Energy Economics*, 103, 105526.
- Rubaszek, M., & Uddin, G. S. (2020). The role of underground storage in the dynamics of the us natural gas market: A threshold model analysis. *Energy Economics*, 87, 104713.
- Ruhnau, O., Stiewe, C., Muessel, J., & Hirth, L. (2023). Natural gas savings in germany during the 2022 energy crisis. *Nature Energy*, 8(6), 621–628.
- Rystad Energy, R. (2023). Gas market cube. *Commercial Database*.
- Samuelson, P. A. (1952). Spatial price equilibrium and linear programming. *The American economic review*, 42(3), 283–303.
- Schorfheide, F., & Song, D. (2024). Real-time forecasting with a (standard) mixed-frequency var during a pandemic.
- Serletis, A., & Herbert, J. (1999). The message in north american energy prices. *Energy Economics*, 21(5), 471–483.
- Silverstovs, B., L'Hégaret, G., Neumann, A., & Von Hirschhausen, C. (2005). International market integration for natural gas? a cointegration analysis of prices in europe, north america and japan. *Energy Economics*, 27(4), 603–615.

- Silvestrini, A., & Veredas, D. (2008). Temporal aggregation of univariate and multivariate time series models: a survey. *Journal of Economic Surveys*, 22(3), 458–497.
- S&P Global Commodity Insights. (2023). *Us lng export utilization rises from recent lows as maintenance weighs on feedgas demand*. Retrieved from <https://www.spglobal.com/commodityinsights/en/market-insights/latest-news/natural-gas/061623-us-lng-export-utilization-rises-from-recent-lows-as-maintenance-weighs-on-feedgas-demand> (Accessed: 2023-06-16)
- Symeonidis, L., Prokopczuk, M., Brooks, C., & Lazar, E. (2012). Futures basis, inventory and commodity price volatility: An empirical analysis. *Economic Modelling*, 29(6), 2651–2663.
- Szafranek, K., Papież, M., Rubaszek, M., & Śmiech, S. (2023). How immune is the connectedness of european natural gas markets to exceptional shocks? *Resources Policy*, 85, 103917.
- Takayama, T., & Judge, G. G. (1971). Spatial and temporal price and allocation models.
- Telser, L. G. (1958). Futures trading and the storage of cotton and wheat. *Journal of Political Economy*, 66(3), 233–255.
- Tiao, G. C. (1972). Asymptotic behaviour of temporal aggregates of time series. *Biometrika*, 59(3), 525–531.
- Toda, H. Y., & Yamamoto, T. (1995). Statistical inference in vector autoregressions with possibly integrated processes. *Journal of econometrics*, 66(1-2), 225–250.
- Tyner, W. E. (2010). The integration of energy and agricultural markets. *Agricultural Economics*, 41, 193–201.
- Valenti, D., Bastianin, A., & Manera, M. (2023). A weekly structural var model of the us crude oil market. *Energy Economics*, 121, 106656.
- Villar, J. A., & Joutz, F. L. (2006). The relationship between crude oil and natural gas prices. *Energy Information Administration, Office of Oil and Gas*, 1, 1–43.
- Wang, Y., Liu, L., & Wu, C. (2017). Forecasting the real prices of crude oil using forecast combinations over time-varying parameter models. *Energy Economics*, 66, 337–348.

Bibliography

- Weiss, A. A. (1984). Systematic sampling and temporal aggregation in time series models. *Journal of Econometrics*, 26(3), 271–281.
- Wiggins, S., & Etienne, X. L. (2017). Turbulent times: Uncovering the origins of us natural gas price fluctuations since deregulation. *Energy Economics*, 64, 196–205.
- Working, H. (1949). The theory of price of storage. *The American Economic Review*, 39(6), 1254–1262.
- Working, H. (1960). Note on the correlation of first differences of averages in a random chain. *Econometrica*, 28(4), 916–918.
- Yang, J., Kolari, J. W., & Min, I. (2003). Stock market integration and financial crises: the case of asia. *Applied Financial Economics*, 13(7), 477–486.
- Zabed, H., Sahu, J., Suely, A., Boyce, A., & Faruq, G. (2017). Bioethanol production from renewable sources: Current perspectives and technological progress. *Renewable and Sustainable Energy Reviews*, 71, 475–501.
- Zellner, A., & Montmarquette, C. (1971). A study of some aspects of temporal aggregation problems in econometric analyses. *The Review of Economics and Statistics*, 335–342.
- Zhang, D., & Ji, Q. (2018). Further evidence on the debate of oil-gas price decoupling: A long memory approach. *Energy Policy*, 113, 68–75.

CURRICULUM VITAE

Markos Farag

PERSONAL DATA

Date of Birth	7th August 1993
Place of Birth	Egypt
Nationality	Egyptian

EDUCATION

Since 2020	Department of Economics, University of Cologne, Germany Doctoral Candidate in Economics
2023	Center for Energy Studies, Louisiana State University, USA Research Stay
2016 - 2019	Cairo University, Egypt Master of Science (M.Sc.) in Economics,
2017	University of Padova, Italy Semester abroad (Erasmus Program)
2011 – 2015	Cairo University, Egypt Bachelor of Science (B.Sc.) in Economics (Minor: Statistics)

WORKING EXPERIENCE

Since 2021	Chair of Energy Economics, University of Cologne Lecturer
2016 – 2019	Economics Department, Cairo University Lecturer Assistant
2015 – 2016	Egyptian Center for Economic Studies Junior Economist

PUBLICATIONS

Articles in Peer-Reviewed Journals:

- Farag, M., Jeddi, S., & Kopp, J. H. (2025). Global Natural Gas Market Integration: The Role of LNG Trade and Infrastructure Constraints. *The World Economy*.
- Farag, M., Musa, D. C., Olayinka, H. A., Ogbonna, A. E., Yaya, O. S., & Olubusoye, O. E. (2025). Forecasting Market Fear: the roles of policy uncertainty and geopolitical Risk. *Applied Economics*, 1-16.
- Ogbonna, A. E., Farag, M., Akintande, O. J., Yaya, O. S., & Olubusoye, O. E. (2024). Re-Validating the Phillips Curve Hypothesis in Africa and the Role of Oil Price: A Mixed Frequency Approach – *Energy*, 131862.
- Farag, M., & Zaki, C. (2024). On the economic and political determinants of trade in natural gas. *The World Economy*, 47(2), 806-836.
- Boulakhbar, M., Farag, M., Benabdelaziz, K., Kouksou, T., & Zazi, M. (2021). A deep learning approach for prediction of electrical vehicle charging stations power demand in regulated electricity markets: The case of Morocco. *Cleaner Energy Systems*, 3, 100039.
- Farag, M., & Zaki, C. (2021) (2021). Price and income elasticities of natural gas demand in Egypt: A bound test approach. *Review of Middle East Economics and Finance*, 17(1), 27-55.

Working Papers:

- Decomposing Return and Volatility Connectedness in Northwest European Gas Markets: Evidence from the R2 connectedness approach. (2024). *EWI Working Paper 24/06*.
- M. Farag, S. Snudden, G. Upton (2014). Can Futures Prices Predict the Real Price of Primary Commodities?. *Laurier Centre for Economic Research and Policy Analysis*.
- Farag, M., Jeddi, S., & Kopp, J. H. (2023). Global natural gas market integration in the face of shocks: Evidence from the dynamics of European, Asian, and US gas futures prices. *EWI Working Paper 23/03*.

Selected Further Publications:

- Boulakhbar, M., Farag, M., Benabdelaziz, K., Zazi, M., Maaroufi, M., & Kousksou, T. (2022). Electric vehicles arrival and departure time prediction based on deep learning: the case of Morocco. In 2022 2nd International Conference on Innovative Research in Applied Science, Engineering and Technology (IRASET) (pp. 1-8). IEEE.
- Theile, P., Farag, M., & Kopp, T. (2022). Does information substitute or complement energy?-A mediation analysis of their relationship in European economies.

Conferences & Seminars

- *2024*: 13th International Ruhr Energy Conference (Essen, Germany); 2024 RCEA International Conference in Economics, Econometrics, and Finance, (UK).
- *2023*: 44th IAEE International Conference (Riyadh, Saudi Arabia); 12th International Ruhr Energy Conference (Essen, Germany); USAEE/IAEE North American 2023 conference (Chicago, USA)
- *2022*: Global Economic Policy Group meeting 2022: Macroeconomic Politics, Integration and Trade (Berlin, Germany); Seminar on Statistics and Econometrics (University of Kiel, Germany); Climate Econometrics Seminar at Nuffield College at the University of Oxford (Virtual)
- *2021*: 16th Annual Conference - Warsaw International Economic Meeting (Virtual); Hagen Workshop on Global Economic Studies (Virtual) ; USAEE/IAEE North American 2021 conference (Virtual) ; 10th International Ruhr Energy Conference (Essen, Germany)
- *2020*: 13th RGS Doctoral Conference in Economics 2020 (Essen, Germany)
- *2019*: EMNES Annual Conference, "Towards A Regional Integration and Employment Driven Socio-Economic Model in the Mediterranean" (Brussels, Belgium); Policy, Awareness, Sustainability, and Systems Workshop (PASS 2019) (University of Cologne, Germany)